

GLUTAMATE RECEPTOR SUBUNITS
IN THE RAT CORNEA

By

BRANDEN KENNETH CARR

Bachelor of Arts, Psychology
University of Central Oklahoma
Edmond, Oklahoma
2010

Bachelor of Science, Biology
Oklahoma State University
Stillwater, Oklahoma
2011

Submitted to the Faculty of the
Graduate College of the
Oklahoma State University
in partial fulfillment of
the requirements for
the Degree of
DOCTOR OF PHILOSOPHY
May, 2017

GLUTAMATE RECEPTOR SUBUNITS
IN THE RAT CORNEA

Dissertation Approved:

Dr. Kenneth Miller

Dissertation Adviser

Dr. Matt Vassar

Dr. Nedra Wilson

Dr. Wouter Hoff

ACKNOWLEDGMENTS

Being a Ph.D. student has its difficulties, but I was fortunate to have a very supportive family both at home and work. My adviser, Dr. Kenneth Miller, has been continuously supportive throughout my time at OSU-CHS, and I cannot thank him enough for everything he has done for me. He has given me knowledge, guidance, and support throughout my time here along with essential skills that I will continue to use throughout my career. Thank you for everything.

I also want to thank my other committee members, Drs. Matt Vassar, Nedra Wilson, and Wouter Hoff. They continuously supported me throughout my time at OSU-CHS by further expanding my knowledge and skills.

I would like to thank all my friends that have helped me throughout my time at OSU-CHS. Thank you Dr. Bernadette Olayinka Ibitokun for teaching me the techniques that I used with the corneas. Also, I would like to thank Dr. Das, Dr. Zijia Zhang, Dr. Ting Wang, Dr. Kellen Myers, Vadim Yerokhin, Michael Anderson, Vikram Gujar, and Radika Pande for being a great and supportive lab group.

I would also like to give a special thanks to Anh Tran-Pham for being there for me throughout the highs and the lows. Finally, I would like to thank my parents, David and Kim Carr, for the unwavering support throughout my life. Without this support, I would not be where I am today. Thank you very much for everything that you have done for me and I love you both very much.

Name: BRANDEN KENNETH CARR

Date of Degree: MAY, 2017

Title of Study: GLUTAMATE RECEPTOR SUBUNITS IN THE RAT CORNEA

Major Field: BIOMEDICAL SCIENCES

Abstract:

The purpose of this study was to identify if topical application of an ionotropic Glutamate receptor (iGluR) antagonist could effectively reduce pain in the cornea and to identify the presence and location of the 16 different iGluR subunits. Furthermore, we assessed the quality of the currently published iGluR literature using the ARRIVE guidelines. We identified DNQX as an effective iGluR antagonist when topically applied to the cornea, we identified the presence of each of the iGluR to the cornea and the trigeminal root ganglion, and we identified the lack of completeness in the currently published iGluR literature. From these results, further investigation of DNQX should be done to identify if it can be used as an effective treatment of corneal pain. Further studies including co-localization of iGluR subunits should be done to identify receptor composition and functionality. Finally, a better reporting of the methods and results of published works should be done to increase translation of results from animal to human.

TABLE OF CONTENTS

Chapter	Page
I. INTRODUCTION	1
Section 1.1 Nociception	2
Section 1.2 Nociceptors	2
Section 1.3 Glutamate as a Neurotransmitter	4
Section 1.4 Glutamate Synthesis	5
Section 1.5 Glutamate Receptors	6
Section 1.6 AMPA Receptors	9
Section 1.7 Kainate Receptors	11
Section 1.8 NMDA Receptors	12
Section 1.9 Delta Receptors	13
Section 1.10 Corneal Structure	13
Section 1.11 Corneal innervation	15
Section 1.12 Glutamate in the Cornea	16
Section 1.13 Glutamate receptor agonists	17
Section 1.14 Glutamate receptor antagonists	18
Section 1.15 Glutamate subunit presence in the cornea	18
Section 1.16 Animal Research: Reporting of In Vivo Experiments (ARRIVE) Guidelines	20
Section 1.17 Prospective implementations	24
Section 1.18 Hypotheses and Specific Aims	24
II. 6,7-DINITROQUINOXALINE-2,3-DIONE (DNQX) AS A TOPICAL EXCITATORY AMINO ACID RECEPTOR ANTAGONIST OF CORNEAL EPITHELIUM: A BEHAVIORAL STUDY	26
Section 2.1 Introduction	27
Section 2.2 Methodology	28
Section 2.3 Results	31
Section 2.4 Discussion	33

Chapter	Page
III. IDENTIFYING THE LOCATION OF THE SIXTEEN CURRENTLY KNOWN GLUTAMATE RECEPTORS IN THE RAT CORNEA: A WESTERN BLOTTING AND IMMUNOHISTOCHEMISTRY STUDY.....	44
Section 3.1 Introduction.....	45
Section 3.2 Methodology.....	46
Section 3.3 Results.....	50
Section 3.4 Discussion.....	97
IV. APPLYING THE ARRIVE GUIDELINES TO PERIPHERAL NOCICEPTIVE EXCITATORY AMINO ACID RECEPTOR LITERATURE: A SYSTEMATIC REVIEW.....	100
Section 4.1 Introduction.....	101
Section 4.2 Methodology.....	101
Section 4.3 Results.....	103
Section 4.4 Discussion.....	108
V. CONCLUSION.....	111
VI. WESTERN BLOT PROTOCOL.....	120
VII. IMMUNOHISTOCHEMISTRY PROTOCOL.....	153
REFERENCES.....	183

LIST OF DIAGRAMS

Diagram	Page
Sensory and motor nerve fiber classification.....	3
Primary sensory afferent in the cornea	4
Postsynaptic neurotransmitter interactions	6
Structure of ionotropic glutamate receptor	8
Nomenclature of the glutamate receptor subunits	9
Corneal layers	15
Sensory innervation of the cornea from the ophthalmic division of the trigeminal nerve	16
Glutamate dose response study.....	17
Glutamate dose response curve.....	17
AMPA dose response curve.....	18
Kainate dose response curve.....	18
NMDA GluN1 immunoreactivity in cornea (whole mount).....	19
NMDA GluN1 immunoreactivity in the rat cornea (10µm sagittal section)	19
AMPA GluA1 immunoreactivity in cornea (whole mount)	20
AMPA GluA2/3 immunoreactivity in the rat cornea (10µm sagittal section).....	20
The first half of the ARRIVE guidelines	22
The second half of the ARRIVE guidelines	23
Figure representing a noxious stimulus being applied to the corneal epithelial layer and the subsequent release of glutamate to activate corneal primary afferents.....	115
Capsaicin behavioral response and log dose response.....	117
Potassium Chloride (KCl) behavioral response and log dose response.....	117

LIST OF FIGURES

Figure	Page
Bar graph of the behavioral responses in each of the respective DNQX treatment groups	32
Dose response curve for DNQX representing the nocifensive behavioral recordings	33
List of Tocris glutamate receptor antagonists with pertinent information	43
List of all primary and secondary antibodies used in this study	50
Preliminary western blots of whole corneas	50
Western blot of GluA2	51
Results of immunofluorescent reactivity for the cornea and trigeminal ganglia	53
Image illustrating immunoreactivity in corneal epithelial cells (GluA2)	54
Image illustrating corneal epithelial nerve fiber staining (GluK1)	54
Image illustrating corneal stromal nerve fiber staining (GluK5)	55
Image illustrating corneal cytoplasmic staining (GluN2D)	55
Image illustrating corneal nuclear staining and enlarged in right panel (GluN2B)	56
Image illustrating Trigeminal large (White arrows) and small (Blue arrows) immunoreactive neuronal cell bodies (GluA2)	57
Image illustrating Trigeminal nuclear (arrows) immunoreactivity (GluK3)	57
Image illustrating Trigeminal nerve fiber (arrows) immunoreactivity (GluN3A)	58
Image illustrating Trigeminal satellite (arrows) immunoreactivity (GluN2D)	58
Image illustrating Trigeminal Schwann (arrows) immunoreactivity (GluN3A)	59
Image illustrating Trigeminal myelin (arrows) immunoreactivity (GluK5)	59
Images illustrating Cornea and Trigeminal root ganglion immunoreactivity of GluA1 (Green) and PGP9.5 (Red)	60
Images illustrating Cornea and Trigeminal root ganglion immunoreactivity of GluA2 (Green) and PGP9.5 (Red)	62
Images illustrating Cornea and Trigeminal root ganglion immunoreactivity of GluA3 (Green) and PGP9.5 (Red)	64
Images illustrating Cornea and Trigeminal root ganglion immunoreactivity of GluA4 (Green) and CGRP (Red)	66
Images illustrating Cornea and Trigeminal root ganglion immunoreactivity of GluK1 (Green) and PGP9.5 (Red)	68
Images illustrating Cornea and Trigeminal root ganglion immunoreactivity of GluK2 (Green) and CGRP (Red)	70
Images illustrating Cornea and Trigeminal root ganglion immunoreactivity of GluK3 (Green) and PGP9.5 (Red)	72

Figure	Page
Images illustrating Cornea and Trigeminal root ganglion immunoreactivity of GluK4 (Green) and PGP9.5 (Red).....	74
Images illustrating Cornea and Trigeminal root ganglion immunoreactivity of GluK5 (Green) and PGP9.5 (Red).....	76
Images illustrating Cornea and Trigeminal root ganglion immunoreactivity of GluN1 (Green) and PGP9.5 (Red).....	78
Images illustrating Cornea and Trigeminal root ganglion immunoreactivity of GluN2A (Green) and PGP9.5 (Red).....	80
Images illustrating Cornea and Trigeminal root ganglion immunoreactivity of GluN2B (Green) and PGP9.5 (Red).....	82
Images illustrating Cornea and Trigeminal root ganglion immunoreactivity of GluN2C (Green) and PGP9.5 (Red).....	84
Images illustrating Cornea and Trigeminal root ganglion immunoreactivity of GluN2D (Green) and PGP9.5 (Red).....	86
Images illustrating Cornea and Trigeminal root ganglion immunoreactivity of GluN3A (Green) and CGRP (Red).....	88
Images illustrating Cornea and Trigeminal root ganglion immunoreactivity of GluN3B (Green) and CGRP (Red).....	90
Images illustrating Cornea and Trigeminal root ganglion immunoreactivity of PSD-95 (Green) and CGRP (Red).....	92
Images illustrating Cornea and Trigeminal root ganglion immunoreactivity of Stargazin (Green) and CGRP (Red).....	94
Images illustrating Cornea and Trigeminal root ganglion immunoreactivity of Glutamate (Green)	96
Adapted PRISMA flow diagram.....	103
Table representing each graded component with description of the ARRIVE guidelines and percentages of articles that met criteria	108

Abbreviations

AMPA - 2-amino-3-(5-methyl-3-oxo-1,2-oxazol-4-yl) propanoic acid

AMPA_r - 2-amino-3-(5-methyl-3-oxo-1,2-oxazol-4-yl) propanoic acid receptor

ANOVA - analysis of variance

ARRIVE - Animal Research: Reporting In Vivo Experiments

CGRP – Calcitonin gene related peptide

CNS – Central nervous system

DNQX - 6,7-dinitroquinoxaline-2,3-dione

DRG – Dorsal root ganglion

EAAR – Excitatory amino acid receptor

ED₅₀ – In vivo dose of a drug that yields 50% of its maximum response

GluR – Glutamate receptor

iGluR – Ionotropic glutamate receptor

IR – Immunoreactivity

ID₅₀ – In vivo dose of drug that yields 50% of the maximum possible inhibition for that drug

KCl – Potassium Chloride

LASIK – Laser assisted in situ keratomileusis

NMDA – N-methyl-D-aspartate

NMDA_r – N-methyl-D-aspartate receptor

NSAIDS – Non-steroidal anti-inflammatory drugs

PBS – Phosphate buffered saline

PSD-95 – Postsynaptic Density-95

PRISMA – Preferred Reporting Items for Systematic Reviews and Meta-Analyses

PVDF – Polyvinylidene difluoride

PNS – Peripheral nervous system

RIPA – Radioimmunoprecipitation Assay

S.E.M. – Standard error of the mean

TRG – Trigeminal root ganglion

TRPV – Transient receptor potential channel

vGluT – vesicular glutamate transporter

CHAPTER I
INTRODUCTION AND REVIEW OF LITERATURE

Introduction

Pain can be detrimental to everyday events leading to decreased productivity within society, including family, social, and work life. To regulate pain in a way to help an individual remain or become a functional member of society would be a huge improvement to many lives and society as a whole. Specifically, the type of pain, acute or chronic, an individual has may influence how their life will proceed within the near and possibly distant future. Acute pain is common from the peripheral nervous system due to an extensive innervation of tissues by primary sensory afferent nerve fibers. The structure, innervation, and sensitivity of the tissue will determine the level of pain intensity that leads to nocifensive (adverse) responses.

Nocifensive responses are present in vertebrates to help fend off adverse stimuli that may be detrimental to existence. In the eye, a noxious stimulus may produce a nocifensive response such as eye blinking. When an irritant has been introduced to the eye, primary sensory afferents of the cornea responsively fire action potentials to signal for a nocifensive response. It has been proposed that glutamate, an excitatory neurotransmitter, has a role in the transduction of external stimuli and a neuronal response (Miller et al. 2011). The action of glutamate occurs by activating Glutamate Receptors (GluRs): α -amino-3-hydroxy-5-methyl-4-isoxazolepropionic acid receptor (AMPAr), Kainate receptor, and N-Methyl-D-aspartic acid receptor (NMDAr) (Bleakman, Alt, & Nisenbaum, 2006). The following literature review will describe in more detail the background of these phenomena and introduce my research hypotheses and specific aims.

Literature Review

1.1: Nociception: Nociception is a response to a noxious stimulus. A noxious stimulus is an adverse stimulus that can cause reflex withdrawals, autonomic responses, and pain (Sherrington, 1903). A noxious stimulus, via application or injection of glutamate (da Silva et al., 2014; Michelotti et al., 2014; Nilsson et al., 2014; Sato et al., 2015; Shimada et al., 2015), mustard oil (Albin, Carstens, & Carstens, 2008; Bonjardim, da Silva, Gameiro, Tambeli, & Ferraz de Arruda Veiga, 2009; Claiborne, Nag, & Mokha, 2009; Merrill, Cuellar, Judd, Carstens, & Carstens, 2008; Ruparel, Patwardhan, Akopian, & Hargreaves, 2008; Sawyer, Carstens, & Carstens, 2009; Zhang et al., 2006), capsaicin (Burness & McCormack, 2016; Deba & Bessac, 2015; Doll et al., 2016; Landmann et al., 2016; Li et al., 2016; Ruparel et al., 2008; Zakharov et al., 2015), and Freund's adjuvant (Atianjoh et al., 2010; Y. S. Lee, Lee, Lee, & Choi, 2013; J. S. Park et al., 2008; Peng et al., 2012), can initiate an action potential from primary sensory afferent nerve fibers innervating peripheral tissue. In order to prevent unwanted harm to a tissue, a reflexive response (including wiping, licking, moving, etc.) occurs to prevent the noxious stimulus from remaining on a tissue for a prolonged period of time (Rossignol, Dubuc, & Gossard, 2006). This type of stimulus also will elicit nociception, or pain.

1.2: Nociceptors: Nociceptors are classified as A δ and C primary afferent fibers, but as seen in table 1.1, primary afferent nerve fibers in general are classified as being large, medium, or small or as type A, B, and C respectively (Basbaum, Bautista, Scherrer, & Julius, 2009; Haines, 2012). Furthermore, table 1.1 represents a distinct breakdown of the classifications of neuron type that is dependent on axon diameter, nerve fiber velocity, and what tissue is supplied by nociceptors.

Peripheral nerve electrophysiologic classification	Afferent Fibers group	Fiber Diameter (μm)	Conduction velocity (m/s)	Receptor supplied
<i>Sensory Fiber</i>				
A α	Ia and Ib	13 - 20	80-120	Primary muscle spindles, Golgi tendon organ
A β	II	6-12	35-75	Secondary muscle spindles, skin mechanoreceptors
A δ	III	1-5	5-30	Skin mechanoreceptors, thermal receptors, and nociceptors
C	IV	0.2-1.5	0.5-2	Skin mechanoreceptors, thermal receptors, and nociceptors
<i>Motor Fiber</i>				
A α	N/A	12-20	72-120	Extrafusal skeletal muscle fibers
A γ	N/A	2-8	12-48	Intrafusal muscle fibers
B	N/A	1-3	6-18	Preganglionic autonomic fibers
C	N/A	0.2-2	0.5-2	Postganglionic autonomic fibers

Table 1.1: Sensory and motor nerve fiber classification (Adapted from (Haines, 2012)).

The nociceptors, or primary sensory afferent neurons, have four specific main parts: the peripheral nerve terminal, axon, neuronal cell body, and a central axon terminal (Woolf & Ma, 2007). The peripheral nerve terminal is present in the peripheral tissue and responds to a noxious stimulus that can produce an axonal action potential to reach the next sensory neuron, a secondary sensory neuron (Mertens, Blond, David, & Rigoard, 2015). The neuronal cell body is located in the Trigeminal Root Ganglion (TRG) or the Dorsal Root Ganglion (DRG) depending if the peripheral tissue is located in the face or body, respectively. Furthermore, these primary sensory afferent neurons are classified as pseudounipolar with one axon from the neuronal cell body that divides to project peripherally and centrally (Ray, Singh, & Mehra, 2010). In order to convey a noxious signal to the secondary neuron, the central axon terminal produces synaptic release, i.e., exocytosis, of neurotransmitters to stimulate the secondary neuron (Mertens et al., 2015).

For a noxious signal to reach the brain, there are four sensory neurons organized in a sequence from the peripheral tissue to the cerebral cortex. The primary neuron, represented by figure 1.1, extends from the peripheral tissue to the brainstem or spinal cord depending if the

primary neuron innervates the face or the body, respectively. This is where a topical stimulus can be applied to the cornea to start a signaling cascade. The primary neuron synapses on a secondary neuron located in a brainstem nucleus or spinal cord. This secondary neuron has an axon that ascends to the thalamus to synapse on a tertiary neuron present in the Ventral Posterior Medial (Nosedá & Burstein, 2013) or Ventral Posterior Lateral (Mertens et al., 2015) nucleus dependent on the primary neuron innervating the face or the body, respectively. Finally, the thalamic neuron synapses on a fourth order neuron in the primary sensory cortex of the brain. The peripheral noxious stimulus will be interpreted cognitively in the cortex as pain (Mertens et al., 2015; Nosedá & Burstein, 2013). At the same time, interneurons in the brainstem or spinal cord produce a fast noxious reflexive response before a full painful interpretation is made (Rossignol et al., 2006). This reflexive nocifensive response is an attempt to eliminate the noxious stimulus before it can cause any harm.

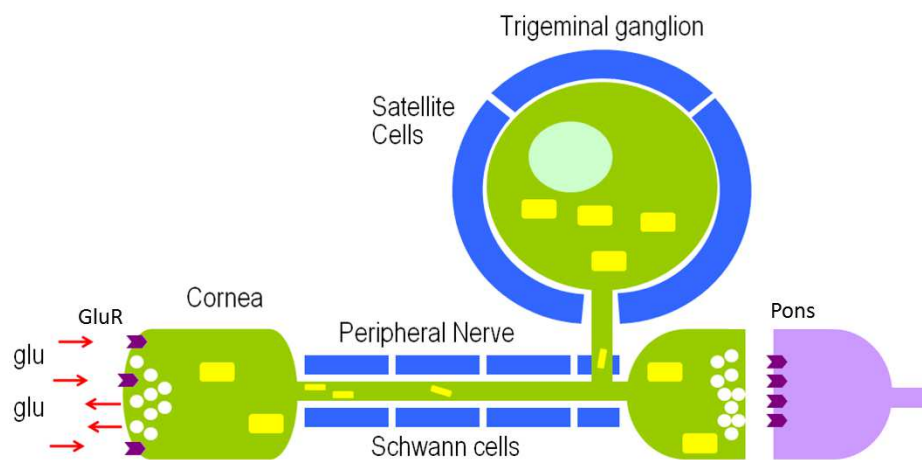


Figure 1.1: Primary sensory afferent in the cornea.

1.3: Glutamate as a neurotransmitter: L-glutamate is the major excitatory neurotransmitter within vertebrates (Miller, Hoffman, Sutharshan, & Schechter, 2011). Once bound to a Glutamate receptor (GluR), a conformational change of the receptor will occur

producing an influx and efflux of ions disrupting the basal, electrochemical balance (Greger, Ziff, & Penn, 2007). If the response is large enough, the neuronal membrane will depolarize to produce an action potential through its axon to signal for neurotransmitter, e.g., glutamate, release into the postsynaptic cleft (Greger et al., 2007). Release of glutamate has the potential to signal the postsynaptic neuron to trigger an action potential.

1.4: Glutamate synthesis: Glutamate is the conjugate base of the amino acid glutamic acid. Glutamic acid is a non-essential amino acid owing to cells being able to synthesize glutamate from glutamine (Miller et al., 2012). Glutamine is a non-essential amino acid under normal conditions, but also is a conditionally essential amino acid when an individual is critically ill. During this critically ill, or stressed state, the individual will require an external source of glutamine to meet the requirements of the body (Lacey & Wilmore, 1990). In the nervous system, a constant store of glutamine, the substrate for glutamate synthesis, is present from the supporting cells, such as astrocytes and Schwann cells, so that neurons will have replenishment of glutamate following synaptic exocytosis (Miller et al., 2011).

As seen in figure 1.2, Glutamine (Gln), stored in the glial cells, can be released for presynaptic neuronal uptake (Popoli, Yan, McEwen, & Sanacora, 2012). Once in the presynaptic neuron, the catalyzing enzyme glutaminase will perform glutaminolysis by hydrolysis of the amide group of glutamine (Miller et al., 2011). This will produce glutamic acid which can convert to its conjugate base after deprotonation of a hydroxyl group, glutamate (Fazzari, Linher-Melville, & Singh, 2016). Glutamate is transported into the synaptic vesicles within the presynaptic neuron by the vesicular glutamate transporter (vGluT) (Miller et al., 2011). Once glutamate is in the synaptic vesicle, the presynaptic neuron can synaptically release, i.e., exocytose, glutamate into the synaptic cleft. At this time, the glutamate can bind to and trigger a conformational change of glutamate receptors on the post synaptic neuron causing membrane

depolarization and action potential production in the secondary neuron. Glutamate is recycled back into the Schwann or satellite cells by cell membrane glutamate transporters. Glutamate is converted back into glutamine by the enzyme glutamine synthetase (Miller et al., 2011) to continue the cycle between glutamine and glutamate.

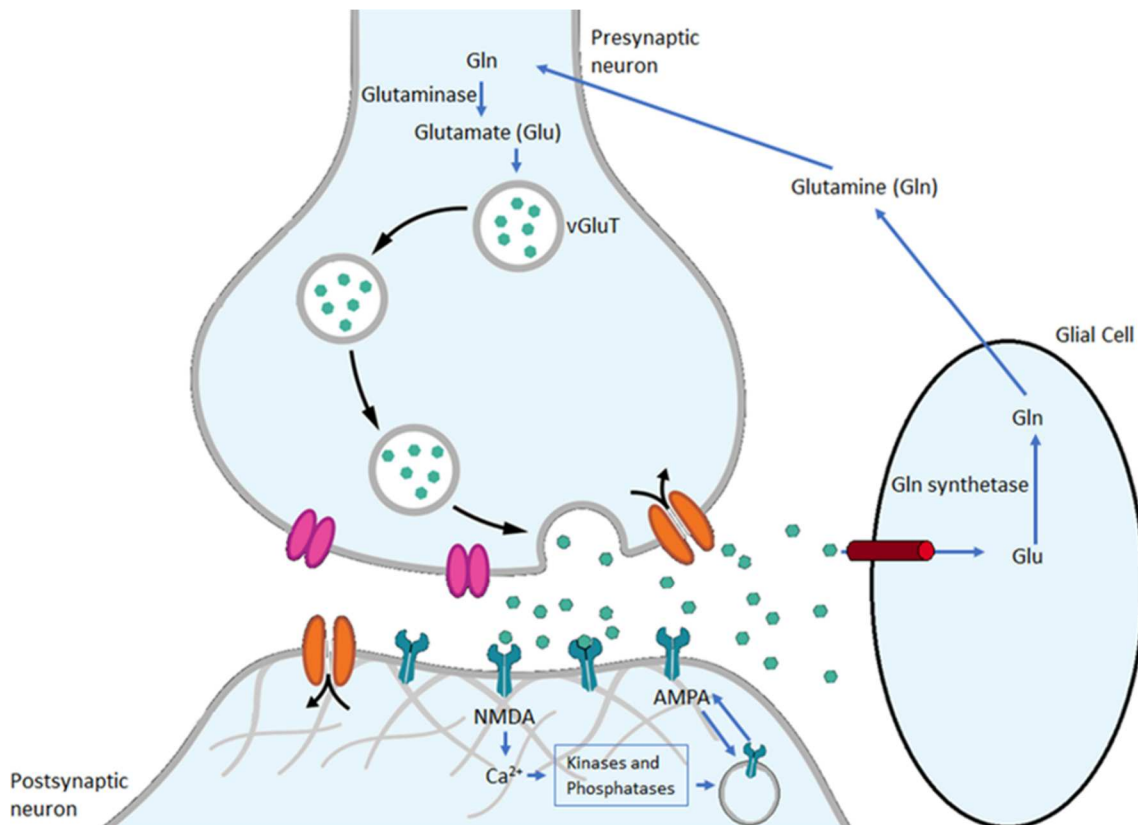


Figure 1.2: Postsynaptic neurotransmitter interactions. (Adapted from Thomas Spletstoeser (www.scistyle.com) - Own work, CC BY-SA 4.0, <https://commons.wikimedia.org/w/index.php?curid=41349083>)

1.5 Glutamate receptors: Ionotropic glutamate receptors (iGluRs) are present in the postsynaptic neurons for regulation of neuronal depolarization and subsequent generation of action potentials (Mayer, 2005b). These iGluRs are also present on the peripheral tissue epithelium and the peripheral nerve terminals of primary afferents (Hatziefthimiou, Gourgoulianis, & Molyvdas, 2002). Currently, there are three recognized iGluRs known in vertebrates: α -amino-3-hydroxy-5-methyl-4-isoxazolepropionic acid receptor (AMPAr), Kainate receptor, and N-Methyl-D-aspartic

acid receptor (NMDAr) (Bleakman et al., 2006). A fourth type of iGluR, the Delta receptor, recently has been described and is currently undergoing characterization (Miyoshi et al., 2014; Yuzaki & Aricescu, 2017). The AMPA, Kainate, and NMDA receptors are all tetramers (Bleakman et al., 2006; Mayer, 2005b), as seen in figure 1.3, meaning four separate subunits combine to make a functional receptor (Popoli et al., 2012). These receptors can all be either heterotetramers, meaning that more than one receptor subtype produce a receptor, or homotetramers, which means that four of the same type of subunit produce a functional receptor (Bleakman et al., 2006).

Even though AMPA, Kainate, and NMDA subunits are all iGluRs, a functional receptor can only be formed when four subunits combine within their respective type. AMPA receptors can also form homotetramers by dimerizing two dimers that both consist of the same type of subunits (Greger et al., 2007). Some of the combinations of AMPA subunits may not be fully functional, so receptor subunit expression is tightly controlled and specific combinations on the cellular membrane will be present (Coleman et al., 2010).

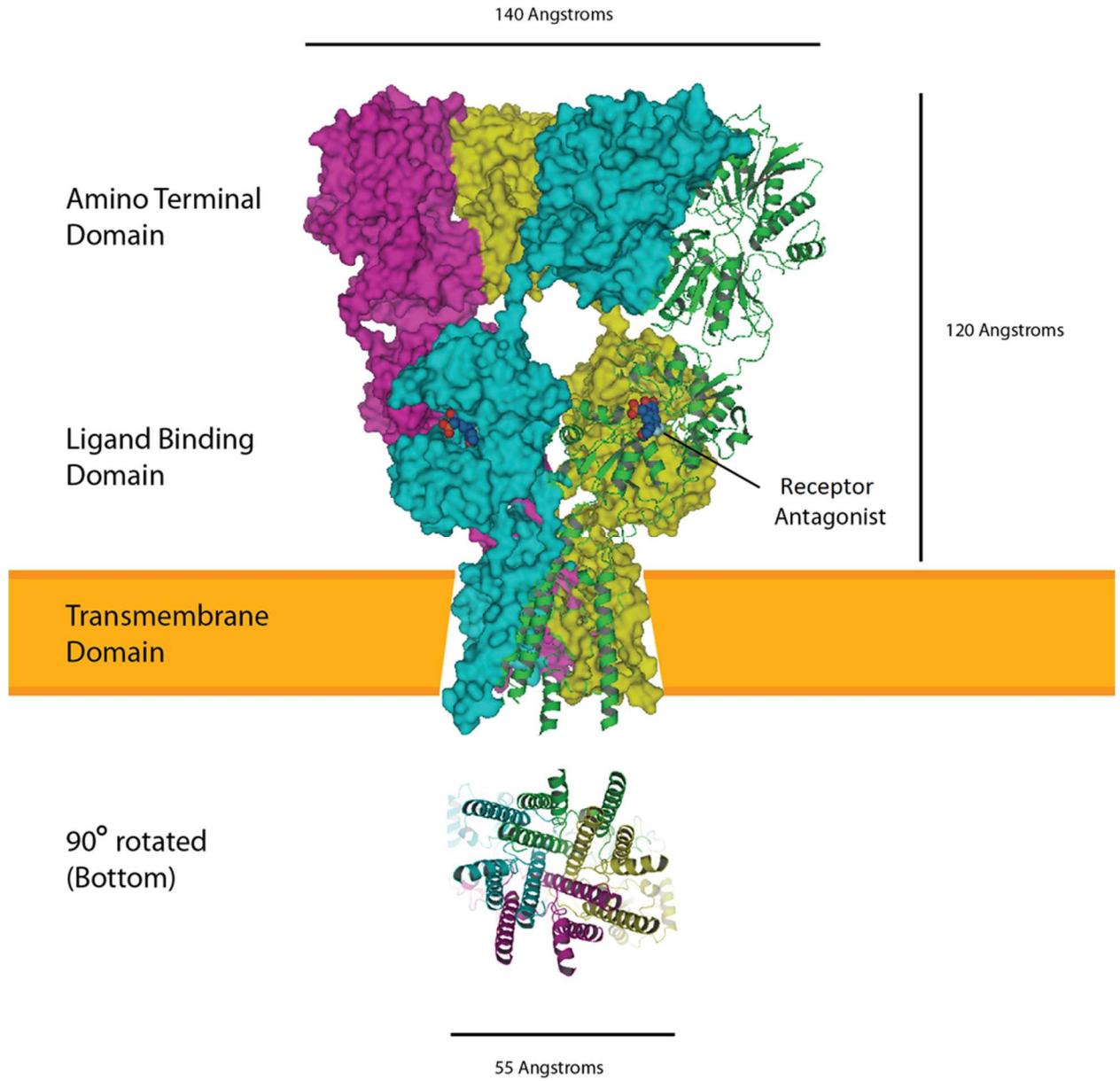


Figure 1.3: Conformation of the glutamate receptor before (Left) and after (Right) a conformational change.

Represented by the GluN1–GluN2B NMDA receptor. (By Curtis Neveu - Own work, CC BY-SA 3.0,

<https://commons.wikimedia.org/w/index.php?curid=16583388>)

NMDA	AMPA	Kainate	Delta
NR1 = GluN1	GluRA = GluR1 = GluA1	GluR5 = GLUK5 = GluK1	δ 1 = GluD1
NR2A = GluN2A	GluRB = GluR2 = GluA2	GluR6 = GLUK6 = GluK2	δ 2 = GluD2
NR2B = GluN2B	GluRC = GluR3 = GluA3	GluR7 = GLUK7 = GluK3	
NR2C = GluN2C	GluRD = GluR4 = GluA4	KA1 = GLUK1 = GluK4	
NR2D = GluN2D		KA2 = GLUK2 = GluK5	
NR3A = GluN3A			
NR3B = GluN3B			

Table 1.2: Nomenclature of the glutamate receptor subunits.

1.6 AMPA receptors: AMPA receptors can be present in the form of homotetramers or heterotetramers, increasing the diversity in the construct of a functioning AMPA receptor (Greger et al., 2007; Mayer, 2005b). The AMPA receptors have four subunits that include GluA1, GluA2, GluA3, and GluA4 (Greger et al., 2007). In the vertebrate nervous system, there appears to be a limit to subunit combinations (Traynelis et al., 2010). Our current knowledge indicates that two of the four AMPA subunits dimerize, then, when forming a heterotetramer, form as a dimer of dimers (Greger et al., 2007). These dimers will then dimerize with another dimer to form a functional receptor with four subunits.

A normally activated AMPA receptor will allow some calcium through the pore along with sodium from the extracellular space to intracellular (Traynelis et al., 2010). An exception to this rule is that the AMPA receptors can further increase diversity by substituting one amino acid for another to decrease calcium permeability (Traynelis et al., 2010). The Glutamine (Q) to Arginine (R) substitution that resides in the pore loop of the receptor dramatically reduces the calcium permeability of receptors containing modified GluA2 subunits (Greger et al., 2007). Furthermore, the GluA2-4 subunits can go through a Glycine (G) to Arginine (R) replacement in the ligand binding domain (LBD) that will allow for a quicker recovery of the receptor after depolarization (Lomeli et al., 1994).

Another way that the AMPA receptors increase their diversity is by the production of two splicing variations called Flip and Flop (Pachernegg, Munster, Muth-Kohne, Fuhrmann, & Hollmann, 2015; Y. H. Park et al., 2016; Pei et al., 2009). The flip/flop splicing site of the AMPAR subunits (Krampfl et al., 2002; Lomeli et al., 1994; Pachernegg et al., 2015; Pei et al., 2009) is found in the C-terminal loop between TMIII and TMIV (Greger et al., 2007). When spliced at the flip/flop site, only one of the two 115 base pair long sequences will be expressed (Pachernegg et al., 2015). The overall kinetics of the receptor show that the flip splice variant is activated faster and the desensitization of the receptors containing these subunit splice variants will be about four times slower than the flop splice variant (Pachernegg et al., 2015; Pei et al., 2009).

The type of AMPAR subunits present in a nerve terminal can help determine the roles they have during persistent, or chronic, pain (Latremoliere & Woolf, 2009; Tao, 2012). Central sensitization occurs as increased responsiveness of a second order, nociceptive neuron (Woolf & Salter, 2000). When NMDA receptors are activated postsynaptically, an increase influx of calcium activates protein kinase enzymes, protein kinase C (PKC), Ca²⁺/calmodulin-dependent protein kinase (CaMKII), protein kinase A (PKA), and extracellular signal-regulated kinases (ERK), that phosphorylate the GluA2 containing AMPA receptors and, in turn, causes endocytosis of the receptors. Furthermore, intracellular GluA1 containing AMPA receptors stored on vesicles will also become phosphorylated allowing them to be inserted into the membrane, replacing the GluA2 AMPAR. This allows for a much higher calcium influx further activating additional protein kinase pathways. These kinases produce phosphorylation of the scaffolding protein stargazin, increasing its affinity to postsynaptic density-95 (PSD-95), an auxiliary protein, and modifying its ectodomain (Latremoliere & Woolf, 2009). This allows for

an increased affinity of the GluA1 receptor subunit for glutamate and allows for higher channel opening probability to further increase the calcium influx (Latremoliere & Woolf, 2009).

1.7 Kainate receptors: Kainate receptors consist of the subunits GluK1-5 and are also present as homotetramers and heterotetramers similar to AMPA and NMDA receptors (Bleakman et al., 2006), but not all of the Kainate receptor subunits can form homotetramers. The GluK1-3 receptor subunits can form homotetramers as well as heterotetramers. The GluK4 and GluK5 subunits are only found in a heterotetrameric conformation and they need to form a heterotetramer with the GluK1-3 subunits (Mollerud, Frydenvang, Pickering, & Kastrup, 2017). The Kainate receptors are located both on pre-and post-synaptic terminals, whereas AMPA receptors are commonly located in post synaptic terminals only (Mollerud et al., 2017). Furthermore, the Kainate receptor subunits GluK4 and GluK5 have been shown to undergo a glutamine (Q) to an arginine (R) post-translational site editing causing a reduction in calcium permeability (Burnashev, Zhou, Neher, & Sakmann, 1995) similar to the AMPA receptors.

The Kainate receptor binding domain of the GluK1 and GluK2 subunits have been described as 40% and 16% larger when compared to the GluA2 subunit (Mayer, 2005a). The larger volume of these Kainate receptor subunit binding domains allows for additional water molecules to become attached to the ligand binding domain (LBD) (Mayer, 2005a). Once the ligand glutamate comes into contact with the LBD, water molecules are displaced and an additional 11° greater domain closure of the GluK2 occurs, compared to the GluA2 subunit (Mayer, 2005a). This corresponds with the greater efficacy for ion gating that is seen by the Kainate receptors (Mayer, 2005a) as compared to the AMPA and NMDA receptors.

Kainate receptor subunits have differing structural characteristics and responses when a ligand binds to the Kainate subunit LBD as compared to the AMPA subunit LBD. For example, Kainate receptors have a strong affinity for the specific ligand, Kainic acid, which causes a rapid

desensitization of the Kainate receptor but a nondesensitizing response at the AMPA receptors (Fleck, Cornell, & Mah, 2003; Patneau, Vyklicky, & Mayer, 1993). Furthermore, Kainate receptors recover from desensitization much slower than AMPA receptors (Fleck et al., 2003). Splice variation and RNA editing also occur for Kainate receptors to greatly increase variability similar to AMPA receptors (Bleakman et al., 2006). Lastly, Kainate receptors seem to play a key role in some diseases including epilepsy, schizophrenia, depression and bipolar disorder (Das et al., 2012; Ibrahim et al., 2000; Pickard et al., 2006).

1.8 NMDA receptors: NMDA receptors occur as homotetramers and heterotetramers similar to that of the AMPA and Kainate receptors (Bleakman et al., 2006). There currently are seven NMDA receptor subunits which include GluN1, GluN2A-D, and GluN3A-B, (Bleakman et al., 2006). A major difference between NMDA receptors and the AMPA and Kainate receptors is that two GluN1 subunits are required to be present in all functional NMDA receptors.

Additionally, these receptor subunits bind coagonists glycine or D-serine (Balu & Coyle, 2015; Mothet, Le Bail, & Billard, 2015). This provides additional complexity to the NMDA receptors since glutamate and a coagonist must be present to trigger a conformational change in the receptor. Furthermore, the GluN3A-B receptor subunits also use glycine or D-serine as a coagonist (Traynelis et al., 2010; Yao & Mayer, 2006). To form a functional GluN3 containing NMDA receptor, a GluN2 and 2 GluN1 subunits need to be present (Traynelis et al., 2010).

NMDA receptors are unique from AMPA and Kainate receptors by having a basal, magnesium channel block preventing the flow of ions until it has been dislodged from the receptor (Mayer, Westbrook, & Guthrie, 1984; Nowak, Bregestovski, Ascher, Herbet, & Prochiantz, 1984). The magnesium block plays a large role in central sensitization by preventing calcium influx until proper membrane depolarization, often by GluA2 containing AMPA receptors (Latremoliere & Woolf, 2009). Once membrane depolarization occurs, magnesium is

dislodged allowing the influx of calcium ions through the NMDA receptor. The increased Ca^{++} will lead to the phosphorylation of GluA2 to cause a switching, endocytosis, of GluA2 containing AMPA receptors to GluA1 containing receptors (Latremoliere & Woolf, 2009) as previously described during central sensitization.

Splice variants also are present for GluN1, further increasing the diversity of NMDA receptors (Bleakman et al., 2006; Dingledine, Borges, Bowie, & Traynelis, 1999). The GluN1 splice variants can be full length, missing exon 21, missing exon 22, or missing both and are represented as GluN1-1, GluN1-2, GluN1-3, GluN1-4, respectively (Dingledine et al., 1999). Furthermore, each of these splice variants can be further classified by inclusion or exclusion of exon 5 (Dingledine et al., 1999).

1.9 Delta Receptors: Delta receptors are currently classified as glutamate receptors due to their similarity to the other three iGluRs, but they are not activated by glutamate (Miyoshi et al., 2014). The delta receptors have two subunits, GluD1 and GluD2, coded by the GRID2 gene (Miyoshi et al., 2014). The delta receptors will not be studied in our analysis. A complete summary of the iGluR nomenclature is present in table 1.2.

1.10 Corneal Structure: The cornea is a transparent and avascular tissue that allows light to enter the eye for the retina (Parekh, Ferrari, Sheridan, Kaye, & Ahmad, 2016). The cornea consists of five main layers including the epithelial cell layer, Bowman's layer, corneal stroma, Descemet's layer, and endothelial cell layer. The corneal epithelium is stratified squamous epithelium. It consists of four to six cell layers in the human and is about 50 μm thick (Eghrari, Riazuddin, & Gottsch, 2015) as seen in figures 1.4. The corneal epithelium is the outermost cellular layer and is directly exposed to external irritants such as dust, chemicals, etc. The large number of tight junctions between corneal epithelial cells (Eghrari et al., 2015) helps to prevent adverse substances from crossing the epithelium to gain access to deeper corneal

structures. Under the epithelial layer is Bowman's layer. Bowman's layer is present in many species, but no major role has been found other than being the basement membrane of the corneal endothelial cells (Wilson & Hong, 2000). The stromal layer resides under Bowman's layer as seen in Fig. 1.4. The stromal layer consists of about 90% of the thickness of the cornea, consisting of extra-cellular matrix proteins secreted by the epithelial and endothelial cells. The stroma has a key role of visual function due to the regular organization pattern of the collagen layers allowing for optimal passage of light (Xuan et al., 2016). The endothelial cells are the innermost layer of the cornea and Descemet's membrane is the basement membrane for the endothelial cells (Parekh et al., 2016). The endothelial cells of the cornea have an incomplete zona occludens which allows nutrients to enter the cornea from the aqueous humor and allows water from the cornea to move towards the aqueous humor to keep the cornea slightly dehydrated to improve its transparency (Parekh et al., 2016).

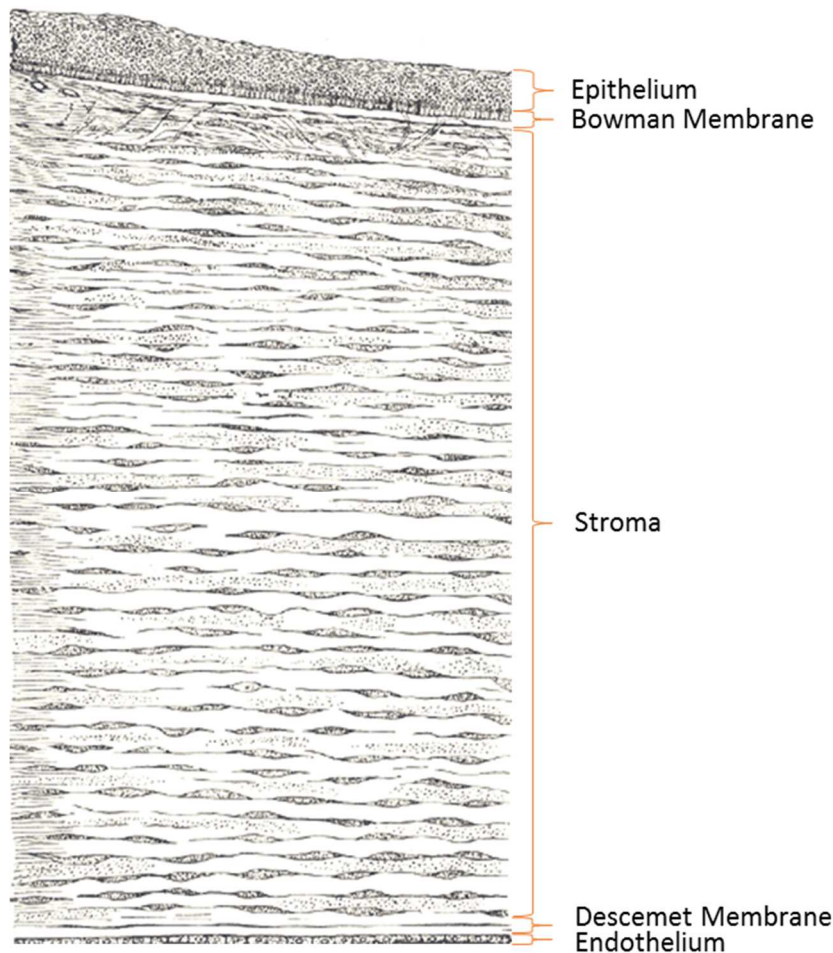


Figure 1.4: Corneal layers (By Henry Vandyke Carter - Henry Gray (1918) Anatomy of the Human Body (See "Book" section below)Bartleby.com: Gray's Anatomy, Plate 871, Public Domain, <https://commons.wikimedia.org/w/index.php?curid=566809>)

1.11: Corneal innervation: The cornea is innervated by the ophthalmic division of the trigeminal nerve (Cranial Nerve V₁) (Marfurt & Del Toro, 1987). As seen in figure 1.5, the ophthalmic division of the trigeminal nerve enters the stroma and primary sensory afferents branch to innervate the corneal epithelium (Chan-Ling, 1989). The peripheral portion of the corneal epithelium is more highly innervated than the central (He, Bazan, & Bazan, 2010). Although glutamate and glutaminase have been reported in corneal afferent fibers (Miller & Ibitokun, 2011), there is a lack of knowledge about glutamate receptor subunit distribution in the corneal epithelium.

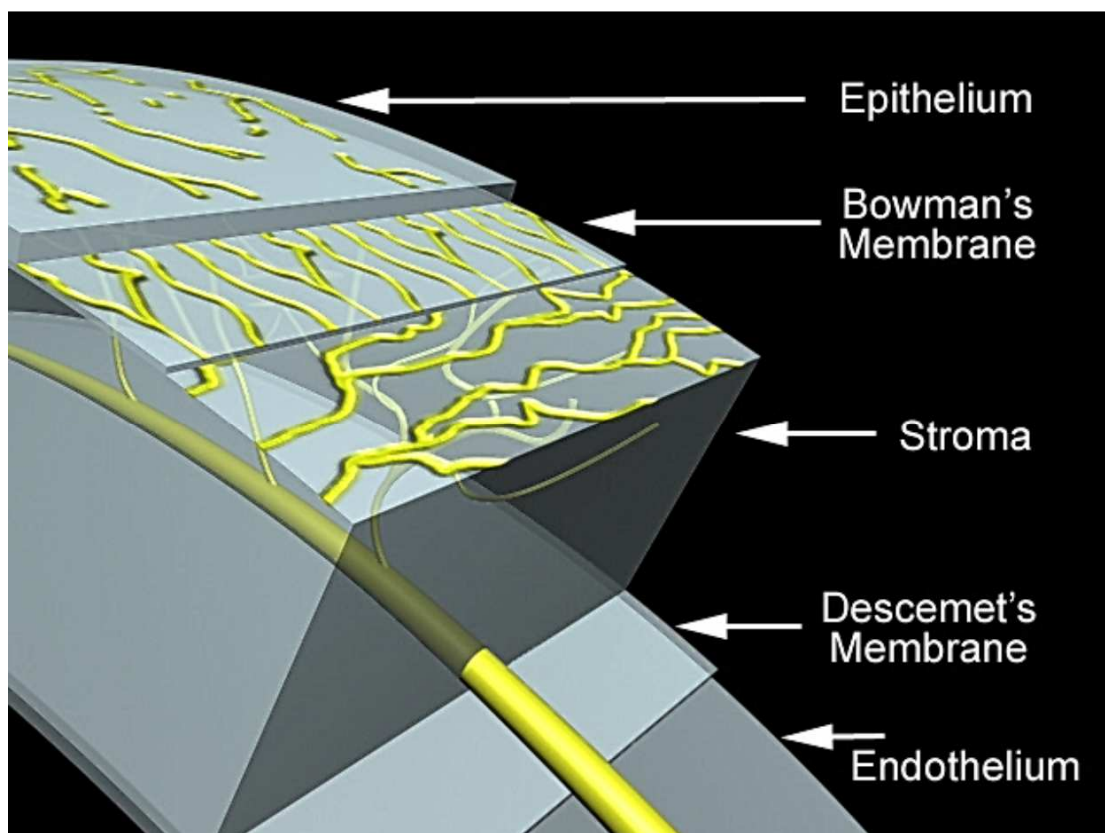


Figure 1.5: Sensory innervation of the cornea from the ophthalmic division of the trigeminal nerve.

1.12: Glutamate in the Cornea: Glutamate is an effective agonist of iGluRs in the rat cornea. Although the corneal epithelial cells are held together by many tight junctions, topical application of glutamate is very effective at inducing a nocifensive response. In figure 1.6, the behavioral response, blinking, wiping, shaking, of Sprague Dawley rats is displayed when glutamate is introduced to the cornea in a topical solution. In figure 1.7, the glutamate dose response and the median effective dose (ED_{50}) is presented (Ibitokun, 2012). The ED_{50} for glutamate-induced nocifensive responses was determined to be 0.5 M. Compared to the CNS, the high concentration of glutamate needed to induce an effective response is due to the tissue organization of the cornea, i.e., multiple cell layers and tight junctions. Since the topical solution of glutamate is applied directly to the eye, glutamate molecules reach the iGluRs by diffusion. In

addition, there is a thin layer of lubricating fluid, known as tear film, on the eye surface that dilutes the glutamate solution once applied.

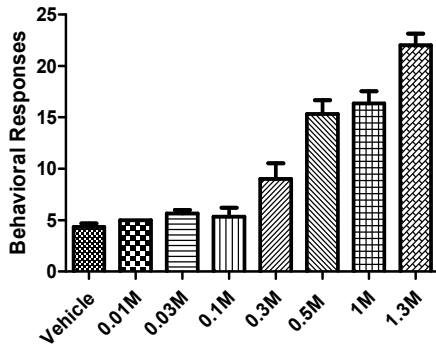


Figure 1.6. Glutamate dose response study. (From (Ibitokun, 2012))

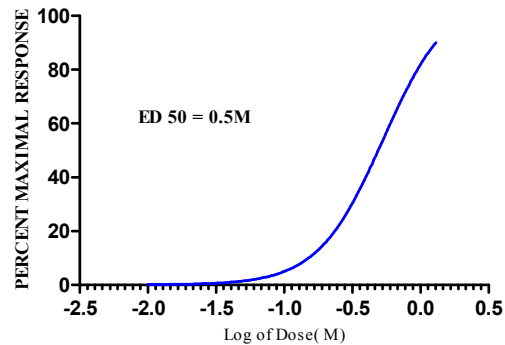


Figure 1.7. Glutamate dose response curve. (From (Ibitokun, 2012))

1.13: Glutamate receptor agonists: AMPA and Kainate are effective agonists of their respective iGluRs in the rat cornea. In our lab, AMPA and Kainate were applied to the rat cornea and the nocifensive response to these agonists is demonstrated in figures 1.8 and 1.9, respectively (Ibitokun, 2012). In figure 1.8 a topical application of AMPA was applied to the cornea and the ED₅₀ was determined to be 0.5mM. In figure 1.9, a topical application of kainate was applied to the cornea and the ED₅₀ was ascertained to be 0.1mM. This further supports that various shape and sizes of molecules can diffuse through the corneal epithelium to gain access to the sensory peripheral afferents.

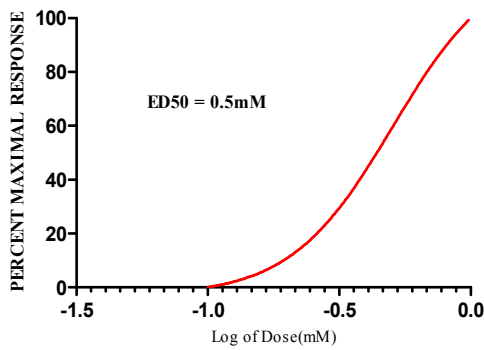


Figure 1.8. AMPA dose response curve.
(From (Ibitokun, 2012))

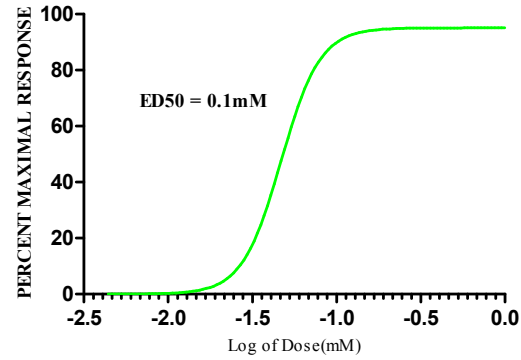


Figure 1.9. Kainate dose response curve.
(From (Ibitokun, 2012))

1.14: Glutamate receptor antagonists: Antagonists of iGluR can be used to prevent activation of iGluRs to elicit action potentials (Alt et al., 2004). These iGluR antagonists include, but are not limited to: DNQX (Fedele & Raiteri, 1996; Lund et al., 2010), NBQX (Alt et al., 2004; Dolman et al., 2005), and GYKI 53655 as AMPA/Kainate antagonists (Bleakman et al., 1996; Bleakman, Ogden, Ornstein, & Hoo, 1999), LY382884 as a Kainate antagonist (Alt et al., 2004), and AP5 as an NMDA antagonist (Lund et al., 2010). These iGluR antagonists competitively inhibit the iGluR by attaching to the ligand binding site making it less likely that the agonist, a glutamate molecule, will bind (Alt et al., 2004). By decreasing the likelihood of the iGluR activation, a reduction of nocifensive behavior can be observed and analyzed to determine the effectiveness of the antagonist (Bonnet et al., 2015).

1.15: Glutamate subunit presence in the cornea: Immunohistochemistry supports the presence of NMDA receptors within the cornea. We have evaluated the presence of NMDA receptors using whole mounts and sagittal sections from the rat cornea (Ibitokun, 2012). Figure 1.12 represents the immunoreactivity of corneal epithelial cells for GluN1 (NMDA subunit) demonstrated by the white arrows. The yellow arrows illustrate the immunoreactive granules that

are found within the nuclei and cell membranes of corneal epithelial cells. In figure 1.13, the white arrows represent the immunoreactivity of GluN1 on the corneal epithelial nerve fibers. This supports the hypothesis that the NMDA receptors are present in the cornea, but other specific NMDA subunits have not been studied. Furthermore, double labeling of NMDA subunits with nerve fiber specific proteins, e.g., peripherin, protein gene product 9.5, beta tubulin, have not been conducted.

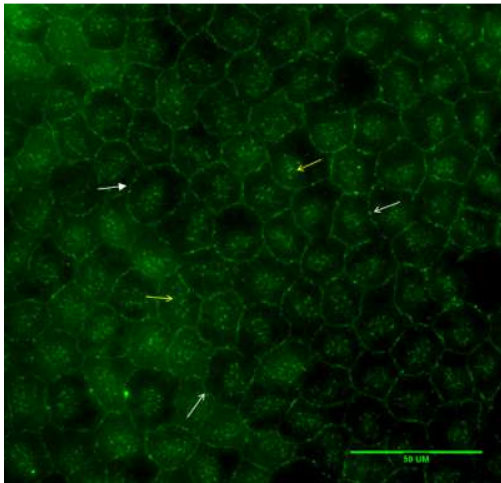


Figure 1.10. NMDA GluN1 immunoreactivity in cornea (whole mount). Corneal epithelial cell membranes are immunoreactive for NMDA GluN1 (white arrows), as well as scattered GluN1 immunoreactive granules within the nucleus (yellow arrows). (From (Ibitokun, 2012))

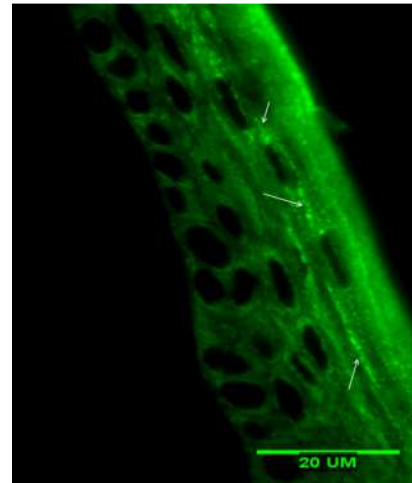


Figure 1.11. NMDA GluN1 immunoreactivity in the rat cornea (10μm sagittal section). NMDA GluN1 immunoreactivity was observed on corneal epithelial nerve fibers (white arrows). These corneal afferent nerve fibers exhibited varicosities and traveled between the superficial corneal epithelial cells. (From (Ibitokun, 2012))

Immunohistochemistry supports the presence of AMPA receptors in the cornea. We have evaluated the presence of AMPA receptors using whole mount and sagittal sectioned corneas (Ibitokun, 2012). Figure 1.12 represents the whole mount immunoreactivity of AMPA GluA1 receptor subunits represented by the white arrows. In figure 1.13, the white arrows demonstrate the GluA2/3 immunoreactivity within the cytoplasm of the corneal epithelial cells and the yellow arrows illustrate the immunoreactivity of GluA2/3 subunits around the nuclei of the epithelial

cells. This supports the hypothesis that AMPA receptors are present within the rat cornea, but the evaluation of other specific AMPA subunits is still understudied. Furthermore, the neuronal innervation associated with the AMPA receptors composition is lacking and can be further explained by double or triple labeling AMPA subunits alongside nerve fiber specific proteins (Ibitokun, 2012).

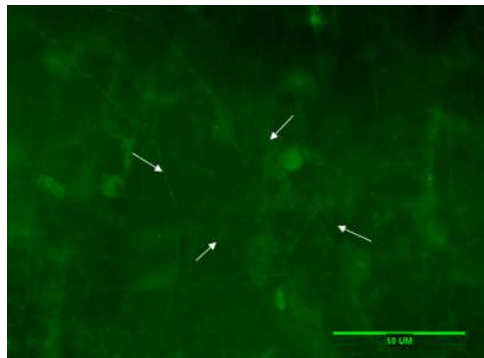


Figure 1.12. AMPA GluA1 immunoreactivity in cornea (whole mount). The cornea shows GluA1 immunoreactivity in the subepithelial nerve plexus as indicated by the white arrows. (From (Ibitokun, 2012))

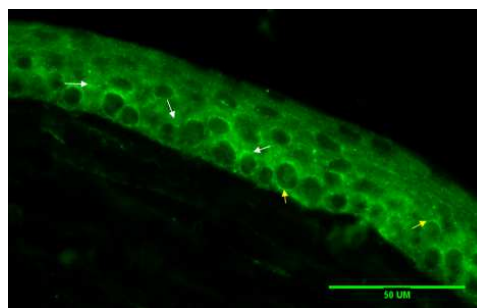


Figure 1.13. AMPA GluA2/3 immunoreactivity in the rat cornea (10μm sagittal section). GluA2/3 immunoreactivity occurred in corneal epithelial cells. The distribution is mainly within the cytoplasm (white arrows) of the epithelial cells with a clustering around the nucleus (yellow arrows). (From (Ibitokun, 2012))

1.16: Animal Research: Reporting of In Vivo Experiments (ARRIVE) Guidelines:

To increase the quality of reporting preclinical trials, a set of standardized guidelines can be used. A set of guidelines commonly accepted for preclinical trials within a wide range of journals is called the Animal Research: Reporting In Vivo Experiments (ARRIVE) Guidelines (Kilkenny, Browne, Cuthill, Emerson, & Altman, 2010). These guidelines were published in Plos Biology in 2010 to help standardize scientific reporting. Many journals have adopted the use of the ARRIVE guidelines to aid in the efforts to increase the quality of reporting. The ARRIVE guidelines are meant to be used during the process of constructing a study, but many

investigators encounter ARRIVE guidelines after the completion or initiation of research study and apply their study to the guidelines rather than applying the guidelines to their study.

Preclinical trials in their current state have consistently underutilized the ARRIVE Guidelines (Baker, Lidster, Sottomayor, & Amor, 2014; Karp et al., 2015; Kilkenny et al., 2010). To increase the reporting of the standards set by the ARRIVE guidelines, in the current study we aim to identify the components that are lacking within the Excitatory Amino Acid Receptor (EAAR) literature, which includes the iGluR literature, so we can apply that knowledge to future preclinical trials. Figure 1.14 and 1.15 represents the first and second half ARRIVE guidelines with all of its components and descriptions, respectively.



The ARRIVE Guidelines Checklist

Animal Research: Reporting In Vivo Experiments

Carol Kilkenny¹, William J Browne², Innes C Cuthill³, Michael Emerson⁴ and Douglas G Altman⁵

¹The National Centre for the Replacement, Refinement and Reduction of Animals in Research, London, UK, ²School of Veterinary Science, University of Bristol, Bristol, UK, ³School of Biological Sciences, University of Bristol, Bristol, UK, ⁴National Heart and Lung Institute, Imperial College London, UK, ⁵Centre for Statistics in Medicine, University of Oxford, Oxford, UK.

	ITEM	RECOMMENDATION	Section/ Paragraph
Title	1	Provide as accurate and concise a description of the content of the article as possible.	
Abstract	2	Provide an accurate summary of the background, research objectives, including details of the species or strain of animal used, key methods, principal findings and conclusions of the study.	
INTRODUCTION			
Background	3	<ul style="list-style-type: none"> a. Include sufficient scientific background (including relevant references to previous work) to understand the motivation and context for the study, and explain the experimental approach and rationale. b. Explain how and why the animal species and model being used can address the scientific objectives and, where appropriate, the study's relevance to human biology. 	
Objectives	4	Clearly describe the primary and any secondary objectives of the study, or specific hypotheses being tested.	
METHODS			
Ethical statement	5	Indicate the nature of the ethical review permissions, relevant licences (e.g. Animal [Scientific Procedures] Act 1986), and national or institutional guidelines for the care and use of animals, that cover the research.	
Study design	6	<p>For each experiment, give brief details of the study design including:</p> <ul style="list-style-type: none"> a. The number of experimental and control groups. b. Any steps taken to minimise the effects of subjective bias when allocating animals to treatment (e.g. randomisation procedure) and when assessing results (e.g. if done, describe who was blinded and when). c. The experimental unit (e.g. a single animal, group or cage of animals). A time-line diagram or flow chart can be useful to illustrate how complex study designs were carried out. 	
Experimental procedures	7	<p>For each experiment and each experimental group, including controls, provide precise details of all procedures carried out. For example:</p> <ul style="list-style-type: none"> a. How (e.g. drug formulation and dose, site and route of administration, anaesthesia and analgesia used [including monitoring], surgical procedure, method of euthanasia). Provide details of any specialist equipment used, including suppliers). b. When (e.g. time of day). c. Where (e.g. home cage, laboratory, water maze). d. Why (e.g. rationale for choice of specific anaesthetic, route of administration, drug dose used). 	
Experimental animals	8	<ul style="list-style-type: none"> a. Provide details of the animals used, including species, strain, sex, developmental stage (e.g. mean or median age plus age range) and weight (e.g. mean or median weight plus weight range). b. Provide further relevant information such as the source of animals, international strain nomenclature, genetic modification status (e.g. knock-out or transgenic), genotype, health/immune status, drug or test naïve, previous procedures, etc. 	

The ARRIVE guidelines. Originally published in *PLoS Biology*, June 2010¹

Figure 1.14: The first half of the ARRIVE guidelines describing the recommended components of an animal research manuscript. (From (Kilkenny et al., 2010))

Housing and husbandry	9	Provide details of: a. Housing (type of facility e.g. specific pathogen free [SPF]; type of cage or housing; bedding material; number of cage companions; tank shape and material etc. for fish). b. Husbandry conditions (e.g. breeding programme, light/dark cycle, temperature, quality of water etc for fish, type of food, access to food and water, environmental enrichment). c. Welfare-related assessments and interventions that were carried out prior to, during, or after the experiment.	
Sample size	10	a. Specify the total number of animals used in each experiment, and the number of animals in each experimental group. b. Explain how the number of animals was arrived at. Provide details of any sample size calculation used. c. Indicate the number of independent replications of each experiment, if relevant.	
Allocating animals to experimental groups	11	a. Give full details of how animals were allocated to experimental groups, including randomisation or matching if done. b. Describe the order in which the animals in the different experimental groups were treated and assessed.	
Experimental outcomes	12	Clearly define the primary and secondary experimental outcomes assessed (e.g. cell death, molecular markers, behavioural changes).	
Statistical methods	13	a. Provide details of the statistical methods used for each analysis. b. Specify the unit of analysis for each dataset (e.g. single animal, group of animals, single neuron). c. Describe any methods used to assess whether the data met the assumptions of the statistical approach.	
RESULTS			
Baseline data	14	For each experimental group, report relevant characteristics and health status of animals (e.g. weight, microbiological status, and drug or test naïve) prior to treatment or testing. (This information can often be tabulated).	
Numbers analysed	15	a. Report the number of animals in each group included in each analysis. Report absolute numbers (e.g. 10/20, not 50%). b. If any animals or data were not included in the analysis, explain why.	
Outcomes and estimation	16	Report the results for each analysis carried out, with a measure of precision (e.g. standard error or confidence interval).	
Adverse events	17	a. Give details of all important adverse events in each experimental group. b. Describe any modifications to the experimental protocols made to reduce adverse events.	
DISCUSSION			
Interpretation/scientific implications	18	a. Interpret the results, taking into account the study objectives and hypotheses, current theory and other relevant studies in the literature. b. Comment on the study limitations including any potential sources of bias, any limitations of the animal model, and the imprecision associated with the results. c. Describe any implications of your experimental methods or findings for the replacement, refinement or reduction (the 3Rs) of the use of animals in research.	
Generalisability/translation	19	Comment on whether, and how, the findings of this study are likely to translate to other species or systems, including any relevance to human biology.	
Funding	20	List all funding sources (including grant number) and the role of the funder(s) in the study.	



References:

1. Kilkenny C, Browne WJ, Cuthill IC, Emerson M, Altman DG (2010) Improving Bioscience Research Reporting: The ARRIVE Guidelines for Reporting Animal Research. *PLoS Biol* 8(6): e1000412. doi:10.1371/journal.pbio.1000412
2. Schulz KF, Altman DG, Moher D, the CONSORT Group (2010) CONSORT 2010 Statement: updated guidelines for reporting parallel group randomised trials. *BMJ* 340:c332.

Figure 1.15: The second half of the ARRIVE guidelines describing the recommended components of an animal research manuscript. (From (Kilkenny et al., 2010))

1.17: Prospective implementations: Many previous experiments have used AMPA, Kainate, and NMDA receptor antagonists injected into tissue to test their effectiveness and examine if these antagonists can access peripheral receptors in the hind paw (J. S. Park et al., 2008), sciatic nerve (Gong, Kung, Magni, Bhargava, & Jasmin, 2014), and masseter (Lund et al., 2010). A missing element in this research on peripheral iGluRs is an examination of one of the most accessible tissues on the body, the cornea. Our study is novel in the sense that the treatment site is the direct application to the cornea. We also will use a iGluR antagonist that may be less selective when compared to other antagonists, but has a good chance of being effective in the cornea due to its low molecular weight. With this in mind, our study may yield a new pharmaceutical drug that can be easily applied to the cornea with a dropper. Furthermore, with a better understanding of the presence of the iGluR subunits in the cornea, more specific drugs can be used to target specific receptors that could have fewer side effects.

1.18: Hypotheses and Specific Aims:

Hypothesis for Aim 1: We hypothesize that the iGluRs can be antagonized with a topical application of the AMPA-kainate antagonist DNQX in the rat cornea.

Specific Aim 1: To behaviorally evaluate the effect of DNQX, a selective AMPA and Kainate GluR antagonist, with co-application of glutamate to the Sprague Dawley rat cornea. In this study, a comprehensive evaluation of the nocifensive responses to glutamate when DNQX is co-administered will be carried out. Nocifensive responses to be recorded include: eye blinking, eye wiping, and eye scratching. The effectiveness of the antagonist will be evaluated by conducting an analysis of variance (ANOVA).

Hypothesis for Aim 2: We hypothesize that specific iGluR subunits are present in the cornea and certain combinations of iGluR subunits contribute to the perception of pain of the cornea.

Specific Aim 2: To use Western blotting and immunohistochemical techniques to determine the presence and location of ionotropic GluR subunits within the Sprague Dawley rat cornea. In this study, Western blotting techniques and immunofluorescent imaging will be used to evaluate the specific subunits of iGluRs in relation to the corneal architecture. Localizing the specific iGluRs along with localizing nerve fibers will allow for a better understanding of the location, presence, and potential functionality of these iGluR subunits.

Hypothesis for Aim 3: We hypothesize that there is an underreporting of the ARRIVE guidelines, particularly in methods sections, in the EAAR literature.

Specific Aim 3: To evaluate Excitatory Amino Acid Receptor literature for the reporting of the ARRIVE guidelines components. In this study, the ARRIVE guidelines will be applied to the published EAAR literature. We will evaluate each of the ARRIVE guidelines to identify the components that are most severely underreported. This will allow for the proper reporting of results according to the ARRIVE guidelines for studies in our laboratory and hopefully other laboratories.

CHAPTER II

6,7-DINITROQUINOXALINE-2,3-DIONE (DNQX) AS A TOPICAL EXCITATORY AMINO ACID RECEPTOR ANTAGONIST OF CORNEAL EPITHELIUM: A BEHAVIORAL STUDY

Abstract

Introduction: 6,7-dinitroquinoxaline-2,3-dione (DNQX) is an AMPA/Kainate antagonist that is water soluble. The aim of this study was to determine the effectiveness of DNQX when topically applied to the Sprague Dawley rat cornea stimulated by glutamate.

Methods: A total of 36 rats were used to quantitatively evaluate the nocifensive behaviors. Glutamate, the ligand for AMPA and Kainate receptors, was used as the agonist. A co-administration of Glutamate/DNQX was used to determine the effectiveness of DNQX as a competitive antagonist when directly applied to the cornea. The Animal Research: Reporting of In Vivo Experiments (ARRIVE) guidelines were used in the writing of this manuscript.

Results: DNQX was shown to significantly ($p < 0.05$) antagonize the effects of glutamate in a dose dependent manner. The half maximal inhibitory concentration (IC₅₀) was determined as 1.18 μ M.

Discussion: DNQX could potentially be beneficial in alleviating ophthalmic pain when topically applied to the cornea.

1. Introduction

Ionotropic glutamate receptors (iGluR) are a class of receptors that are activated by glutamate (Johnson & Ascher, 1987; Kleckner & Dingledine, 1988), allowing for the flow of positively charged sodium and calcium ions to go from the exterior to interior cellular space (Dingledine et al., 1999; Traynelis et al., 2010). This influx of positively charged ions depolarizes neurons to trigger an intracellular cascade leading to an action potential (Latremoliere & Woolf, 2009; Miller et al., 2011; Tao, 2012; Woolf & Salter, 2000). While there is increasing research conducted in the central nervous system (CNS) (Zhuo, 2017), a better understanding of these iGluR is needed for peripheral tissues such as the cornea.

The iGluR are occur in four types: α -amino-3-hydroxy-5-methyl-4-isoxazolepropionic acid (AMPA) receptor, Kainate receptor, N-methyl-D-aspartate (NMDA) receptor, and Delta receptor. The AMPA, Kainate, NMDA, and Delta receptors are subdivided into 4 (GluA1-4), 5 (GluK1-5), 7 (GluNA, GluNB1-4, GluNC1-2), and 2 (GluD1-2) subunits (Bleakman et al., 2006; Dingledine et al., 1999; Traynelis et al., 2010). These subunits will typically dimerize within their class, then form a dimer of those dimers to form a functional heterotetramer (Sobolevsky, Yelshansky, & Wollmuth, 2004; Traynelis et al., 2010) that will be activated by glutamate. Coagonists, glycine or D-Serine, bind to GluN1, GluN3A, or GluN3B containing NMDA receptors (Johnson & Ascher, 1987; Kleckner & Dingledine, 1988; Traynelis et al., 2010).

The cornea is one of the most densely innervated tissues of the body (Eghrari et al., 2015; He et al., 2010) and glutamate receptors have been detected recently in the rat cornea (Ibitokun, 2012). Glutamate was determined to produce dose dependent nocifensive behaviors when applied to the rat cornea (Ibitokun, 2012). These results identified a need for receptor specific antagonists to be directly applied to the cornea for inhibition of glutamate-induced nocifensive behavior. For example, 6,7-dinitroquinoxaline-2,3-dione (DNQX) is an AMPA and Kainate

receptor antagonist that is water soluble and it may easily penetrate the corneal epithelium to antagonize exogenously applied glutamate. These results will translate to human models in procedures such as Lasik Surgery. The animal model of choice was the rat which is superior to the mouse model for correlation to human disease (Iannaccone & Jacob, 2009). In the present study, our aim, therefore, is to determine if DNQX will antagonize nocifensive behaviors produced by the co-application of glutamate directly on the Sprague Dawley rat cornea. We hypothesize that the AMPA and Kainate specific antagonist, DNQX, will antagonize but not completely prevent nocifensive behavior when applied.

2. Methods

Ethical Guidelines

Experimental procedures were conducted in accordance to the guidelines from the National Institutes of Health (NIH Publications No. 80-23) and were approved by the Oklahoma State University Center for Health Sciences Institutional Animal Care and Use Committee. All experiments were structured so that the number of animals and the length of the study were kept to a minimum. This manuscript was written in accordance to the Animal Research: Reporting of *In Vivo* Experiments (ARRIVE) guidelines (Kilkenny et al., 2010).

Animals

Thirty-six randomized naïve male and female Sprague-Dawley rats from Charles River Laboratories, Wilmington, MA, with an age of 3-5 months were used in this study. The exact number of animals in each group is displayed in the table in figure 2.1. The rats were housed as 1-3 rats per transparent plastic cage (17in x 9.25in x 8.5in; L x W x H) with a metal grated top. A 12-hour light/12-hour dark cycle was used at a temperature kept at 22-23 °C and humidity at 38% in a USDA approved animal facility with standard housing conditions (not specific pathogen free). The rats had free access to Teklad 18% protein rat pellets (Envigo, Huntingdon,

United Kingdom) and purified water (Filter: Pentek C1 Carbon Filter Cartridge 2.5" X 9.75" 5 Micron). All cages were bedded with Teklad Sani-Chips (Envigo, Huntingdon, United Kingdom) to cover the bottom of the cage 1 inch deep. The animals were allowed to habituate in the experimental apparatus by placing them in a transparent plexiglass observational chamber (12in x 11in x 10.25in; L x W x H) for exploration before application of any drugs, three consecutive days in advance of experimentation.

Behavioral testing

All experiments were conducted in a quiet room between 1700 and 2300 hours. The animals were randomly assigned to at least one of 9 experimental groups and/or 2 control groups. Each rat was randomly chosen to participate in more than one experimental and/or control group. At least a week occurred between trials to allow for the 5-6 day period of corneal epithelium renewal before the next experiment was conducted. The experimenter was aware of what drug and concentration was used. All rats underwent welfare checks twice per week at the time of bedding replacement and by the experimenter immediately before the administration of the drug. Any changes in the rat health were noted. After all data was collected, all rats were euthanized with carbon dioxide (CO₂).

Drugs

L-Glutamic acid (Sigma, St. Louis, MO, FW= 169.1), 6,7-Dinitroquinoxaline-2,3-dione (DNQX) disodium salt (Tocris bioscience, Bristol, United Kingdom, FW= 252.14) and phosphate buffered saline PBS (pH:7.3) were used in this experiment. L-Glutamic acid was used as an agonist to the primary afferents to cause a nocifensive behavioral response (Ibitokun, 2012) and was considered the best iGluR agonist, being the natural ligand of the AMPA and Kainate receptors. The antagonist DNQX was used due to its low molecular weight compared to other AMPA and Kainate antagonists as seen in table 2.1. We reasoned that this would allow for easier

penetration via diffusion into the corneal epithelium to interact with the AMPA and Kainate receptors. PBS was used as a buffer solution for diluting the L-Glutamate and DNQX as it has minimal, if any, effect on the AMPA and Kainate receptors.

Experimental Design

In this study, 36 naive Sprague Dawley rats were used. Both male and female rats were randomly assigned to each of the 9 experimental and 2 control groups. Power analysis was conducted to determine the number of animals needed for each group (G Power). Each of the experimental groups had a topical dose of 10 μ L DNQX with a Rainin pipette at the respective dose five minutes before a second combination dose of 10 μ L DNQX and glutamate was given. A five minute wait period was to allow for adequate diffusion of DNQX across the epithelial layer to occur. The observational count of eye blinks, eye wipes, and eye scratching occurred for 30 seconds immediately after the combination dose was given in the observational chamber (12in x 11in x 10.25in; L x W x H). For the glutamate and PBS control, the observational recordings for a period of 30 seconds began once the respective dose was given. Water was used to wash out any remaining solution for all animals once the behavioral responses were counted by use of a wash bottle. Experimental doses were made at logarithmically increasing concentrations including 0.01 μ M, 0.033 μ M, 0.1 μ M, 0.33 μ M, 1.0 μ M, 3.0 μ M, 10.0 μ M, 30.0 μ M, and 100.0 μ M to determine an inhibitory dose response and IC₅₀. Glutamate was used at 0.5M as determined from a dose response curve from previous work in our lab (Ibitokun, 2012).

Statistical Analysis

The Kolmogorov–Smirnov test was used to check for the normality of the dataset using GraphPad Prism (Version 7.03). All experimental groups had normally distributed data. One-way Analysis of variance (ANOVA) using GraphPad Prism (Version 5.01) was conducted to determine statistical significance ($p < 0.05$) and post-hoc comparisons were performed using the

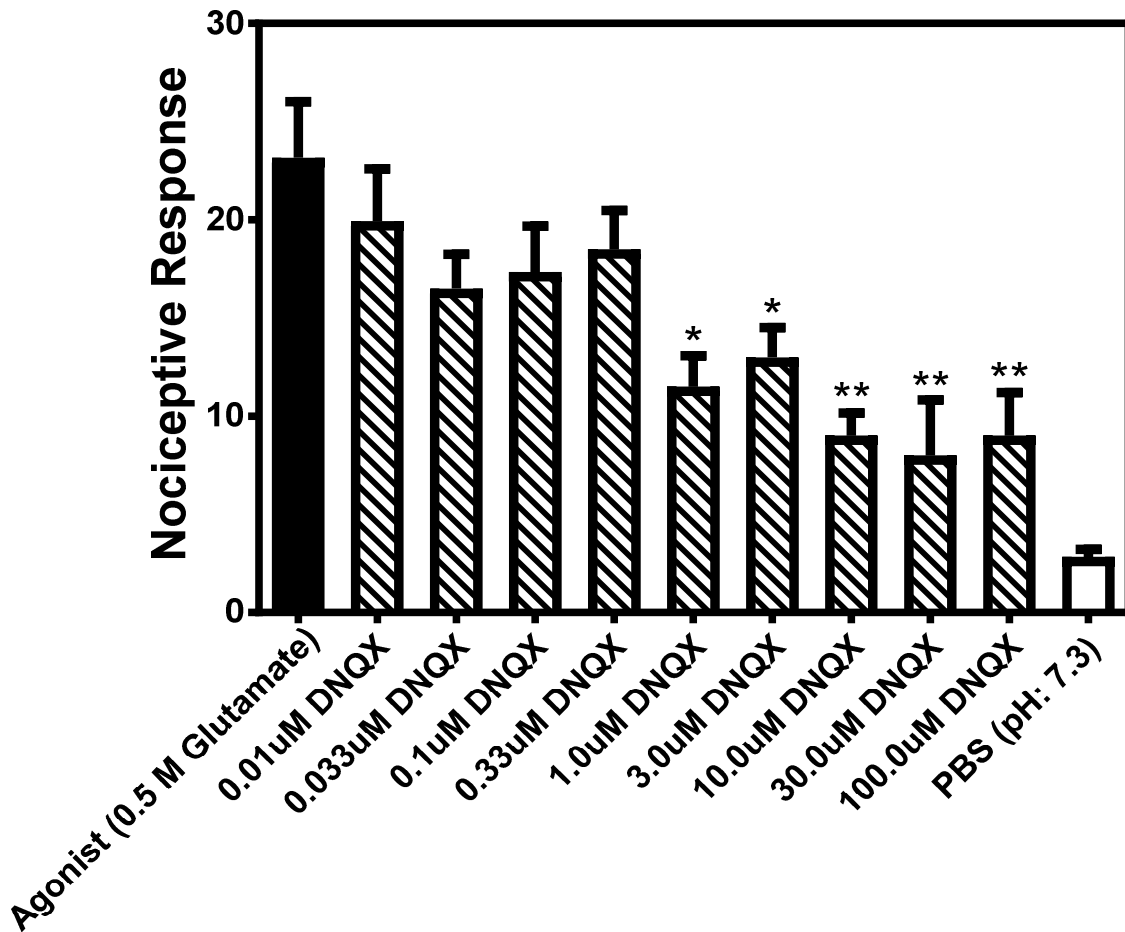
Newman–Keuls method to detect changes between the behavioral responses of experimental groups to the 0.5M L-Glutamate. GraphPad Prism (Version 7.03) was used to construct a log dose response curve. All DNQX data was averaged for each dose, transformed, then normalized. Nonlinear regression was used to determine the IC50.

3. Results

3.1. Corneal stimulation with glutamate

Once the rats appeared to be habituated to the behavioral apparatus and passed health checks, the solutions were topically applied. As seen in table 2.1, the 0.5M glutamate only treatment and PBS only treatment yielded an average of 23 and 3 responses respectively. Application of 0.01, 0.033, 0.1, and 0.33 μ M DNQX + 0.5M glutamate did not significantly decrease the number of nocifensive responses when compared to 0.5M glutamate only. A significant decrease in nocifensive responses ($p < 0.05$) was observed at 1.0 and 3.0 μ M DNQX + 0.5M Glutamate. To further evaluate if there was a further decrease in nocifensive responses, 10, 30, and 100 μ M DNQX + 0.5M Glutamate were used. A further decrease in nocifensive responsive was observed ($p < 0.01$) until a plateau was reached at about 30 μ M. No data was removed from the dataset. No major adverse events occurred during the study, but a water washout period after the conclusion of analysis of each rat was included to decrease any potential side effects of the drugs.

DNQX Dose Response Study



Sample Size	6	12	12	12	12	12	12	6	6	6	6
Mean	23.17	19.92	16.50	17.33	18.50	11.50	13.00	9.00	8.00	9.00	2.83
Standard Deviation	6.97	9.29	6.04	8.08	6.83	5.45	5.26	2.83	6.93	5.40	0.98
Standard Error of the Mean	2.85	2.68	1.74	2.33	1.97	1.57	1.52	1.15	2.83	2.21	0.40

Figure 2.1: Bar graph of the behavioral responses in each of the respective DNQX treatment groups. Experimental groups logarithmically increased in concentration. The table underneath the graph displays the sample size, mean, standard deviation, and the standard error of the mean for each of the experimental and control groups. Statistical significance when compared to agonist of $p \leq 0.05$ was displayed as *. Statistical significance when compared to agonist of $p \leq 0.01$ was displayed as **.

As seen in figure 2.2, a dose response curve was constructed to evaluate the half maximal inhibitory concentration (IC_{50}) of the observed nocifensive responses. The IC_{50} was observed to be $1.18\mu\text{M}$.

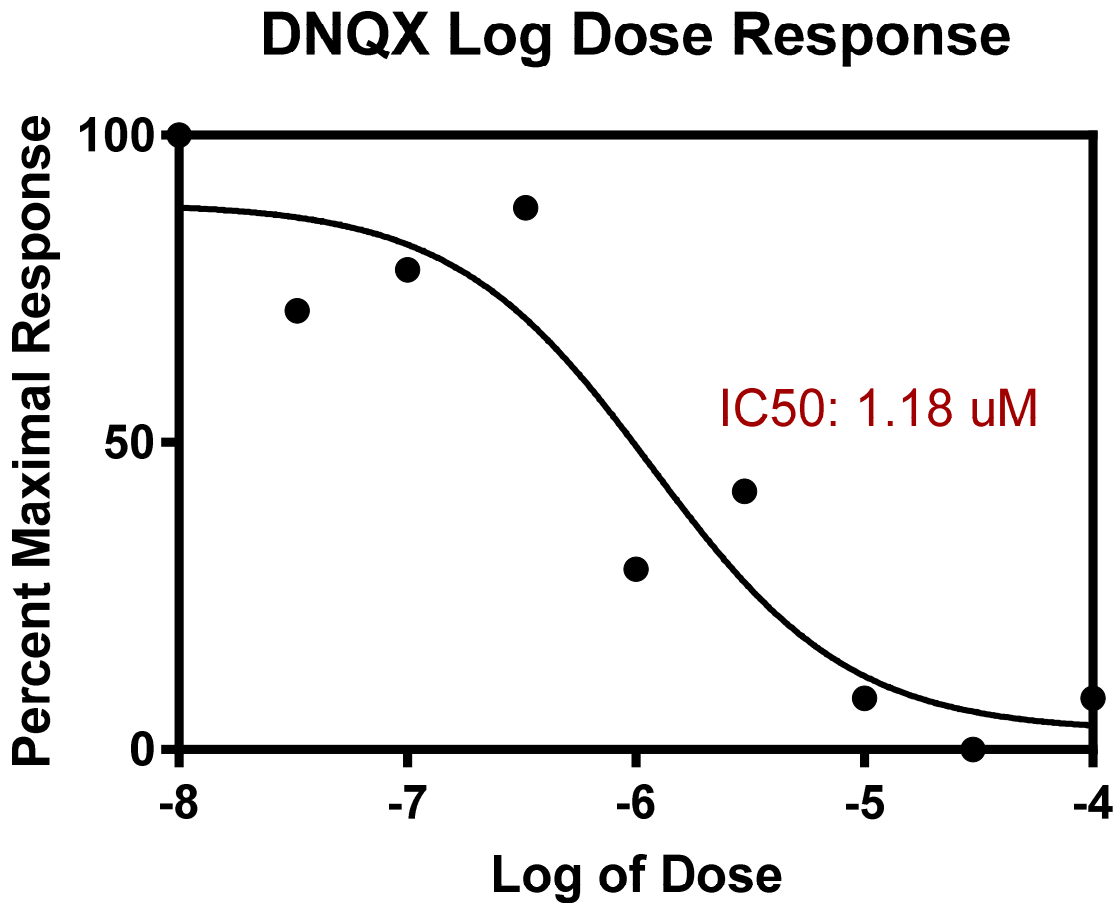


Figure 2.2: Dose response curve for DNQX representing the nocifensive behavioral recordings in Figure 2.1.

4. Discussion

A significant decrease was detected in observed glutamate-induced nocifensive behaviors with topically applied DNQX to the cornea. Compared to previously published work (Gazerani, Dong, Wang, Kumar, & Cairns, 2010), the concentration of glutamate needed to elicit a nocifensive response was greater in the cornea when topically applied as compared to the

subcutaneous injection to the facial skin over the masseter. We theorize that higher concentrations were needed because the topical glutamate solution must dissolve through the protective corneal epithelial cell layer that has more tight junctions per area compared to any other body tissue (Eghrari et al., 2015). Despite the higher concentrations of both glutamate and DNQX, the glutamate elicited nocifensive response was dose dependently reduced by DNQX.

Peripheral neuron terminals release glutamate that activate AMPA, Kainate, and NMDA receptors on nerve terminals in an autocrine or paracrine manner (Miller et al., 2011). During inflammation, an increase in the amount of glutamate receptors occurs on the terminals and the number of peripheral axons with iGluRs increases (Carlton & Coggeshall, 1999). As inflammation progresses, glutamate release can activate more receptors continuing the peripheral sensitization of primary afferents (Miller et al., 2011).

Our results show a reduction of nocifensive responses, but not a total diminishing of the response. This could be in part due to the receptor specificity of the drug of choice. DNQX is an AMPA/Kainate antagonist (Fedele & Raiteri, 1996) that has little to no antagonistic characteristics for the NMDA receptors. To evaluate this, a non-specific iGluR antagonist or a combination of DNQX along with a NMDA receptor antagonist should be used.

The Sprague Dawley animal model used is better at translating to a human model than a mouse model because the clinical implications are better translated (Iannaccone & Jacob, 2009). Furthermore, this study is a good example on how we can reduce and refrain from the extensive use of animals (Flecknell, 2002). We were able to randomly re-use each rat across more than one experimental group which greatly reduced the number of rats needed. We were not able to replace the Sprague Dawley rat model, however, with an in vitro model because human clinical implementation would have been lost.

Future studies should evaluate varying antagonists to determine if a larger molecular weight compound would still cross the corneal epithelial cell layer. As seen in table 2.1, an extensive list of glutamate receptor antagonists from Tocris were identified. Chemical name, common name, molecular weight, chemical formula, solubility, and antagonist site were included. DNQX has a relatively low molecular weight for the water soluble AMPA/Kainate antagonists. Further effectiveness in AMPA, Kainate, and NMDA specific antagonists should be evaluated, but one limitation of our study is that we were not able to antagonize specific glutamate receptor subunits because of the lack of subunit specific antagonists. Finally, some antagonists have a specific target to a specific receptor (Traynelis et al., 2010). Evaluation of the site specific AMPA, Kainate, and NMDA receptor antagonists would help compare the effectiveness to their effects in the CNS.

Chemical Name	Common Name	Molecular weight	Formula	Solubility	Antagonist site
1,4-Dihydro-6-(1H-imidazol-1-yl)-7-nitro-2,3-quinoxalinedione hydrochloride	YM 90K hydrochloride	309.67	C ₁₁ H ₇ N ₅ O ₄ .HCl	Soluble to 10 mM in DMSO with gentle warming	Selective AMPA antagonist
1-(4'-Aminophenyl)-3,5-dihydro-7,8-dimethoxy-4H-2,3-benzodiazepin-4-one	CFM-2	311.34	C ₁₇ H ₁₇ N ₃ O ₃	Soluble to 100 mM in DMSO	Non-competitive AMPA antagonist
2,3-Dioxo-6-nitro-1,2,3,4-tetrahydrobenzo[f]quinoxaline-7-sulfonamide	NBQX	336.28	C ₁₂ H ₈ N ₄ O ₆ S	Soluble to 100 mM in DMSO	Potent AMPA antagonist. More selective than CNQX
4-(8-Methyl-9H-1,3-dioxolo[4,5-h][2,3]benzodiazepin-5-yl)-benzenamine dihydrochloride	GYKI 52466 dihydrochloride	366.24	C ₁₇ H ₁₅ N ₃ O ₂ .2HCl	Soluble to 50 mM in DMSO and to 10 mM in water	Selective non-competitive AMPA antagonist
(±)-4-(4-Aminophenyl)-1,2-dihydro-1-methyl-2-propylcarbamoyl-6,7-methylenedioxyphthalazine	SYM 2206	366.42	C ₂₀ H ₂₂ N ₄ O ₃	Soluble to 100 mM in ethanol and to 100 mM in DMSO	Non-competitive AMPA antagonist

2,3-Dioxo-6-nitro-1,2,3,4-tetrahydrobenzo[f]quinoxaline-7-sulfonamide disodium salt	NBQX disodium salt	380.24	C12H6N4O6SNa2	Soluble to 100 mM in water	Potent AMPA antagonist. More water soluble form of NBQX
4-(8-Chloro-2-methyl-11H-imidazo[1,2-c][2,3]benzodiazepin-6-benzeneamine dihydrochloride	GYKI 47261 dihydrochloride	395.71	C18H15ClN4.2HCl	Soluble to 100 mM in DMSO	Non-competitive AMPA antagonist
N-[3-[[4-[(3-Aminopropyl)amino]butyl]amino]propyl]-1-naphthaleneacetamide trihydrochloride	Naspm trihydrochloride	479.91	C22H34N4O.3HCl	Soluble to 100 mM in water	Ca ²⁺ -permeable AMPA receptor antagonist
3-(2-Chlorophenyl)-2-[2-[6-[(diethylamino)methyl]-2-pyridinyl]ethenyl]-6-fluoro-4(3H)-quinazolinone hydrochloride	CP 465022 hydrochloride	499.41	C26H24ClFN4O.HCl	Soluble to 10 mM in water and to 100 mM in DMSO	Selective, non-competitive AMPA antagonist
(S)-N-[7-[(4-Aminobutyl)amino]heptyl]-4-hydroxy- α -[(1-oxobutyl)amino]benzenepropanamide dihydrochloride	Philanthotoxin 74	507.54	C24H42N4O3.2HCl	Soluble to 100 mM in water and to 100 mM in DMSO	GluR1 and GluR3 AMPA receptor antagonist
6-Cyano-7-nitroquinoxaline-2,3-dione	CNQX	232.16	C9H4N4O4	Soluble to 100 mM in DMSO	Potent AMPA/kainate antagonist
6,7-Dinitroquinoxaline-2,3-dione	DNQX	252.14	C8H4N4O6	Soluble to 100 mM in DMSO	Selective non-NMDA antagonist
6-Cyano-7-nitroquinoxaline-2,3-dione disodium	CNQX disodium salt	276.12	C9H2N4O4Na2	Soluble to 20 mM in water	Potent AMPA/kainate antagonist. More water soluble form of CNQX
6,7-Dinitroquinoxaline-2,3-dione disodium salt	DNQX disodium salt	296.1	C8H2N4O6Na2	Soluble to 100 mM in water	Selective non-NMDA antagonist. Water-soluble salt of DNQX
(α S)- α -Amino-3-[(4-carboxyphenyl)methyl]-3,4-dihydro-2,4-dioxo-1(2H)-pyrimidinepropanoic acid	UBP 282	333.3	C15H15N3O6	Soluble to 100 mM in 1eq. NaOH and to 25 mM in 1eq. HCl	AMPA/kainate antagonist; distinguishes between motoneuron and dorsal root kainate receptors
(8R)-7-Acetyl-5-(4-aminophenyl)-8,9-dihydro-8-methyl-7H-1,3-dioxolo[4,5-h][2,3]benzodiazepine	Talampanel	337.37	C19H19N3O3	Soluble to 100 mM in DMSO	Non-competitive AMPA/kainate antagonist

[[3,4-Dihydro-7-(4-morpholinyl)-2,3-dioxo-6-(trifluoromethyl)-1(2H)-quinoxaliny]methyl]phosphonic acid	ZK 200775	409.25	C14H15N3O6F3P	Soluble to 100 mM in DMSO and to 50 mM in ethanol	Competitive AMPA/kainate antagonist
D-(-)-2-Amino-4-phosphonobutyric acid	D-AP4	183.1	C4H10NO5P	Soluble to 100 mM in 1eq. NaOH	Broad spectrum EAA antagonist
DL-2-Amino-4-phosphonobutyric acid	DL-AP4	183.1	C4H10NO5P	Soluble to 33 mM in water	Broad spectrum EAA antagonist
4-Hydroxyquinoline-2-carboxylic acid	Kynurenic acid	189.17	C10H7NO3	Soluble to 50 mM in DMSO and to 100 mM in 1eq. NaOH	Broad spectrum EAA antagonist
γ -D-Glutamylglycine	γ DGG	204.18	C7H12N2O5	Soluble to 100 mM in 1eq. NaOH and to 100 mM in water with gentle warming	Broad spectrum glutamate receptor antagonist
DL-2-Amino-4-phosphonobutyric acid sodium salt	DL-AP4 Sodium salt	205.08	C4H9NNaO5P	Soluble to 100 mM in water	Broad spectrum EAA antagonist.
4-Hydroxyquinoline-2-carboxylic acid sodium salt	Kynurenic acid sodium salt	211.15	C10H6NNaO3	Soluble to 100 mM in water and to 50 mM in DMSO	Sodium salt of kynurenic acid
(R)-3-Carboxy-4-hydroxyphenylglycine		211.17	C9H9NO5	Soluble to 100 mM in 1eq. NaOH	Ionotropic glutamate receptor antagonist
2,4-Dihydroxyphenylacetyl-L-asparagine		282.25	C12H14N2O6	Soluble to 50 mM in water	Constituent of various spider toxins. Reported to be specific blocker of glutamate receptors.
(RS)-1-(2-Amino-2-carboxyethyl)-3-(2-carboxybenzyl)pyrimidine-2,4-dione	UBP 296	333.3	C15H15N3O6	Soluble to 10 mM in 1eq. NaOH with gentle warming and to 10	Selective, potent kainate antagonist; selective for GluR5-containing receptors

				mM in DMSO	
(S)-1-(2-Amino-2-carboxyethyl)-3-(2-carboxybenzyl)pyrimidine-2,4-dione	UBP 302	333.3	C15H15N3O6	Soluble to 25 mM in 1eq. NaOH and to 20 mM in DMSO with gentle warming	Potent and selective kainate antagonist; active enantiomer of UBP 296
2,3:4,5-Bis-O-(1-methylethylidene)-β-D-fructopyranose sulfamate	Topiramate	339.36	C12H21NO8S	Soluble to 100 mM in DMSO and to 100 mM in ethanol	GluR5 antagonist; inhibits carbonic anhydrase (CA) II and IV
(S)-1-(2-Amino-2-carboxyethyl)-3-(2-carboxy-thiophene-3-yl-methyl)-5-methylpyrimidine-2,4-dione	UBP 310	353.35	C14H15N3O6S	Soluble to 100 mM in DMSO	GLUK5 antagonist
4,6-Bis(benzoylamino)-1,3-benzenedicarboxylic acid	NS 3763	404.38	C22H16N2O6	Soluble to 25 mM in DMSO	Selective non-competitive kainate antagonist; selective for GLUK5
(S)-1-(2-Amino-2-carboxyethyl)-3-(2-carboxy-5-phenylthiophene-3-yl-methyl)-5-methylpyrimidine-2,4-dione	ACET	429.45	C20H19N3O6S	Soluble to 20 mM in 3eq. NaOH	Potent antagonist of GluR5-containing kainate receptors
(αS)-α-Amino-3-[(4-carboxyphenyl)methyl]-3,4-dihydro-5-iodo-2,4-dioxo-1(2H)-pyrimidinepropanoic acid	UBP 301	459.2	C15H14IN3O6	Soluble to 5 mM in DMSO with gentle warming	Kainate receptor antagonist
1-Aminocyclobutane-1-carboxylic acid	ACBC	115.13	C5H9NO2	Soluble to 100 mM in water	NMDA antagonist, acts at glycine site
(R)-(+)-3-Amino-1-hydroxypyrrolidin-2-one	(R)-(+)-HA-966	116.12	C4H8N2O2	Soluble to 100 mM in water	NMDA partial agonist/antagonist; acts at glycine site
(S)-(-)-3-Amino-1-hydroxypyrrolidin-2-one	(S)-(-)-HA-966	116.12	C4H8N2O2	Soluble to 100 mM in water	NMDA antagonist/partial agonist
(R)-4-Carboxyphenylglycine		195.17	C9H9NO4	Soluble to 100 mM in 1eq. NaOH and to 5 mM in water	Moderately potent NMDA antagonist

DL-2-Amino-5-phosphonopentanoic acid	DL-AP5	197.13	C5H12NO5P	Soluble to 10 mM in water and to 100 mM in 1eq. NaOH	Potent, selective NMDA antagonist
(E)-(±)-2-Amino-4-methyl-5-phosphono-3-pentenoic acid	CGP 37849	209.14	C6H12NO5P		Potent and selective NMDA antagonist
(2R*,4S*)-4-(1H-Tetrazol-5-ylmethyl)-2-piperidinecarboxylic acid	LY 233053	211.22	C8H13N5O2	Soluble to 100 mM in water and to 100 mM in DMSO	Competitive NMDA receptor antagonist
3,5-Dimethyl-tricyclo[3.3.1.1 ^{3,7}]decan-1-amine hydrochloride	Memantine hydrochloride	215.77	C12H21N.HCl	Soluble to 100 mM in water	NMDA antagonist; acts at ion channel site
DL-2-Amino-5-phosphonopentanoic acid sodium salt	DL-AP5 Sodium salt	219.11	C5H11NNaO5P	Soluble to 100 mM in water	Sodium salt of DL-AP5
cis-4-[Phosphomethyl]-piperidine-2-carboxylic acid	CGS 19755	223.17	C7H14NO5P	Soluble to 25 mM in water	Potent, competitive NMDA antagonist
4-(Phosphonomethyl)-2-piperazinecarboxylic acid	PMPA (NMDA antagonist)	224.15	C6H13N2O5P	Soluble to 100 mM in water	Competitive NMDA antagonist
DL-2-Amino-7-phosphonoheptanoic acid	DL-AP7	225.18	C7H16NO5P	Soluble to 100 mM in 1eq. NaOH	Specific NMDA antagonist
(E)-(±)-2-Amino-4-methyl-5-phosphono-3-pentenoic acid ethyl ester	CGP 39551	237.19	C8H16NO5P	Soluble to 100 mM in water	Potent, selective and competitive NMDA antagonist
2-Phenyl-1,3-propanedioldicarbamate	Felbamate	238.24	C11H14N2O4	Soluble to 100 mM in DMSO and to 100 mM in ethanol	NMDA antagonist, acts glycine site
(R)-3,4-Dicarboxyphenylglycine	(R)-3,4-DCPG	239.18	C10H9NO6	Soluble to 100 mM in water	AMPA antagonist/weak NMDA antagonist
D-4-[(2E)-3-Phosphono-2-propenyl]-2-piperazinecarboxylic acid	D-CPP-ene	250.19	C8H15N2O5P	Soluble to 100 mM in water	Potent, competitive NMDA antagonist
(2R*,4S*)-4-(3-Phosphonopropyl)-2-piperidinecarboxylic acid	PPPA	251.22	C9H18NO5P	Soluble to 100 mM in water	Competitive NR2A antagonist

3-((R)-2-Carboxypiperazin-4-yl)-propyl-1-phosphonic acid	(R)-CPP	252.21	C8H17N2O5P	Soluble to 100 mM in water	Potent NMDA antagonist; more active enantiomer of (RS)-CPP
(RS)-3-(2-Carboxypiperazin-4-yl)-propyl-1-phosphonic acid	(RS)-CPP	252.21	C8H17N2O5P	Soluble to 100 mM in water	Potent NMDA antagonist
(2R,3S)- β -p-Chlorophenylglutamic acid	(2R,3S)-Chlorpgeg	257.67	C11H12ClNO4	Soluble to 100 mM in 1.1eq. NaOH	Weak NMDA antagonist
5,7-Dichloro-4-hydroxyquinoline-2-carboxylic acid	5,7-Dichlorokynurenic acid	258.06	C10H5Cl2NO3	Soluble to 100 mM in 1eq. NaOH and to 100 mM in DMSO	Potent NMDA antagonist, acts at glycine site
2-Amino-2-(2-chlorophenyl)cyclohexanone hydrochloride	Norketamine hydrochloride	260.16	C12H14ClNO.HCl	Soluble to 100 mM in water	Potent, non-competitive NMDA antagonist; antinociceptive
7-Chloro-3-(cyclopropylcarbonyl)-4-hydroxy-2(1H)-quinolinone	L-701,252	263.68	C13H10ClNO3	Soluble to 50 mM in DMSO	NMDA antagonist, acts glycine site
N,N'-1,4-Butanediylbisguanidine sulfate	Arcaine sulfate	270.31	C6H16N6.H2SO4	Soluble to 25 mM in water	Competitive NMDA antagonist
2-(2-Chlorophenyl)-2-(methylamino)cyclohexanone hydrochloride	Ketamine hydrochloride	274.19	C13H16ClNO.HCl	Soluble to 100 mM in water	Non-competitive NMDA receptor antagonist
[3S-(3 α ,4 α ,6 β ,8 α)]-Decahydro-6-(phosphonomethyl)-3-isoquinolinecarboxylic acid)	LY 235959	277.26	C11H20NO5P	Soluble to 100 mM in water	Competitive NMDA antagonist
1-(1-Phenylcyclohexyl)piperidine hydrochloride	Phencyclidine hydrochloride	279.85	C17H25N.HCl	Soluble to 40 mM in water	Non-competitive NMDA receptor antagonist
5,7-Dichloro-4-hydroxyquinoline-2-carboxylic acid sodium salt	5,7-Dichlorokynurenic acid sodium salt	280.04	C10H4Cl2NNaO3	Soluble to 100 mM in 1eq. NaOH	Sodium salt of 5,7-Dichlorokynurenic acid. Potent NMDA antagonist, acts at glycine site
2-Amino-N-(1-methyl-1,2-diphenylethyl)acetamide hydrochloride	Remacemide hydrochloride	304.82	C17H20N2O.HCl	Soluble to 100 mM in water	NMDA antagonist; blocks ion channel and allosteric modulatory site
(5R,10S)-(-)-5-Methyl-10,11-dihydro-5H-dibenzo[a,d]cyclohepten-5,10-imine maleate	(-)-MK 801 maleate	337.37	C16H15N.C4H4O4	Soluble to 25 mM in water with	NMDA antagonist, less active enantiomer

				gentle warming	
(5S,10R)-(+)-5-Methyl-10,11-dihydro-5H-dibenzo[a,d]cyclohepten-5,10-imine maleate	(+)-MK 801 maleate	337.37	C16H15N.C4H4O4	Soluble to 25 mM in water and to 100 mM in DMSO	Non-competitive NMDA antagonist; acts at ion channel site
1,3-Dihydro-5-[3-[4-(phenylmethyl)-1-2H-benzimidazol-2-one	TCS 46b	345.44	C22H23N3O	Soluble to 100 mM in DMSO and to 100 mM in ethanol	Orally active, subtype-selective NR1A/NR2B antagonist
α -(4-Chlorophenyl)-4-[(4-fluorophenyl)methyl]-1-piperidineethanol	Eliprodil	347.86	C20H23ClFNO	Soluble to 25 mM in DMSO	Non-competitive NR2B-selective NMDA antagonist
(9 α ,13 α ,14 α)-3-Methoxy-17-methylmorphinan hydrobromide	Dextromethorphan hydrobromide	352.31	C18H25NO.HBr	Soluble to 40 mM in water	NMDA receptor antagonist
N,N'-1,10-Decanediyldisguanidine sulfate	Synthalin sulfate	354.47	C12H28N6.H2SO4	Soluble to 5 mM in water	Non-competitive NMDA antagonist
7-Chloro-4-hydroxy-3-(3-phenoxy)phenyl-2(1H)-quinolinone	L-701,324	363.8	C21H14ClNO3	Soluble to 100 mM in DMSO	NMDA antagonist; acts at glycine site
1-[2-(4-Chlorophenyl)ethyl]-1,2,3,4-tetrahydro-6-methoxy-2-methyl-7-isoquinolinol hydrochloride	Ro 04-5595 hydrochloride	368.3	C19H22ClNO2.HCl	Soluble to 15 mM in water and to 100 mM in DMSO	NR2B-selective NMDA antagonist
(S)- α -Amino-2'-chloro-5-(phosphonomethyl)[1,1'-biphenyl]-3-propanoic acid	SDZ 220-581	369.74	C16H17ClNO5P	Soluble to 25 mM in DMSO with gentle warming and to 100 mM in 1.1eq. NaOH	Competitive NMDA antagonist
1-[2-(4-Hydroxyphenoxy)ethyl]-4-[(4-methylphenyl)methyl]-4-piperidinol hydrochloride	Co 101244 hydrochloride	377.91	C21H27NO3.HCl	Soluble to 100 mM in water and to 50 mM in DMSO	Highly selective NR2B antagonist
(2S*,3R*)-1-(Phenanthren-2-carbonyl)piperazine-2,3-dicarboxylic acid	PPDA	378.38	C21H18N2O5	Soluble to 50 mM in 2eq. NaOH and to 100 mM in	Subtype-selective NR2C/NR2D antagonist

				DMSO	
trans-2-Carboxy-5,7-dichloro-4-phenylaminocarbonylamino-1,2,3,4-tetrahydroquinoline	L-689,560	380.23	C17H15Cl2N3O3	Soluble to 25 mM in DMSO and to 100 mM in ethanol	Very potent NMDA antagonist
(±)-1-(1,2-Diphenylethyl)piperidine maleate		381.47	C19H23N.C4H4O4	Soluble to 10 mM in water	NMDA antagonist, acts ion channel site
(6aS,10aS)-3-(1,1-Dimethylheptyl)-6a,7,10,10a-tetrahydro-1-hydroxy-6,6-dimethyl-6H-dibenzo[b,d]pyran-9-methanol	HU 211	386.57	C25H38O3	Soluble to 100 mM in DMSO and to 100 mM in ethanol	NMDA receptor antagonist; also NF-κB inhibitor
4,6-Dichloro-3-[(1E)-3-oxo-3-(phenylamino)-1-propenyl]-1H-indole-2-carboxylic acid sodium salt	Gavestinel	397.19	C18H11Cl2N2O3Na	Soluble to 40 mM in DMSO	Potent and selective glycine site antagonist; orally available and active in vivo
(1R*,2S*)-erythro-2-(4-Benzylpiperidino)-1-(4-hydroxyphenyl)-1-propanol hemi-(DL)-tartrate	Ifenprodil hemitartrate	400.49	C21H27NO2.½C4H6O6	Soluble to 15 mM in water with gentle warming	Non-competitive NMDA antagonist. Also oligand
(1S*,2S*)-threo-2-(4-Benzylpiperidino)-1-(4-hydroxyphenyl)-1-propanol hemitartrate	threo Ifenprodil hemitartrate	400.49	C21H27NO2.½C4H6O6	Soluble to 25 mM in water and to 100 mM in DMSO	NR2B-selective NMDA antagonist; also oagonist
4-[3-[4-(4-Fluorophenyl)-1,2,3,6-tetrahydro-1(2H)-pyridinyl]-2-hydroxypropoxy]benzamide hydrochloride	Ro 8-4304 hydrochloride	406.88	C21H23FN2O3.HCl	Soluble to 10 mM in water and to 100 mM in DMSO	NR2B-selective NMDA antagonist
[(1S)-1-[[[7-Bromo-1,2,3,4-tetrahydro-2,3-dioxo-5-quinoxaliny]methyl]amino]ethyl] phosphonic acid hydrochloride	CGP 78608 hydrochloride	414.58	C11H13BrN3O5P.HCl	Soluble to 100 mM in 2.2eq. NaOH	Potent, selective glycine-site NMDA antagonist
(S)-α-Amino-2',4'-dichloro-4-hydroxy-5-(phosphonomethyl)-[1,1'-biphenyl]-3-propanoic acid	SDZ 220-040	420.19	C16H16Cl2NO6P	Soluble to 100 mM in DMSO	Potent, competitive NMDA antagonist
4-[6-Methoxy-2-[(1E)-2-(3-nitrophenyl)ethenyl]-4-oxo-3(4H)quinazolinyl]benzoic acid	QNZ 46	443.41	C24H17N3O6	Soluble to 10 mM in DMSO with gentle warming	NR2C/NR2D-selective NMDA receptor non-competitive antagonist

(α R, β S)- α -(4-Hydroxyphenyl)- β -methyl-4-(phenylmethyl)-1-piperidinepropanol maleate	Ro 25-6981 maleate	455.55	C22H29NO2.C4H4O4	Soluble to 10 mM in water with gentle warming and to 100 mM in DMSO	NR2B-selective NMDA antagonist
4,4'-(Pentamethylenedioxy)dibenzamidine bis-2-hydroxyethanesulfonate salt	Pentamidine isethionate	592.68	C19H24N4O2.2C2H6O4S	Soluble to 100 mM in water	Antimicrobial that antagonizes NMDA receptors
Conantokin-T		2683.8	C110H175N31O45S		Non-competitive NMDA receptor antagonist
Conantokin-R		3098.4	C127H201N35O49S3		Potent non-competitive NMDA receptor antagonist

Table 2.1: List of Tocris glutamate receptor antagonists with pertinent information.

Acknowledgements

NIH Grant AR047410

CHAPTER III

IDENTIFYING THE LOCATION OF THE SIXTEEN CURRENTLY KNOWN GLUTAMATE RECEPTORS IN THE RAT CORNEA: A WESTERN BLOTTING AND IMMUNOHISTOCHEMISTRY STUDY

Abstract

Introduction: With further evaluation of glutamate receptor subunits in the central nervous system being conducted, a full evaluation is needed to determine the presence and localization of glutamate receptor subunits in the peripheral nervous system. Once an understanding of where each receptor subunit is located in the cornea and trigeminal root ganglion, more specific evaluation can occur.

Aim: To identify and localize GluA1-4, GluK1-5, GluN1, GluN2A-2D, and GluN3A-3B glutamate receptor subunits in the Sprague Dawley rat cornea and trigeminal root ganglion.

Methods: A total of 24 Sprague Dawley rats were used to identify the presence of 16 glutamate receptor subunits by western blots and a total of 24 rats for immunofluorescence.

Results: Each of the 16 glutamate receptor subunits were present in the Sprague Dawley rat cornea and trigeminal root ganglion with a differential distribution in the tissues across the glutamate receptor subunits.

Discussion: Glutamate receptors become functional when four receptor subunits form a tetramer. Identifying the presence and location of each of the subunits separately will further our knowledge on what possible functions a receptor has and what combination of subunits can combine to form a functional receptor in the peripheral nervous system.

Introduction

Currently four ionotropic glutamate receptor subtypes (iGluRs) have been classified: 2-Amino-3-(3-hydroxy-5-methyl-isoxazol-4-yl)propanoic acid (AMPA), Kainate, N-methyl-D-aspartate receptor (NMDA), and Delta (Bleakman et al., 2006). These receptors are all activated by L-glutamate or a combination of L-glutamate and coagonist, e.g., glycine, with Delta receptors being an exception where the endogenous ligand is under current examination (Yuzaki & Aricescu, 2017).

An iGluR requires a dimer of dimer of subunits within the same receptor class to construct a functional tetrameric receptor (Dingledine et al., 1999; Traynelis et al., 2010). Each iGluR has specific subunits included in their receptor class; AMPA: GluA1, GluA2, GluA3, and GluA4; Kainate: GluK1, GluK2, GluK3, GluK4, GluK5; NMDA: GluN1, GluN2A, GluN2B, GluN2C, GluN2D, GluN3A, and GluN3B; Delta: GluD1 and GluD2. Additional subunit variants have been described including flip and flop for AMPA and NMDA receptor subunits (Krampfl et al., 2002; Pachernegg et al., 2015; Y. H. Park et al., 2016; Pei et al., 2009). Certain subunit containing receptors have been described for specific functions such as GluK1 and GluN2B in relation to inflammatory pain (Abe et al., 2005; Bu et al., 2015; Vincent et al., 2016).

Despite the extensive research conducted on iGluRs and their receptor subunits in the central nervous system, there is minimal identification of these iGluR subunits in peripheral tissues, for example the cornea (Carr, 2017). The cornea is the most innervated peripheral tissue in the body (Barry, Petroll, Andrews, Cavanagh, & Jester, 1995; Eghrari et al., 2015; He et al.,

2010) and, during certain human surgery procedures such as Lasik surgery, pain can become debilitating during the recovery phase (Huang & Chen, 2008). With the identification of specific iGluR subunits in the cornea, more accurate targeting could accomplish specific results, e.g., decreased pain, faster healing, etc. A rat model was chosen for this study, because in many ways it is superior to the mouse model for correlation to human disease (Iannaccone & Jacob, 2009).

In our study, we aimed to determine the presence and location of the 16 currently recognized subunits that form the AMPA, Kainate, and NMDA GluRs in the Sprague Dawley rat cornea and trigeminal root ganglion. We hypothesized that some, but not all, of the glutamate receptor subunits will be present in the stromal nerve fibers and corneal epithelial cells and a similar immunoreactivity will be present in neuronal cell bodies of the ophthalmic division of the trigeminal root ganglion. With an understanding of potential subunit combinations in the cornea, we can begin to identify better tissue specific drugs for pain, dry eye, and epithelial healing following injury.

Methods:

Ethical Guidelines

This experiment and experimental procedures were conducted in accordance to the guidelines from the National Institutes of Health (NIH Publications No. 80-23) and were approved by the Oklahoma State University Center for Health Sciences Institutional Animal Care and Use Committee. All experiments were structured so that the number of animals and the length of the study were kept to a minimum. This manuscript was written in accordance to the Animal Research: Reporting of *In Vivo* Experiments (ARRIVE) guidelines (Kilkenny et al., 2010).

Animals

A total of 48 naive male (n=24) and female (n=24) Sprague-Dawley rats (Charles River Laboratories, Wilmington, MA) at an age of 5-10 weeks were used in this study. The rats were housed 1-3 rats in each transparent plastic cage (17in x 9.25in x 8.5in; L x W x H) with a metal grated top. A 12-hour light/12-hour dark cycle was used at a temperature kept at 22-23 °C and humidity at 38% in a USDA approved animal facility with standard housing conditions (not specific pathogen free). The rats had free access to Teklad 18% protein rat pellets (Envigo, Huntingdon, United Kingdom) and purified water (Filter: Pentek C1 Carbon Filter Cartridge 2.5" X 9.75" 5 Micron). All cages were bedded with Teklad Sani-Chips (Envigo, Huntingdon, United Kingdom) to cover the bottom of the cage 1 inch deep.

Western blot

A total of 12 male and 12 female (n=24/48, mean age: 9.54 months (age range: 10.28-8.57 months)) naïve rats were euthanized by 5% isoflurane anesthetic (NDC 11695-0500-2, Henry Schein Animal Health) followed by decapitation once they became unresponsive. A total of 48 whole corneas, trigeminal root ganglia, and hippocampus were taken and combined in a 1:1 Radioimmunoprecipitation assay (RIPA) buffer (50mM Tris HCl buffer (pH 8), 1% NP40, 0.5% sodium deoxycholate, 0.1% SDS, 150mM NaCl, 10% glycerol) and lysis buffer (50mM Tris HCl pH 7.4, 1% triton X 100, 50mM NaCl, 10% glycerol). 1µL Halt Protease & Phosphatase Inhibitor Cocktail (x100, Thermo Scientific, Waltham, MA) solution was added to 1mL RIPA/Triton X-100. The tissues in solution were stored at -80°C until used before homogenization.

All samples were homogenized by a handheld homogenizer with pestles. Bio-Rad, Hercules, CA, Criterion TGX Precast Gels (26 well, 4-20%) at 100V for 10 minutes, 150V for 10 minutes, and 180V for 1 hour 20 mins were used. All blots were transferred to a Polyvinylidene difluoride (PVDF) membrane (Cat. #162-0177). Each glutamate receptor was

examined for the cornea and trigeminal root ganglion. The hippocampus was used as a positive control. A Typhoon 9410 Variable Mode Imager was used to image the western blots. A Chemidoc MP imaging system (BIORAD, Hercules, CA) was used to image GluA2.

Immunofluorescence

A total of 12 males and 12 females (n=24/48, mean age: 7.44 months, age range: 7.14-8.85 months) naïve rats were used for evaluation of the 16 glutamate receptors with immunofluorescence. All animals were euthanized with 3mL of 2.5% Avertin and 1mL of 100mg/mL Xylazine (NDC 59399-111-50, Akorn Animal Health, Lake Forest, IL). Rats were intracardially perfused with a fixative solution (75% picric acid, 0.2% paraformaldehyde, 0.1M phosphate buffer, pH 7.3) when corneal blink and tail flick responses were no longer present. Perfusion and tissue collection were done between 1200 to 1800 hours. Corneas, trigeminal root ganglia, and hippocampus were extracted from the rats and placed in the fixative solution for 4-6 hours at 4°C. All tissue were transferred into 10% sucrose in phosphate buffered saline (PBS, pH: 7.3) for 12 to 48 hours at 4°C.

Corneas were cut 3-4 times with a scalpel blade from the periphery to close to the center, but not enough to separate the tissue into different sections to help keep the tissue flat. Tissue were placed in Shandon M-1 Embedding matrix (Ref: 1310, Thermo Scientific, Waltham, MA) in an embedding mold and frozen into a square block with liquid nitrogen. To keep flat, the corneas were placed epithelium side down in a drop of embedding medium and frozen. Additional medium was placed on top of the frozen tissue and frozen again to allow for coronal sectioning. Tissue sections were coronally cut at 18µm using a Leica cryostat (CM1850) and thaw mounted on gel coated slides (VWR, 48311-600). All slides were placed tissue up on a slide warmer (Fisher Scientific, Waltham, MA, model: 77) for 1 hour at 37°C. The tissues were washed 3 times with PBS (pH: 7.3). The slides were incubated in 0.5% BSA, and 0.5%

polyvinylpyrrolidone in PBS with 0.3% Triton (PBS-T). Sections were incubated for 48 hours at 4°C in each of the primary antisera presented in table 3.1 which includes GluA1-4, GluK1-5, GluN1,2A-2B,3A,3B, PSD-95, stargazin, and glutamate. All primary antisera raised in goat or mouse were colocalized with PGP 9.5 raised in rabbit, all antibodies raised in rabbit were colocalized with Calcitonin gene-related peptide (CGRP) raised in mouse, and glutamate was single labeled without colocalization. The tissue was washed three times with PBS for ten minutes each. Alexa Fluor 488 secondary antisera for iGluRs, PSD-95, Stargazin, and Glutamate, and Alexa Fluor 555 secondary antisera for PGP9.5 and CGRP were added with PBS-T to 1:1000 for their respected species for 1 hour followed by three washes with PBS. Coverslips were placed over the tissue with Prolong Gold antifade reagent (Ref: P36930). All images were taken with a Leica DMI 4000B confocal microscope (Resolution: 2048 x 2048) with a 40X water objective. Images were saved as TIFF and the exposure times were iGluR subunit specific. All final images were a merge of 3-10 confocal images (Resolution: 2048 x 2048) that best represented the particular field of view. Refer to table 3.1 for a full list of antibodies used along with the company, catalog number, species reactivity, monoclonal or polyclonal, and concentration used.

<i>Target</i>	<i>Company</i>	<i>Catalog Number</i>	<i>Species</i>	<i>Mono/Poly</i>	<i>Concentration</i>
<u>Primary antisera</u>					
GluA1	Santa Cruz	sc-7609	Goat	Polyclonal	1:100
GluA2	Millipore	MAB397	Mouse	Monoclonal	1:100
GluA3	Santa Cruz	sc-7613	Goat	Polyclonal	1:100
GluA4	Acris	AP16819PU-N	Goat	Polyclonal	1:100
GluK1	Santa Cruz	sc-7617	Goat	Polyclonal	1:100
GluK2	Abcam	ab53092	Rabbit	Polyclonal	1:100
GluK3	Abcam	ab82148	Goat	Polyclonal	1:100
GluK4	Santa Cruz	sc-8917	Goat	Polyclonal	1:100
GluK5	Santa Cruz	sc-8915	Goat	Polyclonal	1:100
GluN1	Santa Cruz	sc-1467	Goat	Polyclonal	1:100
GluN2A	Santa Cruz	sc-1468	Goat	Polyclonal	1:100

GluN2B	Santa Cruz	sc-1469	Goat	Polyclonal	1:100
GluN2C	Santa Cruz	sc-1470	Goat	Polyclonal	1:100
GluN2D	Santa Cruz	sc-1471	Goat	Polyclonal	1:100
GluN3A	Millipore	07-356	Rabbit	Polyclonal	1:250
GluN3B	Upstate Cell Signaling	07-351	Rabbit	Polyclonal	1:250
PSD-95	Cell Signaling	2507X	Rabbit	Polyclonal	1:500
Stargazin/Cacng2	Upstate Cell Signaling	07-577	Rabbit	Polyclonal	1:100
Glutamate	Sigma	G6642	Rabbit	Polyclonal	1:1000
<u>Colocalized</u> <u>Antisera</u>					
CGRP	Santa Cruz	sc-57053	Mouse	Monoclonal	1:1000
PGP 9.5	Cedarlane	CL7756AP	Rabbit	Polyclonal	1:10,000

Table 3.1: List of all primary antibodies used in this study.

Statistical analysis

Because this was a descriptive study, no statistical analysis was conducted.

Results:

1.1 Western Blot

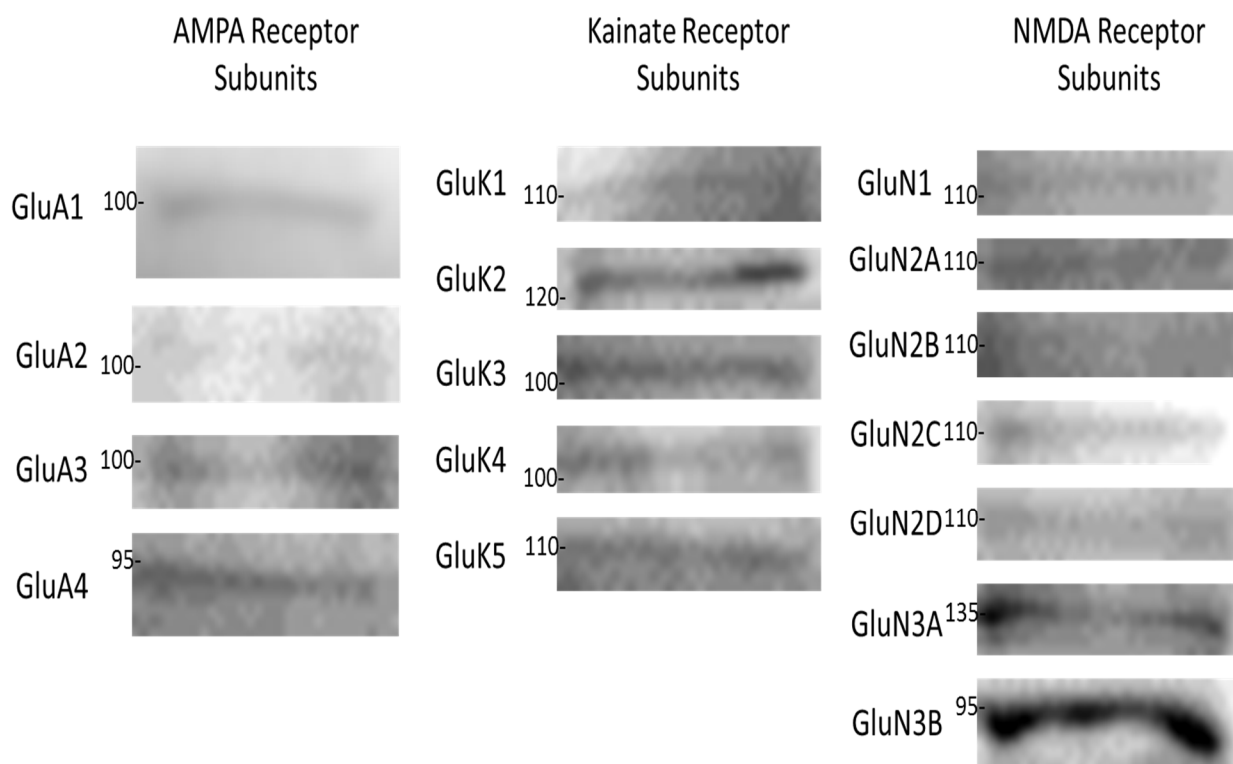


Figure 3.1: Preliminary western blots of whole corneas.

Western blots of each of the iGluR subunits were conducted to support their presence or absence in the cornea. From our preliminary results, figure 3.1, shows that each of the iGluR subunits have some level of expression in the cornea. Because of many nonspecific bands present in the blots in figure 3.1, optimization steps for GluA2 were targeted for further western blot analysis. As represented in figure 3.2, both the whole cornea and trigeminal root ganglion were found to have bands at 130kd. Hippocampal control was found to be at about 110kd.

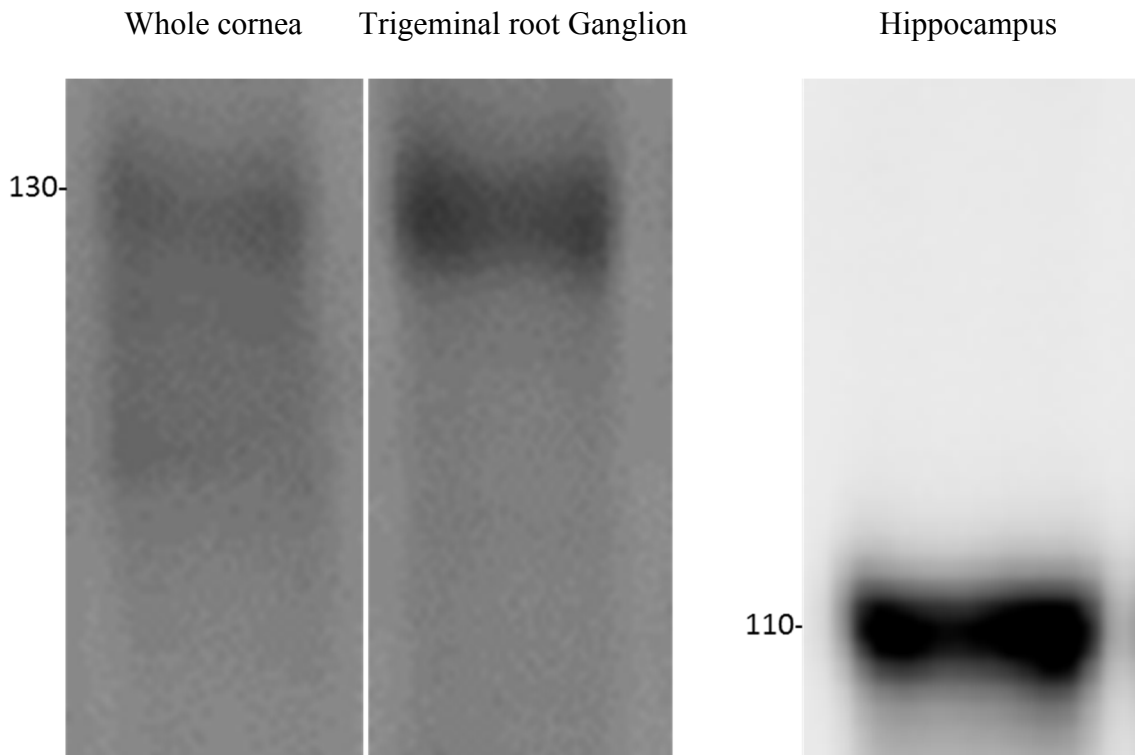


Figure 3.2: Western blot of GluA2.

1.2 Immunohistochemistry

All the glutamate receptor subunits, PSD-95, Stargazin, and glutamate were identified to be present in the corneal epithelium and cytoplasm in the cornea epithelial cells. The intensity of the fluorescence of the corneal epithelial cells made it difficult to identify epithelial nerve fibers. GluA2,3 and GluK1 were identified in the corneal epithelial nerve fibers, but all of the other subunits, PSD-95, Stargazin, and glutamate were undetermined. Perinuclear staining was only

identified in GluA2 and GluK1,4. Nuclear staining was identified in GluK3 and GluN2A,2B,2C. Stromal nerve fibers were undetermined in GluA4 and GluN2B, but, in all the other subunits, PSD-95, Stargazin, and glutamate immunofluorescent staining occurred in the stromal nerve fibers. All results are represented in table 3.2.

All glutamate receptor subunits, PSD-95, Stargazin, and glutamate were identified to be present in both the large and small neuronal cell bodies of the ophthalmic division of the trigeminal root ganglion. Furthermore, for GluA2,3, GluK1,2,4,5, and GluN2C,3B, the large neuronal cell bodies were dimly stained as compared to the brightly stained small neuronal cell bodies. Nuclear staining in the trigeminal root ganglion was not identified for GluA4, GluK2,5, GluN1,2D,3B, PSD-95, Stargazin, and glutamate. Nuclear staining was identified for GluA1,2,3, GluK1,4, and GluN2A3A, but more intense nuclear staining was identified for GluK3 and GluN2B,2C. All of the glutamate receptor subunits, PSD-95, Stargazin, and glutamate were identified in the nerve fibers of the trigeminal root ganglion. GluA1,3, GluK3,4, and GluN1,2C,2D, were identified as having satellite cell staining in the trigeminal root ganglion and the remaining subunits, PSD-95, Stargazin, and glutamate were identified as undetermined. GluN2C,2D,3A,3B were identified to have Schwann cell staining in the trigeminal root ganglion. GluK2,5 and GluN2A,2B were identified to have myelin sheath staining in the trigeminal root ganglion. All results are represented in table 3.2.

Figures 3.2-3.7 represent enlarged examples of the cornea for each of the characteristics identified. Figures 3.8-3.13 represent enlarged examples of the trigeminal root ganglion for each of the characteristics identified. Figures 3.14-3.32 represent each of the glutamate receptor subunits, PSD-95, Stargazin, and glutamate for the cornea and trigeminal root ganglion.

	Cornea					Trigeminal						
	Epithelial cells	Cytoplasm	Nucleus	Epithelial nerve fiber	Stromal nerve fiber	Large neuronal cell bodies	Small neuronal cell bodies	Nuclear	Nerve fibers	Satellite cells	Schwann Cells	Myelin
GluA1	Y	Y	N	U	Y	Y	Y	Y	Y	Y	N	U
GluA2	Y	Y	N	Y	Y	Y	Y	Y	Y	U	N	U
GluA3	Y	Y	N	Y	Y	Y	Y	Y	Y	Y	N	U
GluA4	Y	Y	N	U	U	Y	Y	N	Y	U	N	U
GluK1	Y	Y	N	Y	Y	Y	Y	Y	Y	U	N	U
GluK2	Y	Y	N	U	Y	Y	Y	N	Y	U	N	Y
GluK3	Y	Y	Y	U	Y	Y	Y	Y	Y	Y	N	U
GluK4	Y	Y	N	U	Y	Y	Y	Y	Y	Y	U	U
GluK5	Y	Y	N	U	Y	Y	Y	N	Y	U	N	Y
GluN1	Y	Y	N	U	Y	Y	Y	N	Y	Y	N	U
GluN2A	Y	Y	Y	U	Y	Y	Y	Y	Y	U	N	Y
GluN2B	Y	Y	Y	U	U	Y	Y	Y	Y	U	N	Y
GluN2C	Y	Y	Y	U	Y	Y	Y	Y	Y	Y	Y	U
GluN2D	Y	Y	N	U	Y	Y	Y	N	Y	Y	Y	U
GluN3A	Y	Y	N	U	Y	Y	Y	Y	Y	U	Y	U
GluN3B	Y	Y	N	U	Y	Y	Y	N	Y	U	Y	U
PSD95	Y	Y	N	U	Y	Y	Y	N	Y	U	N	N
Stargazin	Y	Y	N	U	Y	Y	Y	N	Y	U	N	N
Glutamate	Y	Y	N	U	Y	Y	Y	N	Y	U	N	N

Y	Yes (Bright)	Y	Yes (Dim)	N	No
Y	Yes	U	Unclear		

Table 3.2: Results of immunofluorescent reactivity for the cornea and trigeminal root ganglia. Green Y: Presence.

Dark Green Y: Low presence. Bright Green Y: High presence. Yellow U: Unknown presence. Red N: No presence.

1.2.1 Corneal characteristics

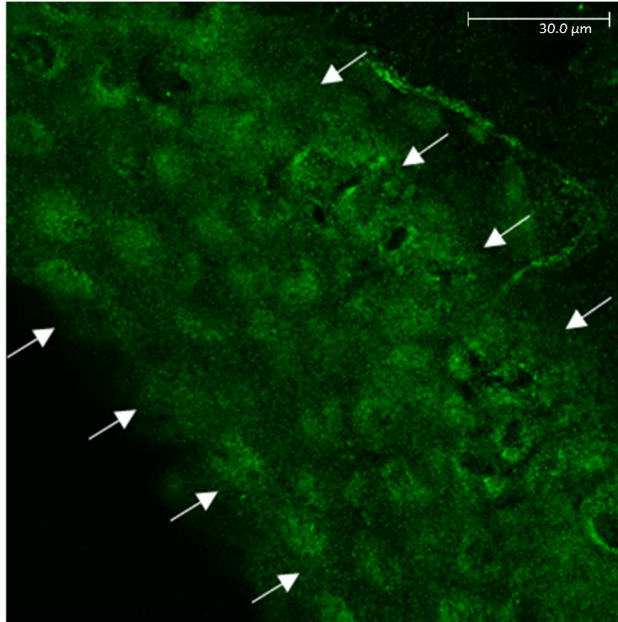


Figure 3.3: Image illustrating immunoreactivity in corneal epithelial cells (GluA2). Arrows illustrate the corneal epithelium.

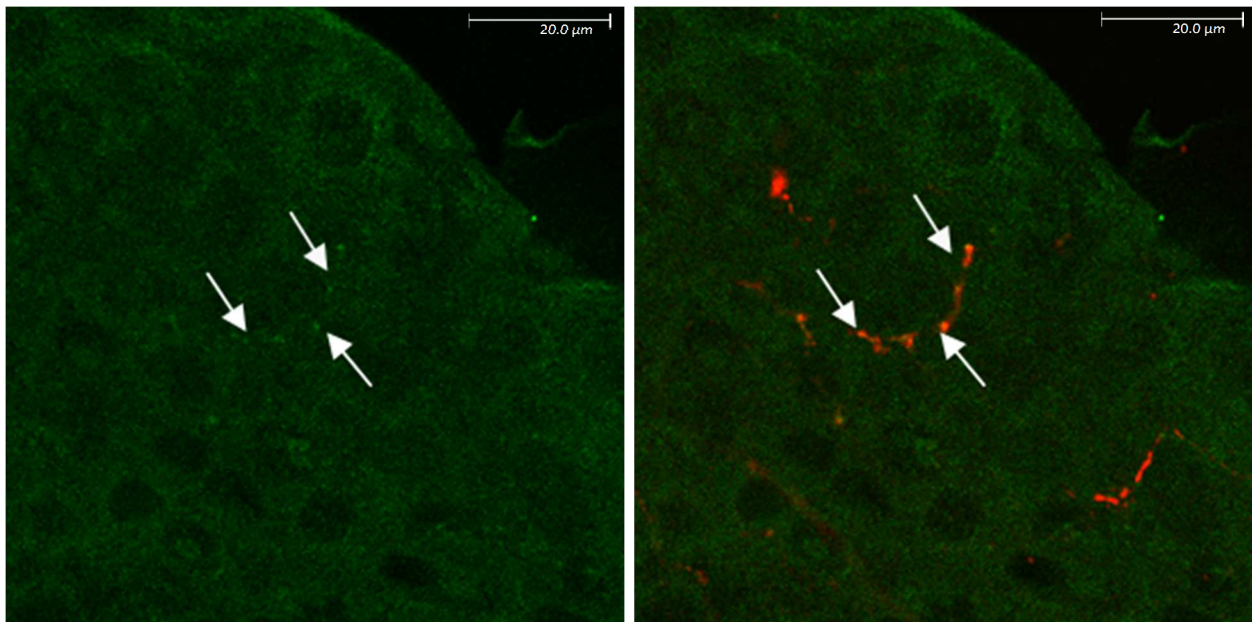


Figure 3.4: Image illustrating corneal epithelial nerve fiber staining (Green: GluK1, Red: PGP 9.5).

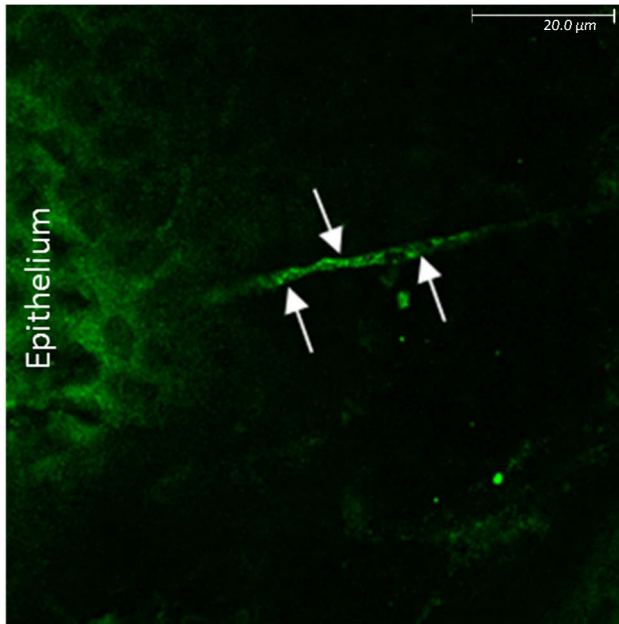


Figure 3.5: Image illustrating corneal stromal nerve fiber staining (GluK5).

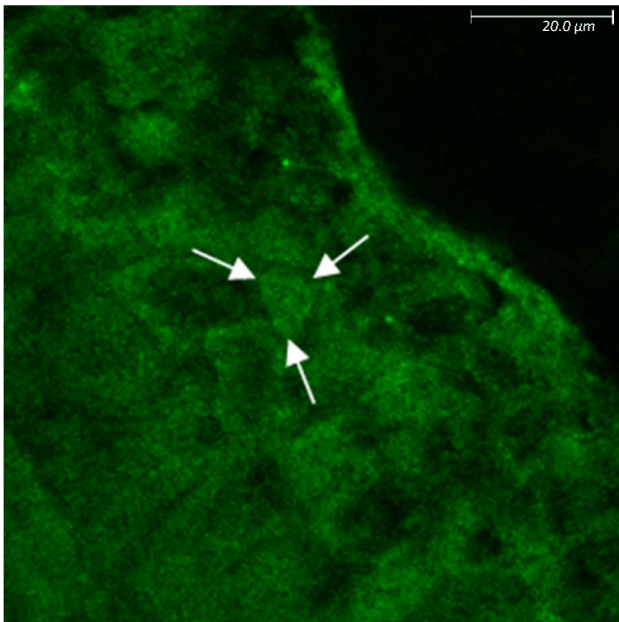


Figure 3.6: Image illustrating corneal cytoplasmic staining (GluN2D).

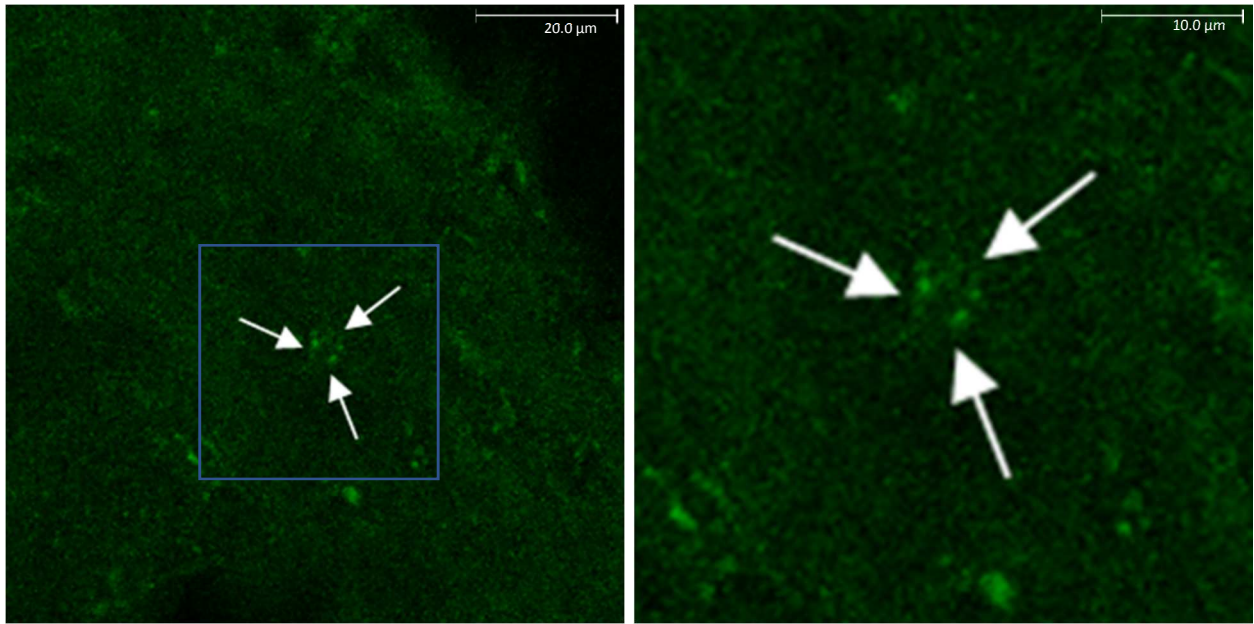


Figure 3.7: Image illustrating corneal nuclear staining and enlarged in right panel (GluN2B).

1.2.2 Trigeminal characteristics

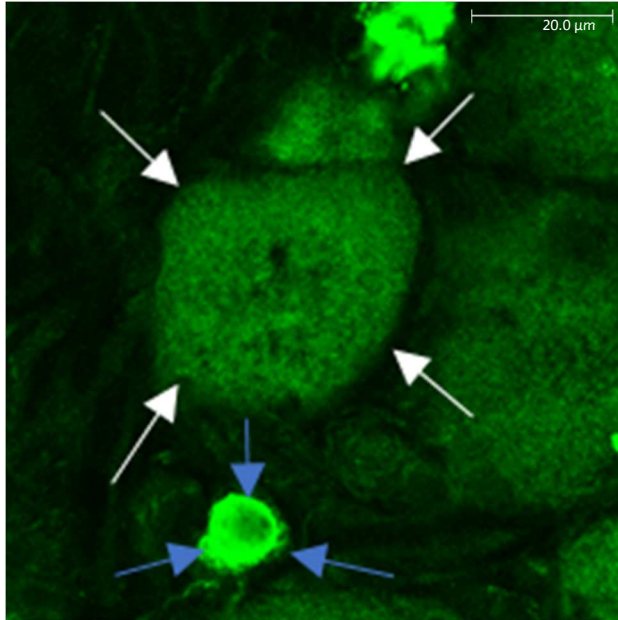


Figure 3.8: Image illustrating Trigeminal large (White arrows) and small (Blue arrows) immunoreactive neuronal cell bodies (GluA2).

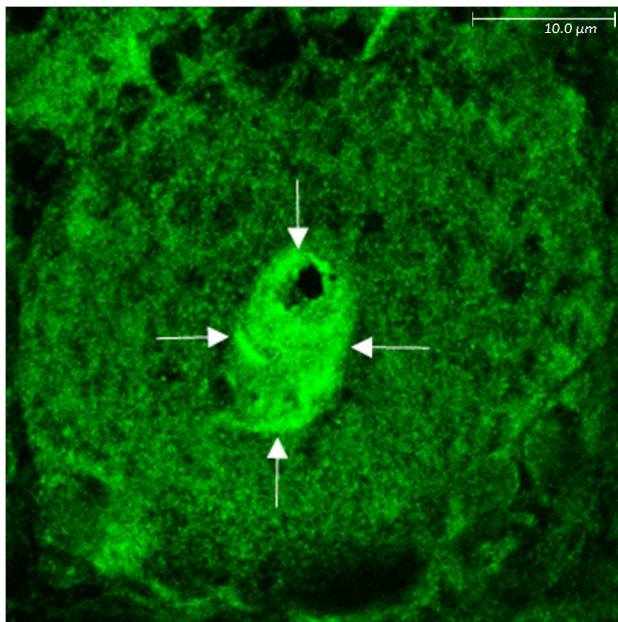


Figure 3.9: Image illustrating Trigeminal nuclear (arrows) immunoreactivity (GluK3) of large neuronal cell body.

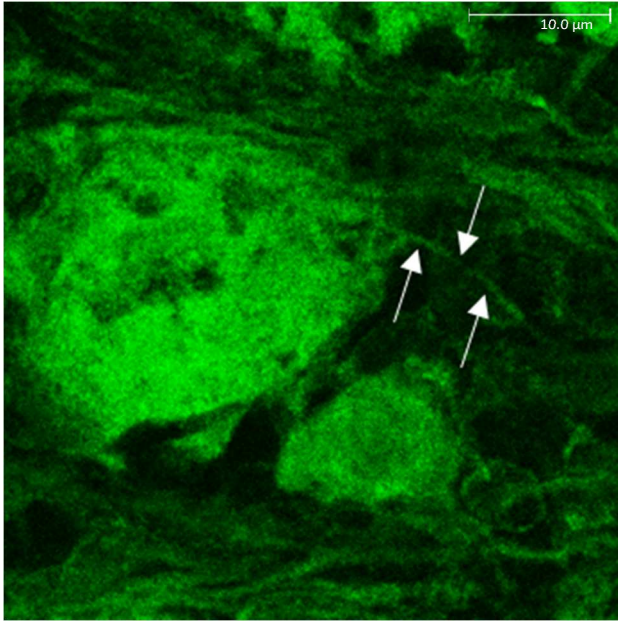


Figure 3.10: Image illustrating Trigeminal nerve fiber (arrows) immunoreactivity (GluN3A).

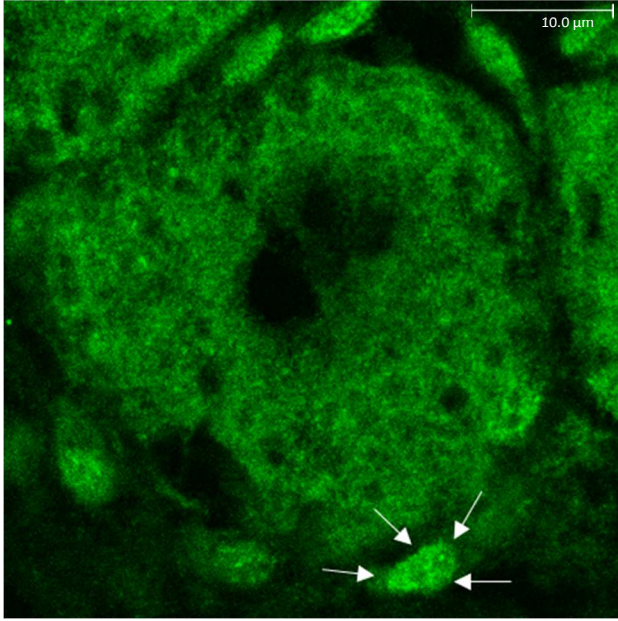


Figure 3.11: Image illustrating Trigeminal satellite (arrows) immunoreactivity (GluN2D).

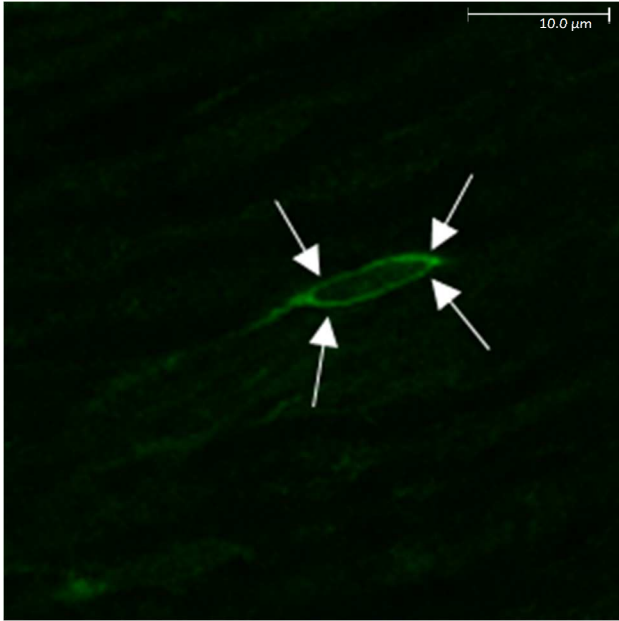


Figure 3.12: Image illustrating Trigeminal Schwann (arrows) immunoreactivity (GluN3A).

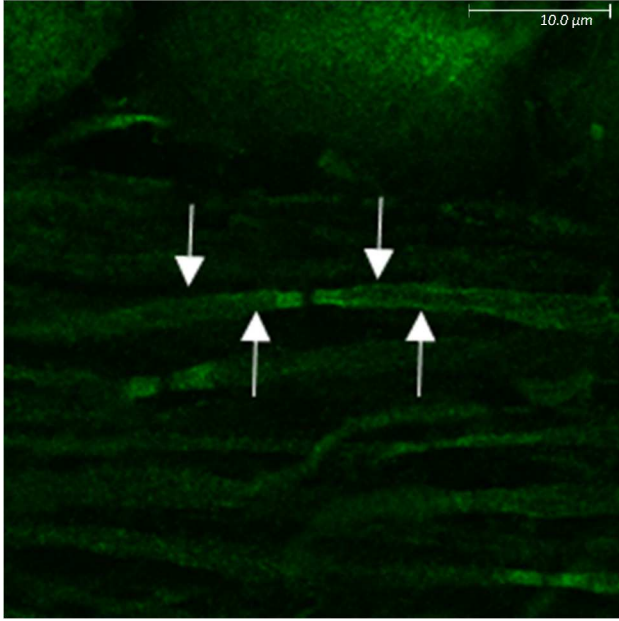


Figure 3.13: Image illustrating Trigeminal myelin (arrows) immunoreactivity (GluK5).

1.2.1 *GluA1*

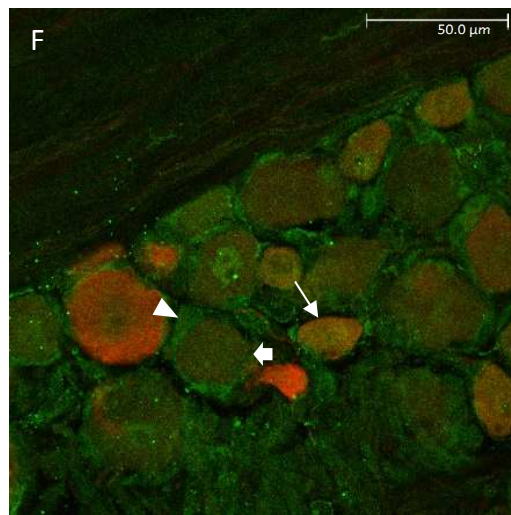
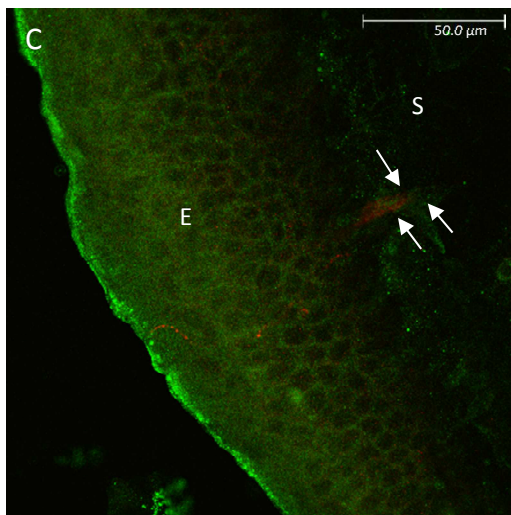
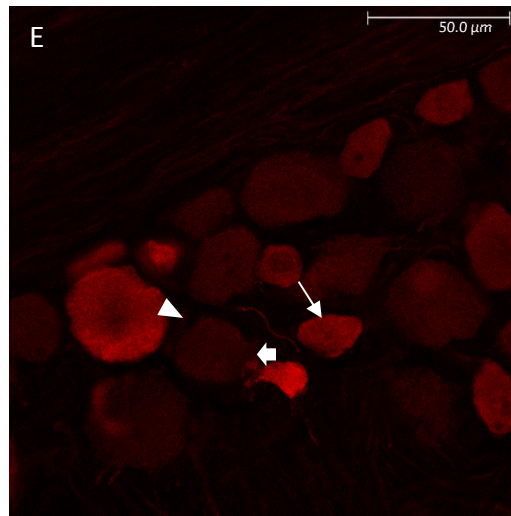
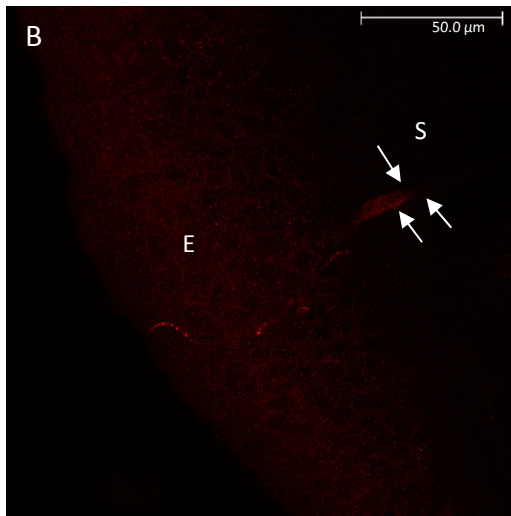
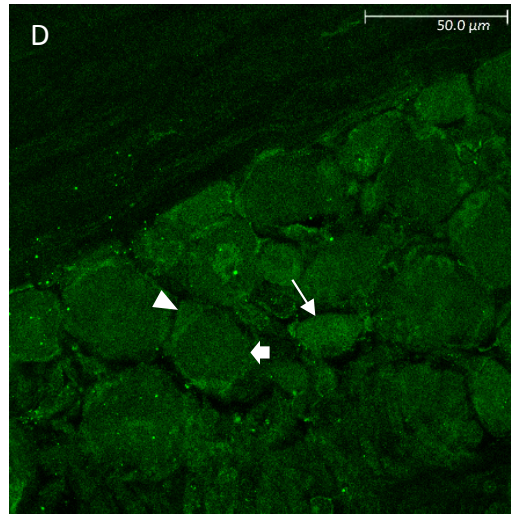
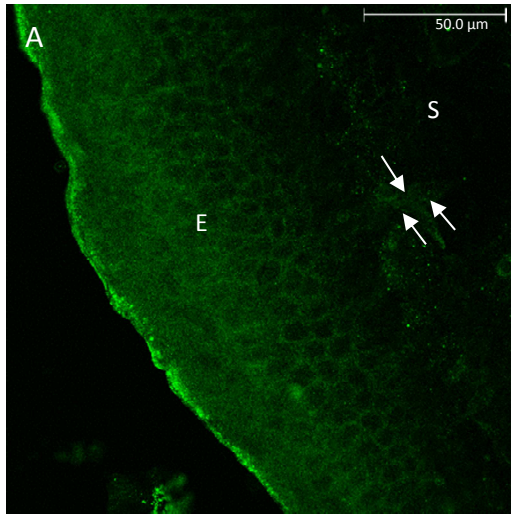


Figure 3.14: Images illustrating Cornea and Trigeminal root ganglion immunoreactivity of GluA1 (Green) and PGP9.5 (Red). Fig1A-C represent immunofluorescent images of GluA1 positive epithelial cells (“E”), Stroma (“S”), and stromal nerve bundles (arrows) in the cornea. Fig1D-F represent immunofluorescent images of GluA1 positive large neuronal cell bodies (thick arrow), small neuronal cell bodies (thin arrow), and satellite cells (arrowhead).

1.2.2 *GluA2*

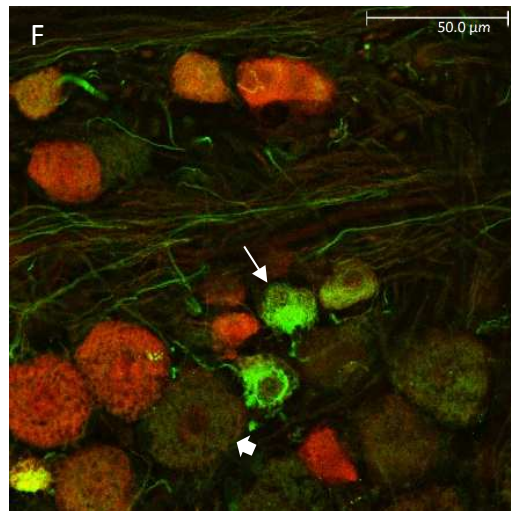
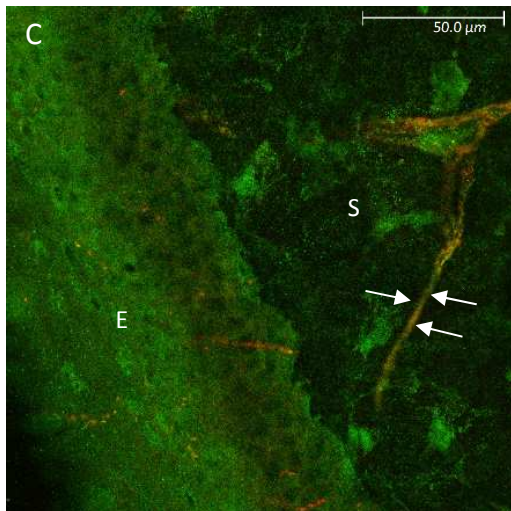
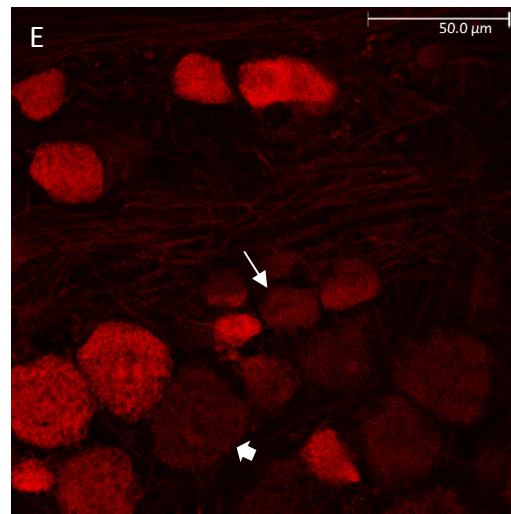
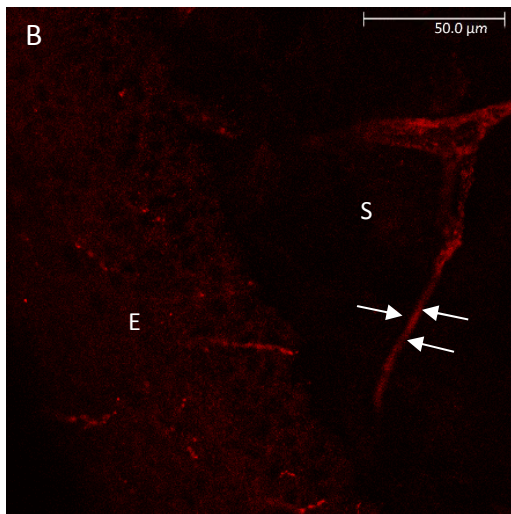
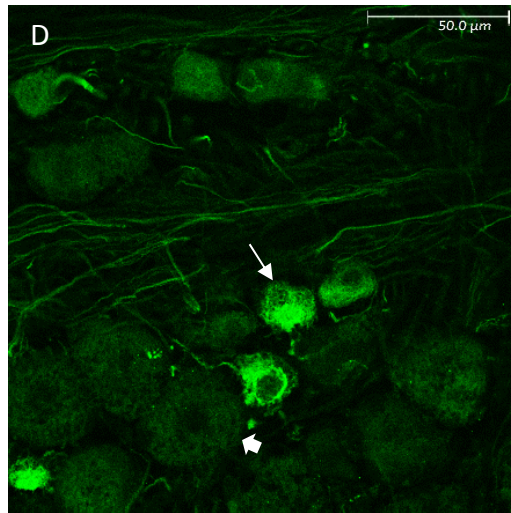
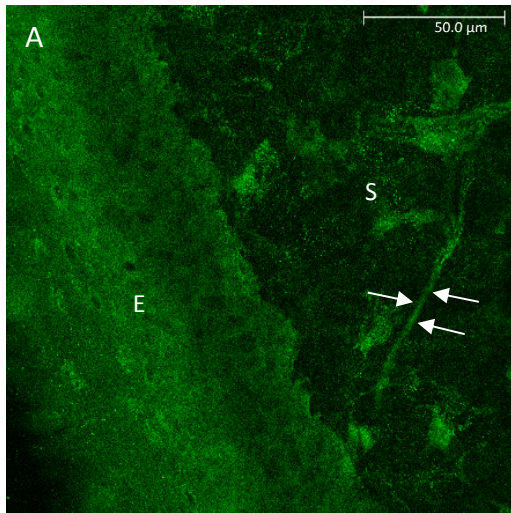


Figure 3.15: Images illustrating Cornea and Trigeminal root ganglion immunoreactivity of GluA2 (Green and PGP9.5 (Red). Fig2A-C represent immunofluorescent images of GluA2 positive epithelial cells (“E”), Stroma (“S”), and stromal nerve bundles (arrows) in the cornea. Fig2D-F represent immunofluorescent images of GluA2 large neuronal cell bodies (thick arrow), and small neuronal cell bodies (thin arrow).

1.2.3 *GluA3*

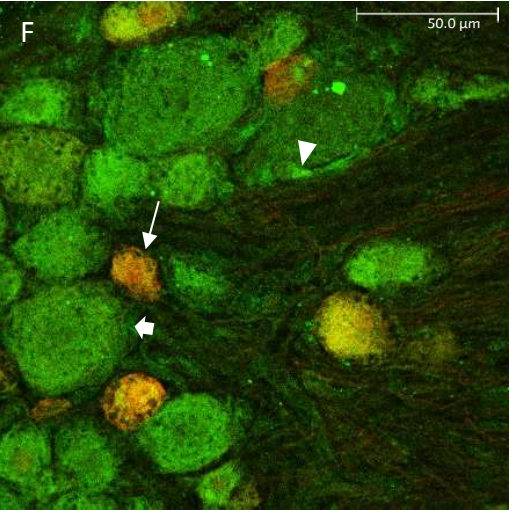
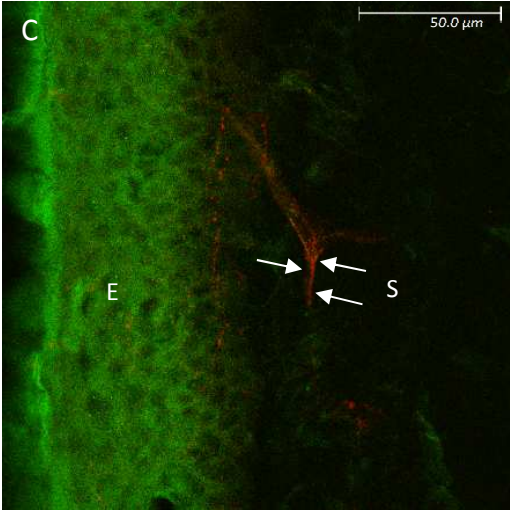
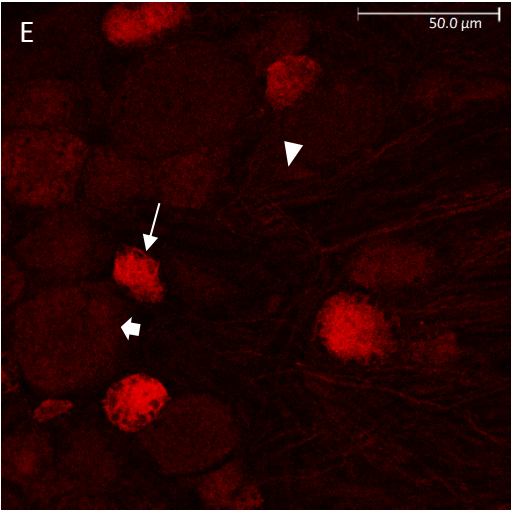
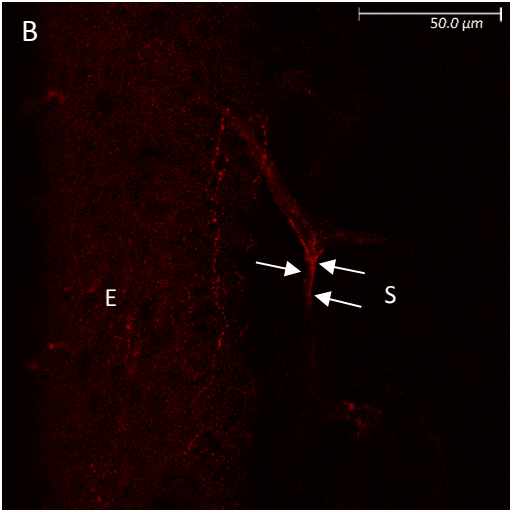
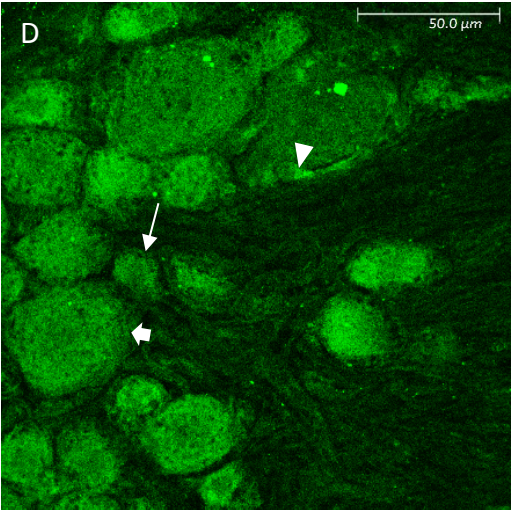
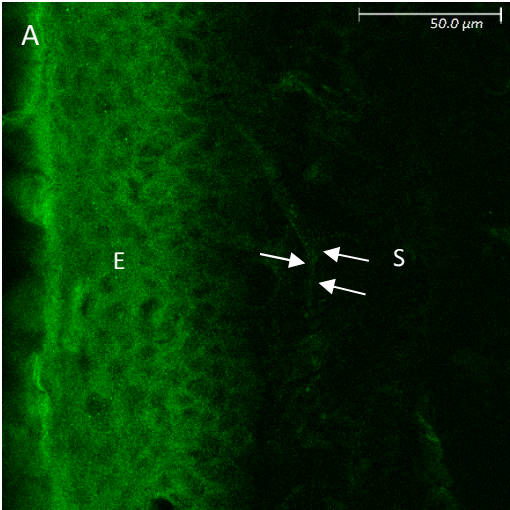


Figure 3.16: Images illustrating Cornea and Trigeminal root ganglion immunoreactivity of GluA3 (Green) and PGP9.5 (Red). Fig3A-C represent immunofluorescent images of GluA3 positive epithelial cells (“E”), Stroma (“S”), and stromal nerve bundles (arrows) in the cornea. Fig3D-F represent immunofluorescent images of GluA3 positive large neuronal cell bodies (thick arrow), small neuronal cell bodies (thin arrow), and satellite cells (arrowhead).

1.2.4 *GluA4*

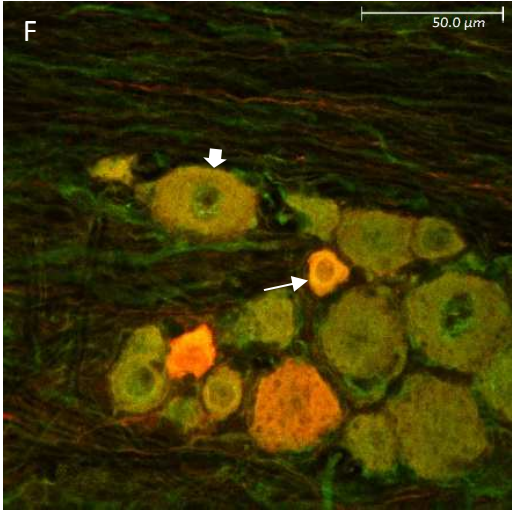
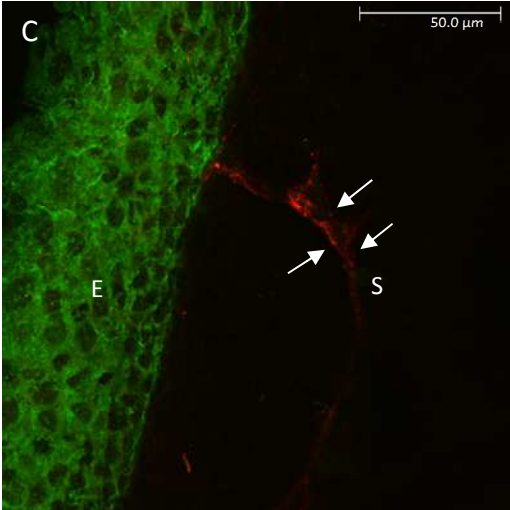
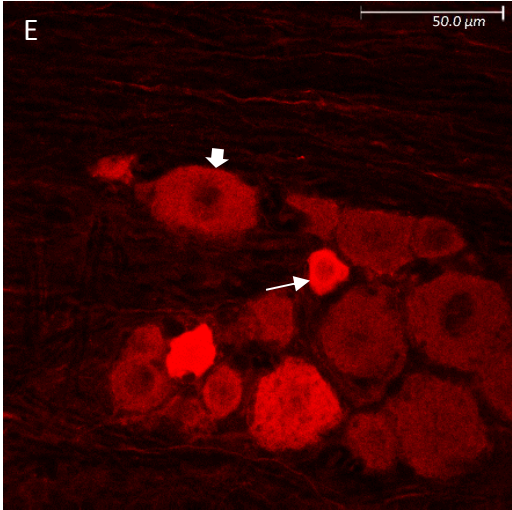
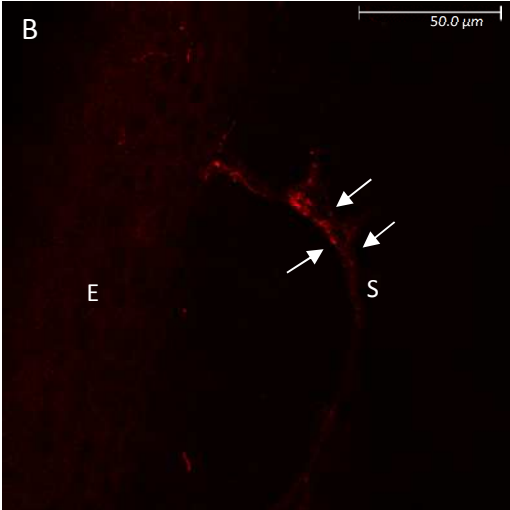
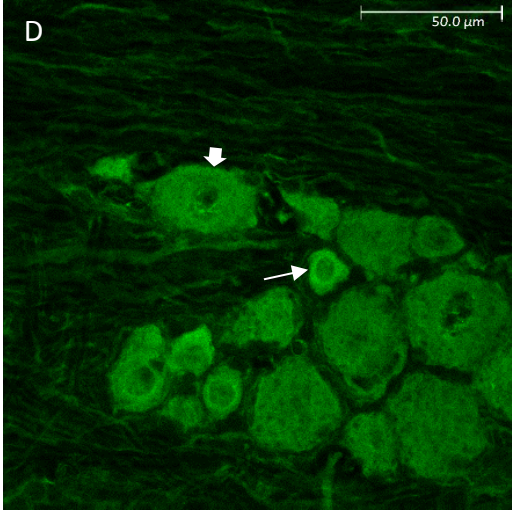
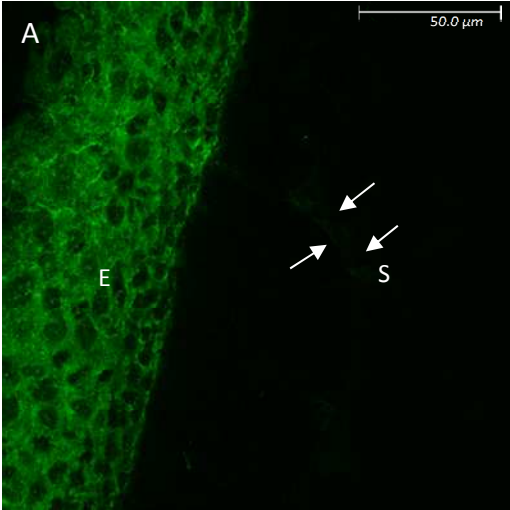


Figure 3.17: Images illustrating Cornea and Trigeminal root ganglion immunoreactivity of GluA4 (Green) and CGRP (Red). Fig4A-C represent immunofluorescent images of GluA4 positive epithelial cells (“E”), Stroma (“S”), and stromal nerve bundles (arrows) in the cornea. Fig4D-F represent immunofluorescent images of GluA4 positive large neuronal cell bodies (thick arrow), and small neuronal cell bodies (thin arrow).

1.2.5 *GluK1*

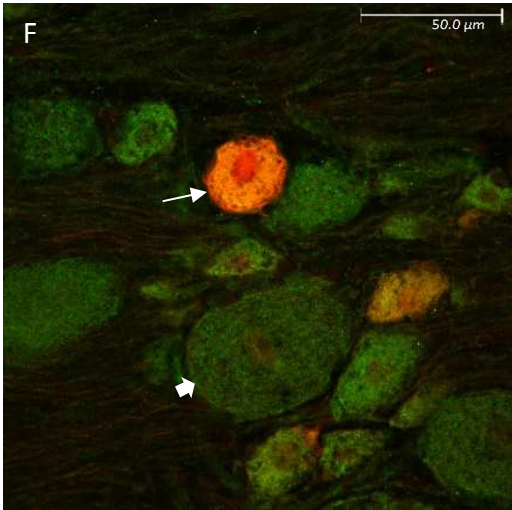
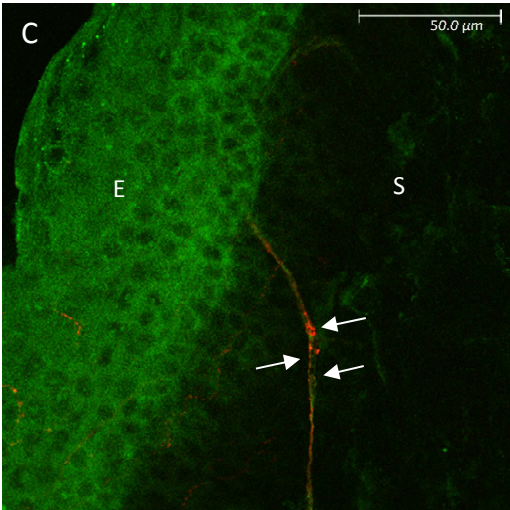
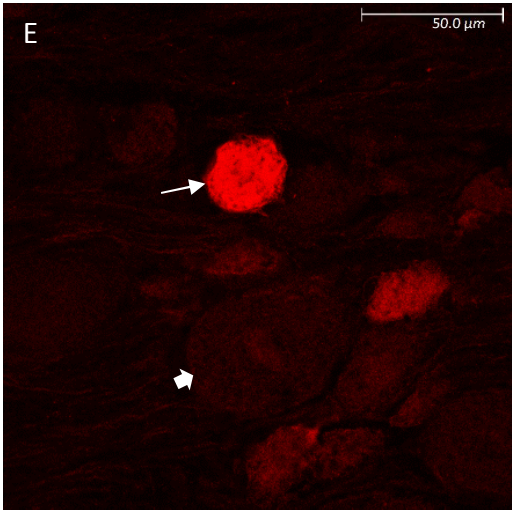
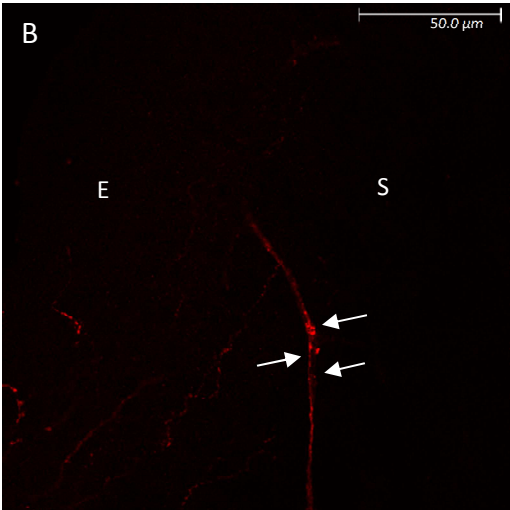
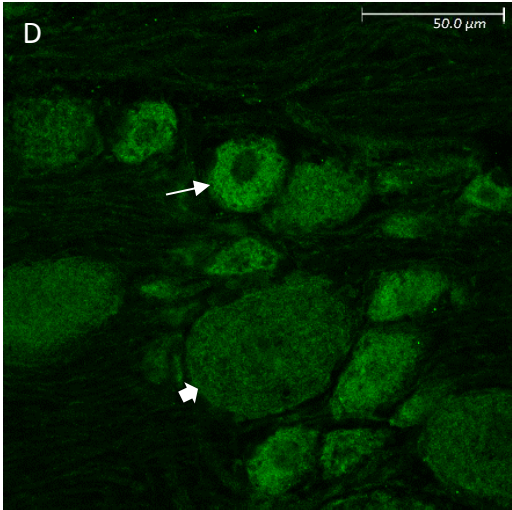
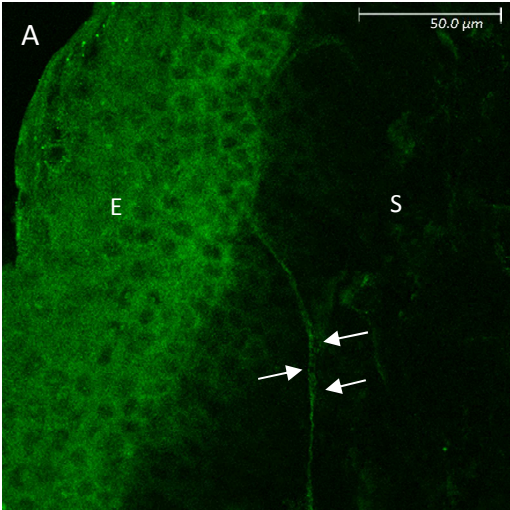


Figure 3.18: Images illustrating Cornea and Trigeminal root ganglion immunoreactivity of GluK1 (Green) and PGP9.5 (Red). Fig5A-C represent immunofluorescent images of GluK1 positive epithelial cells (“E”), Stroma (“S”), and stromal nerve bundles (arrows) in the cornea. Fig5D-F represent immunofluorescent images of GluK1 positive large neuronal cell bodies (thick arrow), and small neuronal cell bodies (thin arrow).

1.2.6 *GluK2*

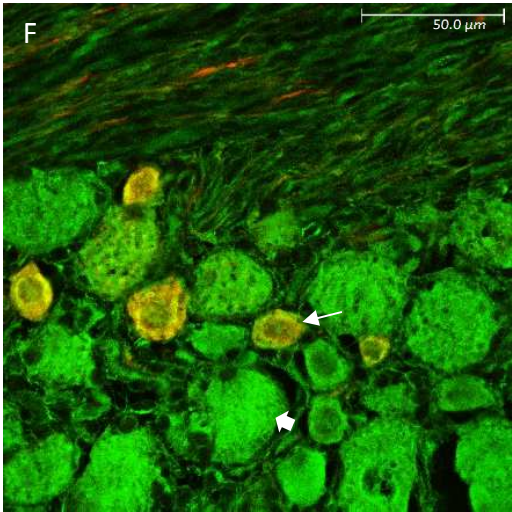
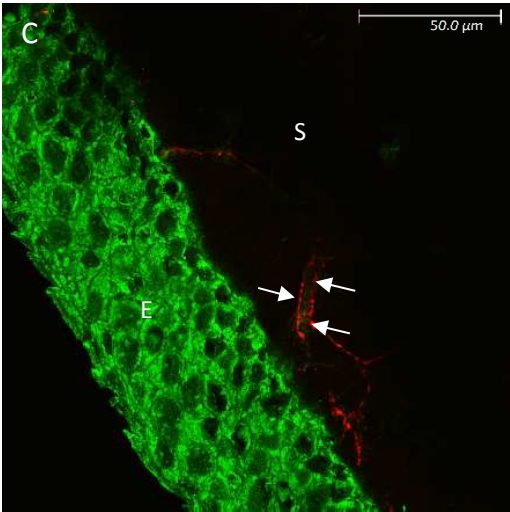
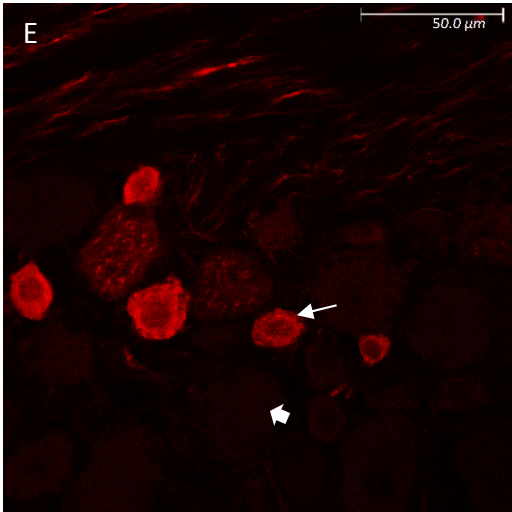
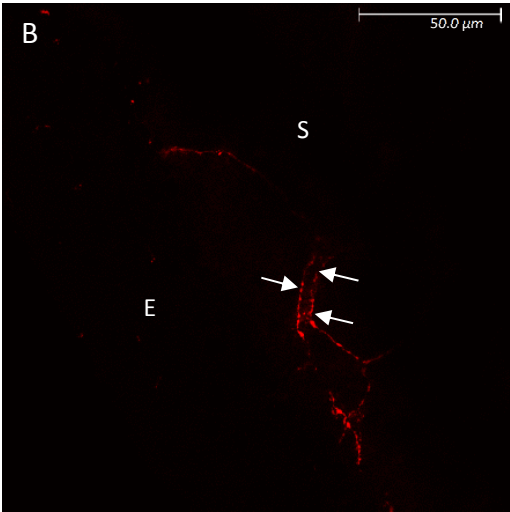
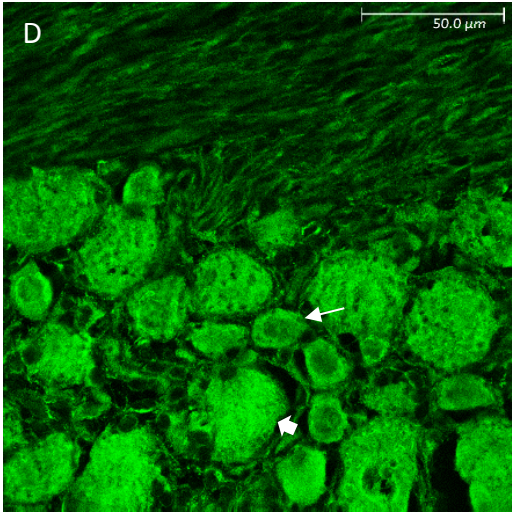
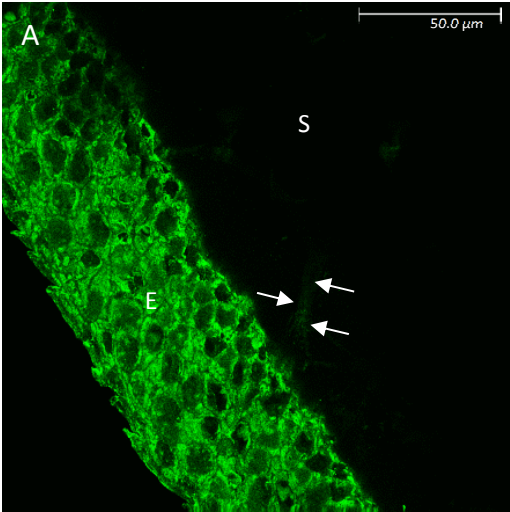


Figure 3.19: Images illustrating Cornea and Trigeminal root ganglion immunoreactivity of GluK2 (Green) and CGRP (Red). Fig6A-C represent immunofluorescent images of GluK2 positive epithelial cells (“E”), Stroma (“S”), and stromal nerve bundles (arrows) in the cornea. Fig6D-F represent immunofluorescent images of GluK2 positive large neuronal cell bodies (thick arrow), small neuronal cell bodies (thin arrow), and satellite cells (arrowhead).

1.2.7 *GluK3*

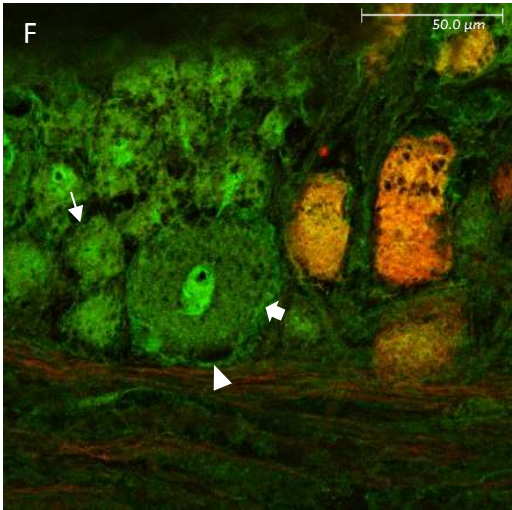
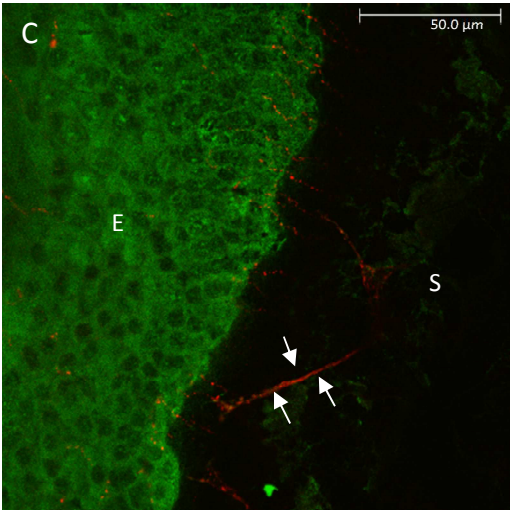
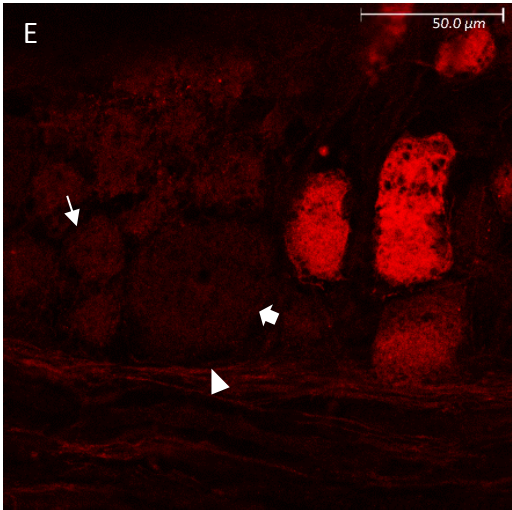
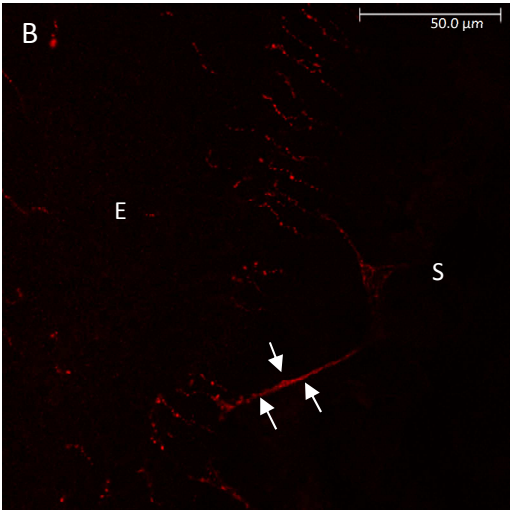
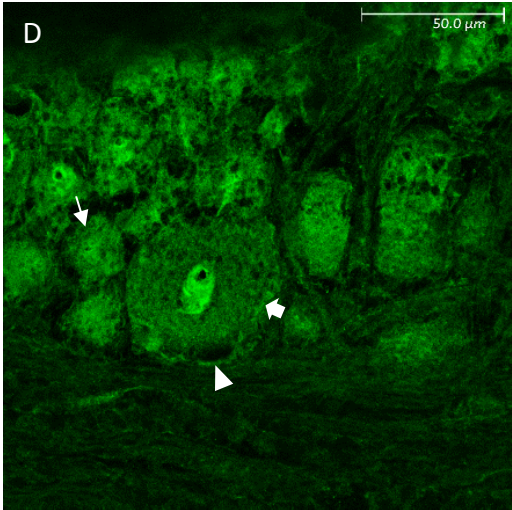
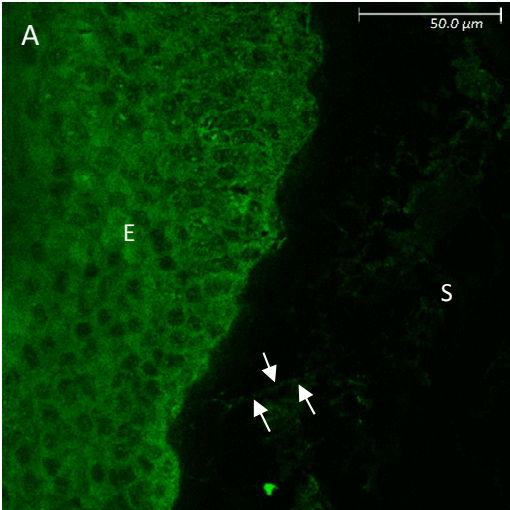


Figure 3.20: Images illustrating Cornea and Trigeminal root ganglion immunoreactivity of GluK3 (Green) and PGP9.5 (Red). Fig7A-C represent immunofluorescent images of GluK3 positive epithelial cells (“E”), Stroma (“S”), and stromal nerve bundles (arrows) in the cornea. Fig7D-F represent immunofluorescent images of GluK3 positive large neuronal cell bodies (thick arrow), small neuronal cell bodies (thin arrow), and satellite cells (arrowhead).

1.2.8 *GluK4*

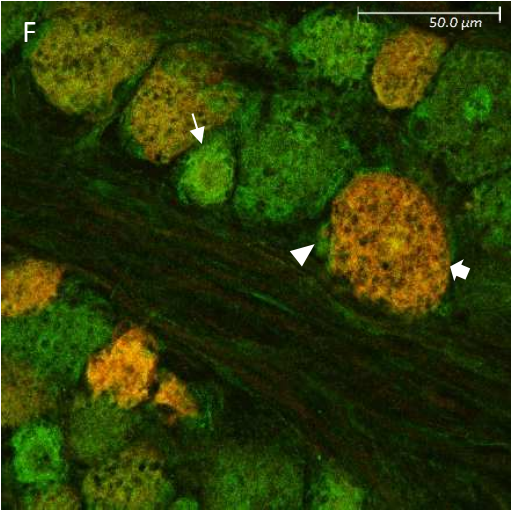
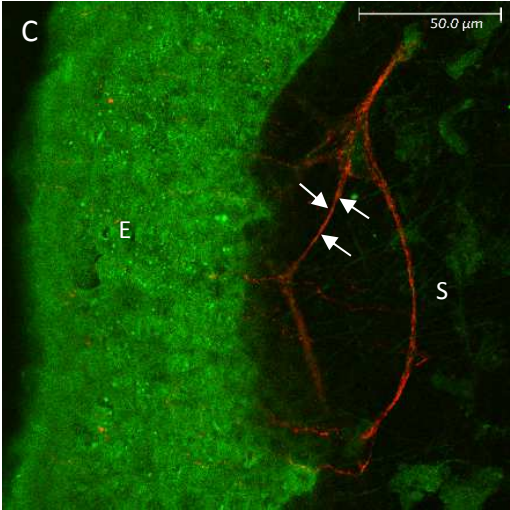
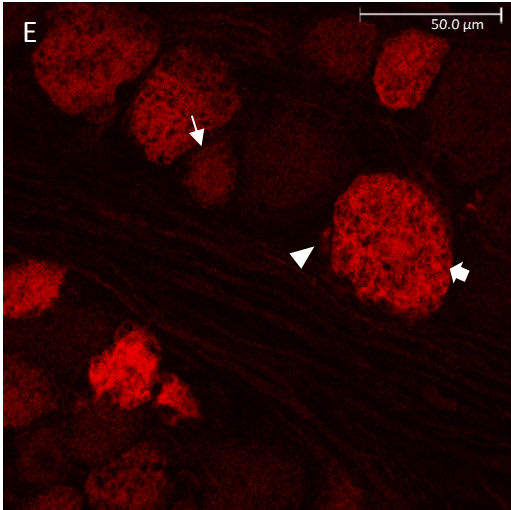
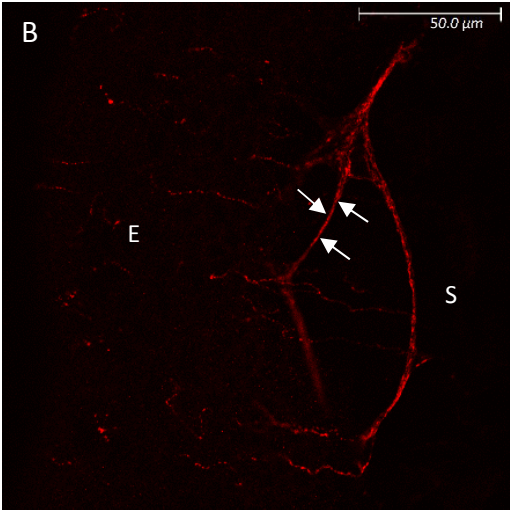
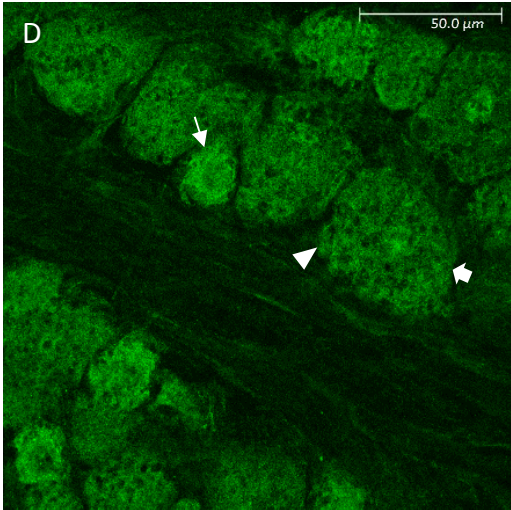
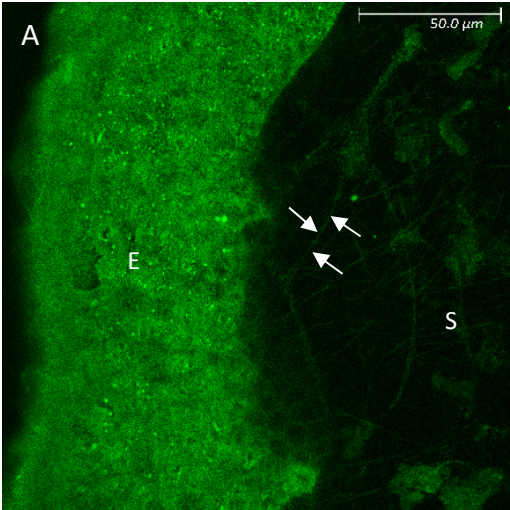


Figure 3.21: Images illustrating Cornea and Trigeminal root ganglion immunoreactivity of GluK4 (Green) and PGP9.5 (Red). Fig8A-C represent immunofluorescent images of GluK4 positive epithelial cells (“E”), Stroma (“S”), and stromal nerve bundles (arrows) in the cornea. Fig8D-F represent immunofluorescent images of GluK4 positive large neuronal cell bodies (thick arrow), small neuronal cell bodies (thin arrow), and satellite cells (arrowhead).

1.2.9 *GluK5*

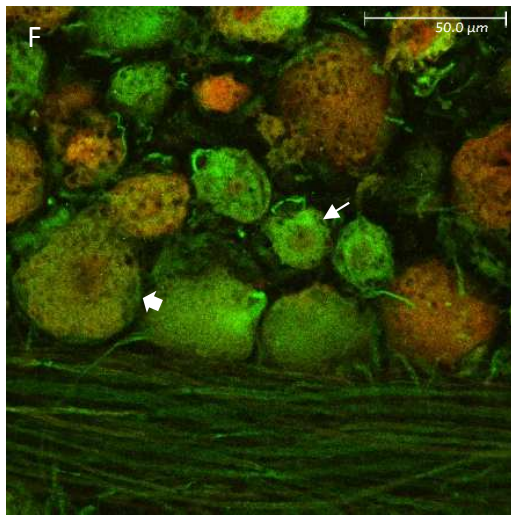
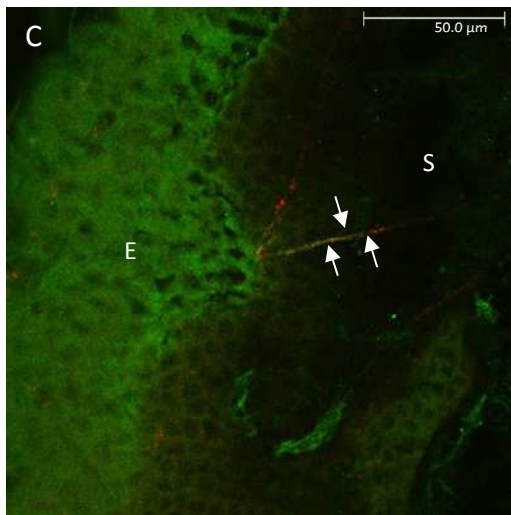
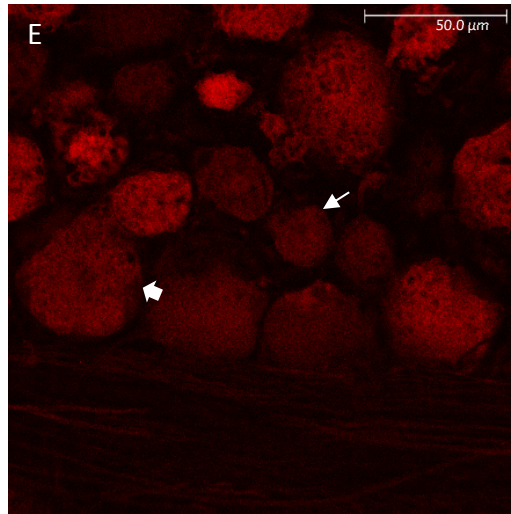
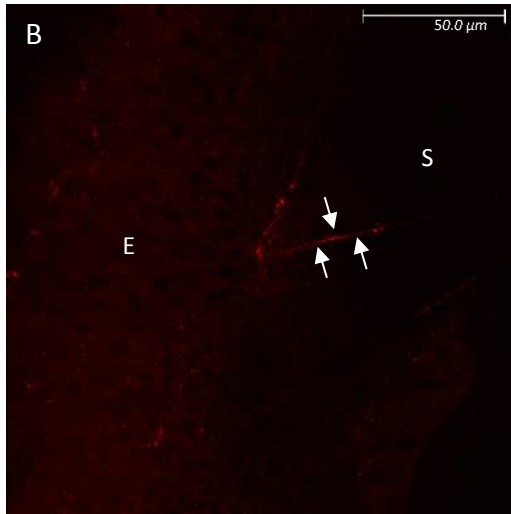
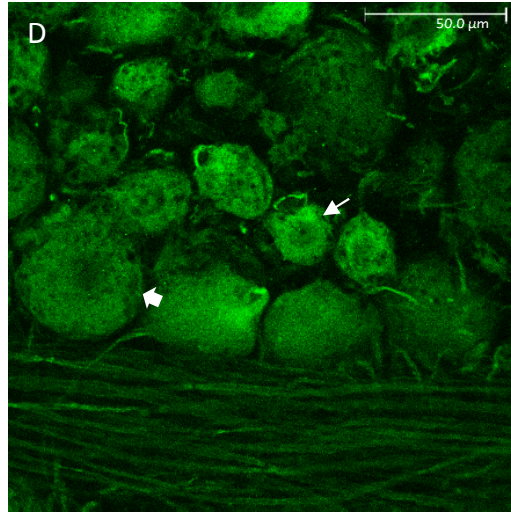
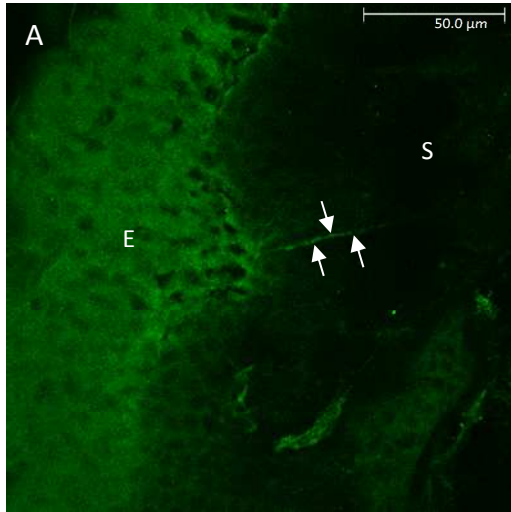


Figure 3.22: Images illustrating Cornea and Trigeminal root ganglion immunoreactivity of GluK5 (Green) and PGP9.5 (Red). Fig9A-C represent immunofluorescent images of GluK5 positive epithelial cells (“E”), Stroma (“S”), and stromal nerve bundles (arrows) in the cornea. Fig9D-F represent immunofluorescent images of GluK5 positive large neuronal cell bodies (thick arrow), and small neuronal cell bodies (thin arrow).

1.2.10 *GluN1*

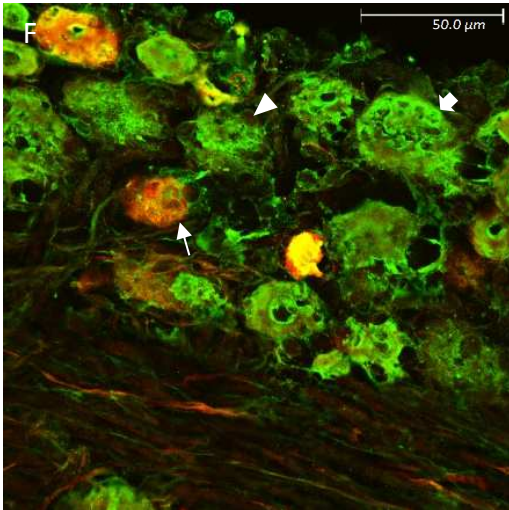
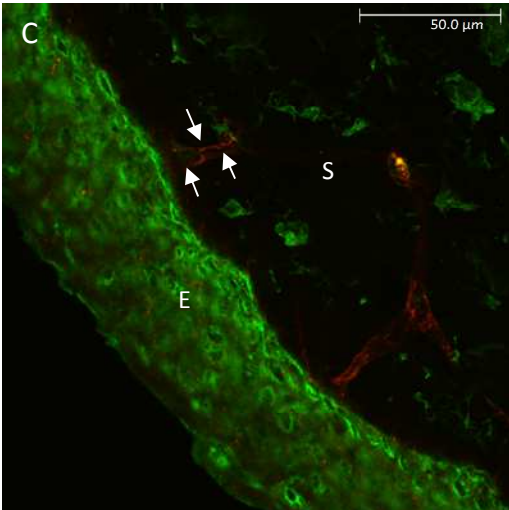
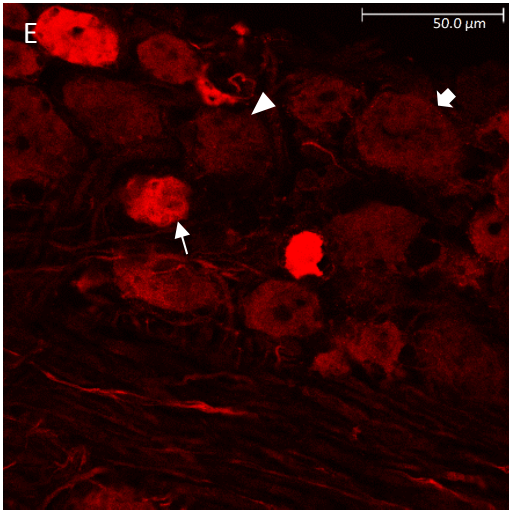
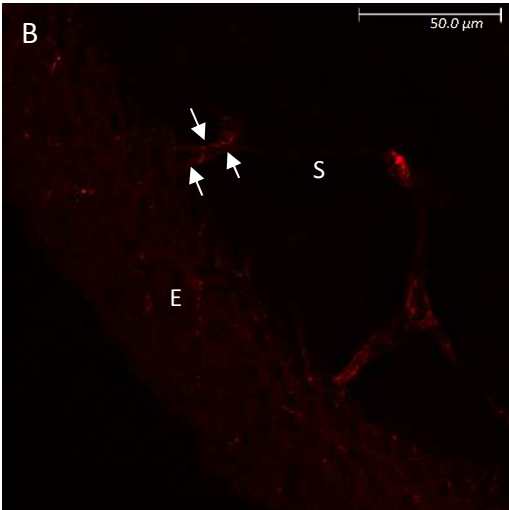
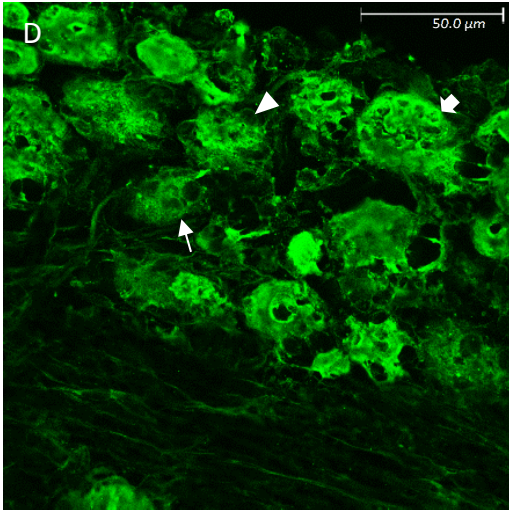
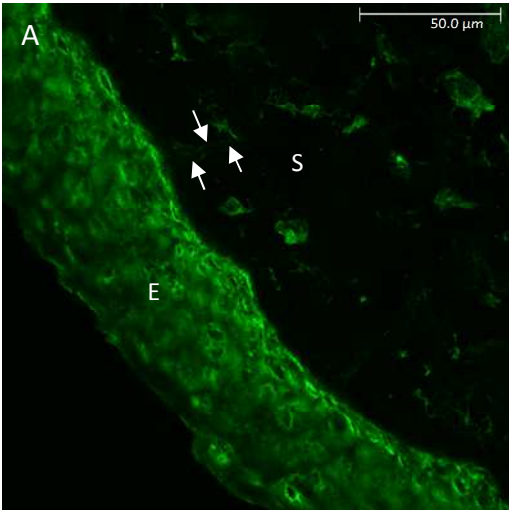


Figure 3.23: Images illustrating Cornea and Trigeminal root ganglion immunoreactivity of GluN1 (Green) and PGP9.5 (Red). Fig10A-C represent immunofluorescent images of GluN1 positive epithelial cells (“E”), Stroma (“S”), and stromal nerve bundles (arrows) in the cornea. Fig10D-F represent immunofluorescent images of GluN1 positive large neuronal cell bodies (thick arrow), small neuronal cell bodies (thin arrow), and satellite cells (arrowhead).

1.2.11 *GluN2A*

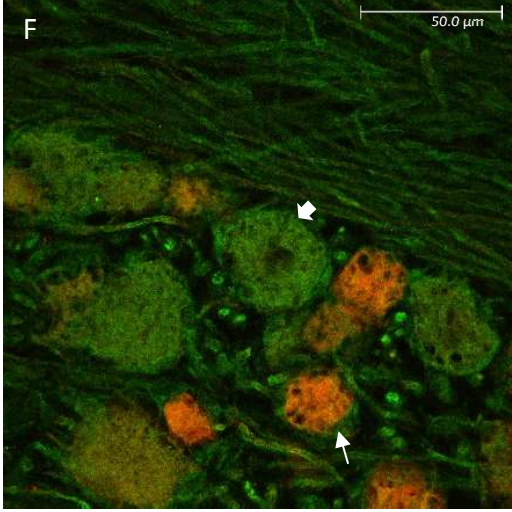
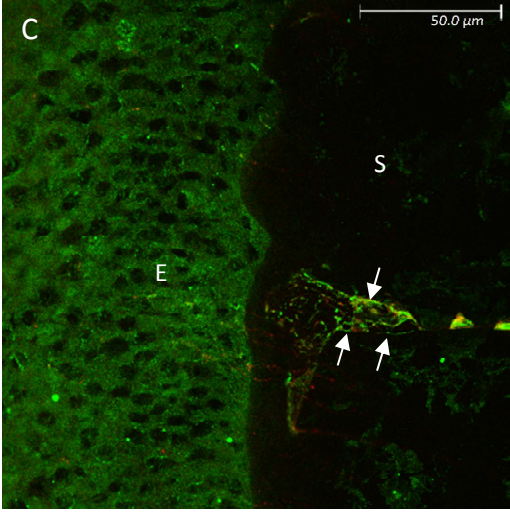
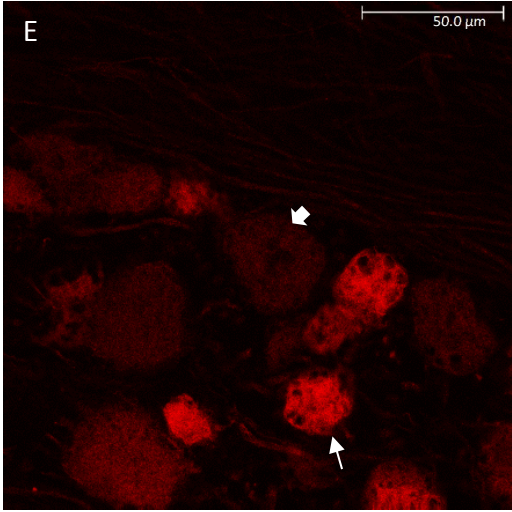
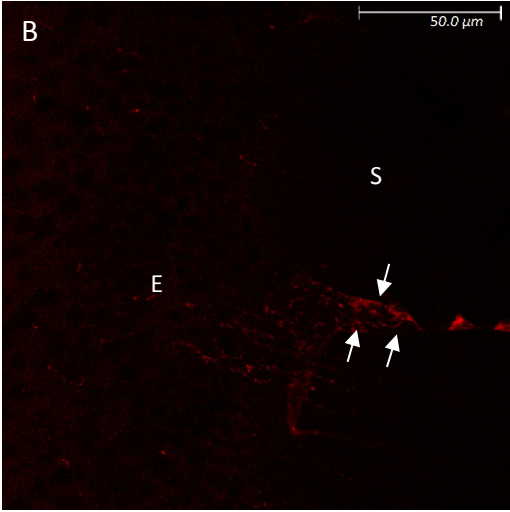
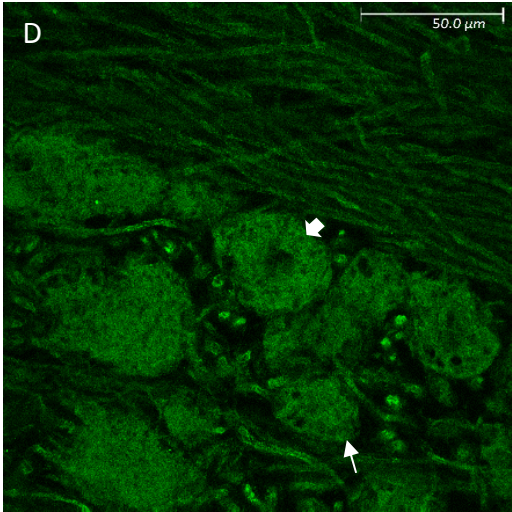
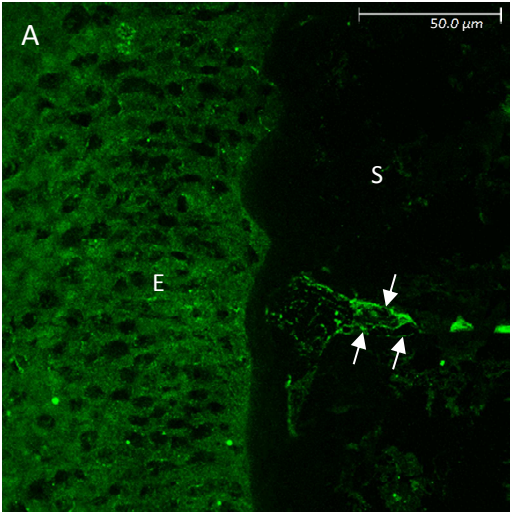


Figure 3.24: Images illustrating Cornea and Trigeminal root ganglion immunoreactivity of GluN2A (Green) and PGP9.5 (Red). Fig11A-C represent immunofluorescent images of GluN2A positive epithelial cells (“E”), Stroma (“S”), and stromal nerve bundles (arrows) in the cornea. Fig11D-F represent immunofluorescent images of GluN2A positive large neuronal cell bodies (thick arrow), and small neuronal cell bodies (thin arrow).

1.2.12 *GluN2B*

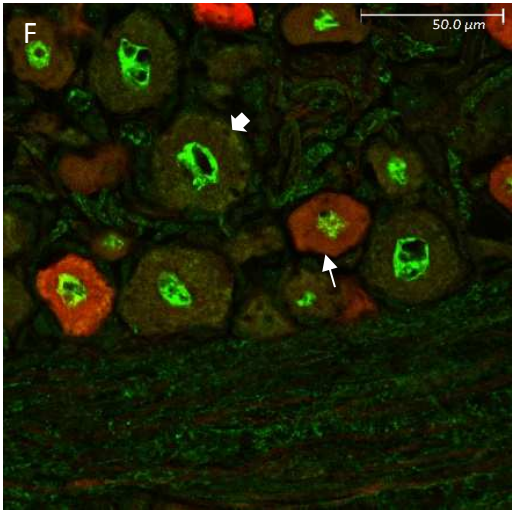
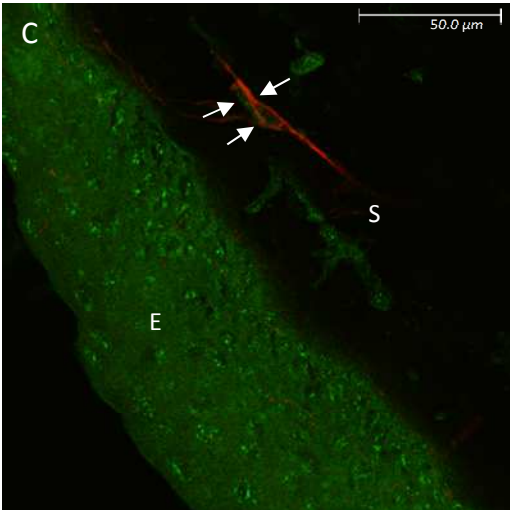
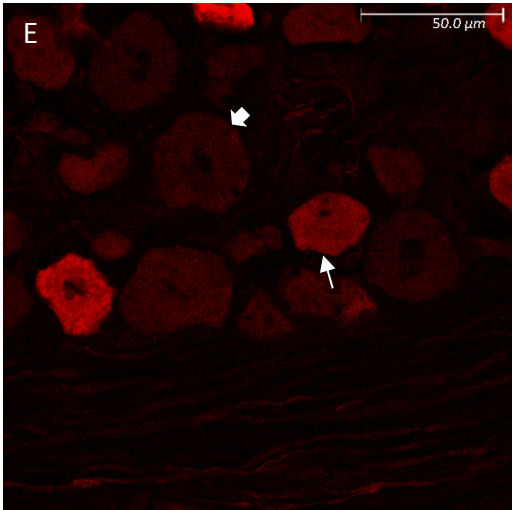
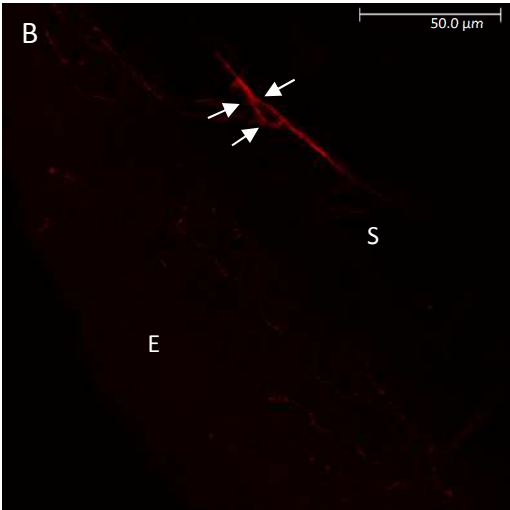
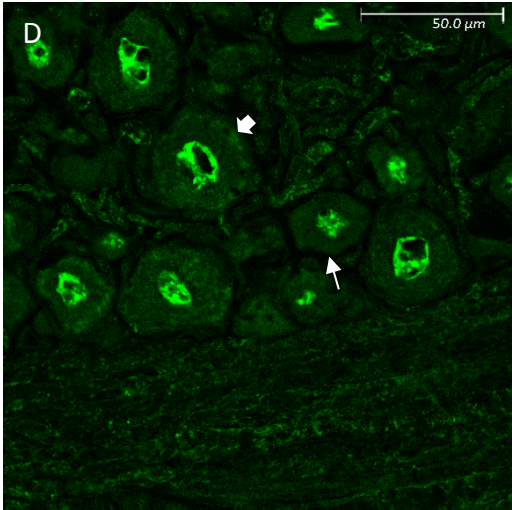
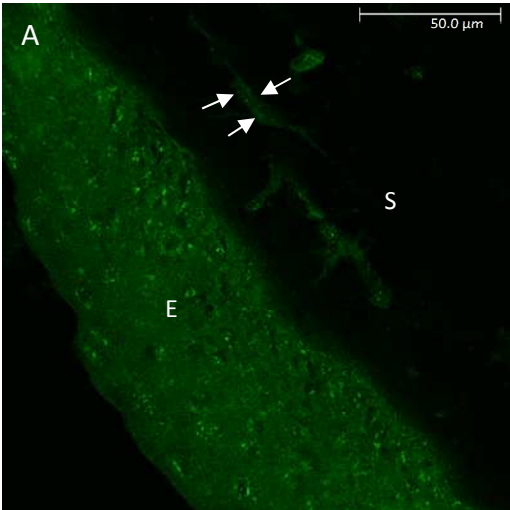


Figure 3.25: Images illustrating Cornea and Trigeminal root ganglion immunoreactivity of GluN2B (Green) and PGP9.5 (Red). Fig12A-C represent immunofluorescent images of GluN2B positive epithelial cells (“E”), Stroma (“S”), and stromal nerve bundles (arrows) in the cornea. Fig12D-F represent immunofluorescent images of GluN2B positive large neuronal cell bodies (thick arrow), and small neuronal cell bodies (thin arrow).

1.2.13 *GluN2C*

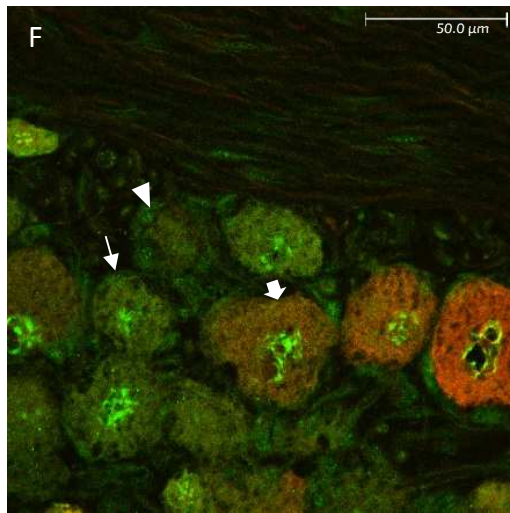
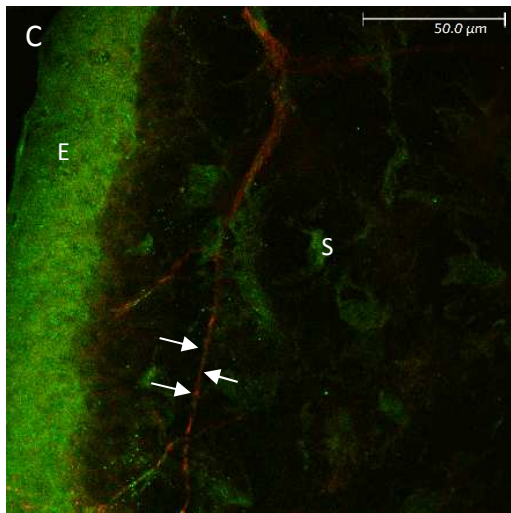
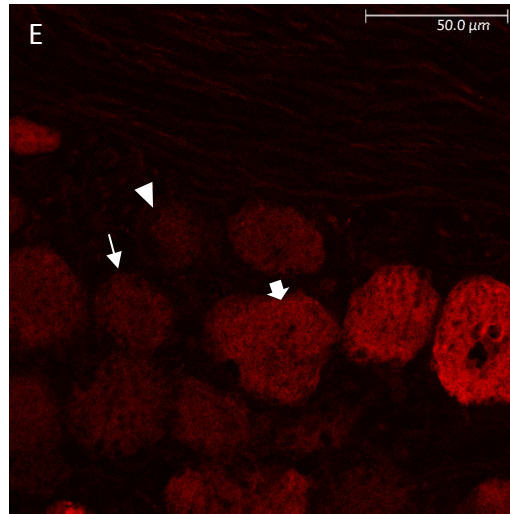
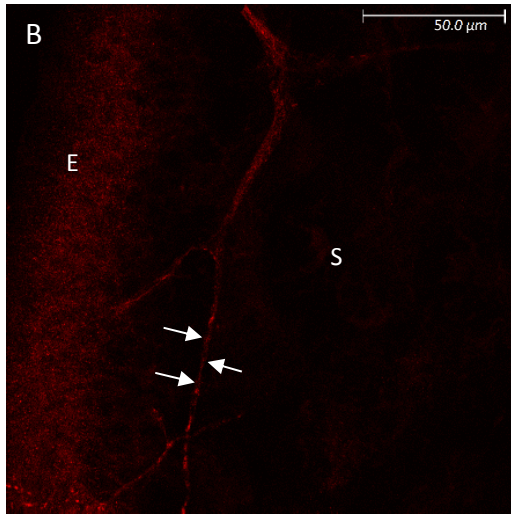
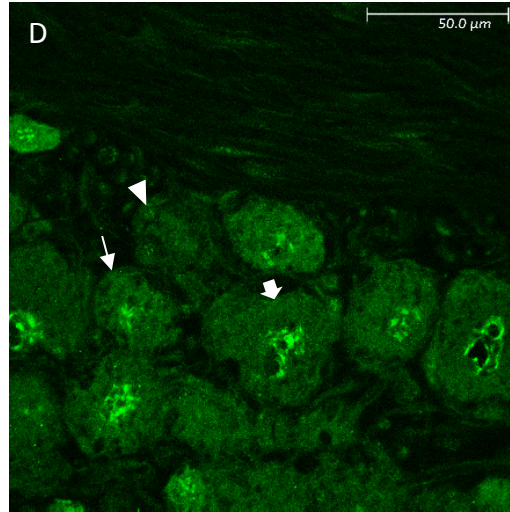
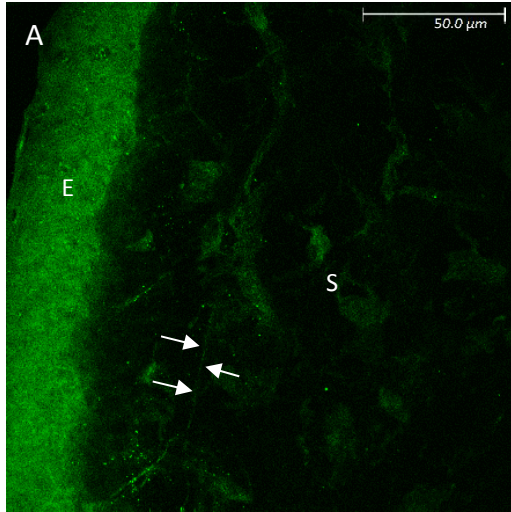


Figure 3.26: Images illustrating Cornea and Trigeminal root ganglion immunoreactivity of GluN2C (Green) and PGP9.5 (Red). Fig13A-C represent immunofluorescent images of GluN2C positive epithelial cells (“E”), Stroma (“S”), and stromal nerve bundles (arrows) in the cornea. Fig13D-F represent immunofluorescent images of GluN2C positive large neuronal cell bodies (thick arrow), small neuronal cell bodies (thin arrow), and satellite cells (arrowhead).

1.2.14 *GluN2D*

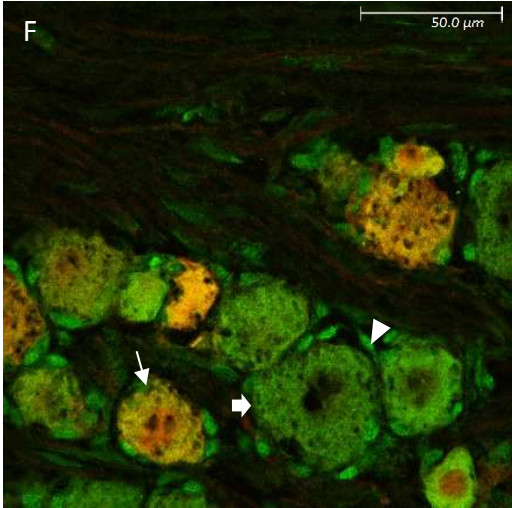
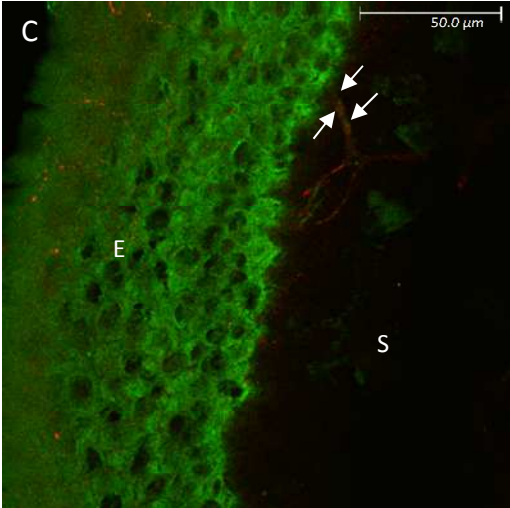
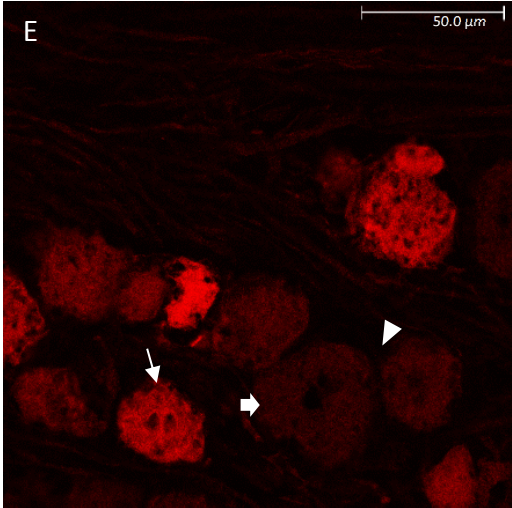
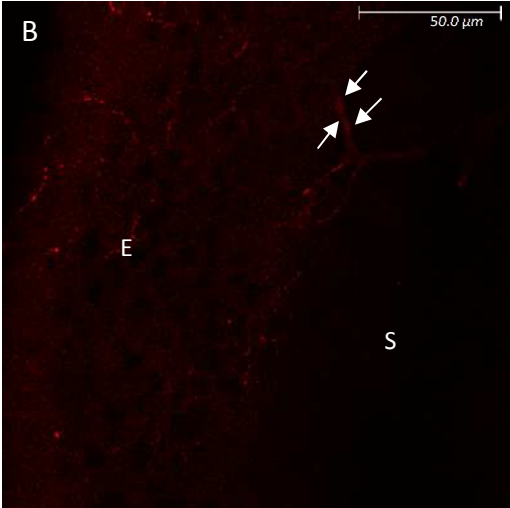
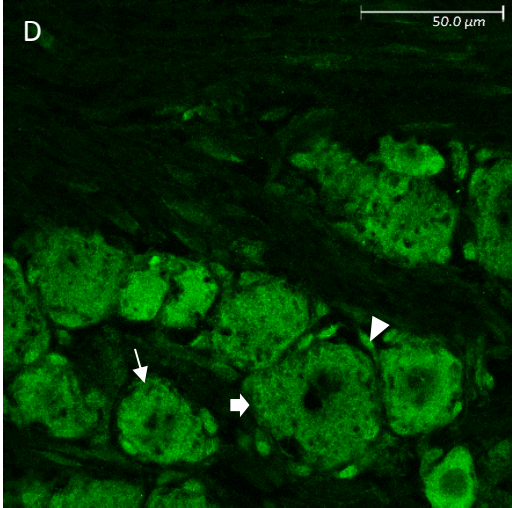
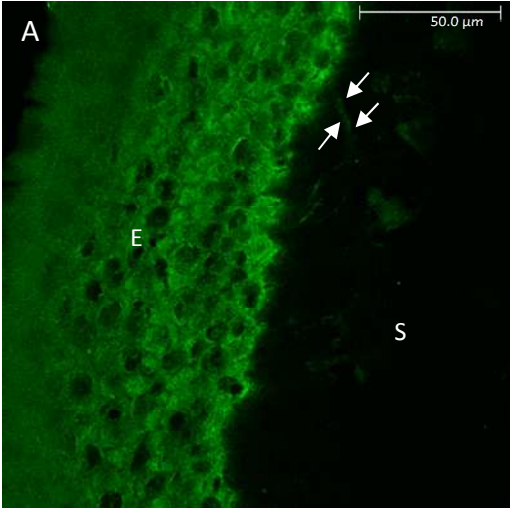


Figure 3.27: Images illustrating Cornea and Trigeminal root ganglion immunoreactivity of GluN2D (Green) and PGP9.5 (Red). Fig14A-C represent immunofluorescent images of GluN2D positive epithelial cells (“E”), Stroma (“S”), and stromal nerve bundles (arrows) in the cornea. Fig14D-F represent immunofluorescent images of GluN2D positive large neuronal cell bodies (thick arrow), small neuronal cell bodies (thin arrow), and satellite cells (arrowhead).

1.2.15 *GluN3A*

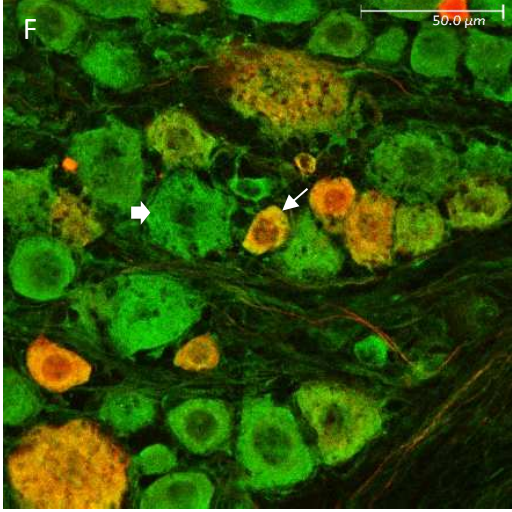
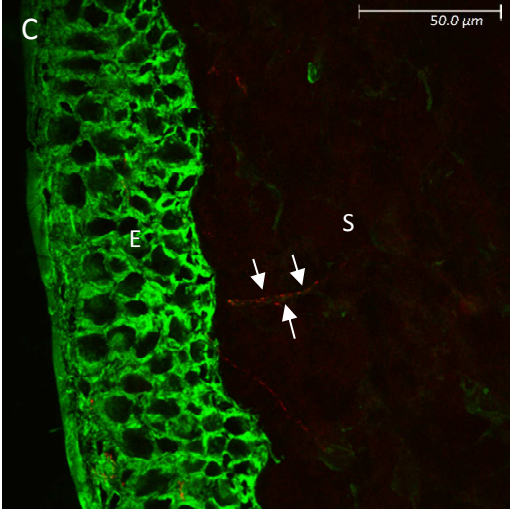
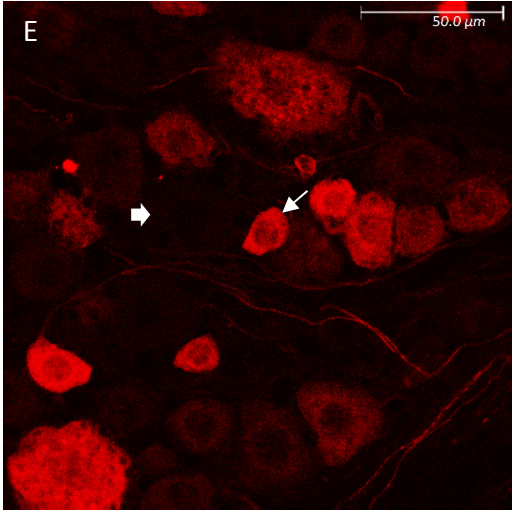
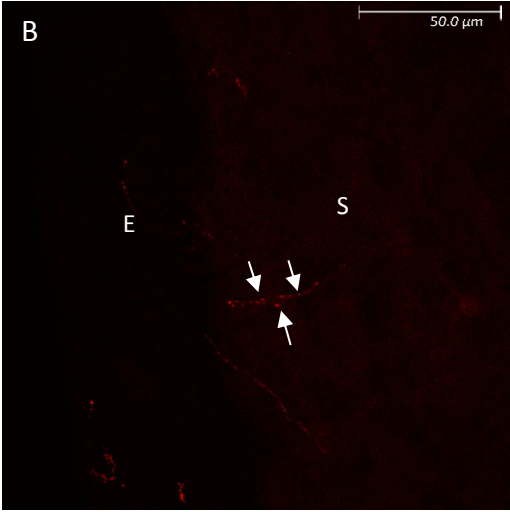
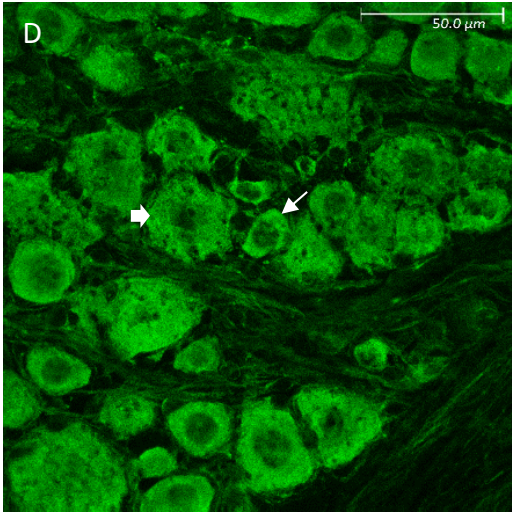
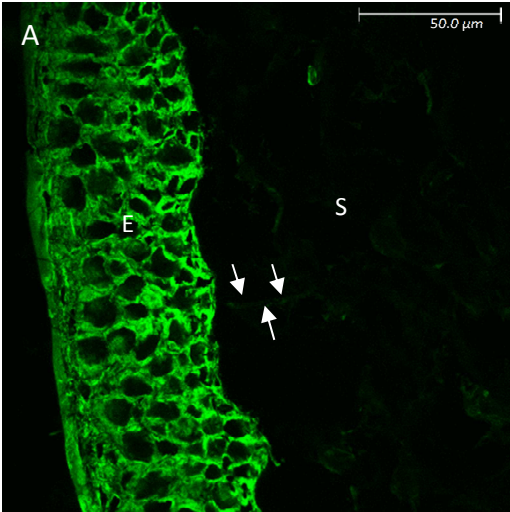


Figure 3.28: Images illustrating Cornea and Trigeminal root ganglion immunoreactivity of GluN3A (Green) and CGRP (Red). Fig15A-C represent immunofluorescent images of GluN3A positive epithelial cells (“E”), Stroma (“S”), and stromal nerve bundles (arrows) in the cornea. Fig15D-F represent immunofluorescent images of GluN3B positive large neuronal cell bodies (thick arrow), and small neuronal cell bodies (thin arrow).

1.2.16 *GluN3B*

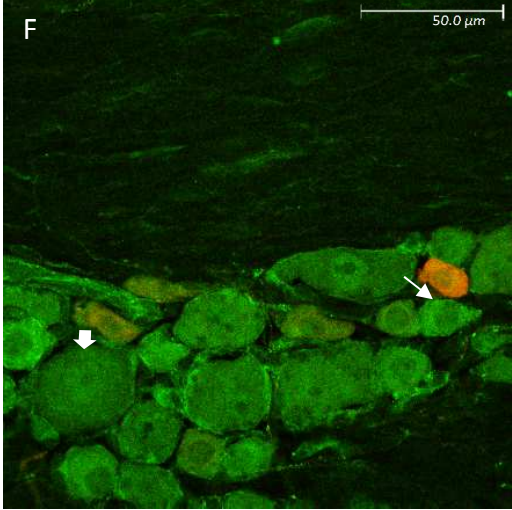
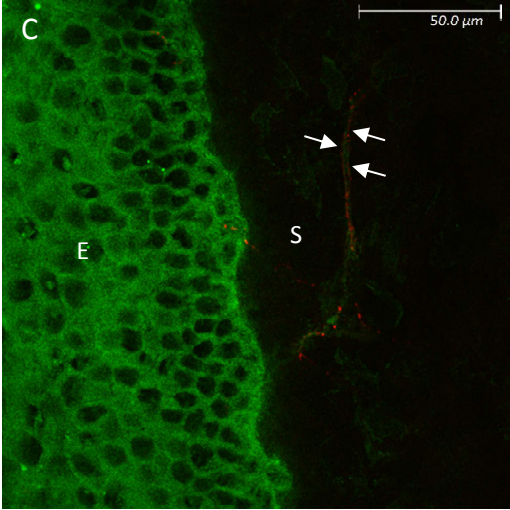
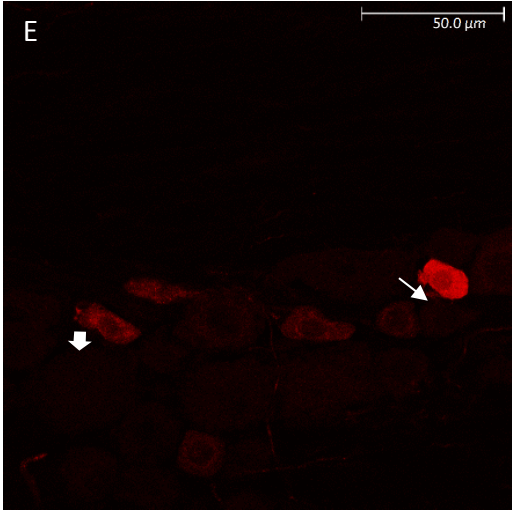
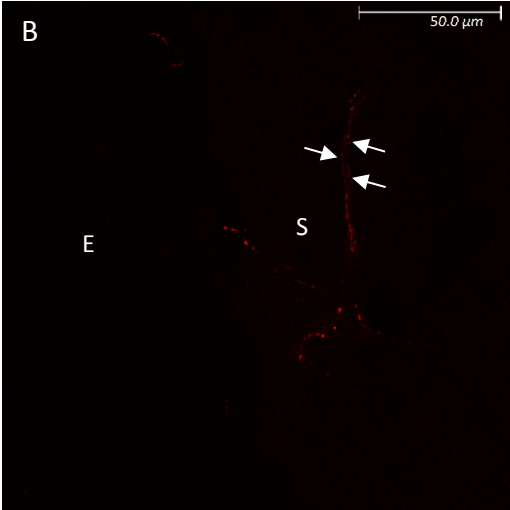
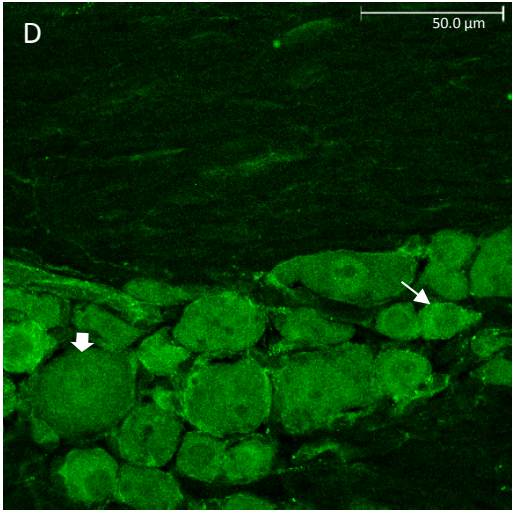
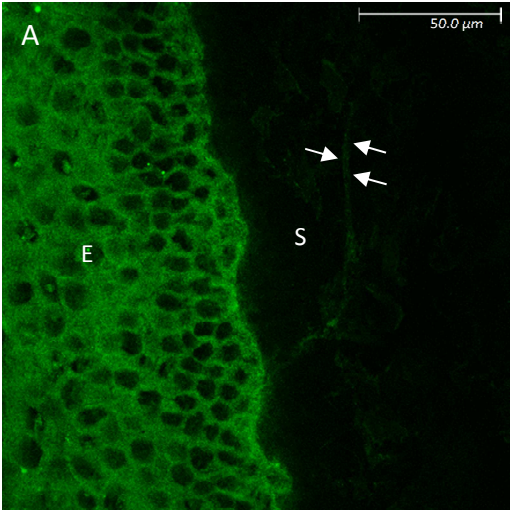


Figure 3.29: Images illustrating Cornea and Trigeminal root ganglion immunoreactivity of Glu3B (Green) and CGRP (Red). Fig16A-C represent immunofluorescent images of GluN3B positive epithelial cells (“E”), Stroma (“S”), and stromal nerve bundles (arrows) in the cornea. Fig16D-F represent immunofluorescent images of GluN3B positive large neuronal cell bodies (thick arrow), and small neuronal cell bodies (thin arrow).

1.2.17 PSD-95

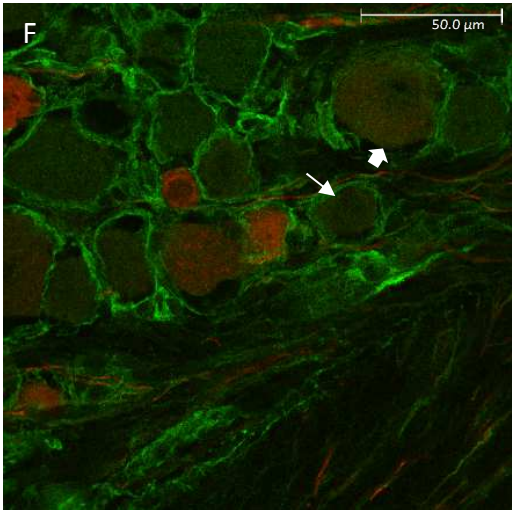
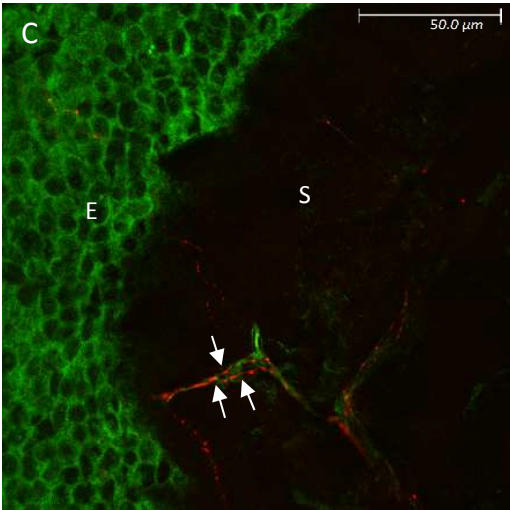
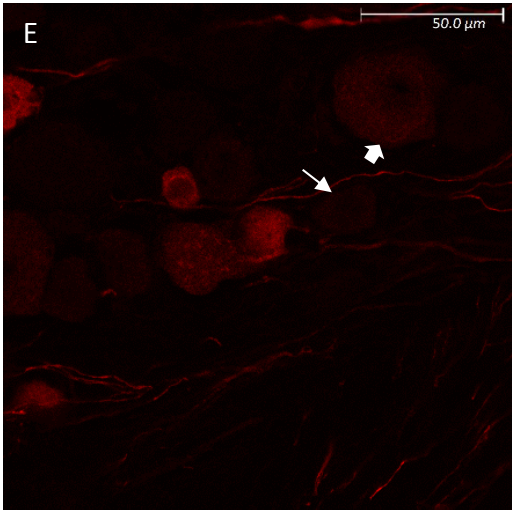
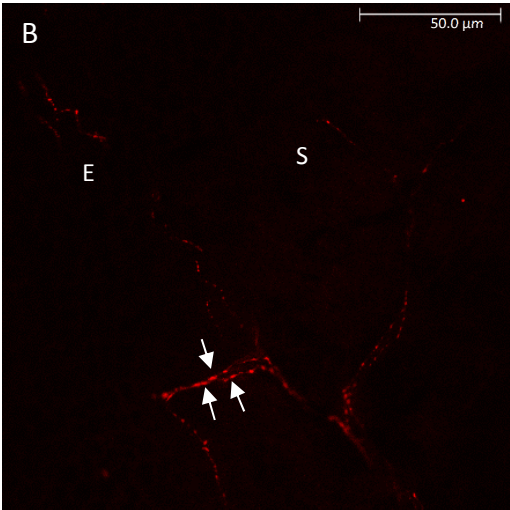
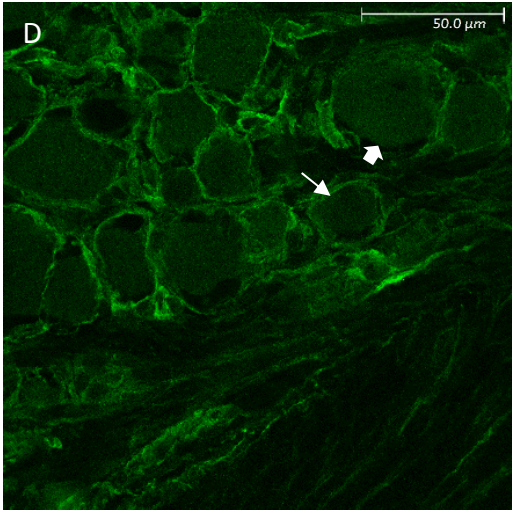
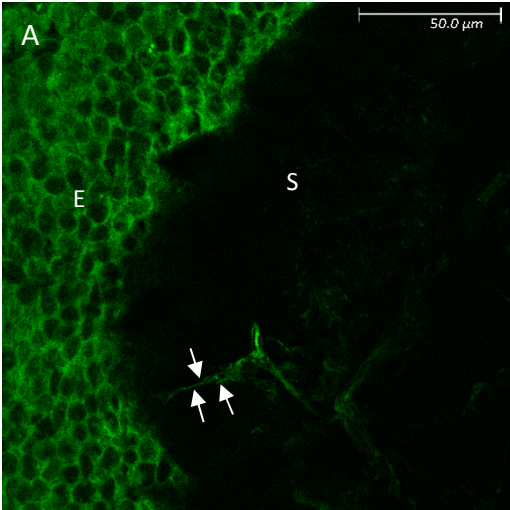


Figure 3.30: Images illustrating Cornea and Trigeminal root ganglion immunoreactivity of PSD-95 (Green) and CGRP (Red). Fig16A-C represent immunofluorescent images of PSD-95 positive epithelial cells (“E”), Stroma (“S”), and stromal nerve bundles (arrows) in the cornea. Fig16D-F represent immunofluorescent images of PSD-95 positive large neuronal cell bodies (thick arrow), and small neuronal cell bodies (thin arrow).

1.2.18 Stargazin

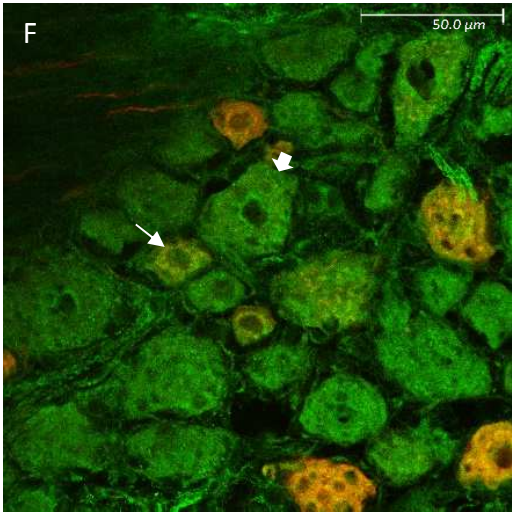
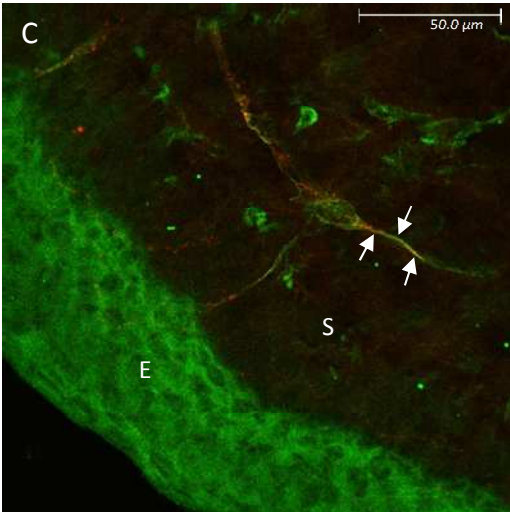
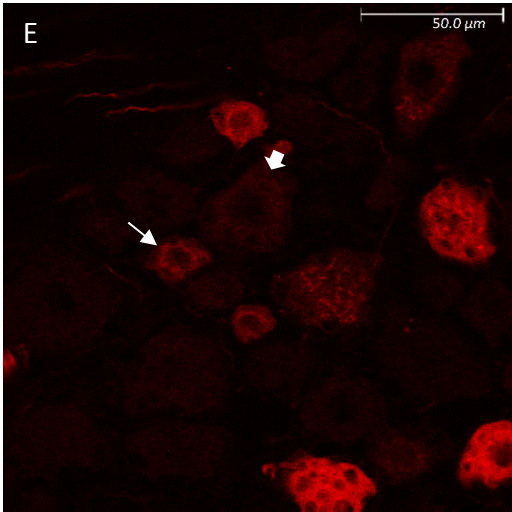
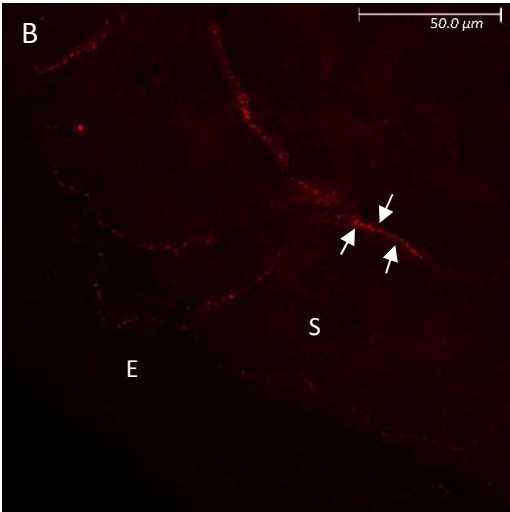
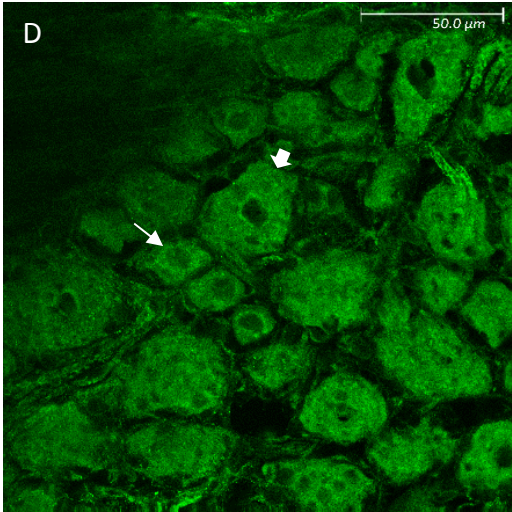
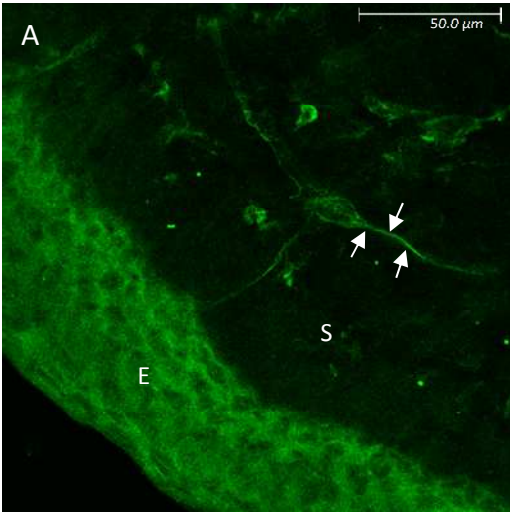


Figure 3.31: Images illustrating Cornea and Trigeminal root ganglion immunoreactivity of Stargazin (Green) and CGRP (Red). Fig16A-C represent immunofluorescent images of Stargazin positive epithelial cells (“E”), Stroma (“S”), and stromal nerve bundles (arrows) in the cornea. Fig16D-F represent immunofluorescent images of Stargazin positive large neuronal cell bodies (thick arrow), and small neuronal cell bodies (thin arrow).

1.2.19 Glutamate

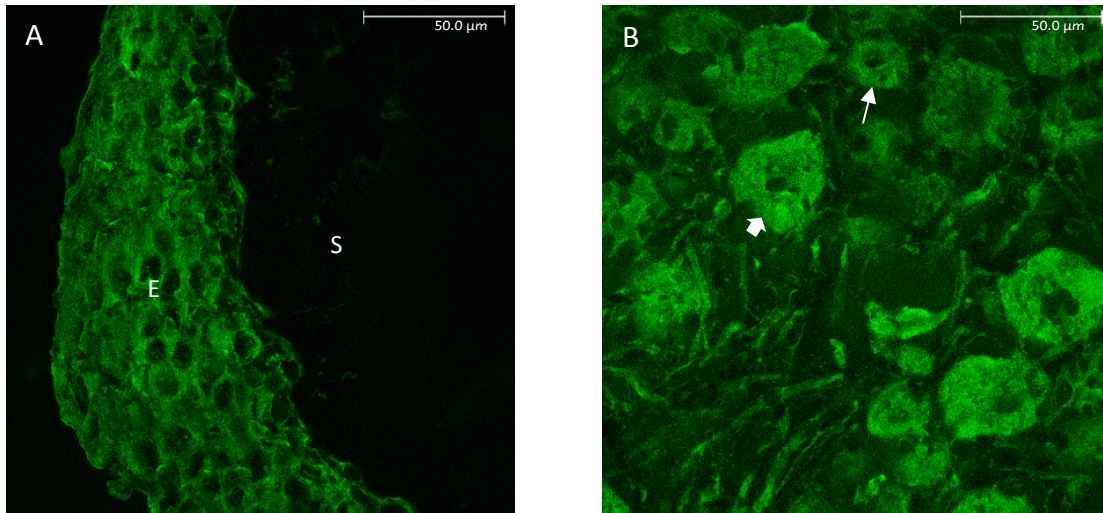


Figure 3.32: Images illustrating Cornea and Trigeminal root ganglion immunoreactivity of Glutamate. Fig16A represent immunofluorescent images of Glutamate positive epithelial cells (“E”), and Stroma (“S”), in the cornea. Fig16B represent immunofluorescent images of Glutamate positive large neuronal cell bodies (thick arrow), and small neuronal cell bodies (thin arrow).

Discussion

In our results, we have identified all the glutamate receptor subunits in both the cornea and trigeminal root ganglion, which directs us to accept the alternative hypothesis that all the iGluR subunits are present in the cornea and trigeminal root ganglion. Interestingly, we have identified differing distributions of immunoreactivity across many of the iGluR subunits, e.g. nuclear staining and Schwann cell staining. Many characteristics, however, were similar across the iGluR subunits, e.g. corneal epithelial cell staining. We identified all iGluR subunits, PSD-95, stargazin, and glutamate in the large and small neuronal cell bodies in the trigeminal root ganglion. These results support that there are specific iGluR subunit combinations that could be responsible for painful responses when glutamate activates the iGluRs. When a noxious stimulus is introduced to a tissue, peripheral neuron terminals release glutamate that activates iGluRs on nerve terminals in an autocrine or paracrine manner (Miller et al., 2011). In skin, there is an increase of iGluR in the nerve terminals during inflammation. Furthermore, the number of peripheral afferents with iGluRs increase (Carlton & Coggeshall, 1999) to produce a more robust nociceptive response due to peripheral sensitization of primary afferents (Miller et al., 2011). With the results of the present study, it is now possible to evaluate if similar occurrences ensue during corneal inflammation.

With immunoblotting, the GluA2 receptor subunit band was identified for the cornea and trigeminal root ganglion at a higher molecular weight than in the hippocampus. Previous studies have also reported findings similar to ours (Kaniakova, Lichnerova, Skrenkova, Vyklicky, & Horak, 2016; Lichnerova et al., 2015; Mollerud, Kastrup, & Pickering, 2016; Tucholski, Pinner, Simmons, & Meador-Woodruff, 2014; Tucholski et al., 2013). The differing number of glycosylation sites between the CNS and PNS can begin to explain the difference in size. Further

evaluation of the glycosylation of these receptor subunits should be conducted to identify further differences between the CNS and PNS.

One limitation to our evaluation is that only the presence or absence of staining of each of the iGluR subunits can be described, but we cannot determine if the iGluR subunits are present in a functional iGluR or if they are present in a nonfunctional aggregation of iGluR subunits (Coleman et al., 2016). Even though each of the iGluR subunits in the cornea and trigeminal root ganglion were detected, further evaluation is required to identify if these iGluR subunits are present in a functional receptor and what types of functions these receptors have.

The Sprague Dawley rat model used has been identified as being a better representative model when translating to humans (Iannaccone & Jacob, 2009). We were able to reduce the number of animals by using multiple corneal sections from each animal for immunohistochemistry of more than one iGluR subunit (Flecknell, 2002). A certain level of bias may have been introduced, however, in the process of identifying the best representative images for each of the iGluR subunits, PSD-95, stargazin, and glutamate. To preserve human clinical implementation of our study, we were not able to replace the Sprague Dawley rat model with an in vitro model.

We identified the GluN2C,2D,3A,3B receptor subunits in the trigeminal root ganglion Schwann cells. Previous work has identified GluN2D and GluN3A in oligodendrocytes and myelin sheath in the optic nerve (Micu et al., 2016) which supports our results. Additional colocalization studies of other iGluR subunits to GluN2C,2D,3A,3B receptor subunits will help in a better understanding of which subunits are present in the Schwann cells and myelin sheath.

Further studies are needed to understand how the events of peripheral sensitization (Latreoliere & Woolf, 2009) occur during cornea inflammation and injury. When a noxious stimulus is introduced to the cornea, phosphorylation of calcium impermeable GluA2 containing

glutamate receptors occurs and these receptors are endocytosed, so calcium permeable GluA1 containing receptors can implant into the cell membrane for a more robust sensitization of nerve fibers (Latremoliere & Woolf, 2009). When topically applied Capsaicin is used as the noxious stimulus, this would support that the corneal epithelial cells could take part in the transduction of a noxious stimulus by autocrine and paracrine release of glutamate from the corneal epithelial cells (Miller et al., 2011).

Acknowledgements

NIH Grant AR047410

CHAPTER IV

APPLYING THE ARRIVE GUIDELINES TO PERIPHERAL IONOTROPIC GLUTAMATE RECEPTOR LITERATURE: A SYSTEMATIC REVIEW

Abstract

Introduction: High quality, basic science publications are needed to further the translational research from animals to humans along with conducting meta-analyses to search for true effects of animal modeled research.

Methods: Two hundred seventy-four published research articles were identified using PubMed in which 169 were coded using the ARRIVE guidelines. Hand coding of each component of the ARRIVE guidelines was done.

Results: Of the 169 studies analyzed, an underreporting of methodological components of the ARRIVE guidelines was observed. To identify the current trend of reporting, the 46 studies that were published after the publication of the ARRIVE guidelines were separately compared to the articles published before 2010. It was determined that there has been little change of efficiently reporting the components of the ARRIVE guidelines over time.

Discussion: Many of the core components of the ARRIVE guidelines were underreported in the peripheral iGluR literature which corresponds to other systematic reviews of a similar assessment type. Better reporting is needed to increase the translation of research from animal models to humans.

Introduction

Animal Research: Reporting of In Vivo Experiments (ARRIVE) guidelines were published in 2010 to improve research reporting and to decrease research redundancy with animal models (Kilkenny et al., 2010). In the interim 7 years, these guidelines often are underutilized within pre-clinical studies (Arora & Ivanovski, 2017; Gulin, Rocco, & Garcia-Bournissen, 2015; Karp et al., 2015). With more evidence indicating inefficient translation of animal research to human studies, (Hackam & Redelmeier, 2006; Ting, Hill, & Whittle, 2015), there is need to increase animal research quality.

In the current study, we examined the use of ARRIVE guidelines in the literature involving ionotropic glutamate receptors (iGluR) in relation to peripheral pain. The iGluRs are located on the peripheral terminals of nociceptive primary sensory afferents and the amino acid glutamate activates and sensitizes the primary sensory afferents by binding to iGluRs (Carr, 2017; Miller et al., 2011). Decreasing pain intensity is a sought-out topic of research (Liu et al., 2008; McRoberts et al., 2001; Medvedev et al., 2004; Zhou, Bonasera, & Carlton, 1996), so increasing the quality of reporting in animal research will undoubtedly aid in increasing translational research.

We hypothesize that when investigating the study quality of the peripheral iGluR literature, the overall efficiency of reporting will not meet the current standards of the ARRIVE guidelines. Furthermore, we hypothesize that will be no significant change of reporting from pre- to post- ARRIVE guidelines publication. Our aim is to evaluate the iGluR literature for each of the ARRIVE guideline components and to compare the efficiency of reporting between pre- and post- ARRIVE guidelines publication.

Methods

Search String

PubMed was used to search Medline to obtain the primary studies with the following search string: “((Excitatory amino acid receptors OR glutamate receptor OR GluA OR gluK OR gluN) AND Pain) AND (Behavior OR Behavioral) AND (Peripheral OR electrophysiology OR microdialysis)” on 2-26-2017. Two hundred seventy-four studies were located from the search and coded using the ARRIVE guidelines. Two on-staff librarians at Oklahoma State University Center for Health Sciences were consulted to identify the most concise yet inclusive search string possible.

Identification of Included Articles

All identified articles were transferred to EndNote. Full text articles were identified and screened for inclusion or exclusion. Articles that included iGluRs and had a component evaluating the peripheral nervous system were included. All articles that were human, a review, not iGluR, not in English, or not retrievable were excluded. Table 4.1 displays an adapted Preferred Reporting Items for Systematic Reviews and Meta-Analyses (PRISMA) flow diagram displaying the included and excluded articles.

Quality assessment

The primary author, B.K.C., reviewed and coded each full text article for each component of the ARRIVE guidelines. The reviewer determined that the publication either included or did not include the requirements for each of the coded components. All subcomponents of the ARRIVE guidelines were individually evaluated by the reviewer. If a single component had multiple requirements, all requirements had to be met to receive an included mark by the reviewer. Table 4.2 contains the 38 coded components with short descriptions.

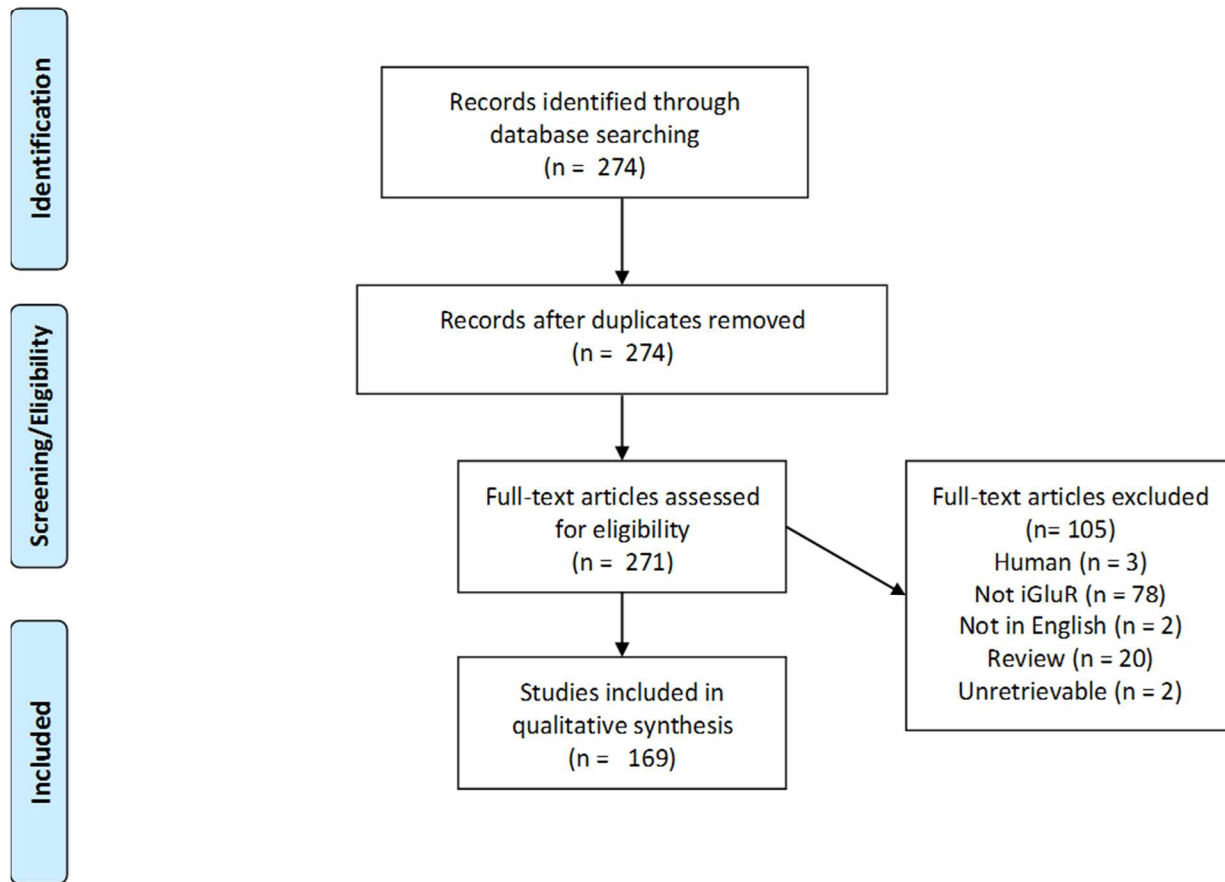


Table 4.1: Adapted PRISMA flow diagram.

Results

After full text screening, a total of 169 studies were included in our study. A total of 46 of these studies were published the same year or after the ARRIVE guidelines were published (Kilkenny et al., 2010). Table 4.2 represents all the coded components and the percentage of reporting when all the 169 articles were combined, when only the articles from before 2010 were combined, and when all of the articles during or after 2010 were combined.

Descriptive and organized abstract

Presenting a descriptive and organized abstract based on each component of a scientific paper has increased before (8.9%) to after (30.4%) ARRIVE guidelines publication.

Ethical statement

An ethical statement of animal usage was reported and increased before (83.7%) to after (100%) the ARRIVE guidelines publication.

Experimental Procedures

Identification of all drugs and doses were highly reported across the articles, before (90.2%), and after (89.1%), but identifying the time of performing the experiment, before (12.2%) and after (8.7%), identifying in detail where the experiment was conducted, before (42.3%) and after (58.7%), and explaining the reason behind choosing the drug and dosages, before (9.8%) and after (4.3%), were underreported.

Experimental Animals

Identifying the average weight and age along with the range of each was not reported, before (2.4%) and after (0.0%). Furthermore, the identification of the animals as naïve or if they participated in a previous experiment and where they were purchased, bred, or found was also underreported, before (7.3%) and after (0.0%).

Housing and Husbandry

Identifying the type, or size, of the cage, bedding used, and the number of animals housed in each cage was underreported, before (7.3%) and after (2.2%). Full reporting of the light/dark cycle, temperature, and quality of food and water was underreported, before (7.3%) and after (2.2%).

Statistics

The statistical methods were highly reported before (91.1%) and after (97.8%) the ARRIVE guidelines publication. Identifying the unit being assessed was moderately reported,

before (62.6%) and after (63.0%). Identifying if data meet the assumptions of statistical approach was underreported, before (3.2%) and after (15.2%).

Outcomes and Estimation

Identifying the standard error of the mean (S.E.M.) for each experimental and control group was underreported, before (26.8%), and after (19.6%).

Interpretation/Scientific Implications

Identifying any bias and limitations to the animal model was underreported, before (2.4%) and after (2.2%). Describing replacement, refinement, and reduction was underreported, before (0.0%) and after (0.0%).

	ARRIVE item	Total (n=169)	Reported (%)	
			Before 2010 (n=123)	2010 to 2017 (n=46)
Title	1	100.0	100.0	100.0
Descriptive and organized abstract.	2	14.8	8.9	30.4
Background a. Reference previous work to describe the motivation of current study.	3a	100.0	100.0	100.0
Background b. Describe how the animal model of choice is the best and how it transfers to humans.	3b	21.9	24.4	15.2
Objectives. Describe the objectives (hypothesis, aims, etc.)	4	89.3	89.4	89.1
Ethical statement. Did they get approval or not?	5	88.2	83.7	100.0
Study design a. Number of Experimental groups and Control groups.	6a	27.2	27.6	26.1
Study design b. Was the study blinded and explain details of who was blinded and when.	6b	30.8	29.3	34.8
Study design c. What was considered an experimental unit? Single animal? Group of animals?	6c	94.7	95.9	91.3

Experimental procedures a. List all drugs that were used (anesthesia, experimental, etc.) and the dose that was administered. Also, where was it administered.	7a	89.9	90.2	89.1
Experimental procedures b. What time of the day was the experiment performed?	7b	11.2	12.2	8.7
Experimental procedures c. Where was the experiment performed? Location of experiment (home cage, water maze, etc).	7c	46.7	42.3	58.7
Experimental procedures d. Explain your reasoning of why you chose the drug, the area of administration, and the dose used.	7d	8.3	9.8	4.3
Experimental animals a. List species, strain, sex, age (mean and range), and weight (mean and range) of animals	8a	1.8	2.4	0.0
Experimental animals b. Are the animals naïve, previously tested, what company did they come from, strain of rat, etc.	8b	5.3	7.3	0.0
Housing and husbandry a. Type of cage (housing), bedding material, number of animals in the cage.	9a	5.9	7.3	2.2
Housing and husbandry b. Light/dark schedule, temperature, quality of food and water.	9b	5.9	7.3	2.2
Housing and husbandry c. Welfare of animal before, during, and after experiment.	9c	1.8	2.4	0.0
Sample size a. Number of animals in whole experiment and number in each group.	10a	11.2	9.8	15.2
Sample size b. How was the number arrived at.	10b	0.0	0.0	0.0
Sample size c. How many independent replications were there.	10c	0.6	0.8	0.0

Allocating animals to experimental groups a. How were the animals sorted into their groups? Randomized? Matching?	11a	8.3	8.1	8.7
Allocating animals to experimental groups b. Describe the order in which the animals were treated and assessed.	11b	1.8	1.6	2.2
Experimental outcomes. What is the outcome that you looking for? Behavioral change, cell death, etc.? Be specific.	12	98.2	98.4	97.8
Statistical methods a. Give specific details about all statistical methods used throughout the experiment.	13a	92.9	91.1	97.8
Statistical methods b. Specify the unit that is being assessed. A group of animals, single animal, neurons, etc.	13b	62.1	62.6	63.0
Statistical methods c. Did the data meet the assumptions of statistical approach?	13c	6.5	3.2	15.2
Baseline data. For each group describe: health, weight, and drug/test naïve.	14	1.2	1.6	0.0
Numbers analyzed a. Report absolute values of the number of animals in each group. Not percent.	15a	46.2	45.5	47.8
Numbers analyzed b. Explain why any animals were taken out of analysis.	15b	0.0	0.0	0.0
Outcomes and estimation. Report results for each analysis with standard error of the mean and/or confidence interval.	16	24.9	26.8	19.6
Adverse events a. Give details about any adverse important events in each experimental group.	17a	0.0	0.0	0.0
Adverse events b. Were there any modifications done to the experimental protocols made to reduce adverse events.	17b	0.6	0.8	0.0

Interpretation/scientific implications a. Interpret the results and consider the aims, current theory, and other literature.	18a	100.0	100.0	100.0
Interpretation/scientific implications b. Comment on the sources of bias, any limitations of the animal model, and the imprecision associated with the results.	18b	2.4	2.4	2.2
Interpretation/scientific implications c. Describe the replacement, refinement, or reduction of the use of animals in research based off of your study.	18c	0.0	0.0	0.0
Generalizability/translation. Comment on how the results translate to other species including humans.	19	28.4	30.9	21.7
Funding. Was this study funded? List all grants and the roles of the funder(s) in this study.	20	56.8	54.5	63.0

Table 4.2: Table representing each graded component with description of the ARRIVE guidelines and percentages of articles that met criteria. All articles combined, articles before 2010, and articles during or after 2010 are represented separately.

Discussion

We found that there were certain components that were well, moderately, or poorly reported. Critical components that were poorly reported include the time of day experiments were performed, identification of the animal origin and if they were naïve, how the experimental animal number was determined, if the data meet the assumptions of statistical approach, and reporting specific standard error of the mean (S.E.M). In many cases the S.E.M. was reported as bars on each data point in a graph, but the numerical value of the S.E.M. of each data point was not located in the published work. With an impetus for conducting meta-analyses in pre-clinical

trials ("Collaborative Approach to Meta analysis and Review of Animal Data from Experimental Studies," 2014), reviewers conducting a meta-analysis would not be able to obtain accurate results when estimating the S.E.M. from graphs. Furthermore, reporting the time of the day an experiment was performed will provide a better understanding of particular factors of the light/dark cycle. Our results indicate that the exact number of animals in specific group often is underreported. Instead of reporting exact values, it was common to find a range of animals for each group. Additionally, how each published work determined the number of animals needed rarely reported.

In our study, we determined that there is low methodological reporting in aspects of animal usage, randomization, blinding, etc. This lack of information may greatly decrease the reproducibility of these preclinical studies. This is a disturbing trend because animals being used in non-reproducible studies are not translated to human research and are difficult for translation to the same or other species of animals in different labs. Increasing the efficiency of reporting and increasing the sample number, for example in the first study conducted in a series, can decrease the amount of subsequent replication and overall reduction of the number of animals used.

In human clinical trials, there are multiple clinical trials registries to enroll research before a study begins and to be updated during and after completion ("ClinicalTrials.gov," 2013). Negative findings can be available to other researchers in these registries. Although clinical trials registries are commonly left unused (Sinnott et al., 2015; Yerokhin, Carr, Sneed, & Vassar, 2016), the concept is one that would bring great benefit to the animal literature. With benefit, risk may follow. For example, introducing an animal trials registry for public use could increase the quality of reporting, but prevention of "research idea theft" might be difficult (Wieschowski, Silva, & Strech, 2016).

Our study contains limitations including determination of the research quality of a publication, but indicates only the efficiency of reporting in a published manuscript. Our study had a more extensive number of articles than similar systematic reviews (Arora & Ivanovski, 2017; Ting et al., 2015), but the total number of articles published after the ARRIVE guidelines were published were still limited (n=46).

In conclusion, our study identified the under-utilization of the ARRIVE guidelines in the peripheral pain iGluR literature, particularly in methodology. We support the use of the ARRIVE guidelines in the pain literature in hope to increase the quality of the published literature. This increase in quality is an important goal to increase the number of preclinical trials that can be translated to human studies and to decrease the potential harm in human research when translational research takes place.

Acknowledgements

NIH Grant AR047410

CHAPTER V

CONCLUSION

Various environmental exposures can damage or activate the corneal primary sensory afferents producing intense pain. The corneal sensory afferents can be damaged or activated by abrasions, drying, and chemicals. For example, autoimmune diseases like Sjogren's syndrome facilitate drying of the cornea (Pedersen & Nauntofte, 2001) leading to primary sensory afferent damage. In each of these cases, it is presumed that glutamate is produced and released as the excitatory neurotransmitter of both the peripheral and central nerve terminals (Miller et al., 2011). Glutamate acts as a ligand to the glutamate receptors which include the AMPA, Kainate and NMDA receptors. When present in peripheral afferent nerve terminals, these receptors participate in the sensitization of primary sensory afferents which in turn increases the rate of neuronal firing. This signal proceeds through the primary, secondary, tertiary, and quaternary neurons to ultimately be perceived in the cortex as intense pain (Basbaum et al., 2009).

Currently, there are several pharmaceutical drugs that help alleviate the pain of an irritated cornea. For example, non-steroidal anti-inflammatory drugs (NSAIDS) can help reduce pain, but side effects may occur such as delayed epithelial regeneration (Aragona & Di Pietro, 2007). Opiates also can be used, but can produce respiratory depression, constipation, and addictive properties that may be more harmful for the patient than the benefits of pain relief (Alam & Juurlink, 2016). A new drug option, therefore, is needed for corneal pain and glutamate

receptor antagonists may be well suited for this need. Glutamate antagonists could alleviate pain by competitively or non-competitively antagonizing glutamate receptors in specific ways. Identifying the right drug along with appropriate solubility, molecular weight, and antagonistic site are all important in determining if a glutamate antagonist will be effective as a pharmaceutical analgesic.

In this study, we focused on corneal and trigeminal root ganglion glutamate receptors. We have evaluated for the functional presence of AMPA and Kainate receptors with behavioral assays, performed immunohistochemistry and preliminary Western blotting for the 16 currently recognized glutamate receptor subunits, and conducted Western blotting to support the presence of GluA2 in the cornea. Finally, we evaluated the literature of iGluRs and peripheral afferents with the ARRIVE guidelines to understand the current reporting of results in the peripheral pain iGluR literature. In previous studies in our lab, we examined GluK1, GluK5, and GluN1 for presence in the cornea using immunohistochemistry and determined the origin of trigeminal root ganglion neuronal cell bodies using retrolabeling with fluorogold (Ibitokun, 2012). These studies demonstrated the presence of these iGluR subunits in both in nerve fibers in the cornea and neuronal cell bodies in the trigeminal root ganglion (Ibitokun, 2012). This indicated that trigeminal root neurons project to the cornea and express specific iGluR subunits. Additionally, our lab determined the glutamate dose response for eliciting nocifensive behavior and determined that an effective topical dose was 0.5M (Ibitokun, 2012). The high dose for eliciting behavior responses, compared to CNS receptor binding studies, is most likely due to two main reasons. First, the cornea always has a layer of tear film that will dilute the exogenously applied glutamate on contact. Secondly, the network of tight junctions between the corneal epithelial cells (Eghrari et al., 2015) will reduce the glutamate that contacts ligand binding sites on peripheral afferents.

In chapter 2, the results that we present support that DNQX is an effective antagonist when topically applied to the cornea and that functional AMPA and Kainate receptors are present in the cornea. We first studied how an AMPA/Kainate antagonist can effectively reduce the glutamate-induced nocifensive response, such as eye blinking, wiping, and shaking. Although glutamate receptor antagonists produce many side effects when given systemically (Bleakman et al., 2006; Traynelis et al., 2010), we believe that a topical application to the cornea may have fewer severe side effects because of the lack of vasculature of the cornea (Eghrari et al., 2015). Still, there could be some adverse effects that need to be evaluated because of the vasculature in the sclera (Sit & McLaren, 2011). We further reviewed a comprehensive list of drugs, table 2.1, that have the potential to have similar antagonistic effects. Three unique characteristics of DNQX caused us to choose it for our behavioral studies: a small molecular weight, specificity for the AMPA and Kainate receptors, and water solubility. With these characteristics, we hypothesized that this drug could diffuse across the corneal epithelium to antagonize the AMPA/Kainate GluRs.

We then aimed to determine the presence and location of all the specific iGluR subunits in chapter 3. Our immunohistochemistry findings supported that all iGluR subunits are present in the cornea. One limitation that needs further research is to determine if these receptor subunits heterotetramerize into a functional glutamate receptor or if they form a nonfunctional aggregate of receptor subunits (Coleman et al., 2016). One step is to use more specific iGluR subunit agonists and/or antagonists to determine if the receptor subunits are functionally active in the cornea. A major limitation to this is the lack of potent subunit specific iGluR antagonists, as displayed in table 2.1, and the incomplete understanding of the functions of certain receptor subunit combinations. Furthermore, there is a lack of specific AMPA and Kainate specific

antagonists in general. As more specific iGluR antagonists are discovered, further analysis in this field can be conducted.

We further evaluated the glutamate receptor subunits for Western blot analysis. Our preliminary data showed presence in each of the iGluR subunits, but many nonspecific bands were present, also. We further optimized detection of the GluA2 subunits by blocking the PVDF membrane with 2.5% bovine serum albumin (BSA) instead of 5% non-fat dried cow milk. After this, GluA2 had a molecular weight that was greater than what was determined for the hippocampus. The most likely explanation for this finding is that the peripheral tissues, in comparison to the CNS, have a greater number of glycosylation sites (Kaniakova et al., 2016; Lichnerova et al., 2015; Mollerud et al., 2016; Tucholski et al., 2014; Tucholski et al., 2013). This would support the claim that the Western blot band with the higher molecular weight is the band of interest for GluA2. Further analysis should be conducted to determine if these subunits are also at an increased molecular weight as compared to the hippocampal iGluR subunits and to further support the presence of the subunits in the cornea and trigeminal root ganglion.

While in the process of identifying a dissertation research project, we became aware the ARRIVE guidelines. These guidelines consist of a set of quality assessment components that aim to help researcher in designing experiments and writing manuscripts as efficiently and effectively as possible. In chapter 4 we used these guidelines to conduct a systematic review of the peripheral pain, iGluR literature. We have identified other similar systematic reviews (Arora & Ivanovski, 2017; Gulin et al., 2015; Ting et al., 2015), but not in this field and not as inclusive. We identified 169 articles and determined that, in many cases, the reporting was insufficient for important aspects that allows for reproducibility of preclinical studies. Furthermore, in the age of meta-analyses, the exact number of animals used per group and the specific S.E.M. were seldom reported. This suggests that changes in scientific publishing must occur in the way data is

reported and/or how journals review and present data. One way to increase the quality of reporting is to require registration of animal trials registries so study updates can be described.

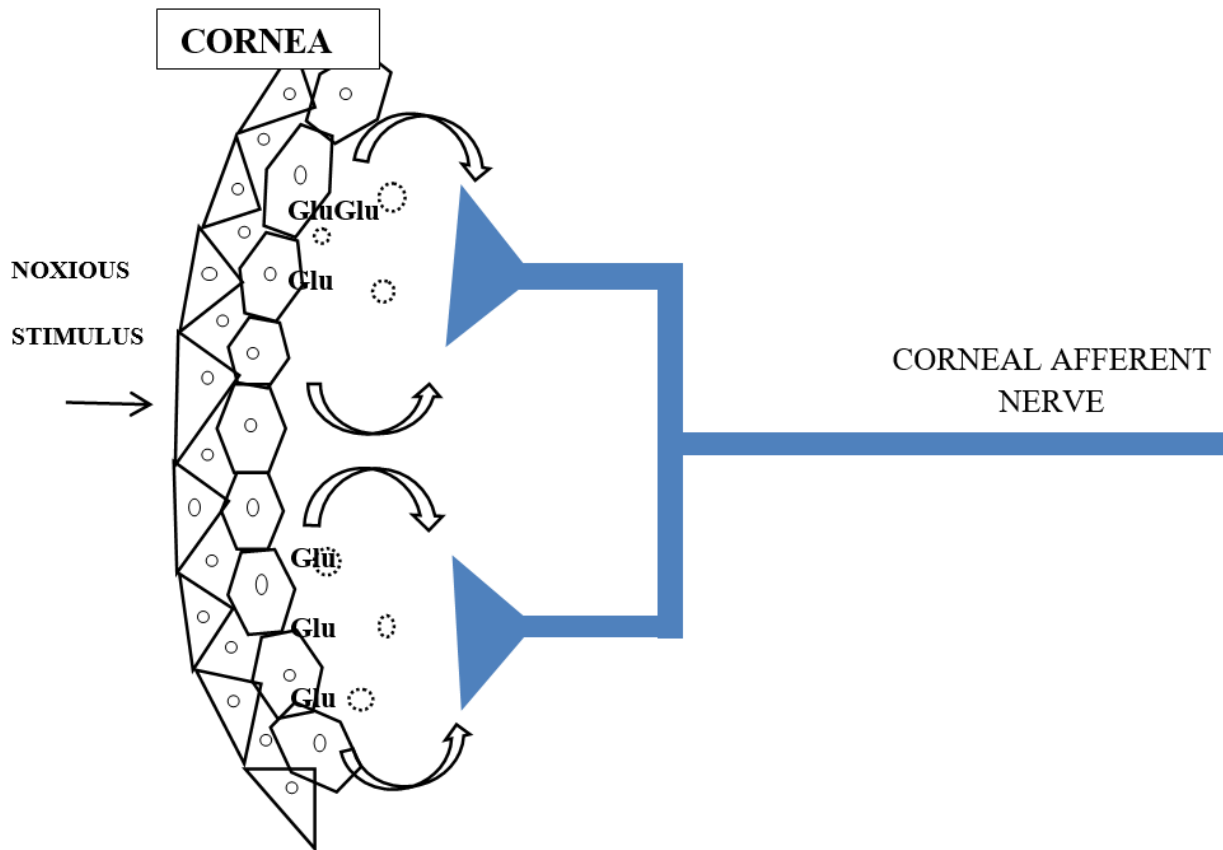


Figure 5.1: Figure representing a noxious stimulus being applied to the corneal epithelial layer and the subsequent release of glutamate to activate corneal primary afferents. (From (Ibitokun, 2012)).

Finally, our study describes the location of glutamate production, release, and activation in the cornea. As seen in figure 7.1, glutamate has been described in this dissertation to be produced in the corneal epithelial cells. When a noxious stimulus interacts with the corneal epithelial cells, glutamate may be released via exocytosis to further stimulate the corneal epithelial cells and to activate the primary sensory afferents. This model, therefore, hypothesizes that the corneal epithelial cells would be a transducer of noxious stimuli into activation of primary sensory nerve terminals. This is supported by the expression of nociceptive-specific

transducer proteins, TRPV1, in cornea cells (Mergler et al., 2014). Furthermore, the presence of iGluRs in both epithelial cells and nerve terminals indicates that the complexity of the cornea is much greater than previously thought. The cornea is one of the most densely innervated tissues for sensation in the body (Eghrari et al., 2015). iGluRs subunits are in many corneal afferents, but an understanding of iGluR subunit composition is lacking. The findings in this dissertation should lead to future research examining the various functionalities of the iGluRs in the cornea, e.g., nociception, wound healing (Por, Choi, & Lund, 2016).

Future research

With the interesting findings of the location of the iGluR subunits in the cornea and trigeminal root ganglion, many future experimental possibilities arose. First, specific iGluR subunits are present at higher levels (immunoreactive intensity) in the small neuronal, TG cell bodies compared to the large neuronal cell bodies, e.g. GluA2-3, GluK1-2, 4-5, and GLUN1, 2C, 3B. We theorize that specific combinations of these receptor subunits are for nocifensive behavior. Colocalizing and immunoprecipitation studies could be conducted to support this theory. A full understanding of the subunit composition of functional nociceptive iGluRs will help identify specific drugs that can act on particular combinations of receptor subunits to decrease the painful response, possibly with much fewer side effects than current drugs.

In chapter 2, we examined the effects DNQX has when topically applied to the cornea. Further research should be conducted to evaluate the effectiveness of DNQX when given topically to the cornea when combined with a potent NMDA antagonist. This may further reduce the number of nocifensive responses seen when glutamate is used as an agonist or a faster reduction of nocifensive responses when compared to DNQX alone.

To further examine corneal epithelial cells as transducers of a noxious stimulus, capsaicin can be topically applied to the cornea to activate the transient receptor potential channel (TRPV)

receptors to produce autocrine and paracrine release of glutamate for activation of the glutamate receptors (Miller et al., 2011). In our preliminary results, figure 5.2, we examined capsaicin as an effective noxious stimulus. Furthermore, in figure 5.3, we examined KCl, which is a noxious stimulus that will depolarize nerve fibers. We plan to examine the effects of these two chemicals on the recruitment of glutamate receptors and to examine the antagonistic effects of DNQX with capsaicin and KCl, along with further combinations of DNQX and NMDA receptor antagonists.

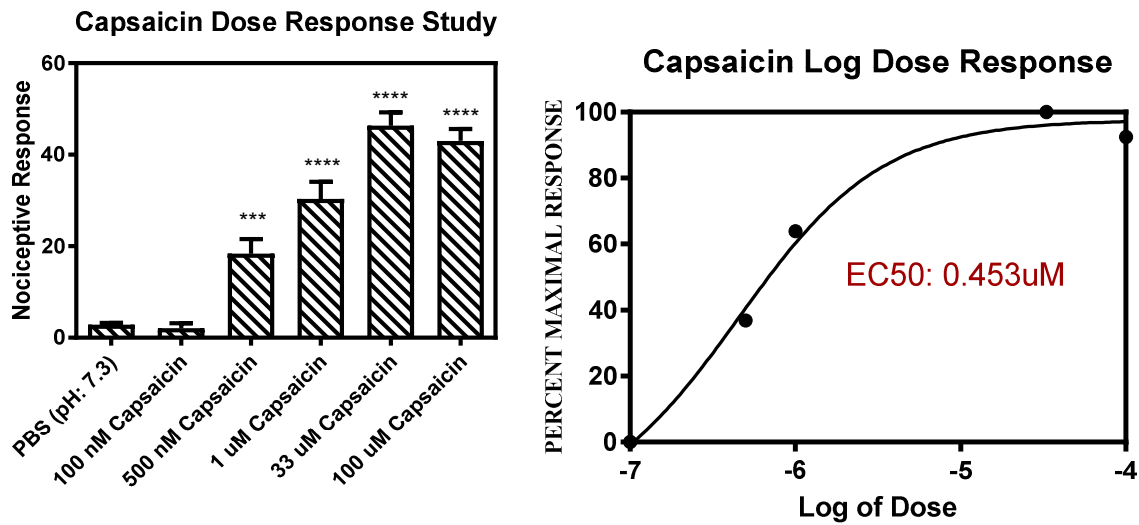


Figure 5.2: Capsaicin behavioral response and log dose response. ($p < 0.001^{***}$, $< 0.0001^{****}$)

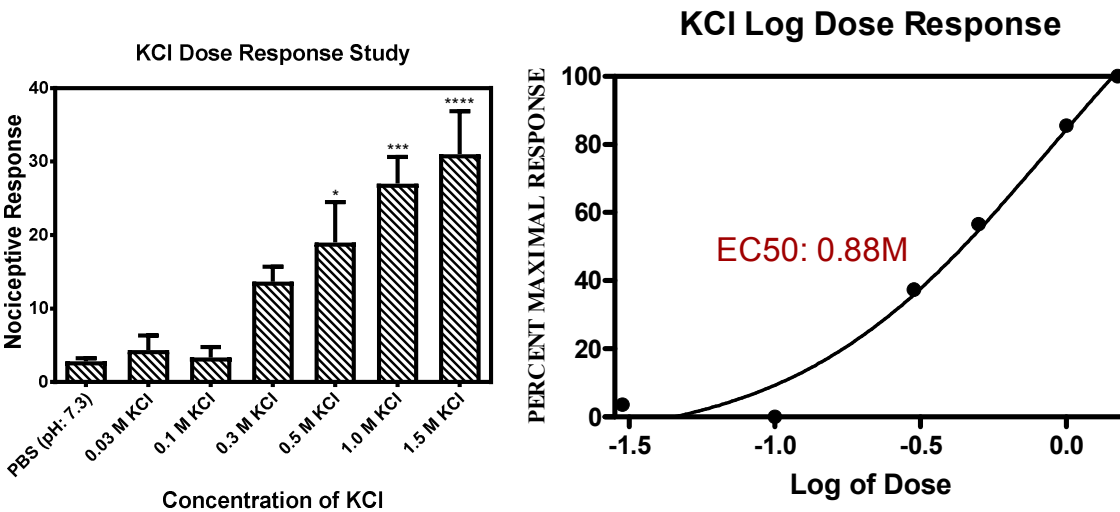


Figure 5.3: Potassium Chloride (KCl) behavioral response and log dose response. ($p = <0.05^*$, $<0.001^{***}$, $<0.0001^{****}$)

Furthermore, we identified GluN2C,2D,3A,3B on the Schwann cells in the trigeminal root ganglion. These data support previous findings that the GluN2D and GluN3A receptor subunits are present in optic nerve oligodendrocytes and myelin sheath (Micu et al., 2016). Our results provide the first report that these subunits occur on peripheral glial cells. Further studies conducted to colocalize iGluR subunits to the Schwann cells would help in a better understanding of which iGluR subunits actively participate in Schwann cell function.

In this dissertation, we showed that glutamate is present in the corneal epithelial cells. Future studies could examine the presence of glutamate synthesizing enzymes such as glutaminase and aspartate aminotransferase. Glutamate, being the ligand to the iGluRs, is transported into cells by glutamate transporters (Hediger & Welbourne, 1999). Further evaluation of specific glutamate transporters including EAAT, GLT1, and GLAST will be conducted to evaluate the similarities and differences between the corneal epithelial cells to the trigeminal root ganglion and CNS neurons. Vesicular glutamate transporters were detected only in corneal nerve fibers and not in corneal epithelial cells (Ibitokun, 2012). The presence of glutamate transporters, therefore, can serve as an export (release) mechanism of the corneal epithelial cells when they are activated by an external nociceptive stimulus.

Conclusion

Evaluating the iGluR in the human cornea has been studied (Feng, Price, McKee, & Price, 2015; A. Lee et al., 2014; Oswald et al., 2012; Seigel et al., 2003; Sloniecka et al., 2015; Staines, 2008), but is ultimately still lacking. Furthermore, a complete evaluation of iGluR subunits in a single tissue has not been conducted. With our results presented in this dissertation, we have examined and worked to fill this gap. With an examination of an AMPA/Kainate antagonist on the cornea and a full examination of all iGluR subunits in a single tissue, our work can help direct researchers to additional iGluR subunits that may not have been considered to have a role in corneal pain. Finally, with the evaluation of peripheral pain iGluR literature using the ARRIVE guidelines, we can begin to produce higher quality publications that makes it easier to reproduce and translate to a human model.

CHAPTER VI

WESTERN BLOT PROTOCOL

Equipment and materials:

Male rat (age between 2-5 months)

Female rat (age between 2-5 months)

Plastic rat home cage and top

Rat bedding

Rat chow

Water in rat dispensable bottle

Two generic green cards and one specifically colored card for you.

- Rat selection
 - 8-10 weeks is good, but no actual age range restriction. (I use 6-8 week rats).
- Tissue collection in surgery room:
 - Anesthesia machine:
 - Set up: Place the blue surgical cloth present in the surgery room over the table with the plastic rat housing cage on one end of the table and the guillotine on the other. You will collect your tissue in the area in between. Place paper towels on either side of the guillotine to absorb the blood.
 - Set up for tissue collection: Obtain a tub of ice and a metal plate for tissue collection. Also, make sure you have enough 1-2 mL tubes for the all of your tissue collection (Use larger sizes for bigger tissues.)
 - Radioimmunoprecipitation Assay buffer (RIPA buffer) -Add 1 mL of RIPA buffer into a 2 mL tube, remove 1 μ L of the RIPA buffer, and add in 1 μ L of the protease/phosphatase inhibitor. The final concentration of the protease/phosphatase will be 1:1000.
 - There are 2 metal gas tanks (1 for carbon dioxide and one for oxygen) and an anesthesia machine for isoflurane in the surgery room.
 - Check the isoflurane level on the anesthesia machine. Add more if needed.

- Make sure the oxygen is plugged into the anesthesia machine and turn the knob until the metal ball on the anesthesia machine is up to the mark (about 5).
 - Make sure the rubber tube on the anesthesia machine is plugged into the plastic box that the rat will be placed in.
 - Place the rat into the box and close the lid before turning on the anesthesia machine.
 - Turn the knob on the anesthesia machine up to 5. This will deeply anesthetize the rat (use 2.5 with a “rat gas mask” if you want to keep the rat anesthetized for a longer period of time.
 - Once the rat appears unconscious; Typically about 3-5 minutes. (INFO: The rat will most likely become hyper aroused as it goes through the stages of anesthesia). Turn the anesthesia machine off and take the rat out of the chamber and close the lid to prevent gas leakage into the room.
 - Immediately place the rat head under the blade of the guillotine, make sure **all your appendages** are away from the blade, and firmly and quickly force the blade through the neck of the rat. (You will need a lot of force to do this; the first time you try it, make sure to slam the blade to feel how it works. Keep fingers, etc., away from the blade!!!!).
 - If you have to readjust the head of the rat, gently grab the nose of the rat with your thumb and index finger and move the head where you want it. This will prevent your fingers from ever going under the blade.
 - Take the head and put it on ice and the body in the sink if it begins to move too much.
- **Tissue Collection:**
 - CORNEA
 - Once the head of the rat is removed and on ice, remove one eye as fast as possible with an 11 sized scalpel blade (the smaller one). Use fine tipped forceps to aid with the process.
 - Note: When removing the eye, place the tip of the 11 sized scalpel blade on the side of the cornea and press straight down without cutting into the eye. Rotate the blade around all the eye to cut all tissue keeping it in place. Use forceps to lift the eye and cut any remaining tissue.
 - Take the eye and place it on the metal plate. Hold the eye with the fine tipped forceps and use the 11 (small) sized scalpel blade to puncture the top side of the cornea next to the sclera.
 - You should be able to obtain a better grip when grabbing the optic nerve, or where the optic nerve was, after a puncture has been made.

- Once a puncture is made, continue to cut along the cornea sclera line until the cornea is completely off. Trim any excess sclera off of the cornea
- Place the cornea in the 99 μ L of RIPA buffer and 1 μ L of Protease/Phosphatase inhibitor solution.
- Homogenize the tissue.
- If saving the tissue for later: Place the eyes of the rat into liquid nitrogen to flash freeze the corneas for storage.
- Place in -80°C freezer until analysis
- TRIGEMINAL ROOT GANGLION
 - Once the eyes are removed, use a scalpel to cut the skin on the top of the skull. Pull the skin back and cut into the muscles around the skull and pull them back as well.
 - Take a pair of large rongeurs and break the bone in between the eyes were.
 - Take the large rongeurs, place rongeur tines on the left and right sides of the skull, and GENTLY crack the skull top (watch movement of the sutures).
 - Once the skull top is cracked, you can gently place the rongeurs under the skull where the eyes were to pull off the entire skull cap. Remove any other bone around the skull and gently begin lifting the brain away from the base of the skull.
 - If done correctly, the brain will come up with ease, but you will have to cut or break the optic nerves as the brain is lifted.
 - Continue lifting the brain and remove any bone that it becomes caught on. The brain should fall out of the skull base.
 - Place the brain on ice for the next step (Hippocampus removal).
 - On the skull base, there will be two large nerves. These nerves appear to have an enlargement and this is the trigeminal root ganglion.
 - Use the 11 (small) sized scalpel to cut through the nerve rostral to the ganglion, cut along both of the long sides of (next to) the ganglion to separate it from the connective tissue, and cut the nerve connected to the caudal side of the ganglion. You should be able to pick the ganglion up with the scalpel tip or a fine tipped forceps.
 - Place the ganglion in the 99 μ L of RIPA buffer and 1 μ L of Protease/Phosphatase inhibitor solution.
 - Homogenize the tissue.
 - If saving the tissue for later: Place the trigeminal root ganglion of the rat into liquid nitrogen to flash freeze the tissue if you want to store it.
 - -80 freezer until analysis
- HIPPOCAMPUS
 - Place the brain that was previously collected on the metal plate located on the ice.

- Cut the cerebellum and brainstem from the brain and place it on ice for the spinal trigeminal nucleus step.
 - With the brain, cut about one fourth of the way from the front of the brain and about one fourth from the back of the brain with the 11 (small) scalpel blade. You should be left with the middle section of the brain.
 - Turn it over and begin to separate the cerebral hemispheres.
 - You should see the corpus callosum (white section) that you can cut through. Underneath is the hippocampus.
 - Keep spreading the cortical hemispheres back until you expose the hippocampus as much as possible.
 - Cut around the hippocampus with the 11 (small) scalpel blade and retrieve the hippocampus.
 - Place the hippocampus in the 99 μ L of RIPA buffer and 1 μ L of Protease/Phosphatase inhibitor solution.
 - Homogenize the tissue.
 - If saving the tissue for later: Place the hippocampus of the rat into liquid nitrogen to flash freeze the tissue if you want to store it.
 - -80 freezer until analysis
- SPINAL TRIGEMINAL NUCLEUS
 - With the remaining cerebellum and brainstem from the previous section, place it on the metal plate.
 - Remove the cerebellum and disregard it.
 - Orient yourself to the brainstem and identify the closed and open medulla. You will want to closed medulla section, so use the 11 (small) scalpel blade to cut at the top of the closed medulla and disregard the open medulla.
 - Trim the bottom part of the brainstem (may not have to depending on the location of the decapitation) to about 25 mm below the beginning of the closed medulla.
 - Place the section upright and obtain the dorsal section of the tissue.
 - This will have the spinal trigeminal nucleus in it.
 - Place the spinal trigeminal nucleus in the 99 μ L of RIPA buffer and 1 μ L of Protease/Phosphatase inhibitor solution.
 - Homogenize the tissue.
 - If saving the tissue for later: Place the spinal trigeminal nucleus of the rat into liquid nitrogen to flash freeze the corneas if you want to store them.
 - -80 freezer until analysis
- Homogenizing the tissue
 - Set up: You will need a green or blue homogenizer plastic rod and the homogenizer machine. The homogenizer machine is a handheld device that will twist and vibrate the homogenizer rod for you.

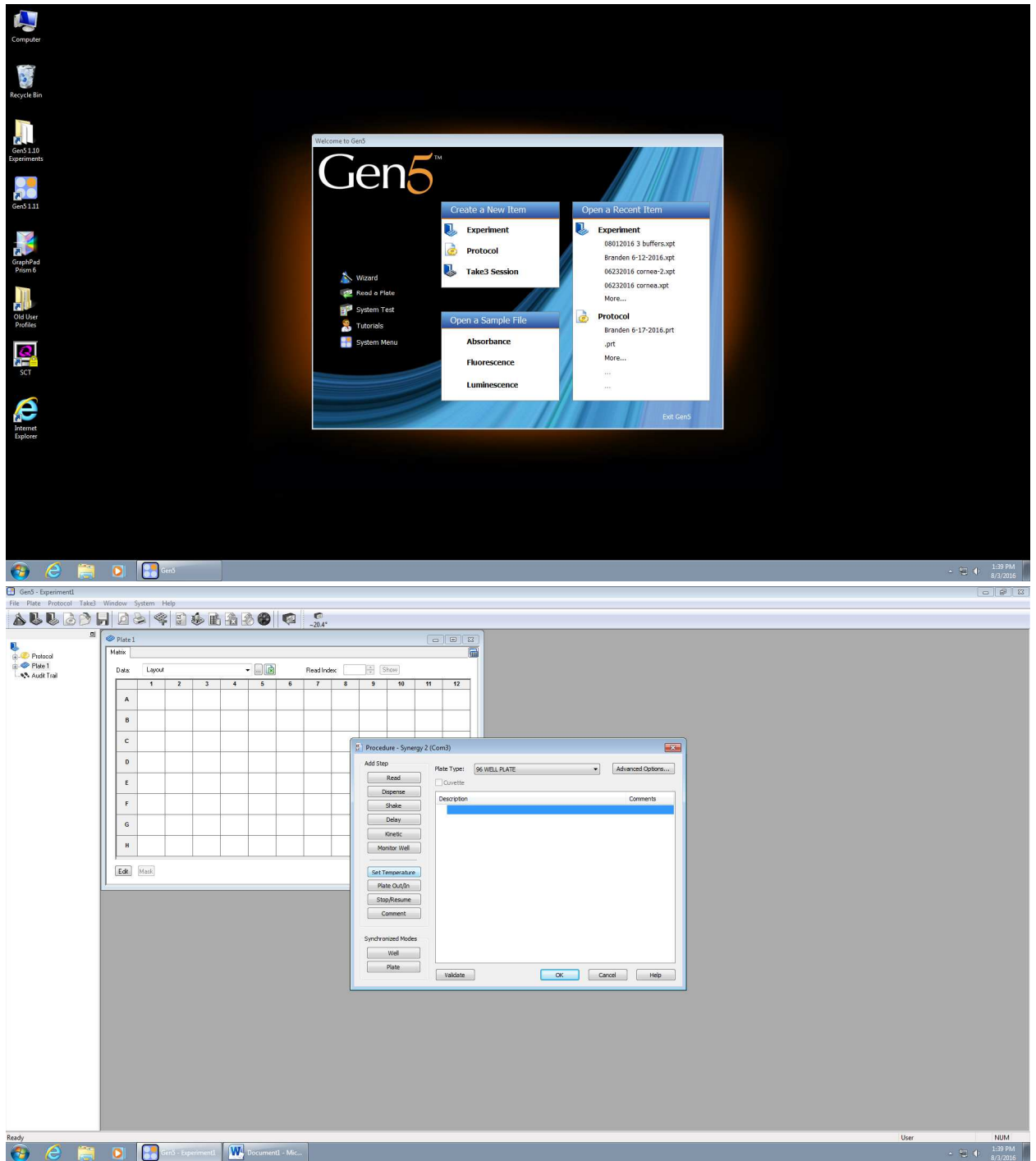
- Take tissue out of the -80 freezer if you stored them.
- If you are using fresh samples that you just collected, it is already in the RIPA/protease inhibitor solution, so you will go to the homogenizing step.
- In the tube that is **ON ICE**, you will smash and twist the tissue to break up and dissolve the proteins in the tissue.
- Place a clean homogenizer rod into the homogenizer machine and gently place the tip into the tube to smash your tissue.
- Press the button to begin the vibrations to aid in the protein extraction.
- The goal is to press the rod hard enough on the bottom of the tube that you do not cause frothing (bubbling) of the fluid in the tube.
- Use the rod to the bottom of the tube and balance between pressing too hard that the vibrations will stop and letting up a little bit that the vibrations will start again.
- Continue with this method for about 1 minute then let the sample sit on ice for about 10 minutes.
- Repeat steps 3-5 times until the tissue is completely homogenized. (The stroma of the whole cornea will not fully homogenize because of very high collagen content.)
- Be sure to use a new rod for each sample and clean the rods that you use after you are finished!
- Once all of the tissue is dissolved into the liquid, bring all of the labeled tubes to a cold microcentrifugation unit.
- Make sure there is nothing in the rotor.
- Place the rotor lid on the rotor, close the lid, set the temperature at 4°C, and push the button that says speed cool. This will cool the machine for you before you use it.
- Bring your homogenized tissue to the centrifuge that you have prepared. Push the off button to end the cooling cycle so you can open the lid.
- Open the lid and place all of your tubes into the centrifuge. Make sure there is a blank tube across from each of the tubes that you place into the centrifuge. Use a loading control tube located next to the centrifuge if you have an odd number of tubes. Pick a tube with a similar amount of fluid in it, but you do not have to be exact.
- Place the lid back on the rotor, shut the centrifuge and have it spin for 10 minutes at 10,000RCF at 4 degrees Celsius.
- Once the cycle is complete, take out only the supernatant with a 200 μ L pipette and place it into a tube labeled accordingly. Either save the pellet in the -80 degree Celsius freezer, or trash them.
 - Trouble shooting tip: If you are not getting a band of interest after all is done, try running the pellet.
 - Suspend the pellet in loading dye, and load it into the gel per normal protocol after boiling.

- Place all of the tubes in the -80 degree Celsius freezer for storage or continue directly into the protein quantifying step.
- BCA assay quantification.
 - Once all of the tissues are homogenized, spun down, and the supernatant is placed into a different identically labeled tube, you are ready to quantify the protein in your tissues. **Keep samples on ice!**
 - Obtain an equal amount of autoclaved PCR tubes and label each as you labeled them on the supernatant tubes.
 - Prepare the solutions for the quantification:
 - Obtain a BCA protein assay kit.
 - Obtain a 50 mL plastic tube and place 49 mL of the reagent A into the tube.
 - Obtain 1 mL of reagent B and put it in the tube for a final volume of 50 mL. This should make it turn green.
 - Obtain a vial of known protein (2 mg/mL vial).
 - Break the glass by applying pressure to the white line away from your body.
 - Take out 1 mL of the fluid and place it into a small tube. Add 1 mL of deionized water to make a final concentration of 1 mg/mL. Mix.
 - Place the broken vial in the broken glass box.
 - You want to dilute a sample of the supernatant for this quantifying step. Here are some examples:
 - 5 times diluted: Take 20 μ L of deionized water and place into each of the tubes for the 5x dilution. Place 5 μ L of your supernatant into the tube as well for a total volume of 25 μ L. Mix. (You will also need to make a tube for the RIPA/Protease inhibitor only solution, as well)
 - 8 times diluted: Take 14 μ L of deionized water and place into each of the tubes for the 8x dilution. Place 2 μ L of your supernatant into the tube as well for a total volume of 50 μ L. Mix. (Will also need to make a tube for the RIPA/Protease inhibitor only solution)
 - 10 times diluted: Take 45 μ L of deionized water and place into each of the tubes for the 10x dilution. Place 5 μ L of your supernatant into the tube as well for a total volume of 50 μ L. Mix. (Will also need to make a tube for the RIPA/Protease inhibitor only solution)
 - Now that the solutions are prepared, it is time to obtain a 96 well plate that is clean and not cloudy. As seen in the image below, each of the wells will have some solution in it via triplicates (3 wells will have the same “stuff” in it).
 - For the first three columns, follow what is shown in the image.
 - The first row of the first three columns will have nothing in it except air.
 - The second row of the first three columns will have 200 μ L of the reagent A/B mix (referred as the green solution from now on).

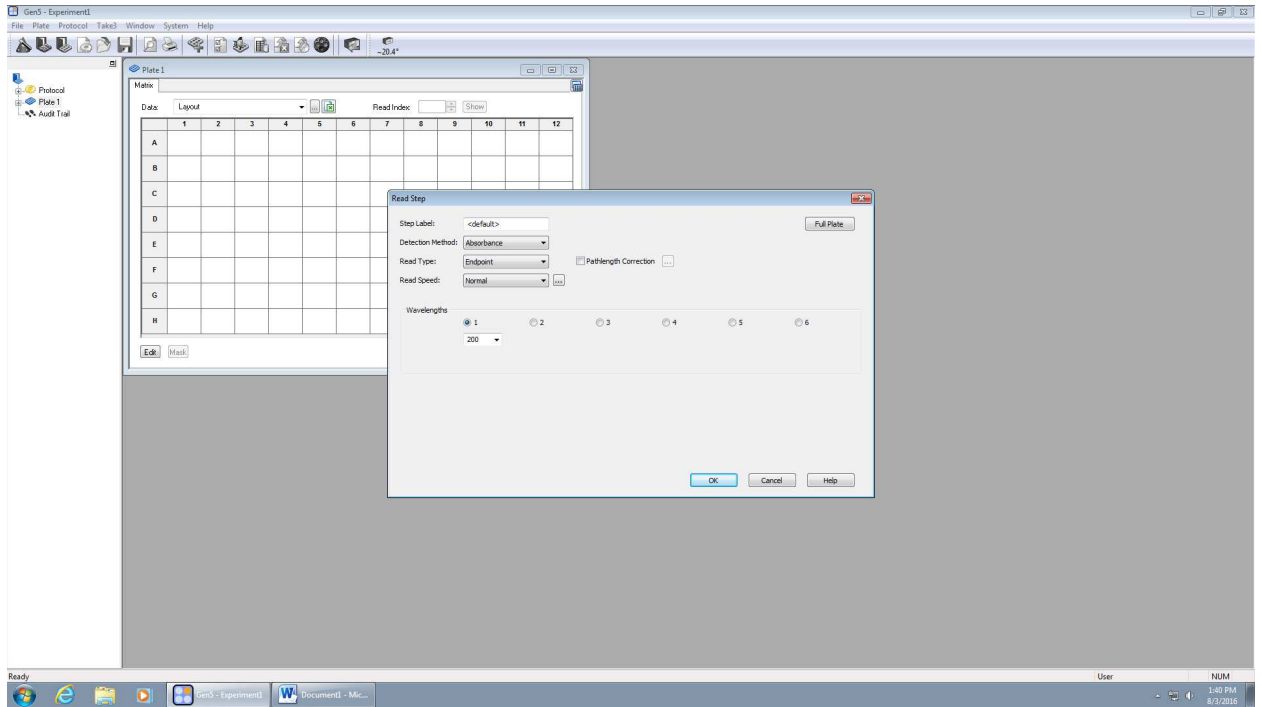
- The third row of the first three columns will have 198 μL of the green solution and 2 μL of the 1 mg/mL solution.
- Continue down the first three columns as the image states.
- The last nine columns will contain your samples in triplicates.
- To do this, you will take a multichannel pipette and place 195 μL of the green solution in all of the wells of columns 4-12.
- You will then add in 5 μL of your sample to each of the wells in triplicate (triplicate means 3 wells will have the exact same material in each of the wells so you can compare and average the difference to account for pipette error).
- Make sure to label what sample you put in which well with the example plate printout that you see below.
- You will begin to see the green solution turn purple over time. (More purple, the more protein is in the well).
- Take the multichannel pipette and take in some of the leftover green solution and pipette it back into the container to wet the pipette tips.
- Go through the wells that you just loaded and mix all of them thoroughly by drawing into and out of the pipette tips. Change tips after each triplicate and re-wet the new tips before placing them in the well for mixing.
- Incubate the plate in the 37°C incubator for 30 minutes. (Make sure to place a lid or Parafilm over the plate before placing it in the incubator).
- Once finished incubating, pop any bubbles in the wells with a tip of a Kimwipe. Carefully just touch the bubble and pop it, do not suck up the solution with the Kimwipe.
- Bring the plate to the Synergy 2 machine in Dr. Champlin's lab for quantification.

	1	2	3	4	5	6	7	8	9	10	11	12
A	Blank	Blank	Blank									
B	200+0	200+0	200+0									
C	198+2	198+2	198+2									
D	196+4	196+4	196+4									
E	194+6	194+6	194+6									
F	192+8	192+8	192+8									
G	190+10	190+10	190+10									
H	188+12	188+12	188+12									

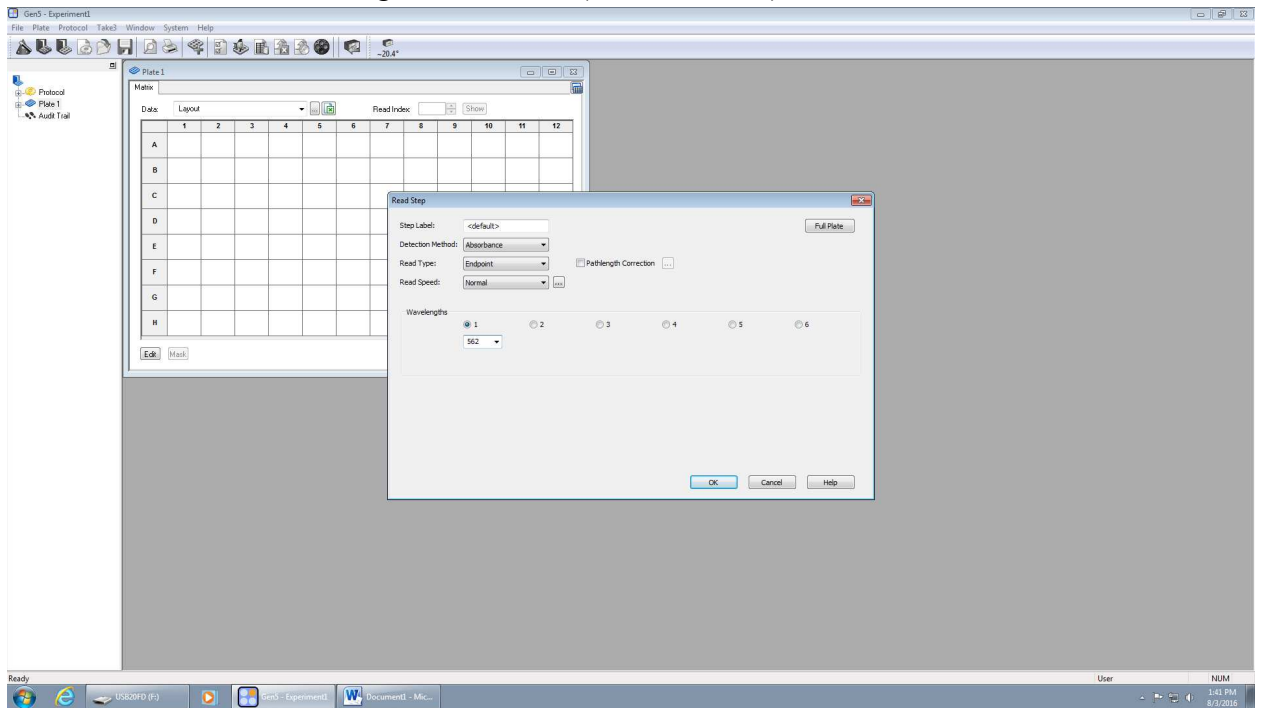
- Reading the plate for protein concentration
 - Take the plate to the plate reader, the Synergy 2 machine.
 - To turn it on, you will need to turn on the power to the right of the machine and the switch at the front bottom left portion of the machine.
 - Launch Gen5 1.11 program on the computer that it is connected to. (Picture Below).
 - Click on “read a plate” when the program is running. (Picture Below).



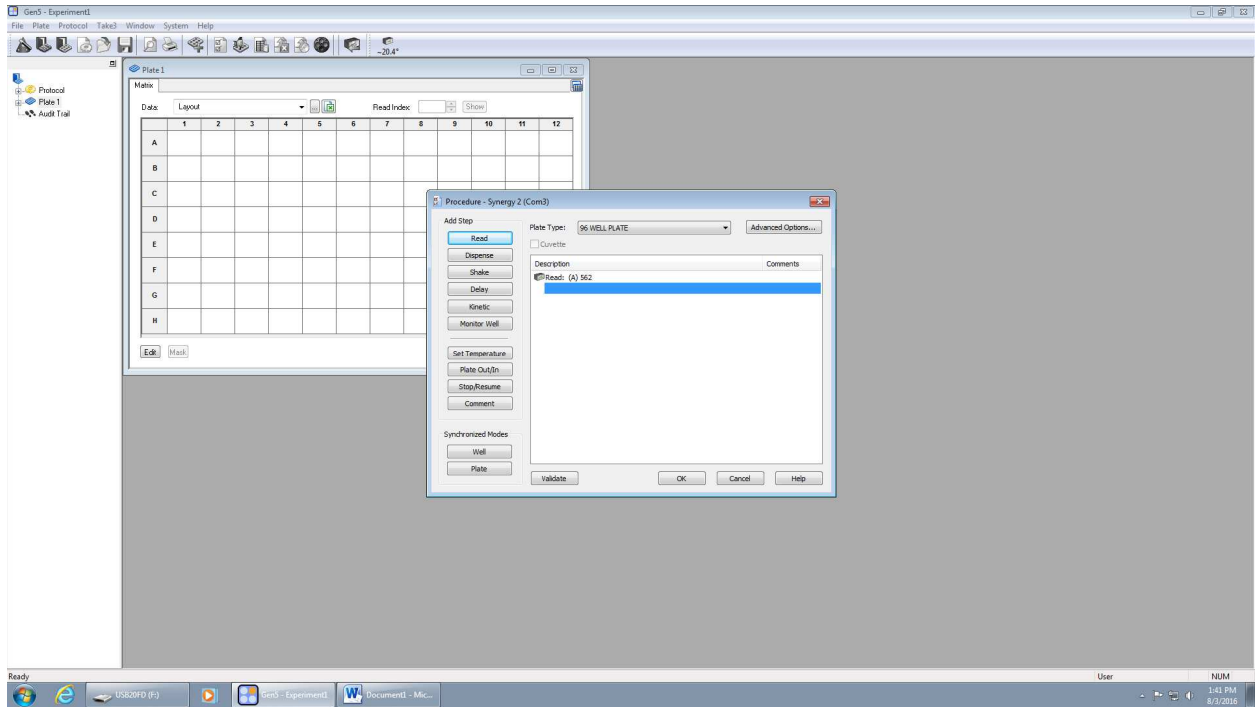
o Click on read and you will be able to enter your wavelength. (Picture Below).



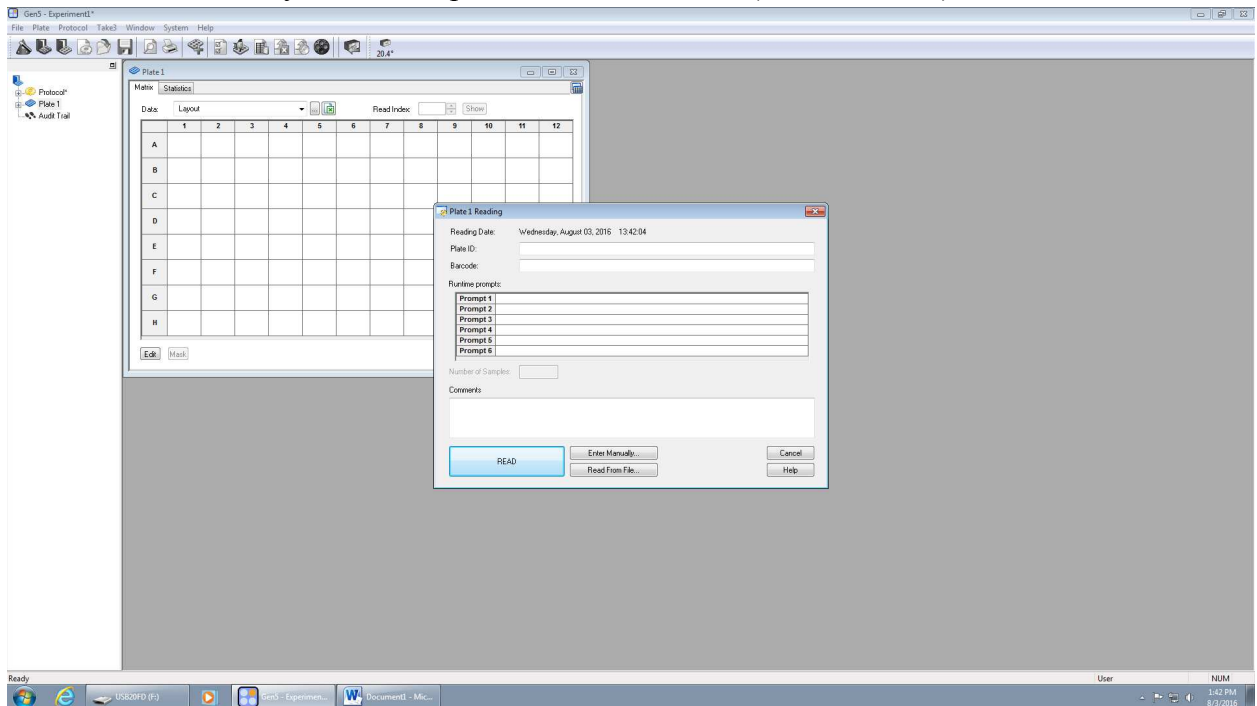
○ Enter 562 as the wavelength then hit ok. (Picture Below).



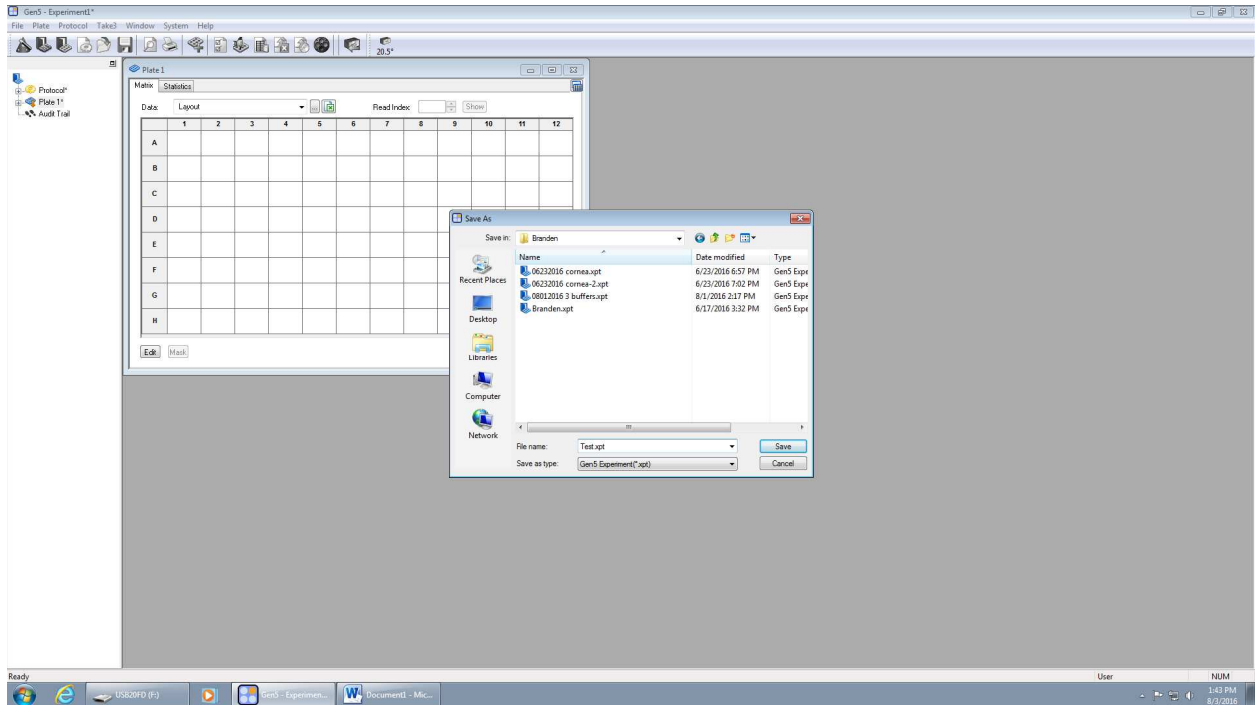
○ Click on ok again. (Picture Below).



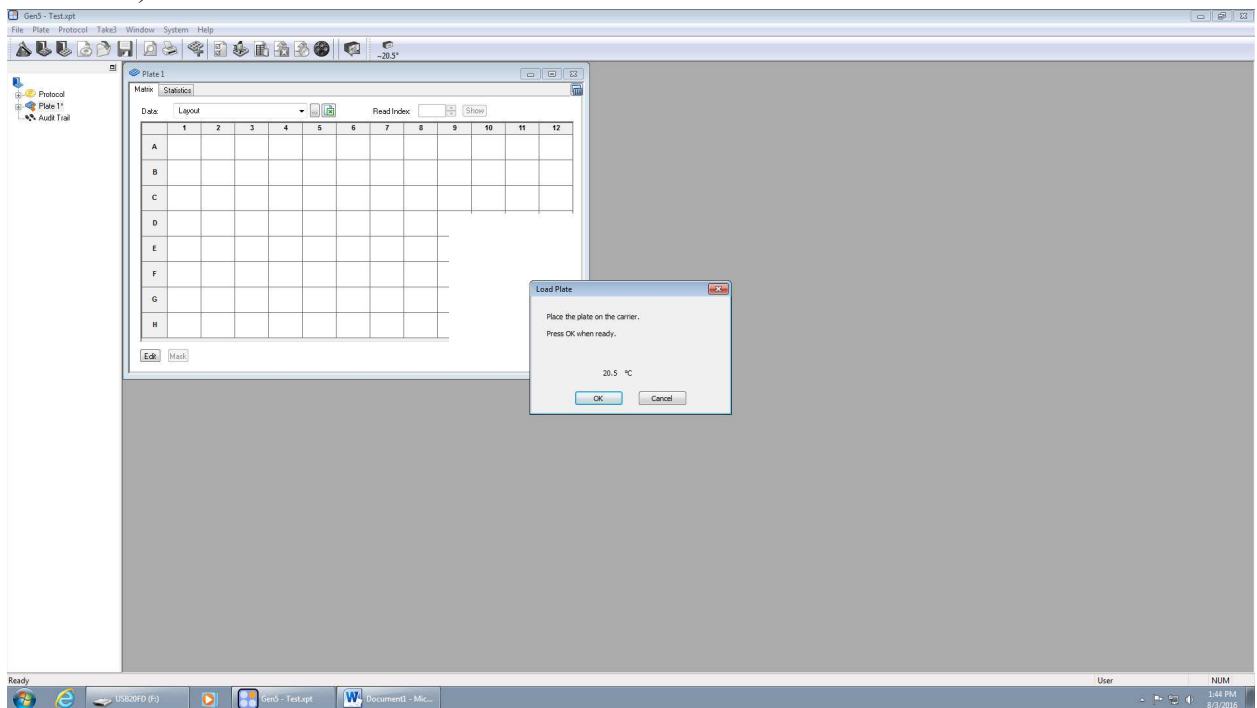
○ You are now ready to read the plate. Click on READ. (Picture Below).



○ This will trigger the ability to identify a location to put your saved results. (Picture Below).

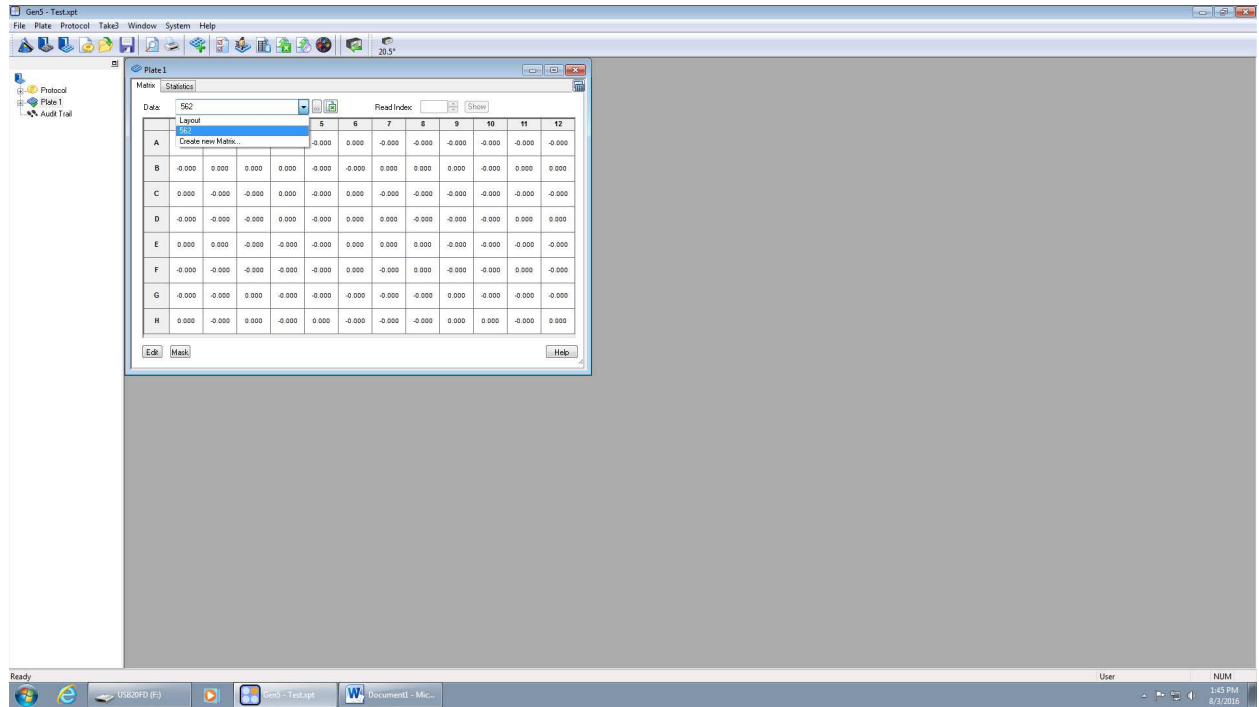


- Find or make your folder under the lab that you are in. Name your file. Save your file in your folder.
- Hit save.
- A warning pop up will appear to make sure your plate is in the machine. (Picture Below).

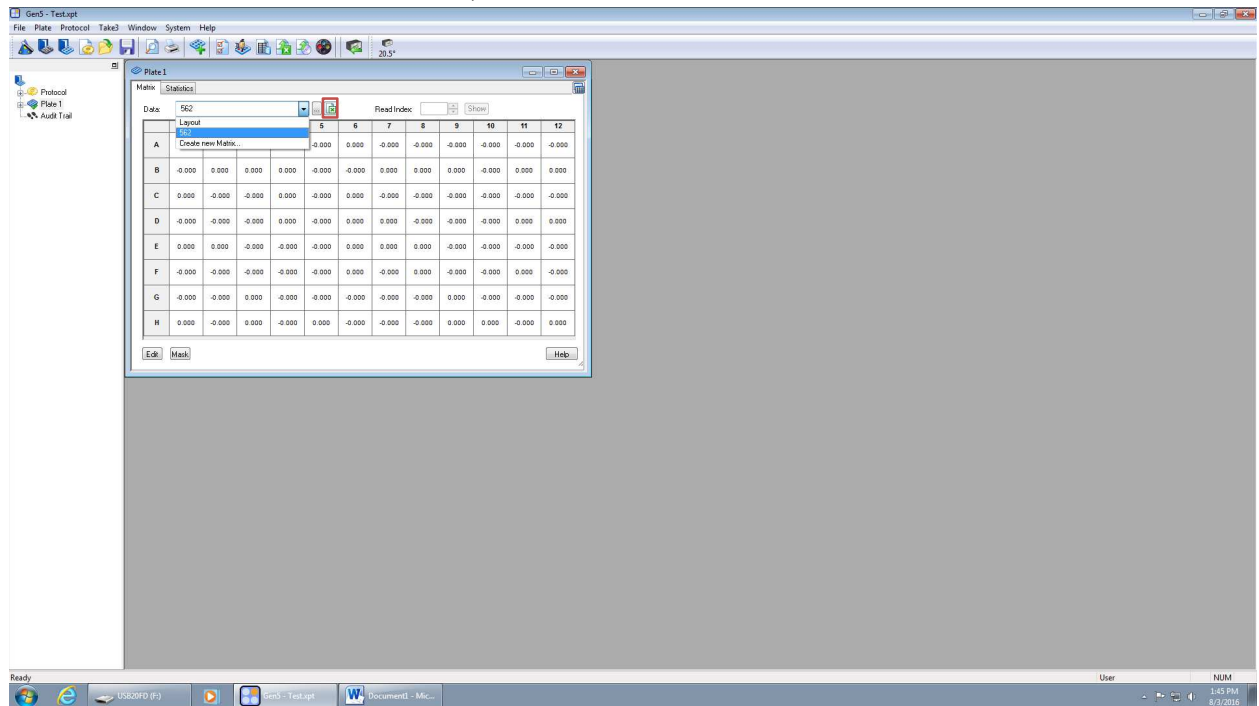


- At this point, place your plate on the machine and hit ok.
- The machine will take in your plate and read it.

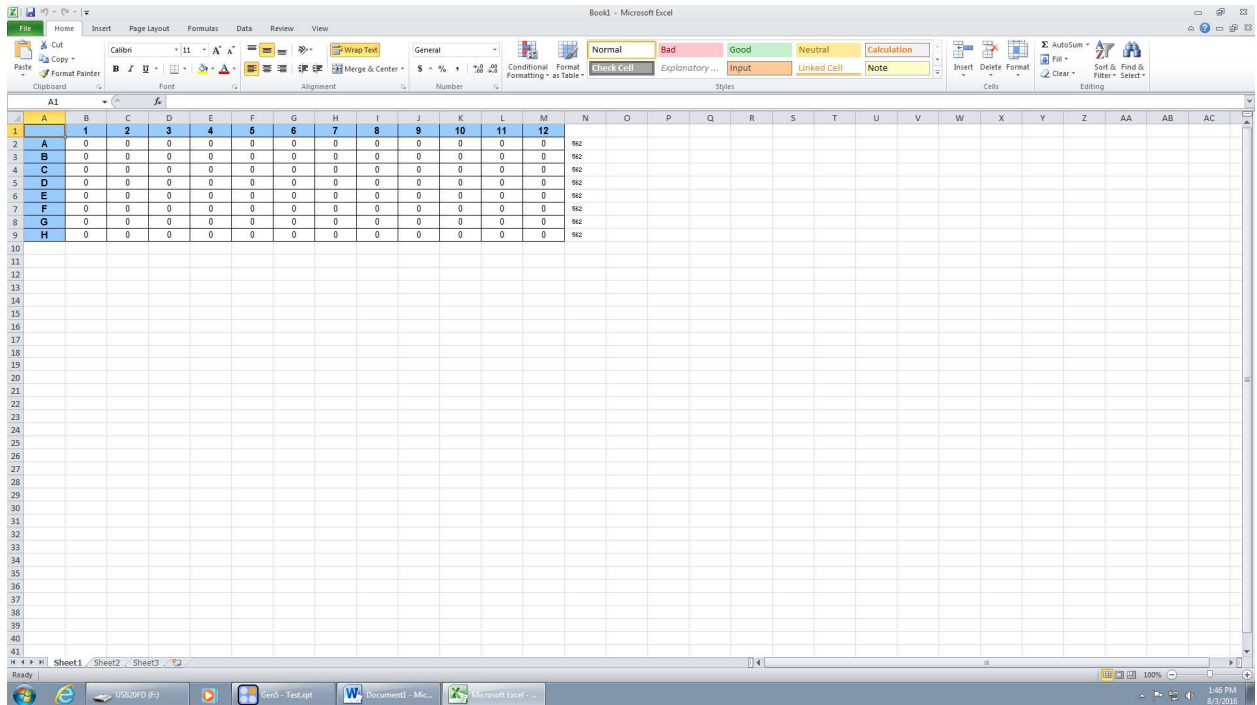
- Hit the layout part on the top and change it to 562 to see your results. (Picture Below)



- Hit the export to excel button to get your results into an excel file. (Picture Below. Look at red box for excel button).



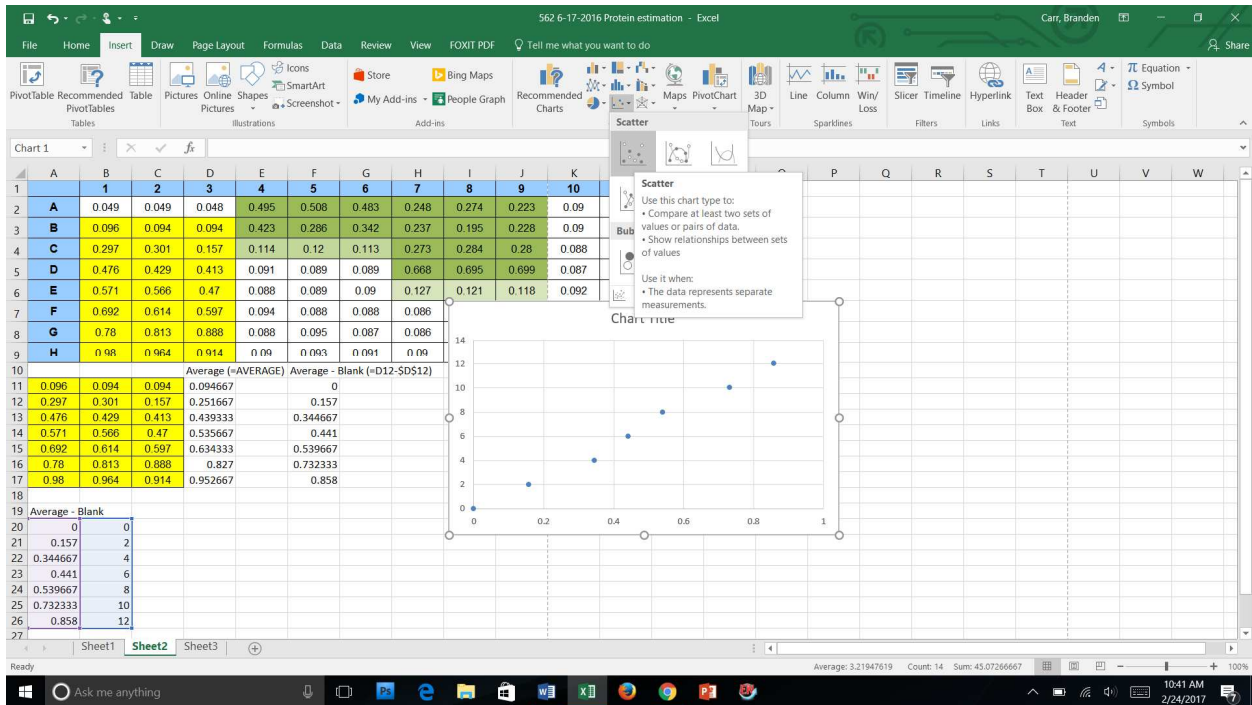
- An excel sheet will open and you can save this file to your folder and/or your flash drive. This is what you need to quantify your protein.



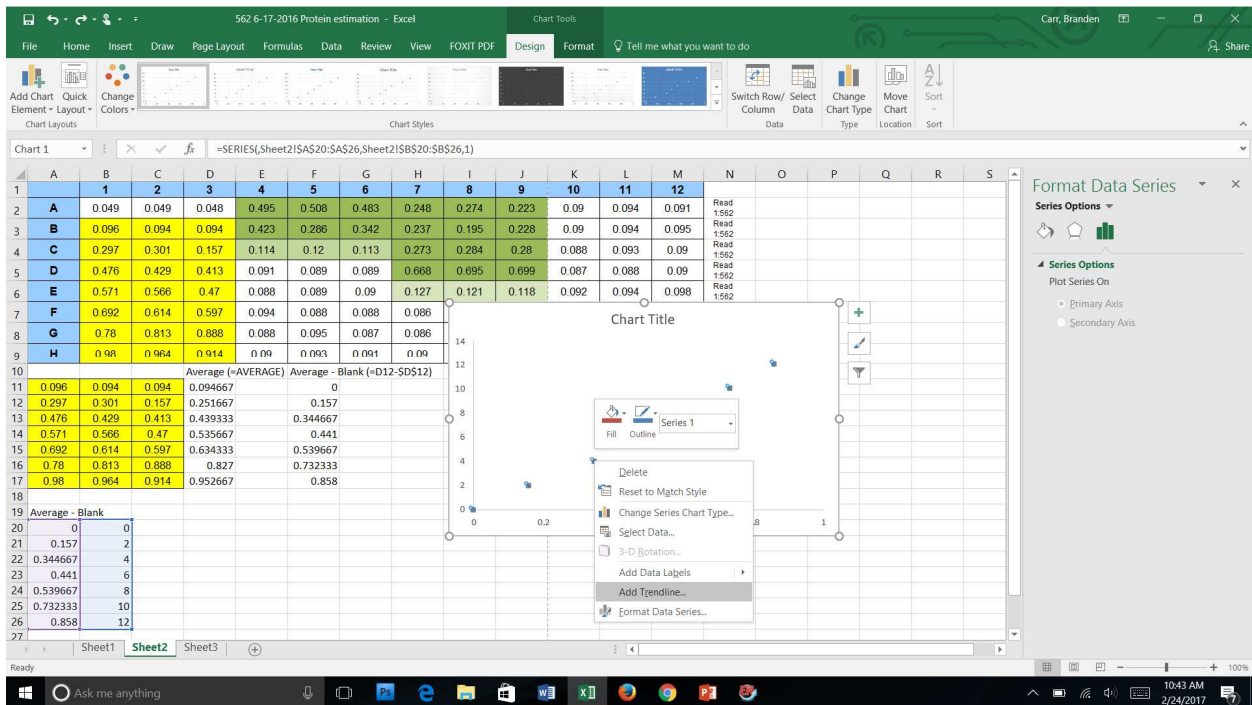
- Determining amount of protein to add to electrophoresis gel wells (BCA protein estimation)
 - After you have scanned your 96 well plate, the excel sheet should look like this:

	A	B	C	D	E	F	G	H	I	J	K	L	M	N
1		1	2	3	4	5	6	7	8	9	10	11	12	
2	A	0.049	0.049	0.048	0.495	0.508	0.483	0.248	0.274	0.223	0.09	0.094	0.091	562
3	B	0.096	0.094	0.094	0.423	0.286	0.342	0.237	0.195	0.228	0.09	0.094	0.095	562
4	C	0.297	0.301	0.157	0.114	0.12	0.113	0.273	0.284	0.28	0.088	0.093	0.09	562
5	D	0.476	0.429	0.413	0.091	0.089	0.089	0.668	0.695	0.699	0.087	0.088	0.09	562
6	E	0.571	0.566	0.47	0.088	0.089	0.09	0.127	0.121	0.118	0.092	0.094	0.098	562
7	F	0.692	0.614	0.597	0.094	0.088	0.088	0.086	0.085	0.091	0.093	0.095	0.095	562
8	G	0.78	0.813	0.888	0.088	0.095	0.087	0.086	0.086	0.088	0.095	0.094	0.099	562
9	H	0.98	0.964	0.914	0.09	0.093	0.091	0.09	0.089	0.089	0.092	0.092	0.091	562
10														
11														

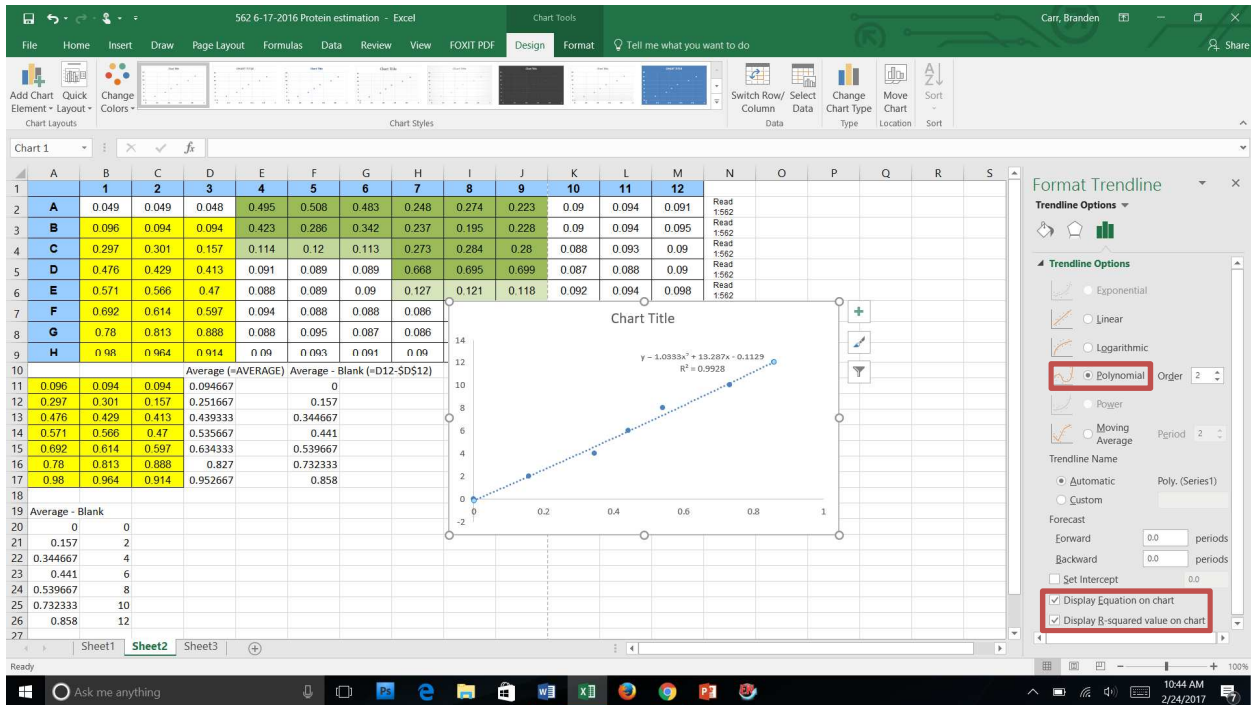
- From this you can prepare a standard curve from the first three columns, (Yellow highlight) and make a graph (Purple and Blue highlights). (Follow instructions in image to get Average-Blank numbers for the graph).



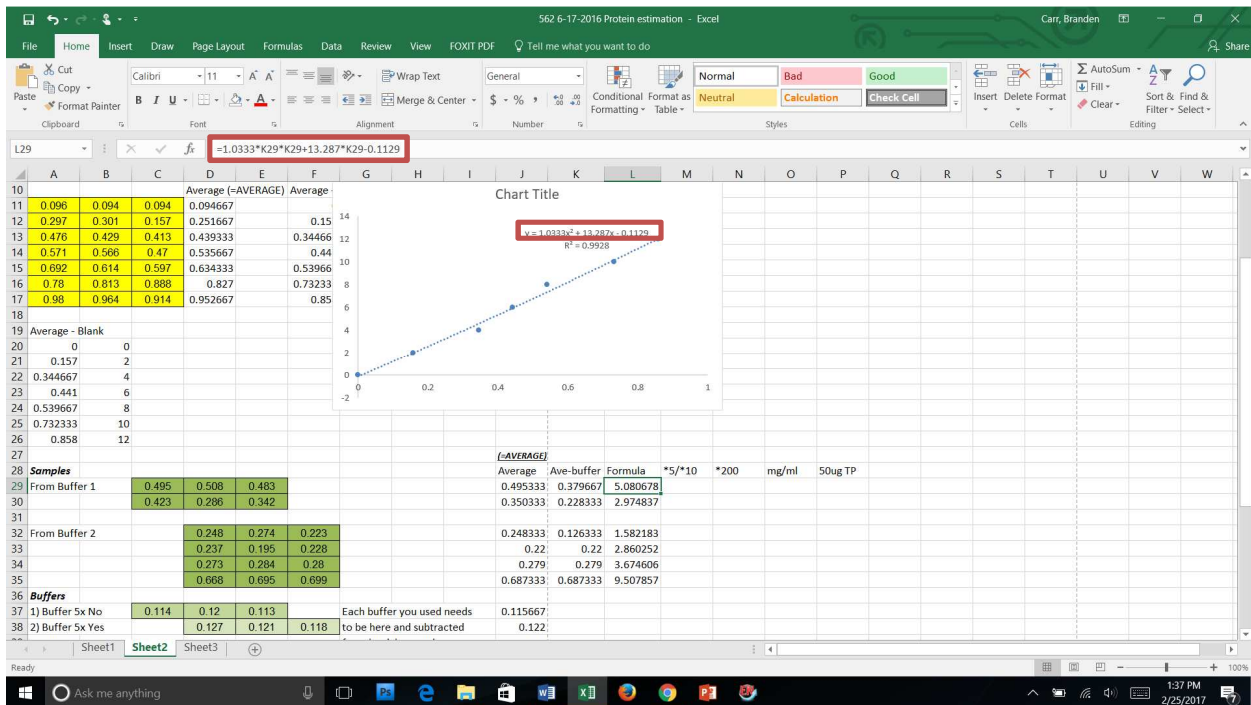
o Add a trendline:



o Add equation, R squared, and polynomial trendline (Red boxes):

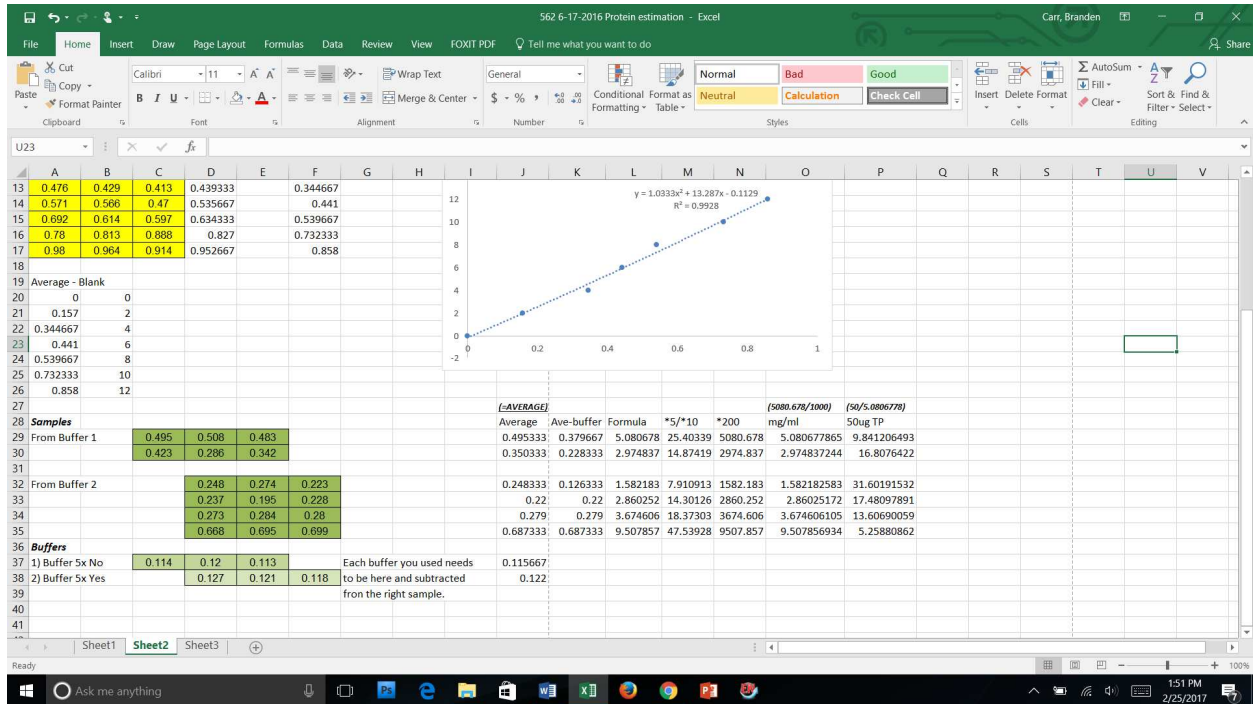


○ Use the formula to get this number:



○ Multiply and divide appropriately. *5/*10 is where you will multiply the previous cell by the dilution factor. *200 is to multiply by 200 since you used a total volume of 200 μ L for each well. The mg/mL is for dividing by 1000 for a conversion factor. The 50 μ g is where you take 50 and divide by the previous cell

to determine how many microliters you need to add in each well to get 50 μ g of total protein in each:



- Once you have the total protein, you can begin to determine how much loading dye and water to add. If you have 30 μ L wells to load into, using the first set of green boxes from buffer 1, you can load 10 μ L of water, 10 μ L of 5x loading dye, and 9.8 μ L of protein, in this order; just in case you mess up, you will not lose your sample.
 - In this case, the loading dye is at a higher concentration, but it is ok to have a little extra, but you do not want to go under the recommended amount or too much in the extreme either.
- Preparing gel for Western blot
 - If using a pre-cast gel, obtain from the refrigerator and bring it to the electrophoresis unit (Protean or Criterion).
 - Protean
 - Can do one or two gels at one time. If doing one, you will need a blank piece of plastic made to mimic a gel so you can pour running buffer between plates.
 - Remove the pre-cast gel from the plastic and REMOVE THE BOTTOM GREEN TAPE ON THE GEL!!!!
 - Put in a blank glass plate where a second gel can be placed in the and the actual gel on the other side.

- The smaller glass plate of the gel must be facing inward!
This will keep running buffer on top of the gel at all times.
- Firmly press down on the plates and place the apparatus in the hinge portion of the device.
- Press firmly and inwardly rotate the colorless plastic pieces to lock in the plates.
- Place the gel and apparatus in the electrophoresis box and add running buffer in between the plates.
 - Troubleshooting tip: If it leaks, take the apparatus out, pour the running buffer into the plastic cell, then place the apparatus on a hard surface.
 - Undo the colorless plastic hinge, then very firmly and forcefully press on the taller glass plate. You should feel about a millimeter drop in height. This will fix your leaking issue.
- Gently place two thumbs on the green well comb and apply steady force upward until the comb exits the gel. Use a well loading pipette tip to fix any wells that might have collapsed.
- Criterion
 - Take a precast gel out of its package, remove the tape at the bottom, and place it in one slot of the Criterion electrophoresis unit.
 - Add Running buffer to the reservoir at the top of the gel cassette and fill the criterion with running buffer to the arrow on the unit.
 - Much more user friendly than the Protean.
- Making your own gel:
 - Mix together these solutions to make the concentration you want (Example is 12% gel)
 - All of this is on the sheet from 5-15% gels:

Polyacrylamide gel %										
	5	6	7	7.5	8	9	10	12	13	15
30% Acrylamide solution	2.5	3	3.5	3.75	4	4.5	5	6	6.5	7.5
4x Resolving Buffer	3.75	3.75	3.75	3.75	3.75	3.75	3.75	3.75	3.75	3.75
Deionized Water	8.75	8.25	7.75	7.5	7.25	6.75	6.25	5.25	4.75	3.75
10% APS	0.05	0.05	0.05	0.05	0.05	0.05	0.05	0.05	0.05	0.05
TEMED	0.01	0.01	0.01	0.01	0.01	0.01	0.01	0.01	0.01	0.01

Stacking gel				
30% Acrylamide solution	4x Resolving Buffer	Deionized Water	10% APS	TEMED
0.65	1.25	3.05	0.025	0.01

- 6 mL of 30% Acrylamide/Bis Solution 29:1 in refrigerator in main lab.
- 5.25 mL of Deionized water
- 3.75 mL of 4x resolving buffer (1.5 M Tris pH 8.5 + 20mL 10% SDS).
- 50 μ L of 10% APS.
- 10 μ L of TEMED (once added, must finish gel quickly since it will begin to set).
- Here is the full list of gels:
 - Get the green stand ready on hard surface and place the smaller plate on the front.
 - Place a small rubber piece on the gel casting stand, then place the green stand with the glass plates on top of the rubber piece.
 - Lock the green stand in onto the casting stand and check for leaks by placing a small (about 1mL) of water in between the plates.

- Troubleshooting: If your gel casting stand is leaking, place a regular pen behind the clamp on top of the casting stand. This will apply additional pressure to the glass and prevent leakage.
 - Remove water by using filter paper. Make sure the plates are dry.
 - Mix the solution together by inverting the tube a couple of times and then begin to place about 7.5mL of the solution between the plates with a pipette.
 - Troubleshooting: If you are having issues with the gel setting too fast, decrease the amount of TMED used. If you are having issues with the gel casting too slow, increase the amount of TMED.
 - Place water on top of the solution between the glass plates very slowly to remove bubbles. Once solidified, remove the water with filter paper.
 - Let solidify and prepare for the stacking gel (Amount in chart above).
 - Place 2 mL of it on top of the previous gel.
 - Place a green comb in between the glass starting with the right most well then rotate the comb between the gel until all of the wells are in. Make sure to prevent a lot of air bubbles from going in between the wells.
 - Troubleshooting: decide how much of the sample you need and how many samples you have. You can choose the number of wells with varying sized combs.
 - Let solidify and the gel is ready to use like the precast gels (without the tape on the bottom).
 - Once in the apparatus, you will have to use a pipette and blow out any extra debris in the wells. To do this, take in running buffer that is on top of the plate in the apparatus, then gently expel the running buffer into the wells. This will get the debris out of the wells and they will sink to the bottom of the cell so they will not interfere with the movement of the loaded proteins
 - You can wrap the gels with saran wrap and place in the 4° C refrigerator for up to three days.
 - Make the running buffer (100 mL of 10x running buffer into 900 mL of deionized water.
 - Set up the apparatus with the short plate on the inside and a plate to hold in the running buffer in between the plates.
 - Pour the running buffer in between the glass plates and let it overflow.
 - Take a 1 mL pipette and suck in some of the running buffer and use it to flush out all the wells to remove debris.
- Preparing sample for western blot
 - Label 500 µL tubes the same name as your samples.

- You want 30 μL total, so: Example= if need 8 μL of sample, load 12 μL deionized water, 10 μL blue dye, and 8 μL sample in that order. Total volume is 30 μL .
 - Blue dye is in the freezer in the box that says Loading Buffer (5x) SDS and 10% APS.
- Once you have your samples prepared, bring to the Perkin Elmer DNA Thermal Cycler to boil the samples at a constant temperature of 100°C.
 - Turn switch on—PRESS: file—1—enter—step—100—enter—enter—start. Let it run for 10 minutes then PRESS: Stop—stop.
 - Can also do this step in mildly boiling water on a hot plate for 10 minutes.
- Be careful when removing the tubes. Grab the tube by the cap/body joint to lift them up, NOT THE CAP ITSELF. They may pop open and you will lose your sample.
- Spin the samples down using the small centrifuge for all the tubes for about 3 seconds each. This should bring any evaporated fluid to the bottom of the tube.
- Turn down the speed on a vortex machine and gently vortex all of the samples for about 1 second. DO NOT ALLOW THE SAMPLE TO FROTH (make bubbles)!
- Prepare the gel so you can load your samples.
- Loading gels
 - Take a 100 μL pipette and have it set to take up about 40 μL of fluid.
 - Place a well loading pipette tip on the pipette and move your entire sample; try to prevent the intake of bubbles.
 - Bring the pipette tip into the well where you want your sample and, up on top of the well, expel any bubbles that may be present. Once gone, enter further into the well and pipette out your sample into the well.
 - Troubleshooting: Be careful not to load your sample behind the glass plate. Gently press the pipette tip on the larger plate and slide into the well to prevent loss of sample.
 - Make sure the tip is above the sample in the well. You can bring the tip up as the well fills.
 - Continue loading all your samples.
 - Once all the samples are loaded, use the last remaining well to load 8 μL of a protein ladder which will tell you how large your protein is (You can place the ladder in any well you want as long as it is only the ladder and not your sample.
 - Protein ladder is in the freezer section in room E453. It is called Spectra Multicolor Broad Range Protein Ladder. Product number: 26634.
 - Troubleshooting: You can do a curtain gel by using multiple samples and ladders. You can cut the final membrane into multiple sections after your transfer is complete. This way you can stain for multiple antibodies by just doing one gel.

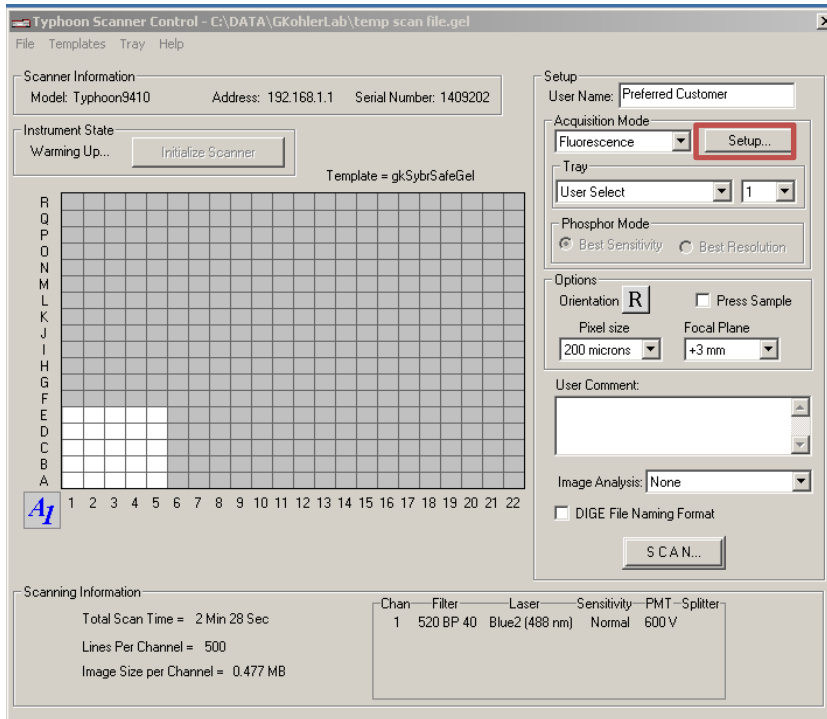
- Conducting a Western blot (Electrophoresis step)
 - Once all your protein is loaded and it is in the cell, place the lid on the cell (red to red, black to black), plug the lid into the powerpac, and turn it on.
 - Set the powerpac to ten minutes to pass 100 volts until the protein has gone through the stacking gel and has entered the bottom gel. Once all the protein has entered the gel, you can turn up the powerpac to 150 volts for 1 hour 20 minutes to allow the protein to travel faster down the gel.
 - For the Criterion, begin with 100 volts for ten minutes, then 150 volts for 10 minutes, then 180 volts for 1hour 20 minutes or until your ladder is in the location you want it.
 - Troubleshooting: This step varies with your protein of interest and other variables. Make sure you understand what voltage you need for your protein of interest beforehand to prevent unnecessary work. Easiest way is to just keep checking the gel and stop the powerpac when your bands are where you want them. Record the time and repeat thereafter.
 - Watch the ladder travel down the gel. Depending on your protein, you may want one of two of the colored bands from the ladder to go all the way to the bottom and through the bottom of the gel.
 - For me, I allow the bottom green and blue bands to exit the gel. This will allow me to visualize my protein of interest (about 100 kilo Daltons) clearly.
- Blotting onto the membrane
 - Once the ladder is just where you want it to be on the gel, turn off the powerpac to prevent excess protein from exiting the gel.
 - To prepare for the blotting step, prepare a transfer buffer by:
 - Add 200 mL of methanol, 700 mL of deionized water, and 100 mL of 10x transfer buffer, then mix. (Can mix with a gloved hand over the top of a 1L graduated cylinder and invert a couple of times.)
 - Pour about 200mL of the transfer buffer into a container.
 - Place 2 black sponges, 4 sheets of filter paper that you cut that is a little larger than your gel, and plastic blotting piece into this transfer buffer for about 5 minutes in a separate container.
 - Cut a PVDF membrane from a roll about the size of the gel that you just ran.
 - Also, cut a small section of the top left corner of the PVDF membrane. This will help you determine what side your protein is on.
 - Obtain a small container to fit your cut PVDF membrane and place enough methanol in it to cover the PVDF membrane. Once the methanol is in the container, place the PDVF membrane and allow it to soak for about 5 minutes.
 - Once soaked, take the PDVF membrane out of the container, and place it into the container with transfer buffer along with the filter paper, etc. Allow it to soak for about 5 minutes. **DO NOT TOUCH THE PVDF MEMBRANE!!!!** Only use a flat head tweezers to transport.

- Take the gel out of the glass plates by taking it out of the apparatus and use a green glass plate opener to pry the edges apart.
 - Self made gel: you can reuse the glass plates, so do not break them when you pry.
 - Pre made gel: you cannot reuse the plastic plates, so you will have to pry harder to break the plastic between the plates.
 - Place the gel in transfer buffer to soak for about 5 minutes. Do not allow it to touch the PVDF membrane.
- Take the plastic blotting piece out of the buffer and hold it in your hand where the colorless/red piece is in your palm and the black piece is on your fingers. (You may have a special container for this step; if so, place the plastic piece on the increasing wall of the tray instead of your hand. Have transfer buffer in this portion as well.)
- Place one sponge on the black portion of the plastic blotter piece.
- Place two pieces of filter paper from the tub on top of the sponge. Roll out any bubbles.
- Place the gel on top of the filter paper. Roll out any bubbles.
- Place the PVDF membrane on the gel and make sure there are no bubbles under the membrane by rolling them out with a roller.
- **MAKE SURE THE PVDF MEMBRANE IS PLACED FACE DOWN!!!** (The cut corner will be on the top right when placed down properly.)
- Place two more pieces of filter paper on the PVDF membrane.
- Place the final sponge on top, close the plastic blotting piece and place it in the transfer cell.
 - Troubleshooting: You need to make sure there are no bubbles in this step or they will show up in your image at the end. Also, make sure the whole sandwich stays wet. Do not let it dry, so do not take a lot of time putting it together if it is not submerged in a specialized western blot sandwich maker.
- Pour the remaining transfer buffer in the soaking container into the transfer cell.
- Place your 2 sandwiches, or your 1 sandwich and an extra plastic piece into the transfer cell.
- Use the remaining transfer buffer in the 1L graduated cylinder to make sure your sandwich is covered.
- Place a stir bar into the cell and check to make sure it will spin using a stir bar plate. If it does, you are good to go; if not, you need to get a smaller one, but not too small.
- Place an ice pack into the cell.
- Place the lid of the cell with the black colored wire on the black electrode, and the colorless portion of the plastic blotting piece towards the red electrode.

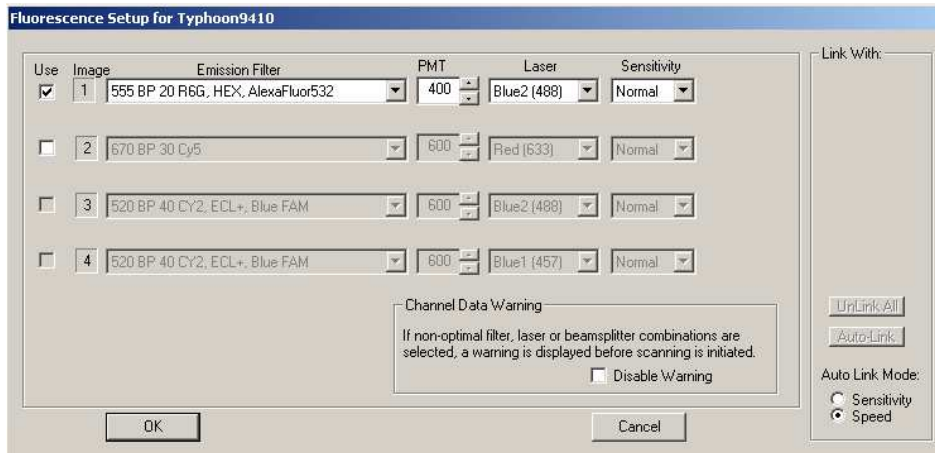
- Obtain a large container that the cell can fit in. Fill the container with ice (Can use a spare transfer container to place the ice around, so you will mold the ice for your own.). Place your transfer cell with your sandwich in the ice. Use some more ice and cover the top of the cell as well.
 - Troubleshooting: The Criterion runs hotter than the Protean. Pouring cold water into the container with ice will increase the ability to extract the extra heat from the cell. This will decrease the overall amps you will have when transferring. (The amps typically stay at around 0.65, if done right.)
 - Troubleshooting: To further make sure your amps will be low, have the transfer cell with transfer buffer in the ice bath for 1 hour before you place the sandwich and ice pack in.
- Turn the powerpac to 110 Volts.
 - Troubleshooting: If the voltage does not go up to 110, and/or the amps max out or are very high, your transfer buffer has gone bad. Pour out the 10 X stock transfer buffer and make a new batch.
- Allow it to sit for 1 hour with precast gel, 1 hour 30 minutes for 10% self-made gel. (You want to see all the bands transfer out of the gel and onto the PVDF membrane. You may need to adjust the time to your liking.).
 - Troubleshooting: If you are looking for small weight proteins, you can use 2 PVDF membranes. If the protein passes through the first one, they hopefully can be seen on the second one.
- Make blocking buffer: Can try nonfat dry milk or Bovine Serum Albumin (BSA):
 - Make 5% milk (2.5 grams of dried milk into a 50 mL tube. Bring to 50 mL mark with TBST) and place about 10 mL of it into a 50 card trading card container (Or go to Vintage Stock and buy a plastic trading card container for a fraction of the price to put it in. Same thing.)
 - Make 2.5% BSA (add 2.5 grams of dried milk into about 70mL of deionized water in a 200mL beaker. Bring the final volume to 100 mL using a graduated cylinder. Distribute 50mL into one 50mL conical tube and 50mL into a different 50mL conical tube. Add 25 μ L of TWEEN 20 into one conical tube and mix by inverting. Label each tube respectively as BSA-T and BSA. Place about 10 mL of BSA-T into a perfect Western container (Or go to Vintage Stock and buy a plastic trading card container for a fraction of the price to put it in. Same thing. Costs 49 cents compared to 15 dollars.)
- Place your PVDF membrane that was just blotted FACE UP into the container with the 5% milk or 2.5% BSA (Cut corner will be on the top left when placed properly.). (You may need to trim the membrane to make it fit into the container. Be sure to cut only the sections of the PVDF membrane where you are sure there are no bands or protein.).
- Primary antisera

- Remove the PVDF membrane from the blotting machine and place it in a 50 card trading card container FACE UP (Cut corner will be at the top left of the PVDF membrane; cut if needed with scissors) with 5% milk (2.5 grams of dried milk into a 50 mL tube; bring to 50 mL mark with TBST) or BSA-T.
- Place on shaker at about 4-5 speed (somewhat gentle) for 2 hours. Should see the membrane sliding back and forth with the flow of the milk or BSA-T.
- After 2 hours, remove the milk or BSA-T and replace it with another 10 mL of milk or BSA (I just use BSA, not BSA-T here). Measure this time with the electronic pipette.
- You typically want a 1:1000 dilution of your primary antiserum, but the concentration of antiserum will depend on how much you need to add to the 5% milk or BSA.
 - Example: For Santa Cruz antisera, they typically come in a concentration of 200 μ g/mL, or 0.2 μ g/ μ L. You want the final concentration to be 1 μ g/ μ L, so you will need to x5 your concentration. Instead of using 10 μ L, you will need to use 50 μ L in this case.
- Pipette CALCULATE μ L of your primary antiserum of interest and place it next to the PVDF membrane to allow for it to diffuse across the membrane. Place in the cold room overnight on the rotator machine.
- Secondary Antisera
 - Take the PVDF membrane in the 50 card, trading card case submerged in the primary antibody out of the cold room.
 - Let it sit for about 1 hour to stabilize at room temperature.
 - Pour the milk/primary antibody out of the container and replace with TBST.
 - You will want to wash with TBST 1 time at “0” minutes (Place in, swirl, pour out) and then 4 times for 15 minutes each.
 - Once washed, prepare 5% milk (2.5 g of dried milk and bring up to 50 mL with TBST) and place 10 mL on the membrane with the electronic pipette.
 - Add 10 μ L of the secondary antiserum in the milk next to the membrane and allow for it to diffuse over the membrane on the rotator machine.
 - Ex: if your primary antiserum was rabbit anti-Kainate receptor subunit, you will need a rabbit secondary antiserum.
 - Ex: if your primary antiserum was mouse anti-Kainate receptor subunit, you will need a mouse secondary antiserum.
 - Note: Depending on the way you would like to image your blot will determine which secondary antisera you will use.
 - Chemifluorescence: Has alkaline phosphatase enzyme conjugated to the secondary antibody. This protocol follows Chemifluorescence.
 - Chemiluminescence: Has horse radish peroxidase enzyme conjugated to the secondary antibody.

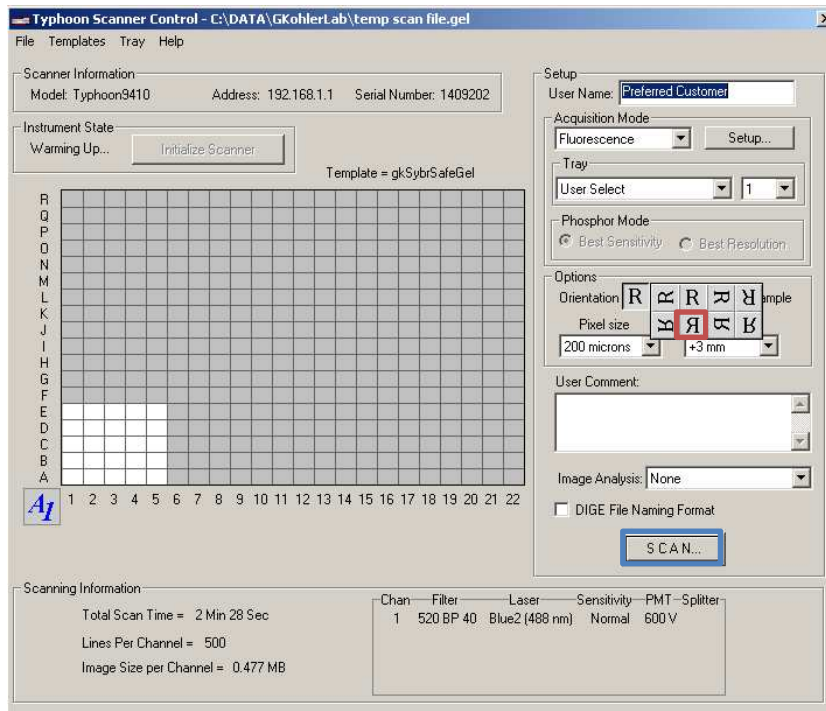
- Once the secondary antiserum is added, allow rotatory shaking for 2 hours.
- Once the 2 hours are finished, remove the milk and wash four times with TBST for 15 minutes each.
- Obtain tweezers that have a square flat head (flat head tweezers), a tube with 1mL substrate labeled ECF substrate for WB RPN5785, and a 1 mL pipette set at 0.5mL.
- Take your PVDF membrane over to the imaging machine. (Typhoon).
- “Wake up” the computer by moving the mouse and double click on Typhoon Scanner Control v5.0.
- Open the machine lid and spray a little bit of isopropyl alcohol on the bottom left portion of the glass piece under the lid and wipe with Kimwipes to clean.
- Let dry for a couple of seconds and then apply 0.5 mL of substrate to the area on the bottom left that you washed in an area you think will fit your membrane. (Drag the pipette tip in a “wave motion” as you eject the substrate).
- Earlier, the top left corner of your membrane was cut. That is face up. The membrane must be faced down, so place the membrane down in a way that has the cut on the top right. This has to be done on the substrate placed on the machine and it must be done quickly. Use the flat head tweezers and run the membrane through the substrate once to soak it and then lift it. Gently place the end way from your tweezers on the glass plate and gently allow the membrane to make contact with the glass/substrate. Make sure you prevent bubbles from being caught underneath the membrane. It helps if you do not have any bubbles when pipetting the solution.
- Once on the glass, (should take no more than 1 minute, aim for about 30 seconds) close the lid and open the Typhoon Scanner control v5.0.
- You will see this picture and you want to click on the setup box highlighted by the red box:



- Once pressed, you will want it to look like this. Change all of the components to match this if you are using alkaline phosphatase secondary antibodies that are excited at 488nm:

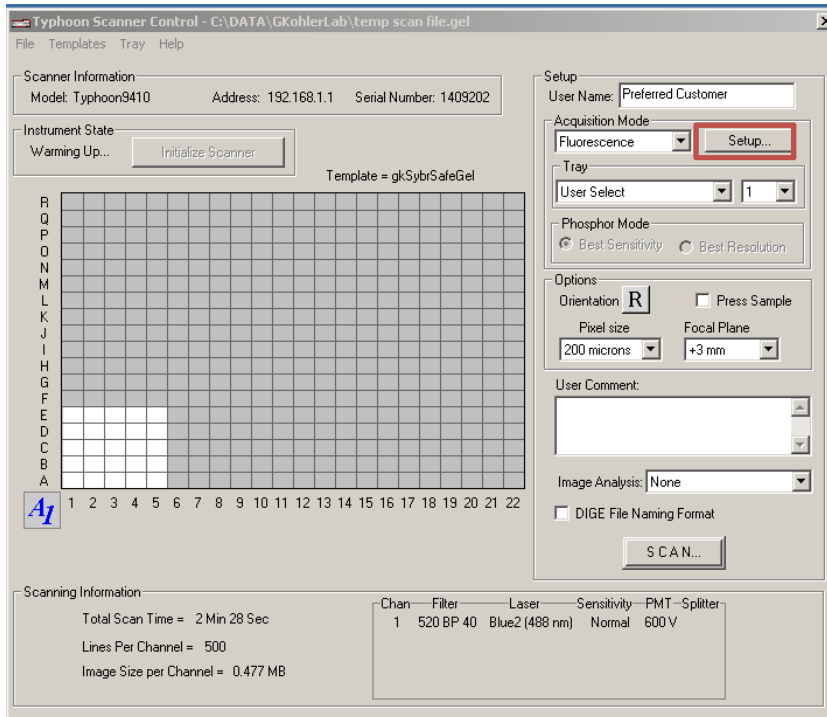


- Press OK, and you will get a message saying that you are changing the laser away from the default. Click yes.
- Once finished, you want to change the orientation of the image to properly view your membrane. Click and hold on the R button and move your arrow to the R that has a red box around it:

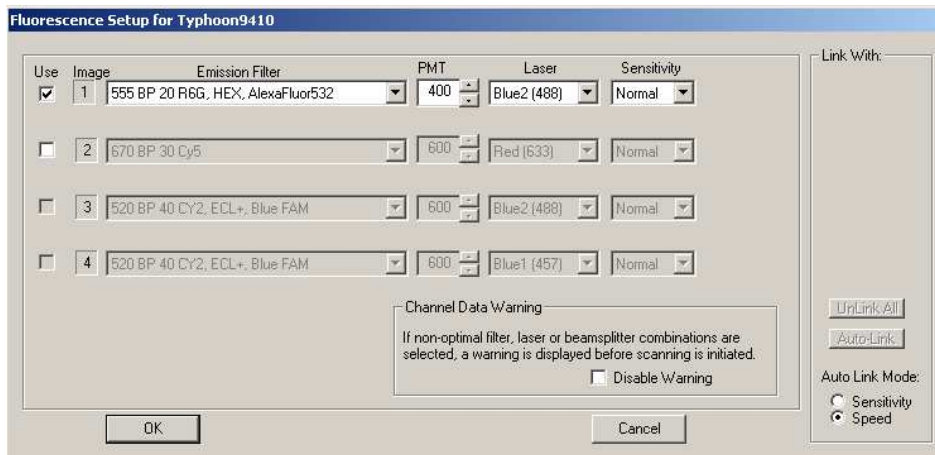


- Once finished, press the SCAN button. It has a blue box around it in the previous image. You will get a box to save your data. Find the folder that says DATA. You should see a lot of folders with names on them. Right click on a portion of the window and click on new folder. Name it (your name) and click off of it. Double click it and you should open your folder. Press the save button.
- It will take about 5 minutes to scan your membrane.
- Stripping and reblotting (Primary antibody)
 - After you have finished the imaging step, bring the PVDF membrane back into the lab and apply about 10 mL of stripping buffer.
 - Place the container that has your PVDF membrane on the shaker for 20 minutes.
 - Remove the fluid after 20 minutes and wash with TBST 3 times with no waiting time.
 - Continue to wash the membrane with TBST for 5 minutes each time until you have eliminated the odor of the stripping buffer.
 - Remove from the final wash (once the smell is gone) and block the membrane a second time with 2.5% milk or BSA-T for 2 hours.
 - After 2 hours, replace the milk with 10 mL of 2.5% milk with an electric pipette, and place 10 μ L (1:1000) of antiserum next to the membrane so it can diffuse across.
 - Place on a rotatory shaker overnight in the cold room.
- Stripping and reblotting (Secondary antiserum)
 - Take the PVDF membrane in the 50 card trading card case submerged in the primary antiserum out of the cold room.
 - Pour the milk/primary antiserum out of the container and replace with TBST.

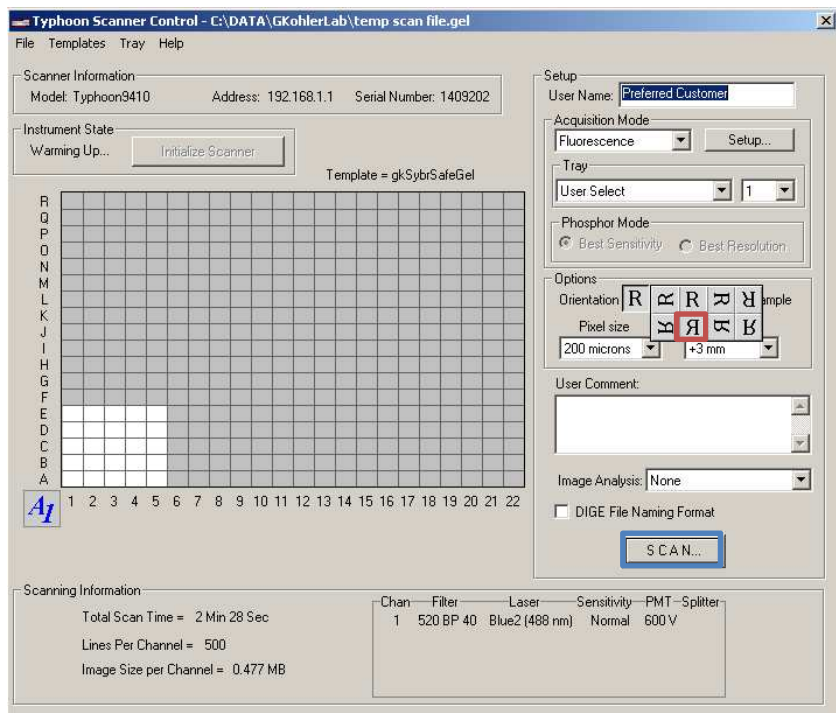
- Wash with TBST 3 times for 20 minutes each.
- Once washed, prepare 5% milk (2.5 g of dried milk and bring up to 50 mL with TBST) and place 10 mL on the membrane with the electronic pipette.
- Add 10 μ L of the secondary antiserum in the 5% milk next to the membrane and allow for it to diffuse over the membrane on the rotator machine.
 - Ex: if your primary antiserum was rabbit anti-Kainate receptor subunit, you will need a rabbit secondary antiserum.
 - Ex: if your primary antiserum was mouse anti-Kainate receptor subunit, you will need a mouse secondary antiserum.
- Once the secondary antiserum is added, allow rotatory shaking for 2 hours.
- Once the 2 hours are finished, remove the milk and wash four times with TBST for 15 minutes each.
- Obtain flat head tweezers, a tube of 1 mL substrate out of the freezer in the box labeled ECF substrate for WB RPN5785, and a 1 mL pipette set at 0.5mL.
- Take your PVDF membrane to the imaging machine next to the cold room.
- Wake up the computer by moving the mouse and double click on Typhoon Scanner Control v5.0.
- Open the machine lid and spray a little bit of isopropyl alcohol on the bottom left portion of the glass piece under the lid and wipe with Kimwipes to clean.
- Let dry for a couple of seconds then apply 0.5 mL of substrate to the area on the bottom left that you washed in an area that you think will fit your membrane. (Drag the pipette tip in a wave motion as you eject the substrate).
- Earlier, you cut the top left corner of your membrane. That is face up. We want you membrane to be faced down, so place the membrane down in a way that has the cut on the top right. This has to be done on the substrate that you just put on it and has to be done fast. Use the tweezers with the square flat head and run the membrane through the substrate once to soak it and then lift it. Gently place the end way from your tweezers on the glass plate and gently allow the membrane to make contact with the glass/substrate. Make sure you prevent bubbles from being caught underneath it. It helps if you do not have any bubbles when pipetting the solution.
- Once on the glass, should take no more than 1 minute, aim for about 30 seconds, close the lid and open the Typhoon Scanner control v5.0 on the computer.
- You will see this picture and you want to click on the setup box highlighted by the red box:



- Once pressed it, you will want it to look like this. Chance all of the components to match this:



- Press OK, and you will get a message saying that you are changing the laser away from the default. Click yes.
- Once finished, you want to change the orientation of the image to properly view your membrane. Click and hold on the R button and move your arrow to the R that has a red box around it:



- Once finished, press the SCAN button. It has a blue box around it in the previous image. You will get a box to save your data. Find the folder that says DATA. You should see a lot of folders with names on them. Right click on a portion of the window and click on new folder. Name it and click off of it. Double click it and you should open your folder. Press the save button.
- It will take about 5 minutes to scan your membrane.
- To save your result gel results as an image, open the program ImageQuant 5.1.
- Go to file then open and find the gel you wish to take to an image.
- Open the file then go back to file then save as.
- Name the file and change the “Save as type:” portion to TIFF Files.
- Save to your designated folder of interest and you have an image file to use. You can open this file on your own computer now.

Making solutions

10X TBS

- 60.6g of Tris HCl pH 7.6
- 87.7g of NaCl
- Bring to 1L of water

Making TBST

- A concentrated solution of TBST is already made. It is 10 times more concentrated than need.
- Take the bottle labeled 10x TBS and measure 100 mL using a graduated cylinder and place the fluid in a 1 L bottle. Add water up to the 1 L mark (900 mL).
- Add 1 mL using a 1 mL pipette of TWEEN 20.
- Swirl to mix and it is ready to use.

Making 5% nonfat dry milk

- Weigh out 2.5 grams of milk powder and pour it into a 50 mL tube. Add TBST up to the 50 mL mark (50 is a plastic line, not a marked black line on the tube.).

Making 2.5% Bovine serum albumin (BSA).

- Weigh out 1.25 grams of BSA and pour it into a 50 mL tube. Add TBST up to the 50 mL mark (50 is a plastic line, not a marked black line on the tube.).

Making 10x Running Buffer

- 144g Glycine
- 30.3g Tris HCl
- 10g SDS
- Bring to 1L of water

Making 10x Transfer Buffer

- 30.3g Tris HCl
- 144g Glycine
- 20% methanol
- Bring to 1L of water

5x Loading buffer

- 1g Sodium dodecyl sulfate (10%)
- 1.67 mL of 1.5M tris-HCl (pH 6.8).
- 5mL of glycerol
- 50 μ L of BME per 1mL of loading buffer.
- 0.001% bromoethanol blue
- Bring to 10mL of water.

1x RIPA buffer

- 50mM Tris HCl buffer (pH 8)
- 1% NP40 (Can use 1% triton X 100)
- 0.5% sodium deoxicholate
- 0.1% SDS

- 150mM NaCl
- 10% glycerol
- Add protease inhibitor

1x Lysis buffer (Triton X-100)

- 50mM Tris HCl pH 7.4
- 1% triton X 100
- 50mM NaCl
- 10% glycerol

APS

- 1g APS.
- Bring to 10mL of water.

LEGEND:

Set up

Making a solution

Set up

Information for a different method

Important step

CHAPTER VII

IMMUNOHISTOCHEMISTRY PROTOCOL

Immunohistochemistry

- Rat selection
 - 8-10 weeks is good, but no actual age range restriction. (I use 6-8 week rats).
- Preparing gel coated slides (wear gloves and lab coat).
 - Obtain a slide metal rack. Do not use rack if rusted.
 - Obtain a square or rectangular glass container that will fit the metal rack.
 - Place glass slides in all the slots of the metal container. Try to get all the slides facing the same direction.
 - Place the metal rack with all the glass slides into the glass container and place under the hood.
 - Obtain the chromic acid solution (recipe provided below) which is in the cabinet under the hood and pour it on the slides in the glass container until the slides are fully submerged.
 - Allow the acid to remain on the slides for 20 minutes. (The acid solution will make holes in your clothes if it gets on you.)
 - Once finished, bring out the metal rack and slides with a bent clothes hanger (attached to the left side of the hood).
 - The hanger is made in a way that you can squeeze it and place the ends in the holes of the metal rack for transport. Be careful not to drop the metal rack with the slides.
 - Place the metal rack with the slides into another empty glass container for transport.
 - Turn on the hot water in the sink and allow the water to wash the slides in the metal rack for 10 minutes. (Keep the hot water flowing over the slides for the full time).
 - Take a ceramic filter that has a flat inside portion for a filter paper to fit in. I have made a template filter paper so you can use it to cut out the right size.

- Place the filter with the filter paper on a 1000mL Büchner flask (vacuum flask) and hook up the vacuum with a tube in the cabinet to the left of the hood. You may need to seal the connection between the flask and the filter by applying parafilm to the connection.
 - Turn on the vacuum and place a little bit of the chromic acid solution on the filter paper to wet it. This ensures it will go through the filter paper and not around and underneath it.
 - Once wet, gently pour the rest of the solution into the filter.
 - Pour the filtered solution back into its original bottle and place it back in the cabinet under the hood.
 - Throw away the filter paper and rinse clean the vacuum filter with water.
- Once the 10 minutes has passed, remove the rack and gently shake any excess water from the rack with slides.
- Take the gelatin slide coating solution (also located in the cabinet under the hood) and pour it into another glass container that fits the metal rack and slides. (The same glass container can be used that held the chromic acid solution after filtering the solution and placing it back in its original bottle and after the container has been rinsed clean with water.)
- Dip the metal rack with the slides 5 times into the gelatin solution. (Nothing special here, just dip once every 3 seconds for 5 times. Takes less than a minute to do.). Drain the solution from the rack by tilting one edge of the rack against the inside lip of the glass container.
- Place the metal rack with the slides in the 37°C incubator for 12-24 hours. Filter the slide coating solution with the filter and new filter paper.
- After 12-24 hrs, remove the slide rack from the oven. Run your finger across the top part of the white portion of the slide to disconnect the slides from the metal so the next coat can be applied evenly.
- Pour the gelatin slide coating solution into a glass container. Dip the metal rack with the slides 5 more times, drain, and allow the slides to remain in the 37°C incubator for another 12-24 hours. Once again, filter the slide coating solution.
- The slides can be left in the 37°C incubator over the weekend if needed.
- **Remember to clean up after yourself after each step.**

Making the Acid Cleaning Solution

- 100 Grams of Potassium Dichromate or Bichromate
- 850mL of DD H₂O.
- 100mL of 95% H₂SO₄.
 - Mix the Potassium Dichromate with deionized H₂O while stirring on low temperature setting until it is completely in solution. This should be done in the hood.
 - Let cool to room temperature.
 - Add the acid and stir. Bring to 1000 mL with DD H₂O.

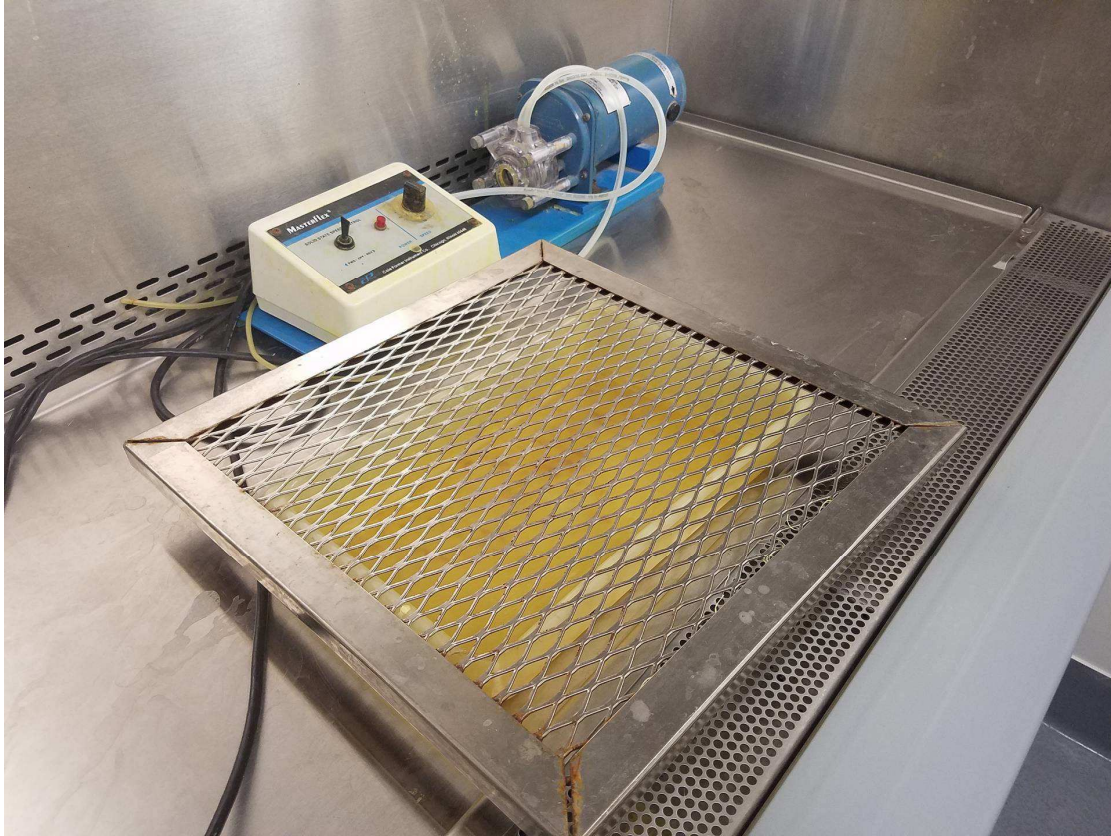
Making the Slide Coating Solution

- 7.5g of Gelatin
- 0.75g of Chrom Alum (Chromium Potassium Sulfate -12 H₂O).
- 0.01 g of Sodium Azide.
- 900 mL of DH₂O.
 - Dissolve gelatin in water by heating to about 50°C, but do not exceed 58°C.
 - Let it cool to room temperature.
 - Add the Chrom Alum (Chromium Potassium Sulfate -12 H₂O).
 - Bring to 1000 mL with deionized H₂O.
 - Filter and skim off any bubbles with filter paper.
- Solution preparation for rat transcardial perfusion:
 - Each rat will need about 100 mL of calcium free Tyrodes buffer and about 240 mL Picric acid, 81 mL 0.4 M phosphate buffer, and 4 mL of paraformaldehyde. Before you continue, determine how many rats you will use and make the solutions accordingly.
 - Calcium free Tyrodes buffer
 - Obtain a large flask (1 L for fewer rats, 2 L for more rats) and place a stir bar in it to mix the solution well without hitting the sides of the glass.
 - Using a graduated cylinder, measure 800 mL of deionized water.
 - Pour the water in the beaker or flask, place a stir bar in the flask, and turn on the stir plate to mix the water.
 - For one liter, weigh and place the following chemicals in the beaker or flask:
 - 6.8 g of NaCl
 - 0.40 g of KCl
 - 0.15 g of MgCl₂.
 - 0.10 g of MgSO₄-7H₂O.
 - 0.19 g of NaH₂PO₄-2H₂O. (Or use 0.098 g of anhydrous NaH₂PO₄-2H₂O).
 - 1.00 g of Glucose.
 - 2.20 g of NaHCO₃.
 - Completely mix.
 - Pour the solution into a 1 L graduated cylinder and add deionized water to the 1 L mark.
 - Pour back into the flask and mix.
 - Using a pH probe attached to a pH meter, add NaOH to raise the pH and HCl to decrease the pH until the solution reaches 7.31-7.35.
 - Place a piece of Parafilm over the top of the flask (or place in a capped bottle) and a piece of tape describing what is in the flask with the date and your name on it.

- Store at room temperature overnight.
- Check the pH right before use on the next day and adjust pH back to 7.31-7.35 if needed.
- Paraformaldehyde (This should be done in the hood.)
 - Obtain a 100mL beaker, a thermometer, and 2 hot plates. Place these items in the ventilated hood.
 - Place the beaker on top of the hot plate with 40 mL of deionized water in it.
 - Place the thermometer in a metal bar holder and place the tip into the water.
 - The temperature should be kept between 50-55 degrees Celsius. DO NOT GO OVER 55 DEGREES CELSIUS!!!!
 - Place a small stir bar into the 100mL beaker and turn on the stirring and heating functions.
 - Measure 8 grams of paraformaldehyde under the hood.
 - Bring the temperature up to 50°C.
 - Once the temperature reaches 50°C, place the 8g of paraformaldehyde in the beaker and allow to mix.
 - Once the temperature again reaches 50°C, place the beaker on a different hotplate and only turn on the stirring function.
 - Place the paraformaldehyde into the 100mL beaker with the water.
 - Obtain about 8 pellets of sodium hydroxide (NaOH) and place into the 100mL beaker.
 - After about 30 seconds of mixing, place the 100mL beaker back on the hotplate with the thermometer and bring the temperature back up to 50°C.
 - Once at 50°C, remove the 100mL beaker and place back on the stirring only plate.
 - Repeat moving the 100mL beaker back and forth until the solution has cleared. (You will move the solution back and forth about 3 times and the solution will not be perfectly clear, but close).
 - Once the solution is clear, let it sit until it has reached room temperature.
 - Obtain a funnel, graduated cylinder, and a round piece of filter paper.
 - Fold the round piece of filter paper in half twice and separate the edges from each other to be able to place it into the funnel.
 - Place the funnel with the filter paper in on top of the graduated cylinder.
 - Pour the paraformaldehyde solution and let it filter through the paper.
 - You will filter deionized water with the same filter paper after the paraformaldehyde is all filtered out.
 - You want the final volume to be 50mL.
 - After filtered, your solution should be completely colorless and not cloudy.

- 0.4 M phosphate buffer
 - Obtain a 1000mL beaker and add 900mL of deionized water into it.
 - Place a stir bar in the beaker and begin mixing.
 - Add these chemicals together in the beaker:
 - 43.6g of Na_2HPO_4 (Anhydrous) to the beaker.
 - 12.8g of NaH_2PO_4 (Anhydrous) to the beaker.
 - Allow for the chemicals to completely dissolve.
 - It will take some time to dissolve. The chemical mixture becomes hard when it hits the water.
 - Place the 900mL with the dissolved chemicals into a 1000 mL graduated cylinder and bring the volume to 1000mL with deionized water.
 - Pour the 1000mL back into the beaker for mixing.
 - The 0.4 M phosphate buffer is ready to use.
- Picric acid
 - Under the hood are plastic rectangle jugs of a yellow solution. This is picric acid. You will need 240 mL of picric acid per rat
 - Obtain a 1 L vacuum flask, a large ceramic funnel with multiple holes, and a filter paper cut to fit the funnel.
 - Once the filter paper is in and it does not look like it will leak around the edges, place the tubing on the nozzle of the flask and turn on the vacuum until you see the filter paper settle onto the funnel.
 - Begin to pour the picric acid in the center of the filter paper and be careful not to pour in too much, too fast. If the filter paper moves and the solid get into the flask, you must start over filtering the solution.
 - Keep pouring in as much as needed (240 mL per rat) and then place it in a large graduated cylinder to determine the exact volume collected.
 - Once you have obtained the volume needed, pour all of the picric acid into a large bottle and place a stir bar in the bottle as well.
 - Pour 81 mL of 0.4 M phosphate buffer PER RAT into the picric acid.
 - NOTE: Do not use Sorenson's phosphate buffer or you will get a red precipitate when mixing it with the picric acid.
 - Pour 4 mL of Paraformaldehyde PER RAT into the picric acid.
 - pH the solution to about 7.31-7.35.
 - Store at room temperature overnight.
 - Check the pH right before use on the next day and adjust pH back to 7.31-7.35 if needed.
- 2.5% Avertin
 - Take out 1 mL of 2-methyl-2-butanol and place into a 10mL beaker.
 - Take 1g of 2,2,2-Tribromoethanol and place into the same 10mL beaker.
 - Place a very small (micro) stir bar into the 10mL beaker and stir.

- Allow the chemicals to dissolve completely (about 10 minutes) and place into a microcentrifuge tube.
 - Take 350 μ L of the solution and put into 10mL of phosphate buffered saline (PBS) to make the final concentration of 2.5%. (You will need 3 mL per rat, so make the solution for the number of rats needed.)
- Anesthesia and euthanasia of the animals
 - Obtain the rat for perfusion.
 - Obtain 3mL of Avertin, with a 5mL syringe.
 - Remove the rat from its cage and place a towel over its head and front feet.
 - Turn over rat and use your hip to hold its tail against the counter as you apply pressure with your hand to cross the front feet and keep it still. You may need to try a few times until you get the rat in the right position.
 - Once positioned correctly, quickly penetrate the needle through the abdominal skin and into the peritoneal cavity of the rat. Inject the rat and then quickly remove the needle.
 - Place the rat back into the cage and it will slowly be anesthetized.
 - Take up 1mL of Xylazine with a 1mL syringe.
 - Once again, quickly penetrate the peritoneal cavity of the rat, inject, and remove the needle.
 - Weigh the rat and then place back into the cage.
 - Regularly check the rat by touching its eye to check for the eye blink reflex and pinch its tail and hind paws for a flick response.
 - If there is no response when these tests are done, move on to the next step.
- Perfusion of the animals
 - Place a flat plastic container into the hood to collect the blood and other solutions.
 - There also should be a metal grate that can go on top of the plastic container. (Thick metal, not thin and flimsy). (Image below)



- Turn on the perfusion machine (a pump) and get familiar with it. Play around with some water and see which tube will take in water and which will push out water.
- Place a cannula on the side that expels water.
- Once ready, place the side of the tube that sucks the fluid, into a beaker containing the calcium free Tyrodes buffer.
- Let the machine operate to get out any bubbles until all the water and bubbles have come out. (Do not waste too much of your calcium free Tyrodes).
- Turn off the pump until you have the cannula in the left atrium of the rat.
- Place the rat on its back on the metal grate and test for any reflexes in the cornea, hind paw, and tail:

Touch Cornea



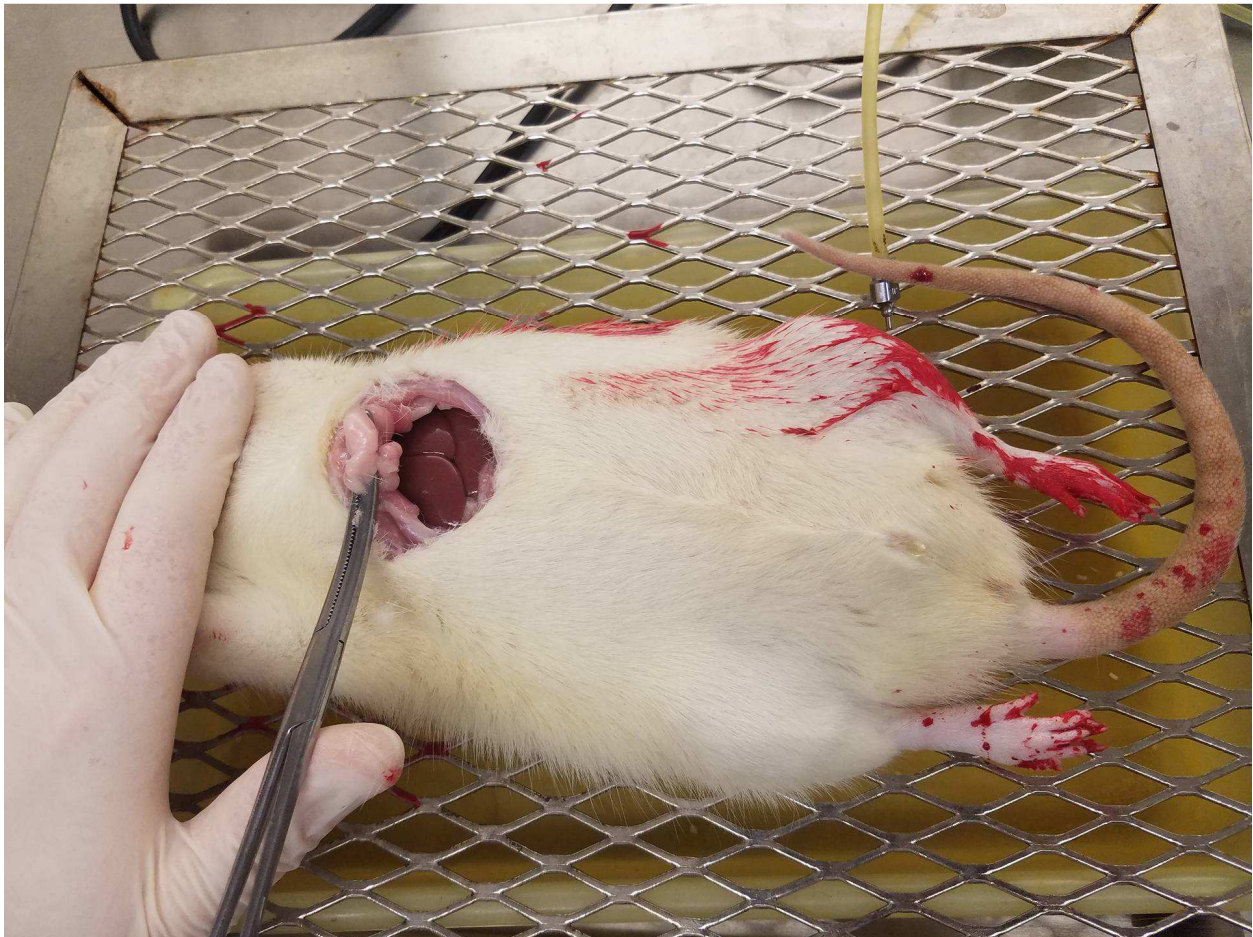
Pinch Hind paw



Pinch Tail



- If you observe any reflexes, wait another minute then retest for reflexes. Do not continue with the perfusion until all three reflexes are not present.
- Feel for the bottom of the rib cage and pinch the skin and muscle to pull it up. With scissors, cut the fur, skin, and muscle below the rib cage.
- Once through the tissue, you should see the xiphoid process.
- Take a hemostat and clip onto the xiphoid process. (Image below)



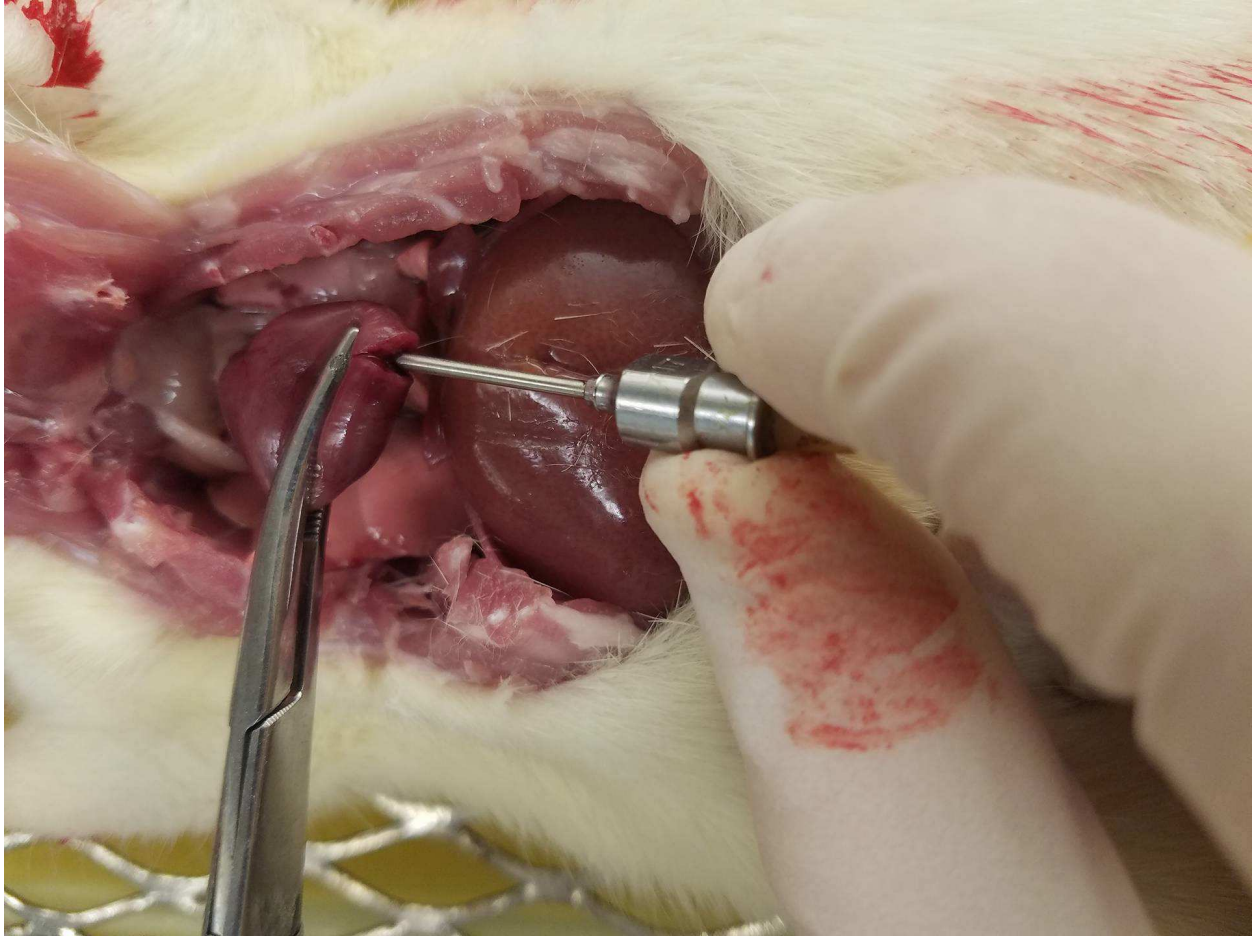
- Pull up to allow an opening and continue to cut on the two peripheral sides of the rat. You must cut through the diaphragm.
- Cut through the ribs and you will eventually see the heart. (Image below)



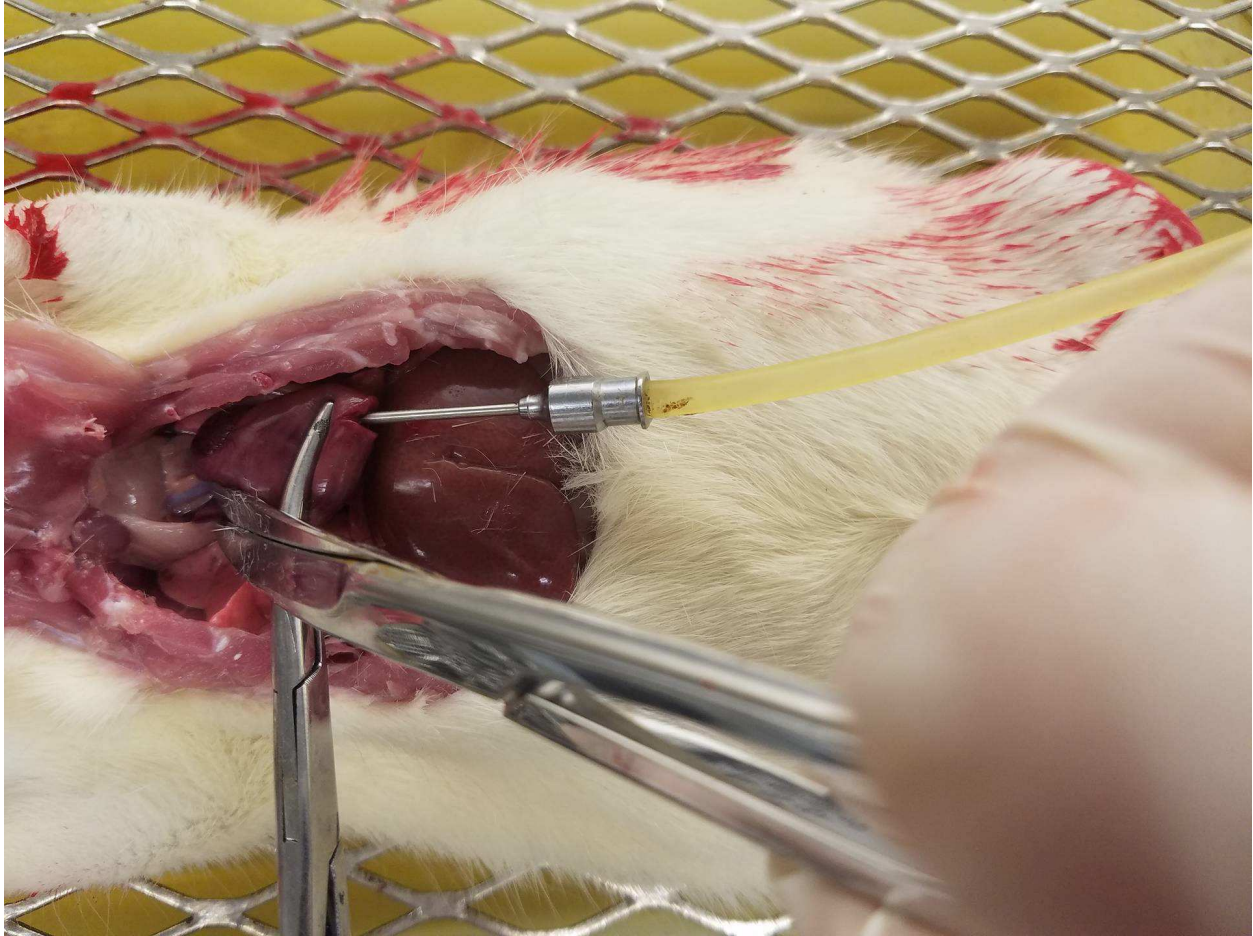
- Expose the heart without cutting it and place the hemostat that is on the xiphoid process in a way to hold the cut ribcage up.
- If the head of the rat is facing to the left, incise the portion of the heart that is further from you and at the base (The left ventricle).(Image below)



- Take the cannula connected to the perfusion tube and insert it through the incision that you made in the left ventricle. Push the tip into the left ventricle and clamp it in place with a hemostat at the site of incision of the ventricle. (Image below)



- Slowly turn on the pump to a very low setting.
- Wait about 3 seconds and cut open the right atrium with surgical scissors. (This allows the blood to make a full passage through the rat systemic circulation and exit at the entrance to the right atrium. Make sure to do this, otherwise the vessels will rupture and cause a mess.). (Image below)



- Slowly turn on the pump to about a rate of 3.5 to 4.
- Allow about 100mL of the calcium free Tyrodes buffer to flow through the vasculature of the rat to clear the blood (watch the “clearing” of the liver). At this point, the rat tissues should be turn white/colorless. Look at the eyes and they should be transparent.
- Turn off the pump and gently move the tube from the calcium free Tyrodes buffer into the picric acid/paraformaldehyde solution (watch out for bubbles getting into the tubing).
 - Troubleshooting: If you get a large bubble in the tube, you can keep the cannula in the heart, but remove the tube. Let the fluid flow through until the bubble is gone, then put the tube back on the cannula.
- Turn the pump back on to about 3.5 to 4 and allow about 240 mL of picric acid/paraformaldehyde to flow through the rat.
- Once finished, drain excess fluid out of the rat and bring the carcass to a cutting board for tissue collection.
- Place each piece of tissue into a labeled microcentrifuge tube containing picric acid/paraformaldehyde fixative.
- Place tubes on ice.

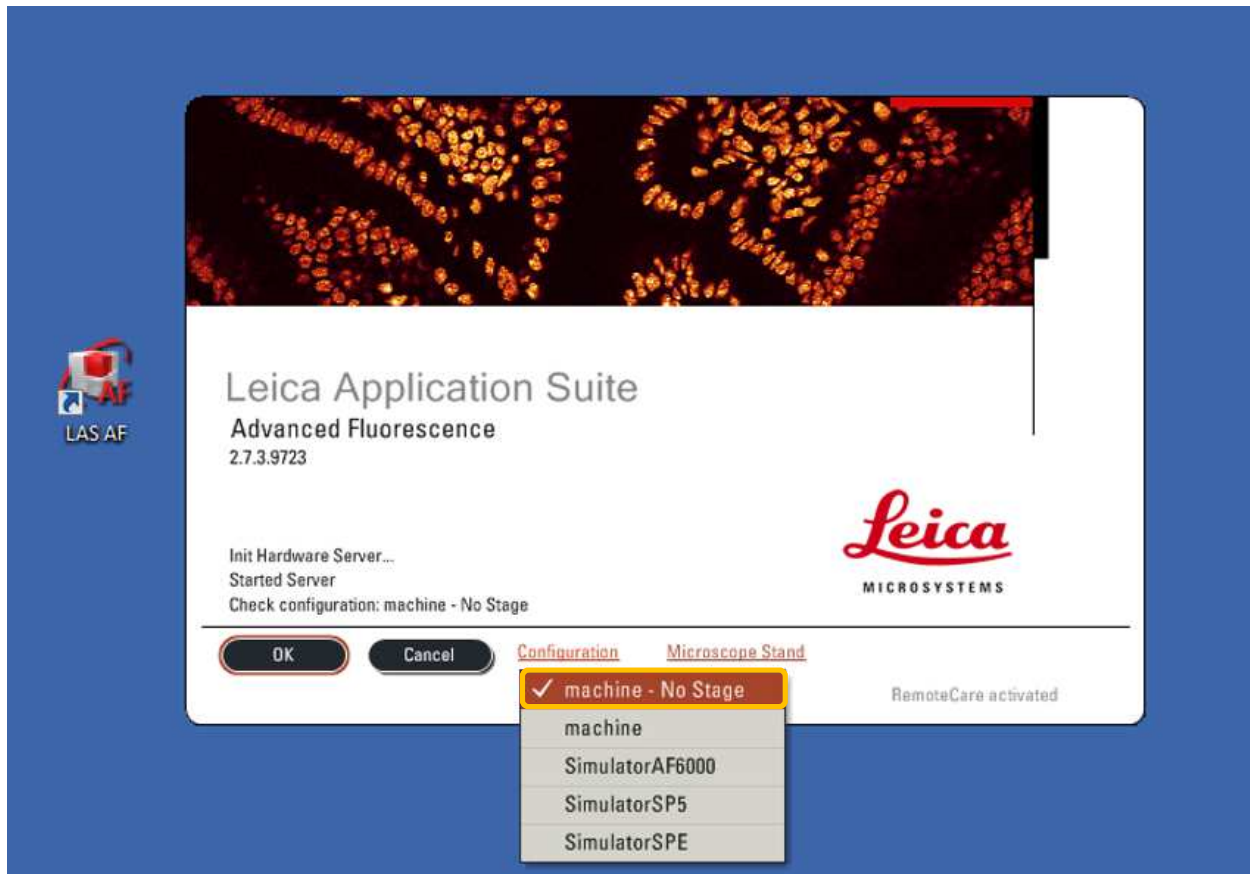
- Place the remains in a Ziploc bag and put into the used animal freezer for disposal.
- Return to the pump and flush the tubes with water by placing the intake tube into a beaker water and running the pump for a little while. (About 30 seconds).
- Place the intake tube back into the calcium free tyrodes and flush the water out.
- You are now ready to move on to the second rat.
- Continue until you have finished all the rats for your experiment.
- Preparing the tissue
 - Once you have the tissue collected on ice, bring tubes to the refrigerator for 4 hours at 4°C.
 - Prepare a 10% sucrose, phosphate buffered-saline solution.
 - Take 5g of sucrose and add to a 50mL tube.
 - Fill with PBS until the 50mL mark is reached.
 - After the tissue has undergone “post-fixation”, use a plastic pipette to remove the picric acid/paraformaldehyde solution from each tube.
 - Fill tubes with 10% sucrose solution and place in the refrigerator overnight (Can keep for about 3 days).
- Preparing cornea in frozen matrix block
 - Turn temperature of the cryostat to -20°C, twist the knob to 18 micrometers, and turn on the light. The temperature should drop to -20°C by the time you prepare your tissue.
 - Take the tubes with tissue and obtain a cutting board, embedding liquid, and embedding plastic containers, and liquid nitrogen.
 - For the cornea, grab the optic nerve area with forceps and cut off the cornea with a small scalpel. Cut about 3 to 4 radial cuts into the cornea to make it lie flat.
 - Do not cut the cornea into multiple section. Keep it all together.
 - Place one drop of embedding matrix into the plastic embedding mold.
 - Place the cornea with epithelial side down in the embedding matrix in the plastic embedding mold.
 - You can place up to 6 corneas in one medium sized plastic embedding mold.
 - Place some liquid nitrogen into a small Styrofoam container. Should be enough liquid nitrogen to surround the plastic embedding piece but not enough to cover it completely.
 - Holding the embedding mold with forceps, freeze the corneas in the plastic embedding mold.
 - Fill the plastic embedding mold with additional embedding matrix until it is full.
 - Wait about 5 seconds for the previous frozen embedding matrix to melt a little bit, but the corneas are mostly still frozen.
 - Freeze the corneas in the embedding matrix for a second time.
 - The block is ready to bring to the cryostat for cutting.

- Cutting the cornea at 18 μm sections
 - Bring the block to the cryostat (temperature was turned down to -20 degrees Celsius and the black knob turned to 18 μm). Place the block in the cryostat and let the temperature equilibrate.
 - Take the cornea block out of the plastic embedding matrix mold.
 - Troubleshooting: Easy way to make sure you get it out without breaking the block is to blow on the plastic piece of the mold until the frozen condensation melts. The block will still be completely frozen, but it will come out with ease.
 - When ready, freeze the cornea block to a round “chuck” in the cryostat.
 - You do this with placing some of the Optical Cutting Temperature (OCT) Embedding Compound (TissueTec #4583) located by the cryostat onto the round portion of the chuck and then place the back of the cornea block OCT.
 - Place it back into the cryostat to freeze.
 - Tighten the chuck post into the microtome. You can slightly move the whole metal piece with the block in it to make it cut straight.
 - Due to the epithelium being the first portion that will be cut, be careful not to hit the knife edge to cube at an angle.
 - Make sure when you are cutting to see the whole (or most) of the block being cut evenly before starting.
 - Once ready, cut the sections into sheets and collect by placing a gel coated slide face down onto the tissue to make it adhere to it.
 - Determine how many pieces you want on one slide.
 - To use the least amount of antibodies as possible, place the tissue as close to the bottom of the gel coated slide as possible.
 - Troubleshooting: If your corneas do not cut all evenly at the same time, you can take certain sections that you want out of a cut with paint brushes and mount that where it belongs on the slide.
 - Five slides can fit into one mailer, so 5 slides are used for each antibody that you are interested in.
 - Troubleshooting: If you use less than 5 slides, you can use blank slides and blank plastic pieces that go in between the blank slides. I will typically try to get everything on 3 slides and as close to the bottom as possible (about 1cm from the bottom of the gel coated slide.). This way I can add in two blank slides and two blank plastic pieces. With this, I will only need 2mL of solution to completely cover the tissue.
 - Continue to cut and place at the end of the slide until you have what you need.
 - Once your slides are cut, place on the warm plate (long black warm plate) in the lab. Turn on the dial to about 2.5 for 1 hour.
- Primary antibodies

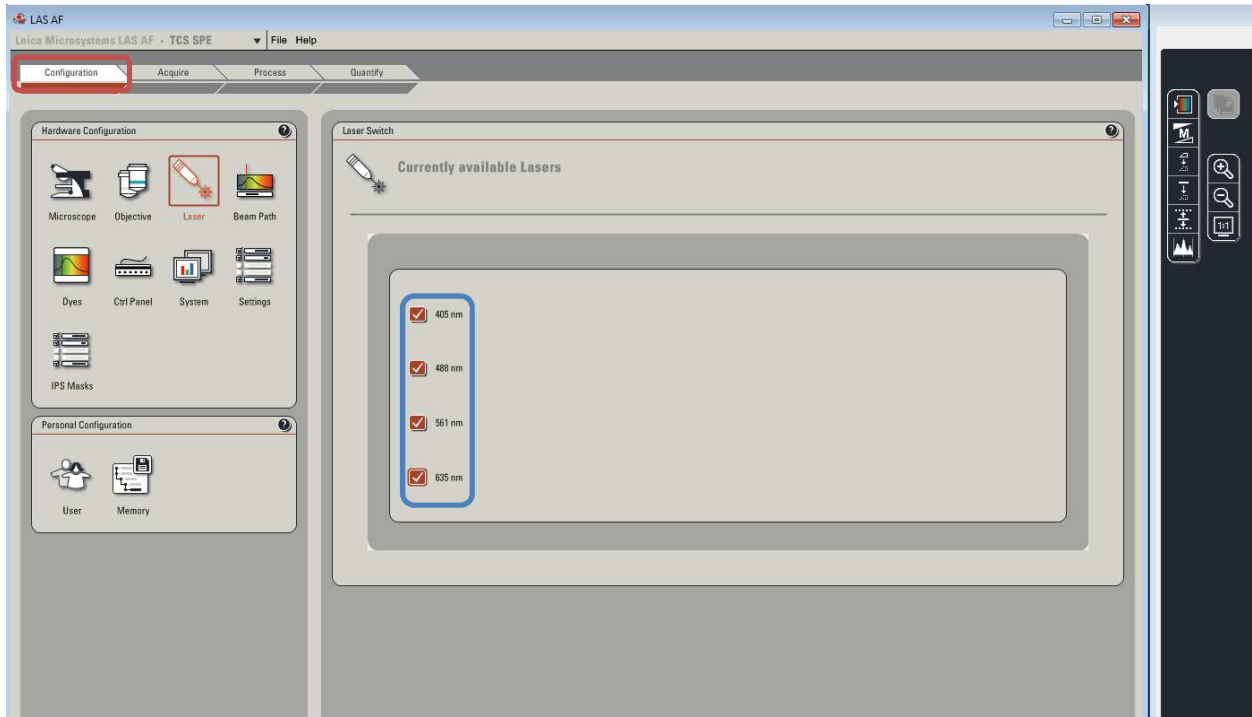
- Take all the slides from the warm plate and place them in mailers (Plastic glass slide holders that hold 5 slides each).
- Place each one in a glass rectangular container and place paper towels around the mailers to prevent them from falling.
- Add PBS to each of the mailers and let it wash for 15 minutes.
 - Troubleshooting: If you find that your tissue has fallen off the slide, the gel coating was not sufficient.
- Repeat 2 more times so each mailer has been washed 3 times for 15 minutes each.
- Make ***PBS-T-BSA-PVP***
 - PBS-T: Take
 - To make PBS-T, obtain a 100mL beaker with a stir bar and a 1000 μ L pipette.
 - Add 63mL of PBS to the 100mL beaker and begin stirring.
 - Use the 1000mL pipette and take out 188 μ L of Triton X-100. (It is very thick, so slowly take it out and allow the pipette tip to stay in the Triton X-100 for about 10 seconds before removing it.
 - Quickly bring the solution over to the 63mL of PBS in the 100mL beaker and dispense the Triton X-100 into the beaker.
 - Allow for it to mix, and the solution is ready to use.
 - PBS-T-BSA-PVP: Take 20 mL of PBS-T and add 0.10 g of BSA and 0.10g of PVP. Mix carefully since it will bubble.
 - Diluent: We want PBS-T with 0.5% bovine serum albumin (BSA), 0.5% PVP. Take 0.05 g of BSA and PVP to each 10mL you need. In this case use $(0.5\text{g})/(100\text{ml}) = (x\text{g})/(20\text{ml}) \rightarrow x = 0.10\text{g}$ bovine serum albumin (BSA) and polyvinylpyrrolidone (PVP). ***Take 20ml PBS-T and add 0.10g of BSA and 0.10g of PVP.*** Mix, but will bubble if mixed too hard.
- Place 2 mL of the PBS-T-BSA-PVP solution into a 15mL tube. (This will be added to the mailers, so depending on how far your tissue is up the slide will determine if you need to use more or less PBS-T-BSA-PVP.
- For each mailer, prepare an additional 15 mL tube with 2 mL of the PBS-T-BSA-PVP solution in it.
- You will want to add in your primary antibodies into each 15mL tube with the PBS-T-BSA-PVP in it. If you are using 2 antibodies and one of them is the same antibody across all of the mailers, you can add in that antibody into the 20 mL solution directly and mix.
 - Example: if you are using PGP 9.5 at a 1:10,000 dilution, you can place 2 μ L of PGP 9.5 into 20 mL of PBS-T-BSA-PVP and distribute 2 mL to each of the 15 mL tubes.
- For the second antibody, make sure it was raised in a different species without cross reactivity.
 - For example, the PGP 9.5 is an anti-rabbit antibody. You can use a GluA1 antibody if it is anti-goat.
 - **Example: G α GluA1**

- Gently take a glass coverslip that will completely cover your tissue and touch the end of it to the Prolong Gold, but not the tissue itself.
- The Prolong will come across the slide and you can gently place the coverslip to the end of the slide, apply slight pressure and gently bring the coverslip across the tissue and the rest of the slide.
- You can get a slight bend in the coverslip, this will help prevent bubbles from accumulating as you place the coverslip on the slide.
- Look for any bubbles that may have become stuck under the coverslip and gently use the forceps to push the bubbles out. Do not go over the area where your tissue is located to avoid possible scratching.
- You can also wrap the coverslip with a Kimwipe and gently apply pressure across the coverslip to remove any bubbles or excess prolong gold.
- Soak up any excess prolong gold with a Kimwipe.
- Place in a cardboard slide holder overnight in a dark drawer to let the prolong gold harden.
- Confocal Microscope.
 - After the prolong gold has hardened overnight, you can view your slides with the confocal microscope.
 - **You will need personal training to use the microscope. Do this before you start your experiment. After training, activate your card to get access to the room**
 - Sign up for the confocal microscope on the calendar.
 - MOST IMPORTANT STEP!!!!
 - When you walk into the microscope room you will take off the plastic cover from the confocal microscope.
 - Look at the microscope and make sure everything looks like it should.
 - **You need to make sure the objectives are all the way down!!!!**
 - The confocal microscope will calibrate itself when you turn it on automatically, if the stage is not all the way down, the stage will catch one of the objectives, put deep scratches in the objective and tear up the stage. This is a VERY expensive mistake.
 - **You need to make sure the objective that is in the useable position is an empty slot!!!!**
 - The water and oil lenses are always placed in and taken out for each experiment, so the empty slot where one of those will be located should be in the useable position when the confocal microscope goes through its calibration steps.
 - Turning the microscope on.
 - There are pieces of tape labeled 1-5 on each of the pieces of machinery that needs to be turned on.

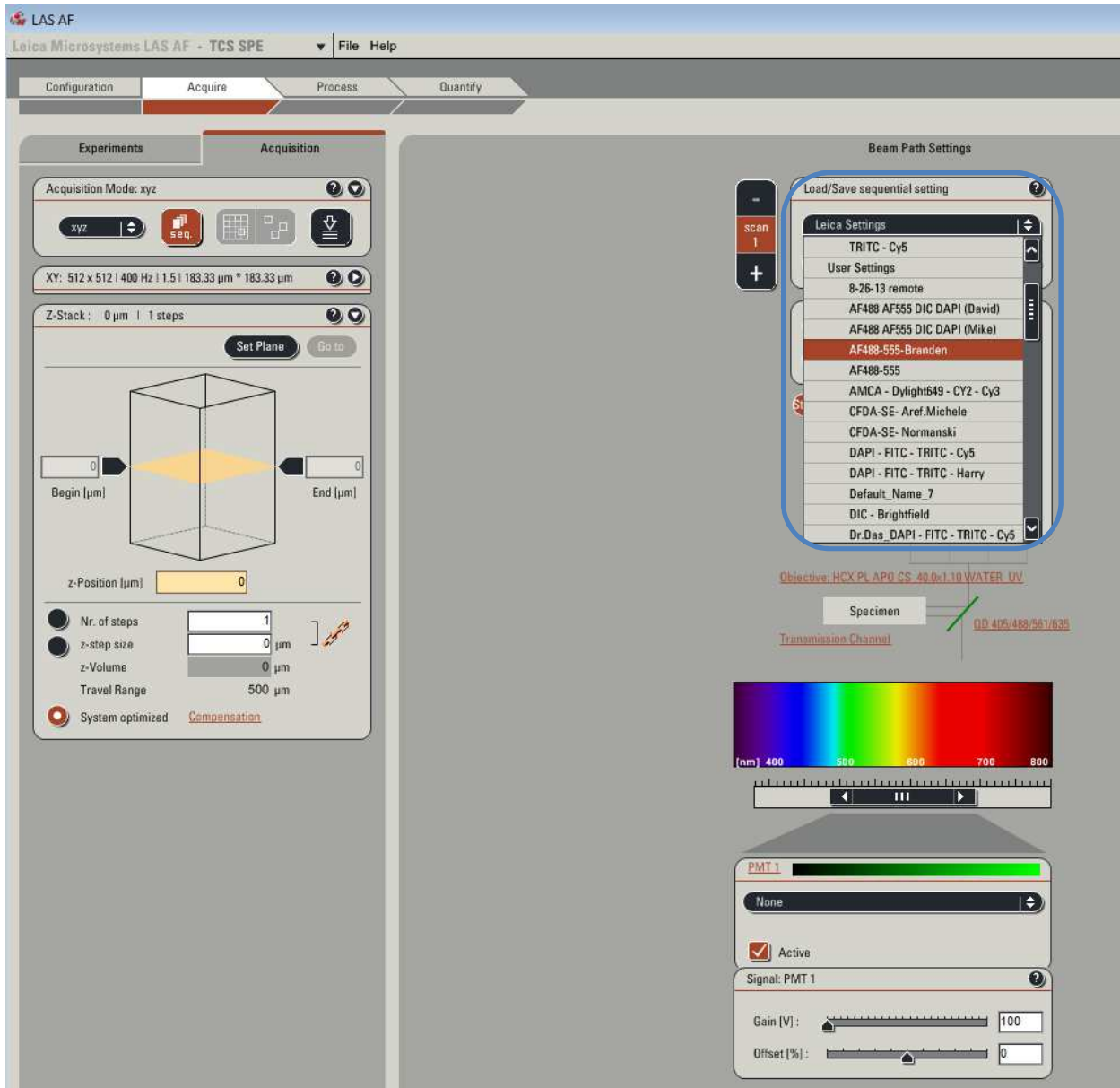
- Turn on the machine by starting with 1 and wait 3-5 seconds, then 2, then 3, then 4, then 5.
- Once the computer is turned on, select SPE_User.
- Then double click on LAS AF.
- Make sure the program is in Machine No Stage (Orange box) mode then click OK (Red outline):



- The confocal microscope will go through its calibration steps.
 - Takes about 1-2 minutes.
- Click on Configuration (Red box) and click on each laser (Blue box):



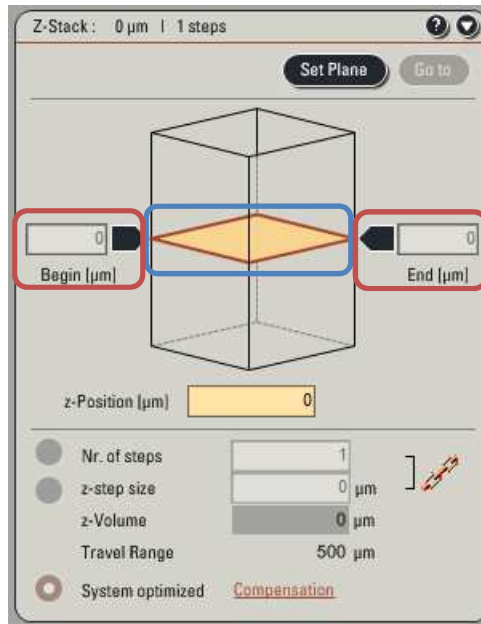
- Identify the settings you need for your fluorophore(s) (Blue box). You can also save your settings if you will be using it a lot:



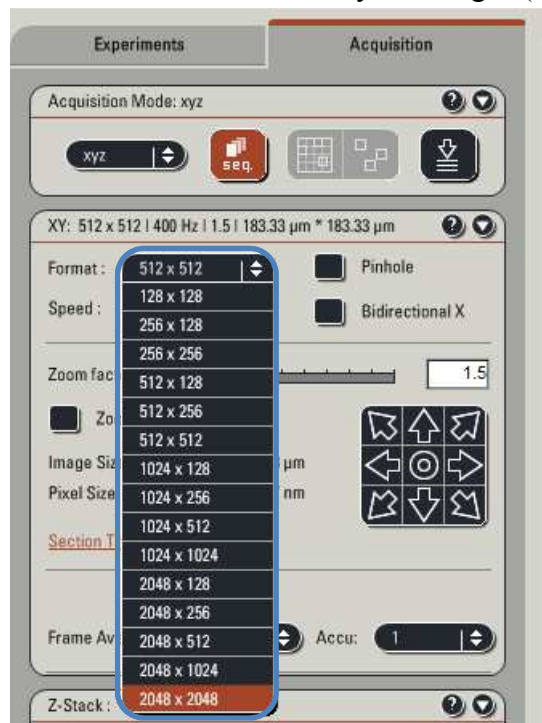
- Placing the objective in the confocal microscope.
 - The 40X Water lens is in a box in the desk. It also has a number written on it. The number indicates the objective location where it belongs. Make sure to put it in the right spot.
 - Unscrew the objective container next to the microscope and on top of the table the microscope is on. Do not take the objective out just yet. Leave the cap loose.
 - Move back the top of the confocal microscope. This is on a hinge system that is not protected. Make sure you firmly grasp the top of the confocal microscope and slowly bring it back until it is all the way back. If you do not guide it, you will damage the microscope.

- Unscrew the cap that is on the objective location for the objective you plan to use.
 - If you do not plan to use the water or oil lens, you do not have to do this.
 - Once again, leave the cap unscrewed on top of the hole that the objective screws into.
 - If dust and other debris manages its way into the objective position hole or in the objective itself, your images will be blurry and it is another expensive mistake.
 - Take the objective out of its casing and unscrew it.
 - After the cap is off the objective, remove the cap on the hole that the objective attaches to the confocal microscope and then screw the objective in.
 - Minimize the time that the transfer happens, but do not slam the objective into its spot.
 - Place the cap in the objective container then screw the cap back on.
- Placing your slide on the stage.
 - Place a drop of autoclaved water on the 40X water objective.
 - Take the slide you want to view with the confocal microscope and wipe it off with water and a Kimwipe.
 - Bring your slide and place it face down (Coverslip down) on the stage.
 - Place your slide on the right side of the stage and bring the left side to the edge of your slide.
 - If you have your tissue all the way at the bottom of the slide, you will not be able to fully bring the left side of the stage to your slide. Just make a judgement and place it where it keeps the stage horizontal over the objectives, but it also does not block the view of your tissue.
 - Slowly bring the 40X water objective up to your slide until the water contacts your slide.
 - You can move the stage at this point to place the objective at the tissue of interest.
 - Carefully bring the arm (Top of the microscope) back in its downright position.
 - You are ready to view your slide.
- Viewing your slide.
 - Press the top left button on the confocal microscope (The one that looks like an eye).

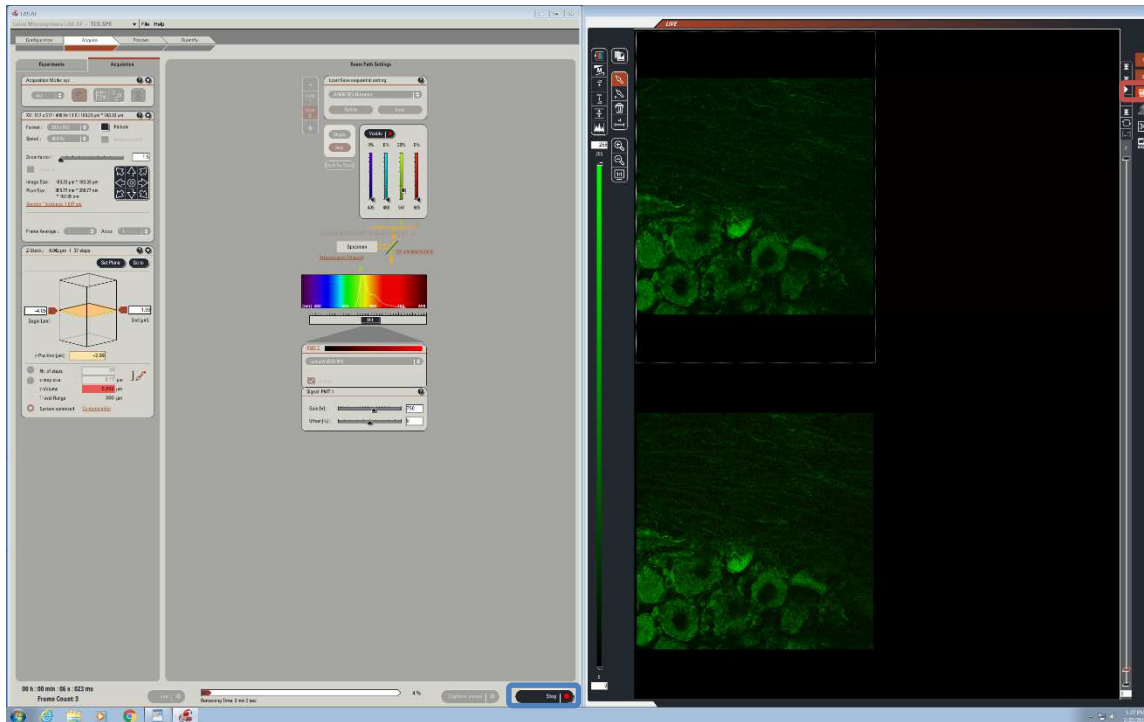
- Press the laser that is at the proper wavelength that will excite the fluorophores that are attached to your secondary antibody.
 - FITC= Excitation: 490, Emission: 525
 - Rhodamine= Excitation: 555, Emission: 565
 - DAPI= Excitation: 350, Emission: 470
 - Texas Red= Excitation: 596, Emission: 615
- Press the center SHUTTER button to view the slide.
- Focus on your tissue of interest and identify what you would like to photograph.
 - You will not be able to photograph the whole field of view you are examining. Place the most interesting part in the very center of what you see.
- Press the SHUTTER button again to close the shutter.
 - Troubleshooting: You do not want to overexpose the fluorophore of the secondary because of photobleaching.
- Taking a Z-Stack photoset.
 - Press on Live to view your tissue on the computer.
 - Slightly adjust the stage to where you want, so you get the image that you want.
 - Adjust the gain to where you want, so you best display the color intensity you are interested in.
 - If you are looking for a good image, gain does not really matter too much.
 - If you want to quantify your images, keep the same gain and laser intensity no matter what. Be sure to record what you use.
 - If the tissue is double labeled, you can switch filters by clicking on scan 2.
 - You will have to readjust everything for the second fluorophore.
 - Click on the yellow box, scroll down with the scroll wheel on the mouse (Blue Box) to the point where you want to start taking images, and click on the banner to the left (Red box left). Click on the yellow box again, scroll up to where you want to finish taking images, and click on the banner to the right (Red box right):



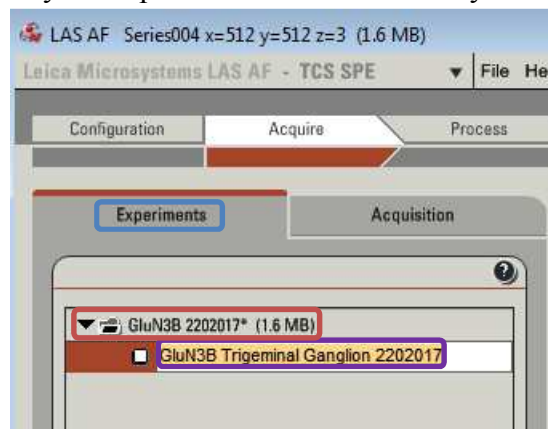
- Select the resolution for your images (Blue Box):



- Click on Start on the bottom right of the left screen.
- Click start (Blue box, where it would indicate start) and you can see the two fluorophores and the combined image by clicking this (Red box):

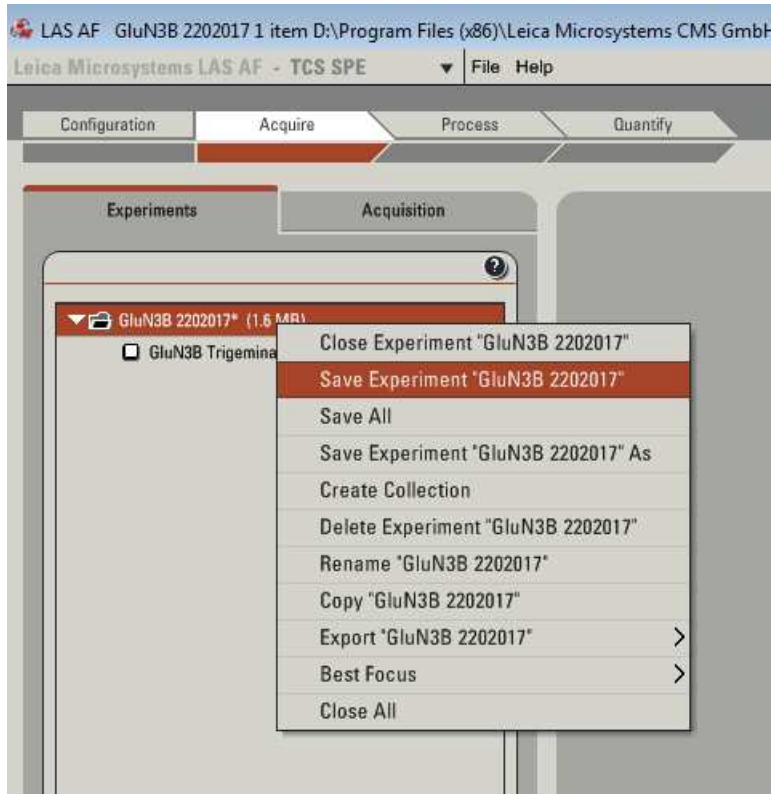


- Naming and saving experiments
 - Click on the experiments tab:
 - PICTURE
 - Click on the experiments tab (Blue box), right click and rename your experiment with the antibody or antibodies you used:

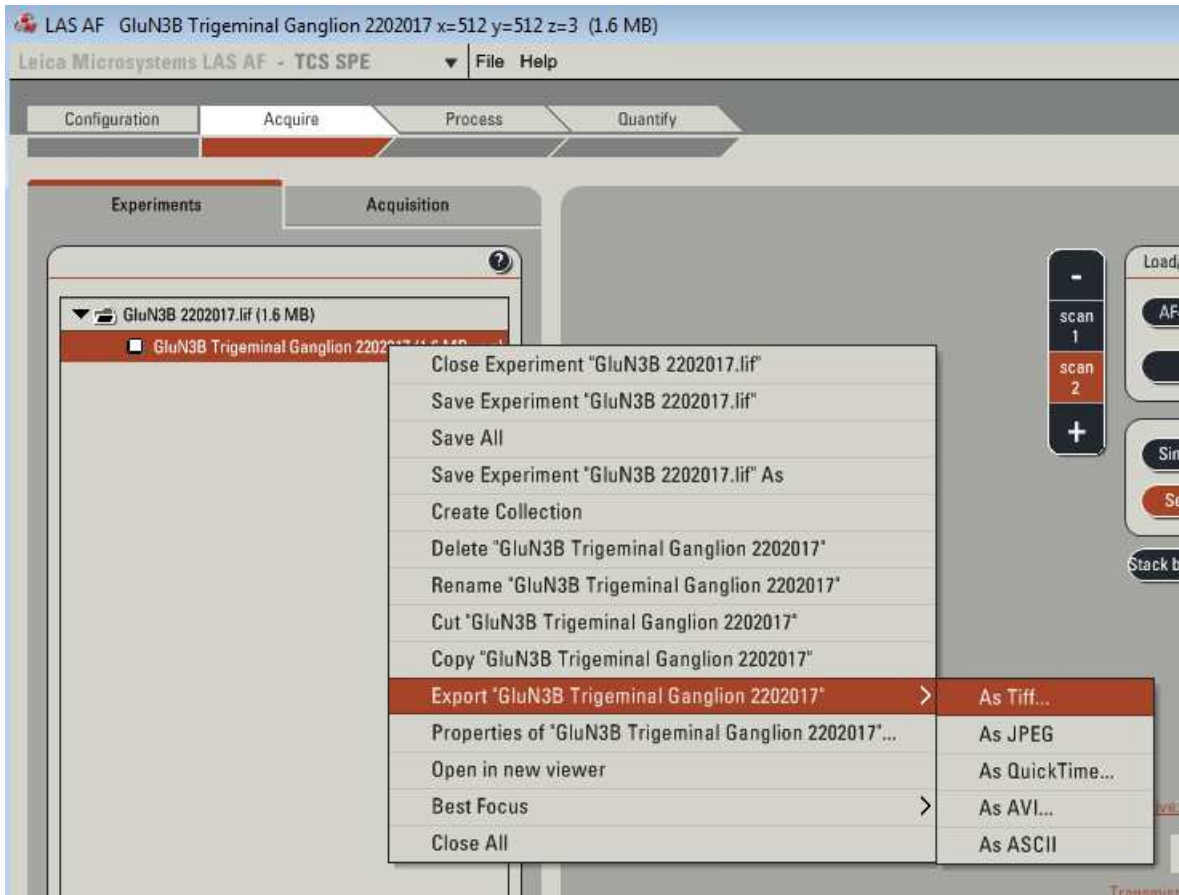


- Also, right click and rename each image set that is located under the main experiment. Add the tissue type and experimental number to the name (Purple box, above image).
 - All the names here will transfer over to your final images. Make sure that you typed it in right before you move on.
 - Find the folder where you will save your images:

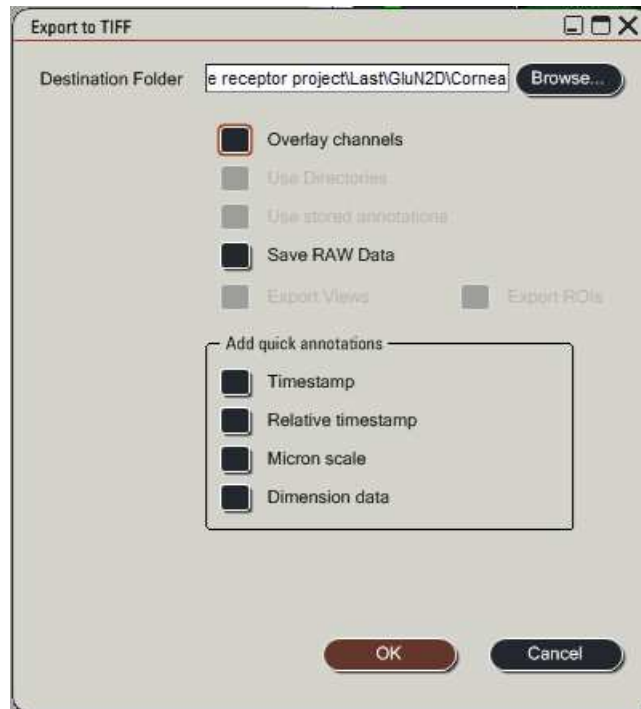
- Save your experiment in the folder you made for it (Red highlight):



- Export the image set as a tiff file to the folder you made for it:



- You must save your image two separate times if you have a co-labeled tissue section. One for the single images, one for the combination of the single labeled to make co-labeled images.
 - Single images



○ Co-labeled images



- Once all your images are in the correct folder, you can move on to formatting and/or analyzing.
- Cleaning up after yourself!!!!
 - You will need to return and properly turn off everything on the confocal microscope. If this is not done correctly, another expensive error may occur.

- After you have saved everything, turn off the program on the computer.
- Go to the start menu and click on shut down computer.
- Once the computer is completely turned off, you can begin to turn off the confocal microscope.
 - Turn off the machine in the right order: 4, then 3, then 2, then 1.
- Carefully guide the top of the confocal microscope back.
- Place your slide back in your slide box.
- **Bring the objectives back to their lowest position!!!**
- Take the cap back out of the objective container.
- Unscrew the 40X water lens. Directly after, set the cap over the hole. Do not screw it in yet.
- Screw the 40X water lens back into the top of the objective container, then screw it back into the objective container.
- Finish by screwing in the cap over the objective lens hole.
- Gently bring the top of the microscope back into the downright position.
- Check to make sure the objectives are in the furthest down position, then cover the confocal microscope with its plastic dust protector.
- Place the 40X water lens back into the cardboard box and place it back in the desk drawer.
- Sign the log with the time that you started and finished in the log book and identify any issues that may have occurred. If you find the confocal microscope in a position or if something was out of place, make a comment in the log. Place it back where it should be, not where you found it.
 - Troubleshooting: There are more functions that the confocal microscope has. Learn about them and try to expand.
- Image processing
 - Once you have the images, you will need to download and bring the images to Image J Fiji.
 - You will also need to go to the website and add the deconvolution lab plugin.
 - First, you will need to identify the images that you want to deconvolute and merge.
 - Make sure you know where you saved your images on your computer and make a new folder for each of the filters and one for the merged images.

- Make a copy of the images you want to deconvolute and merge and separate them into their respective folders.
 - You will not need the folder with the combined images since you will make another combined image with the program.
- Copy the images that you will work on into their respected folders.
- Open Image J Fiji.
- Go to file/import/image sequence.
- Find one of the filter folders and select the first image in the set and select open.
- The program will tell you how many images you have in the folder. Press ok.
- Go to file/import/image sequence again and select your second filter set.
- Continue until you have all the filters that you are working with for that single set of images.
- Now you should have two or more image stacks open for the same image, but in different colors (filters).
- Go to Plugins/Deconvolution Lab/Deconvolution lab and press ok.
- Now you should have the add on in Fiji image J for the deconvolution lab open.
- Select Tikhonov-Miller from the dropdown box to find the deconvolution method that we use.
 - We use the default features which include 10 iterations.
- Click on the image stack that you would like to deconvolute first and select Run.
 - The program is set to conduct commands based from the last image that you clicked on. Keep this in mind.
 - Note: If you have multiple images open, the last one that you clicked on is the one that will go through the deconvolution. Be sure to deconvolute each image set by clicking on the next set and redoing the deconvolution after the previous one has concluded.
- Press Run, then ok. This will start the deconvolution.
- This may take a while depending on how many images you have. You must wait.
- Redo this method for the remaining image stacks.
- You will have a greyscale image stack once this is complete.
- Now, you will want a total of 3 images if you have two filters.
 - One being the green filter, one being the red filter, and one being the combination.
 - There are also other colors, change according to your liking or what it was originally.
- First you will combine your stacks to make one image.
 - This will layer all the images on top of one another to allow you to see all the images at once.
 - Note: You can try this with any images that are not similar to see what is going on. Try taking an image of a tree and a separate

image of a building and see what it looks like when combined.

This will give you an understanding of what the program is doing.

- 'X' out of the deconvolution lab window.
- Select the grey image set that you are interested in combining.
- Go to Image/Stacks/Z Project then press ok.
- You will notice that you can no longer scroll through the images on the stack window. This is because all the images are in a final single image.
 - This image is still greyscale.
- Repeat for the remainder of the filters.
- Go to Image/Color/Merge Channels.
- There will be a window that asks which image belongs to which filter (channel).
- Identify and select the greyscale image in the correct channel and select ok.
- Click on the merged image and go to file/Save As/PNG. Name your image and save it where you want it.
- Click on the merged image to make it active, then you can split the channels by:
 - Image/Color/Split Channels.
- This will split the images that you just combined, but they will be in color.
- Click on the one you want to save first, then select file/Save As/PNG to save it.
- Continue saving all the split images.
- Now you can make a montage if you want.

REFERENCES

- Abe, T., Matsumura, S., Katano, T., Mabuchi, T., Takagi, K., Xu, L., . . . Ito, S. (2005). Fyn kinase-mediated phosphorylation of NMDA receptor NR2B subunit at Tyr1472 is essential for maintenance of neuropathic pain. *Eur J Neurosci*, *22*(6), 1445-1454. doi:10.1111/j.1460-9568.2005.04340.x
- Alam, A., & Juurlink, D. N. (2016). The prescription opioid epidemic: an overview for anesthesiologists. *Can J Anaesth*, *63*(1), 61-68. doi:10.1007/s12630-015-0520-y
- Albin, K. C., Carstens, M. I., & Carstens, E. (2008). Modulation of oral heat and cold pain by irritant chemicals. *Chem Senses*, *33*(1), 3-15. doi:10.1093/chemse/bjm056
- Alt, A., Weiss, B., Ogden, A. M., Knauss, J. L., Oler, J., Ho, K., . . . Bleakman, D. (2004). Pharmacological characterization of glutamatergic agonists and antagonists at recombinant human homomeric and heteromeric kainate receptors in vitro. *Neuropharmacology*, *46*(6), 793-806. doi:10.1016/j.neuropharm.2003.11.026
- Aragona, P., & Di Pietro, R. (2007). Is it safe to use topical NSAIDs for corneal sensitivity in Sjogren's syndrome patients? *Expert Opin Drug Saf*, *6*(1), 33-43. doi:10.1517/14740338.6.1.33
- Arora, H., & Ivanovski, S. (2017). Melatonin as a pro-osteogenic agent in oral implantology: a systematic review of histomorphometric outcomes in animals and quality evaluation using ARRIVE guidelines. *J Periodontol Res*, *52*(2), 151-161. doi:10.1111/jre.12386
- Atianjoh, F. E., Yaster, M., Zhao, X., Takamiya, K., Xia, J., Gauda, E. B., . . . Tao, Y. X. (2010). Spinal cord protein interacting with C kinase 1 is required for the maintenance of complete Freund's adjuvant-induced inflammatory pain but not for incision-induced post-operative pain. *Pain*, *151*(1), 226-234. doi:10.1016/j.pain.2010.07.017
- Baker, D., Lidster, K., Sottomayor, A., & Amor, S. (2014). Two years later: journals are not yet enforcing the ARRIVE guidelines on reporting standards for pre-clinical animal studies. *PLoS Biol*, *12*(1), e1001756. doi:10.1371/journal.pbio.1001756
- Balu, D. T., & Coyle, J. T. (2015). The NMDA receptor 'glycine modulatory site' in schizophrenia: D-serine, glycine, and beyond. *Curr Opin Pharmacol*, *20*, 109-115. doi:10.1016/j.coph.2014.12.004
- Barry, P. A., Petroll, W. M., Andrews, P. M., Cavanagh, H. D., & Jester, J. V. (1995). The spatial organization of corneal endothelial cytoskeletal proteins and their relationship to the apical junctional complex. *Invest Ophthalmol Vis Sci*, *36*(6), 1115-1124.
- Basbaum, A. I., Bautista, D. M., Scherrer, G., & Julius, D. (2009). Cellular and molecular mechanisms of pain. *Cell*, *139*(2), 267-284. doi:10.1016/j.cell.2009.09.028
- Bleakman, D., Alt, A., & Nisenbaum, E. S. (2006). Glutamate receptors and pain. *Semin Cell Dev Biol*, *17*(5), 592-604. doi:10.1016/j.semcdb.2006.10.008
- Bleakman, D., Ballyk, B. A., Schoepp, D. D., Palmer, A. J., Bath, C. P., Sharpe, E. F., . . . Lodge, D. (1996). Activity of 2,3-benzodiazepines at native rat and recombinant human glutamate receptors in vitro: stereospecificity and selectivity profiles. *Neuropharmacology*, *35*(12), 1689-1702.
- Bleakman, D., Ogden, A. M., Ornstein, P. L., & Hoo, K. (1999). Pharmacological characterization of a GluR6 kainate receptor in cultured hippocampal neurons. *Eur J Pharmacol*, *378*(3), 331-337.
- Bonjardim, L. R., da Silva, A. P., Gameiro, G. H., Tambeli, C. H., & Ferraz de Arruda Veiga, M. C. (2009). Nociceptive behavior induced by mustard oil injection into the temporomandibular joint is blocked by a peripheral non-opioid analgesic and a central opioid analgesic. *Pharmacol Biochem Behav*, *91*(3), 321-326. doi:10.1016/j.pbb.2008.08.001

- Bonnet, C. S., Williams, A. S., Gilbert, S. J., Harvey, A. K., Evans, B. A., & Mason, D. J. (2015). AMPA/kainate glutamate receptors contribute to inflammation, degeneration and pain related behaviour in inflammatory stages of arthritis. *Ann Rheum Dis*, *74*(1), 242-251. doi:10.1136/annrheumdis-2013-203670
- Bu, F., Tian, H., Gong, S., Zhu, Q., Xu, G. Y., Tao, J., & Jiang, X. (2015). Phosphorylation of NR2B NMDA subunits by protein kinase C in arcuate nucleus contributes to inflammatory pain in rats. *Sci Rep*, *5*, 15945. doi:10.1038/srep15945
- Burnashev, N., Zhou, Z., Neher, E., & Sakmann, B. (1995). Fractional calcium currents through recombinant GluR channels of the NMDA, AMPA and kainate receptor subtypes. *J Physiol*, *485* (Pt 2), 403-418.
- Burness, C. B., & McCormack, P. L. (2016). Capsaicin 8 % Patch: A Review in Peripheral Neuropathic Pain. *Drugs*, *76*(1), 123-134. doi:10.1007/s40265-015-0520-9
- Carlton, S. M., & Coggeshall, R. E. (1999). Inflammation-induced changes in peripheral glutamate receptor populations. *Brain Res*, *820*(1-2), 63-70.
- Carr, B. K., Miller, K. E. (2017). *Localization of Glutamate Receptors and Scaffold Proteins in Sprague Dawley Rat Cornea and Trigeminal Ganglion* Poster. Anatomy and Cell Biology. Oklahoma State University Center for Health Sciences. OSU-CHS annual research day.
- Chan-Ling, T. (1989). Sensitivity and neural organization of the cat cornea. *Invest Ophthalmol Vis Sci*, *30*(6), 1075-1082.
- Claiborne, J. A., Nag, S., & Mokha, S. S. (2009). Estrogen-dependent, sex-specific modulation of mustard oil-induced secondary thermal hyperalgesia by orphanin FQ in the rat. *Neurosci Lett*, *456*(2), 59-63. doi:10.1016/j.neulet.2009.03.106
- ClinicalTrials.gov. (2013). Retrieved from <https://clinicaltrials.gov/>
- Coleman, S. K., Hou, Y., Willibald, M., Semenov, A., Moykkynen, T., & Keinanen, K. (2016). Aggregation Limits Surface Expression of Homomeric GluA3 Receptors. *J Biol Chem*, *291*(16), 8784-8794. doi:10.1074/jbc.M115.689125
- Coleman, S. K., Moykkynen, T., Hinkkuri, S., Vaahtera, L., Korpi, E. R., Pentikainen, O. T., & Keinanen, K. (2010). Ligand-binding domain determines endoplasmic reticulum exit of AMPA receptors. *J Biol Chem*, *285*(46), 36032-36039. doi:10.1074/jbc.M110.156943
- Collaborative Approach to Meta analysis and Review of Animal Data from Experimental Studies. (2014). Retrieved from <http://www.dcn.ed.ac.uk/camarades/>
- da Silva, L. B., Kulas, D., Karshenas, A., Cairns, B. E., Bach, F. W., Arendt-Nielsen, L., & Gazerani, P. (2014). Time course analysis of the effects of botulinum neurotoxin type A on pain and vasomotor responses evoked by glutamate injection into human temporalis muscles. *Toxins (Basel)*, *6*(2), 592-607. doi:10.3390/toxins6020592
- Das, A., Wallace, G. C. t., Holmes, C., McDowell, M. L., Smith, J. A., Marshall, J. D., . . . Banik, N. L. (2012). Hippocampal tissue of patients with refractory temporal lobe epilepsy is associated with astrocyte activation, inflammation, and altered expression of channels and receptors. *Neuroscience*, *220*, 237-246. doi:10.1016/j.neuroscience.2012.06.002
- Deba, F., & Bessac, B. F. (2015). Anoctamin-1 Cl(-) channels in nociception: activation by an N-aroylaminothiazole and capsaicin and inhibition by T16A[inh]-A01. *Mol Pain*, *11*, 55. doi:10.1186/s12990-015-0061-y
- Dingledine, R., Borges, K., Bowie, D., & Traynelis, S. F. (1999). The glutamate receptor ion channels. *Pharmacol Rev*, *51*(1), 7-61.
- Doll, R. J., van Amerongen, G., Hay, J. L., Groeneveld, G. J., Veltink, P. H., & Buitenweg, J. R. (2016). Responsiveness of electrical nociceptive detection thresholds to capsaicin (8 %)-induced changes in nociceptive processing. *Exp Brain Res*. doi:10.1007/s00221-016-4655-z

- Dolman, N. P., Troop, H. M., More, J. C., Alt, A., Knauss, J. L., Nistico, R., . . . Jane, D. E. (2005). Synthesis and pharmacology of willardiine derivatives acting as antagonists of kainate receptors. *J Med Chem*, *48*(24), 7867-7881. doi:10.1021/jm050584l
- Eghrari, A. O., Riazuddin, S. A., & Gottsch, J. D. (2015). Overview of the Cornea: Structure, Function, and Development. *Prog Mol Biol Transl Sci*, *134*, 7-23. doi:10.1016/bs.pmbts.2015.04.001
- Fazzari, J., Linher-Melville, K., & Singh, G. (2016). TUMOUR-DERIVED GLUTAMATE: LINKING ABERRANT CANCER CELL METABOLISM TO PERIPHERAL SENSORY PAIN PATHWAYS. *Curr Neuropharmacol*.
- Fedele, E., & Raiteri, M. (1996). Desensitization of AMPA receptors and AMPA-NMDA receptor interaction: an in vivo cyclic GMP microdialysis study in rat cerebellum. *Br J Pharmacol*, *117*(6), 1133-1138.
- Feng, M. T., Price, F. W., Jr., McKee, Y., & Price, M. O. (2015). Memantine-associated corneal endothelial dysfunction. *JAMA Ophthalmol*, *133*(10), 1218-1220. doi:10.1001/jamaophthalmol.2015.2476
- Fleck, M. W., Cornell, E., & Mah, S. J. (2003). Amino-acid residues involved in glutamate receptor 6 kainate receptor gating and desensitization. *J Neurosci*, *23*(4), 1219-1227.
- Flecknell, P. (2002). Replacement, reduction and refinement. *Altex*, *19*(2), 73-78.
- Gazerani, P., Dong, X., Wang, M., Kumar, U., & Cairns, B. E. (2010). Sensitization of rat facial cutaneous mechanoreceptors by activation of peripheral N-methyl-d-aspartate receptors. *Brain Res*, *1319*, 70-82. doi:10.1016/j.brainres.2010.01.018
- Gong, K., Kung, L. H., Magni, G., Bhargava, A., & Jasmin, L. (2014). Increased Response to Glutamate in Small Diameter Dorsal Root Ganglion Neurons after Sciatic Nerve Injury. *PLoS One*, *9*(4). doi:10.1371/journal.pone.0095491
- Greger, I. H., Ziff, E. B., & Penn, A. C. (2007). Molecular determinants of AMPA receptor subunit assembly. *Trends Neurosci*, *30*(8), 407-416. doi:10.1016/j.tins.2007.06.005
- Gulin, J. E., Rocco, D. M., & Garcia-Bournissen, F. (2015). Quality of Reporting and Adherence to ARRIVE Guidelines in Animal Studies for Chagas Disease Preclinical Drug Research: A Systematic Review. *PLoS Negl Trop Dis*, *9*(11), e0004194. doi:10.1371/journal.pntd.0004194
- Hackam, D. G., & Redelmeier, D. A. (2006). Translation of research evidence from animals to humans. *Jama*, *296*(14), 1731-1732. doi:10.1001/jama.296.14.1731
- Haines, D. E. (2012). *Fundamental Neuroscience for Basic and Clinical Applications* (4th ed.): Elsevier - Health Sciences Division.
- Hatziefthimiou, A. A., Gourgoulianis, K. I., & Molyvdas, P. A. (2002). Epithelium-dependent effect of L-glutamate on airways: involvement of prostaglandins. *Mediators Inflamm*, *11*(1), 33-38. doi:10.1080/09629350210312
- He, J., Bazan, N. G., & Bazan, H. E. (2010). Mapping the entire human corneal nerve architecture. *Exp Eye Res*, *91*(4), 513-523. doi:10.1016/j.exer.2010.07.007
- Hediger, M. A., & Welbourne, T. C. (1999). Introduction: glutamate transport, metabolism, and physiological responses. *Am J Physiol*, *277*(4 Pt 2), F477-480.
- Huang, S. C., & Chen, H. C. (2008). Overview of laser refractive surgery. *Chang Gung Med J*, *31*(3), 237-252.
- Iannaccone, P. M., & Jacob, H. J. (2009). Rats! *Dis Model Mech*, *2*(5-6), 206-210. doi:10.1242/dmm.002733
- Ibitokun, B. O. (2012). *The role of glutamate in corneal nociception*. Oklahoma State University Center for Health Sciences.
- Ibrahim, H. M., Hogg, A. J., Jr., Healy, D. J., Haroutunian, V., Davis, K. L., & Meador-Woodruff, J. H. (2000). Ionotropic glutamate receptor binding and subunit mRNA expression in thalamic nuclei in schizophrenia. *Am J Psychiatry*, *157*(11), 1811-1823. doi:10.1176/appi.ajp.157.11.1811
- Johnson, J. W., & Ascher, P. (1987). Glycine potentiates the NMDA response in cultured mouse brain neurons. *Nature*, *325*(6104), 529-531. doi:10.1038/325529a0

- Kaniakova, M., Lichnerova, K., Skrenkova, K., Vyklicky, L., & Horak, M. (2016). Biochemical and electrophysiological characterization of N-glycans on NMDA receptor subunits. *J Neurochem*, *138*(4), 546-556. doi:10.1111/jnc.13679
- Karp, N. A., Meehan, T. F., Morgan, H., Mason, J. C., Blake, A., Kurbatova, N., . . . Brown, S. D. (2015). Applying the ARRIVE Guidelines to an In Vivo Database. *PLoS Biol*, *13*(5), e1002151. doi:10.1371/journal.pbio.1002151
- Kilkenny, C., Browne, W. J., Cuthill, I. C., Emerson, M., & Altman, D. G. (2010). Improving bioscience research reporting: the ARRIVE guidelines for reporting animal research. *PLoS Biol*, *8*(6), e1000412. doi:10.1371/journal.pbio.1000412
- Kleckner, N. W., & Dingledine, R. (1988). Requirement for glycine in activation of NMDA-receptors expressed in *Xenopus* oocytes. *Science*, *241*(4867), 835-837.
- Krampfl, K., Schlesinger, F., Zorner, A., Kappler, M., Dengler, R., & Bufler, J. (2002). Control of kinetic properties of GluR2 flop AMPA-type channels: impact of R/G nuclear editing. *Eur J Neurosci*, *15*(1), 51-62.
- Lacey, J. M., & Wilmore, D. W. (1990). Is glutamine a conditionally essential amino acid? *Nutr Rev*, *48*(8), 297-309.
- Landmann, G., Lustenberger, C., Schleinzer, W., Schmelz, M., Stockinger, L., & Rukwied, R. (2016). Short lasting transient effects of a capsaicin 8% patch on nociceptor activation in humans. *Eur J Pain*. doi:10.1002/ejp.867
- Latremoliere, A., & Woolf, C. J. (2009). Central sensitization: a generator of pain hypersensitivity by central neural plasticity. *J Pain*, *10*(9), 895-926. doi:10.1016/j.jpain.2009.06.012
- Lee, A., Derricks, K., Minns, M., Ji, S., Chi, C., Nugent, M. A., & Trinkaus-Randall, V. (2014). Hypoxia-induced changes in Ca(2+) mobilization and protein phosphorylation implicated in impaired wound healing. *Am J Physiol Cell Physiol*, *306*(10), C972-985. doi:10.1152/ajpcell.00110.2013
- Lee, Y. S., Lee, J. H., Lee, I. S., & Choi, B. T. (2013). Effects of electroacupuncture on spinal alpha-amino-3-hydroxy-5-methyl-4-isoxazole propionic acid receptor in rats injected with complete Freund's adjuvant. *Mol Med Rep*, *8*(4), 1130-1134. doi:10.3892/mmr.2013.1633
- Li, W., Wang, J. X., Zhou, Z. H., Lu, Y., Li, X. Q., Liu, B. J., & Chen, H. S. (2016). Contribution of capsaicin-sensitive primary afferents to mechanical hyperalgesia induced by ventral root transection in rats: the possible role of BDNF. *Neurol Res*, *38*(1), 80-85. doi:10.1080/01616412.2015.1135570
- Lichnerova, K., Kaniakova, M., Park, S. P., Skrenkova, K., Wang, Y. X., Petralia, R. S., . . . Horak, M. (2015). Two N-glycosylation Sites in the GluN1 Subunit Are Essential for Releasing N-methyl-d-aspartate (NMDA) Receptors from the Endoplasmic Reticulum. *J Biol Chem*, *290*(30), 18379-18390. doi:10.1074/jbc.M115.656546
- Liu, X. J., Gingrich, J. R., Vargas-Caballero, M., Dong, Y. N., Sengar, A., Beggs, S., . . . Salter, M. W. (2008). Treatment of inflammatory and neuropathic pain by uncoupling Src from the NMDA receptor complex. *Nat Med*, *14*(12), 1325-1332. doi:10.1038/nm.1883
- Lomeli, H., Mosbacher, J., Melcher, T., Hoyer, T., Geiger, J. R., Kuner, T., . . . Seeburg, P. H. (1994). Control of kinetic properties of AMPA receptor channels by nuclear RNA editing. *Science*, *266*(5191), 1709-1713.
- Lund, J. P., Sadeghi, S., Athanassiadis, T., Caram Salas, N., Auclair, F., Thivierge, B., . . . Kolta, A. (2010). Assessment of the Potential Role of Muscle Spindle Mechanoreceptor Afferents in Chronic Muscle Pain in the Rat Masseter Muscle. *PLoS One*, *5*(6). doi:10.1371/journal.pone.0011131
- Marfurt, C. F., & Del Toro, D. R. (1987). Corneal sensory pathway in the rat: a horseradish peroxidase tracing study. *J Comp Neurol*, *261*(3), 450-459. doi:10.1002/cne.902610309
- Mayer, M. L. (2005a). Crystal structures of the GluR5 and GluR6 ligand binding cores: molecular mechanisms underlying kainate receptor selectivity. *Neuron*, *45*(4), 539-552. doi:10.1016/j.neuron.2005.01.031

- Mayer, M. L. (2005b). Glutamate receptor ion channels. *Curr Opin Neurobiol*, *15*(3), 282-288. doi:10.1016/j.conb.2005.05.004
- Mayer, M. L., Westbrook, G. L., & Guthrie, P. B. (1984). Voltage-dependent block by Mg²⁺ of NMDA responses in spinal cord neurones. *Nature*, *309*(5965), 261-263.
- McRoberts, J. A., Coutinho, S. V., Marvizon, J. C., Grady, E. F., Tognetto, M., Sengupta, J. N., . . . Mayer, E. A. (2001). Role of peripheral N-methyl-D-aspartate (NMDA) receptors in visceral nociception in rats. *Gastroenterology*, *120*(7), 1737-1748.
- Medvedev, I. O., Malyshkin, A. A., Belozertseva, I. V., Sukhotina, I. A., Sevostianova, N. Y., Aliev, K., . . . Besselov, A. Y. (2004). Effects of low-affinity NMDA receptor channel blockers in two rat models of chronic pain. *Neuropharmacology*, *47*(2), 175-183. doi:10.1016/j.neuropharm.2004.01.019
- Mergler, S., Valtink, M., Takayoshi, S., Okada, Y., Miyajima, M., Saika, S., & Reinach, P. S. (2014). Temperature-sensitive transient receptor potential channels in corneal tissue layers and cells. *Ophthalmic Res*, *52*(3), 151-159. doi:10.1159/000365334
- Merrill, A. W., Cuellar, J. M., Judd, J. H., Carstens, M. I., & Carstens, E. (2008). Effects of TRPA1 agonists mustard oil and cinnamaldehyde on lumbar spinal wide-dynamic range neuronal responses to innocuous and noxious cutaneous stimuli in rats. *J Neurophysiol*, *99*(2), 415-425. doi:10.1152/jn.00883.2007
- Mertens, P., Blond, S., David, R., & Rigoard, P. (2015). Anatomy, physiology and neurobiology of the nociception: a focus on low back pain (part A). *Neurochirurgie*, *61 Suppl 1*, S22-34. doi:10.1016/j.neuchi.2014.09.001
- Michelotti, A., Cioffi, I., Rongo, R., Borrelli, R., Chiodini, P., & Svensson, P. (2014). Effects of muscle pain induced by glutamate injections during sustained clenching on the contraction pattern of masticatory muscles. *J Oral Facial Pain Headache*, *28*(3), 252-260. doi:10.11607/ofph.1239
- Micu, I., Plemel, J. R., Lachance, C., Proft, J., Jansen, A. J., Cummins, K., . . . Stys, P. K. (2016). The molecular physiology of the axo-myelinic synapse. *Exp Neurol*, *276*, 41-50. doi:10.1016/j.expneurol.2015.10.006
- Miller, K. E., Balbas, J. C., Benton, R. L., Lam, T. S., Edwards, K. M., Kriebel, R. M., & Schechter, R. (2012). Glutaminase immunoreactivity and enzyme activity is increased in the rat dorsal root ganglion following peripheral inflammation. *Pain Res Treat*, *2012*, 414697. doi:10.1155/2012/414697
- Miller, K. E., Hoffman, E. M., Sutharshan, M., & Schechter, R. (2011). Glutamate pharmacology and metabolism in peripheral primary afferents: physiological and pathophysiological mechanisms. *Pharmacol Ther*, *130*(3), 283-309. doi:10.1016/j.pharmthera.2011.01.005
- Miller, K. E., & Ibitokun, B. (2011). Localization of glutamate, glutaminase, and aspartate aminotransferase in rat corneal afferents. *ARVO*, *52*:315.
- Miyoshi, Y., Yoshioka, Y., Suzuki, K., Miyazaki, T., Koura, M., Saigoh, K., . . . Hayasaka, N. (2014). A new mouse allele of glutamate receptor delta 2 with cerebellar atrophy and progressive ataxia. *PLoS One*, *9*(9), e107867. doi:10.1371/journal.pone.0107867
- Mollerud, S., Frydenvang, K., Pickering, D. S., & Kastrup, J. S. (2017). Lessons from crystal structures of kainate receptors. *Neuropharmacology*, *112*(Pt A), 16-28. doi:10.1016/j.neuropharm.2016.05.014
- Mollerud, S., Kastrup, J. S., & Pickering, D. S. (2016). A pharmacological profile of the high-affinity GluK5 kainate receptor. *Eur J Pharmacol*, *788*, 315-320. doi:10.1016/j.ejphar.2016.06.049
- Mothet, J. P., Le Bail, M., & Billard, J. M. (2015). Time and space profiling of NMDA receptor co-agonist functions. *J Neurochem*, *135*(2), 210-225. doi:10.1111/jnc.13204
- Nilsson, M., Lassen, D., Andresen, T., Nielsen, A. K., Arendt-Nielsen, L., & Drewes, A. M. (2014). Intradermal glutamate and capsaicin injections: intra- and interindividual variability of provoked hyperalgesia and allodynia. *Clin Exp Pharmacol Physiol*, *41*(6), 423-429. doi:10.1111/1440-1681.12229

- Nosedá, R., & Burstein, R. (2013). Migraine pathophysiology: anatomy of the trigeminovascular pathway and associated neurological symptoms, cortical spreading depression, sensitization, and modulation of pain. *Pain, 154 Suppl 1*, S44-53. doi:10.1016/j.pain.2013.07.021
- Nowak, L., Bregestovski, P., Ascher, P., Herbet, A., & Prochiantz, A. (1984). Magnesium gates glutamate-activated channels in mouse central neurones. *Nature, 307*(5950), 462-465.
- Oswald, D. J., Lee, A., Trinidad, M., Chi, C., Ren, R., Rich, C. B., & Trinkaus-Randall, V. (2012). Communication between corneal epithelial cells and trigeminal neurons is facilitated by purinergic (P2) and glutamatergic receptors. *PLoS One, 7*(9), e44574. doi:10.1371/journal.pone.0044574
- Pachernegg, S., Munster, Y., Muth-Kohne, E., Fuhrmann, G., & Hollmann, M. (2015). GluA2 is rapidly edited at the Q/R site during neural differentiation in vitro. *Front Cell Neurosci, 9*, 69. doi:10.3389/fncel.2015.00069
- Parekh, M., Ferrari, S., Sheridan, C., Kaye, S., & Ahmad, S. (2016). Concise Review: An Update on the Culture of Human Corneal Endothelial Cells for Transplantation. *Stem Cells Transl Med, 5*(2), 258-264. doi:10.5966/sctm.2015-0181
- Park, J. S., Yaster, M., Guan, X., Xu, J. T., Shih, M. H., Guan, Y., . . . Tao, Y. X. (2008). Role of spinal cord alpha-amino-3-hydroxy-5-methyl-4-isoxazolepropionic acid receptors in complete Freund's adjuvant-induced inflammatory pain. *Mol Pain, 4*, 67. doi:10.1186/1744-8069-4-67
- Park, Y. H., Broyles, H. V., He, S., McGrady, N. R., Li, L., & Yorio, T. (2016). Involvement of AMPA Receptor and Its Flip and Flop Isoforms in Retinal Ganglion Cell Death Following Oxygen/Glucose Deprivation. *Invest Ophthalmol Vis Sci, 57*(2), 508-526. doi:10.1167/iovs.15-18481
- Patneau, D. K., Vyklicky, L., Jr., & Mayer, M. L. (1993). Hippocampal neurons exhibit cyclothiazide-sensitive rapidly desensitizing responses to kainate. *J Neurosci, 13*(8), 3496-3509.
- Pedersen, A. M., & Nauntofte, B. (2001). Primary Sjogren's syndrome: oral aspects on pathogenesis, diagnostic criteria, clinical features and approaches for therapy. *Expert Opin Pharmacother, 2*(9), 1415-1436. doi:10.1517/14656566.2.9.1415
- Pei, W., Huang, Z., Wang, C., Han, Y., Park, J. S., & Niu, L. (2009). Flip and flop: a molecular determinant for AMPA receptor channel opening. *Biochemistry, 48*(17), 3767-3777. doi:10.1021/bi8015907
- Peng, H. Y., Chen, G. D., Hsieh, M. C., Lai, C. Y., Huang, Y. P., & Lin, T. B. (2012). Spinal SGK1/GRASP-1/Rab4 is involved in complete Freund's adjuvant-induced inflammatory pain via regulating dorsal horn GluR1-containing AMPA receptor trafficking in rats. *Pain, 153*(12), 2380-2392. doi:10.1016/j.pain.2012.08.004
- Pickard, B. S., Malloy, M. P., Christoforou, A., Thomson, P. A., Evans, K. L., Morris, S. W., . . . Muir, W. J. (2006). Cytogenetic and genetic evidence supports a role for the kainate-type glutamate receptor gene, GRIK4, in schizophrenia and bipolar disorder. *Mol Psychiatry, 11*(9), 847-857. doi:10.1038/sj.mp.4001867
- Popoli, M., Yan, Z., McEwen, B. S., & Sanacora, G. (2012). The stressed synapse: the impact of stress and glucocorticoids on glutamate transmission. *Nat Rev Neurosci, 13*(1), 22-37. doi:10.1038/nrn3138
- Por, E. D., Choi, J. H., & Lund, B. J. (2016). Low-Level Blast Exposure Increases Transient Receptor Potential Vanilloid 1 (TRPV1) Expression in the Rat Cornea. *Curr Eye Res, 41*(10), 1294-1301. doi:10.3109/02713683.2015.1122812
- Ray, S. B., Singh, S. S., & Mehra, R. D. (2010). Small-sized neurons of trigeminal ganglia express multiple voltage-sensitive calcium channels: a qualitative immunohistochemical study. *Indian J Exp Biol, 48*(6), 538-543.
- Rossignol, S., Dubuc, R., & Gossard, J. P. (2006). Dynamic sensorimotor interactions in locomotion. *Physiol Rev, 86*(1), 89-154. doi:10.1152/physrev.00028.2005

- Ruparel, N. B., Patwardhan, A. M., Akopian, A. N., & Hargreaves, K. M. (2008). Homologous and heterologous desensitization of capsaicin and mustard oil responses utilize different cellular pathways in nociceptors. *Pain*, *135*(3), 271-279. doi:10.1016/j.pain.2007.06.005
- Sato, H., Castrillon, E. E., Cairns, B. E., Bendixen, K. H., Wang, K., Nakagawa, T., . . . Svensson, P. (2015). Intramuscular temperature modulates glutamate-evoked masseter muscle pain intensity in humans. *J Oral Facial Pain Headache*, *29*(2), 158-167. doi:10.11607/ofph.1332
- Sawyer, C. M., Carstens, M. I., & Carstens, E. (2009). Mustard oil enhances spinal neuronal responses to noxious heat but not cooling. *Neurosci Lett*, *461*(3), 271-274. doi:10.1016/j.neulet.2009.06.036
- Seigel, G. M., Sun, W., Salvi, R., Campbell, L. M., Sullivan, S., & Reidy, J. J. (2003). Human corneal stem cells display functional neuronal properties. *Mol Vis*, *9*, 159-163.
- Sherrington, C. S. (1903). Qualitative difference of spinal reflex corresponding with qualitative difference of cutaneous stimulus. *J Physiol*, *30*(1), 39-46.
- Shimada, A., Castrillon, E., Baad-Hansen, L., Ghafouri, B., Gerdle, B., Ernberg, M., . . . Svensson, P. (2015). Muscle pain sensitivity after glutamate injection is not modified by systemic administration of monosodium glutamate. *J Headache Pain*, *16*, 68. doi:10.1186/s10194-015-0546-0
- Sinnett, P. M., Carr, B., Cook, G., Mucklerath, H., Varney, L., Weiher, M., . . . Vassar, M. (2015). Systematic Reviewers in Clinical Neurology Do Not Routinely Search Clinical Trials Registries. *PLoS One*, *10*(7), e0134596. doi:10.1371/journal.pone.0134596
- Sit, A. J., & McLaren, J. W. (2011). Measurement of episcleral venous pressure. *Exp Eye Res*, *93*(3), 291-298. doi:10.1016/j.exer.2011.05.003
- Sloniecka, M., Le Roux, S., Boman, P., Bystrom, B., Zhou, Q., & Danielson, P. (2015). Expression Profiles of Neuropeptides, Neurotransmitters, and Their Receptors in Human Keratocytes In Vitro and In Situ. *PLoS One*, *10*(7), e0134157. doi:10.1371/journal.pone.0134157
- Sobolevsky, A. I., Yelshansky, M. V., & Wollmuth, L. P. (2004). The outer pore of the glutamate receptor channel has 2-fold rotational symmetry. *Neuron*, *41*(3), 367-378.
- Staines, D. R. (2008). Does autoimmunity of endogenous vasoactive neuropeptides cause retinopathy in humans? *Med Hypotheses*, *70*(1), 137-140. doi:10.1016/j.mehy.2007.04.016
- Tao, Y. X. (2012). AMPA receptor trafficking in inflammation-induced dorsal horn central sensitization. *Neurosci Bull*, *28*(2), 111-120. doi:10.1007/s12264-012-1204-z
- Ting, K. H., Hill, C. L., & Whittle, S. L. (2015). Quality of reporting of interventional animal studies in rheumatology: a systematic review using the ARRIVE guidelines. *Int J Rheum Dis*, *18*(5), 488-494. doi:10.1111/1756-185x.12699
- Traynelis, S. F., Wollmuth, L. P., McBain, C. J., Menniti, F. S., Vance, K. M., Ogden, K. K., . . . Dingledine, R. (2010). Glutamate receptor ion channels: structure, regulation, and function. *Pharmacol Rev*, *62*(3), 405-496. doi:10.1124/pr.109.002451
- Tucholski, J., Pinner, A. L., Simmons, M. S., & Meador-Woodruff, J. H. (2014). Evolutionarily conserved pattern of AMPA receptor subunit glycosylation in Mammalian frontal cortex. *PLoS One*, *9*(4), e94255. doi:10.1371/journal.pone.0094255
- Tucholski, J., Simmons, M. S., Pinner, A. L., McMillan, L. D., Haroutunian, V., & Meador-Woodruff, J. H. (2013). N-linked glycosylation of cortical N-methyl-D-aspartate and kainate receptor subunits in schizophrenia. *Neuroreport*, *24*(12), 688-691. doi:10.1097/WNR.0b013e328363bd8a
- Vincent, K., Cornea, V. M., Jong, Y. J., Laferriere, A., Kumar, N., Mickeviciute, A., . . . Coderre, T. J. (2016). Intracellular mGluR5 plays a critical role in neuropathic pain. *Nat Commun*, *7*, 10604. doi:10.1038/ncomms10604
- Wieschowski, S., Silva, D. S., & Strech, D. (2016). Animal Study Registries: Results from a Stakeholder Analysis on Potential Strengths, Weaknesses, Facilitators, and Barriers. *PLoS Biol*, *14*(11), e2000391. doi:10.1371/journal.pbio.2000391

- Wilson, S. E., & Hong, J. W. (2000). Bowman's layer structure and function: critical or dispensable to corneal function? A hypothesis. *Cornea*, *19*(4), 417-420.
- Woolf, C. J., & Ma, Q. (2007). Nociceptors--noxious stimulus detectors. *Neuron*, *55*(3), 353-364. doi:10.1016/j.neuron.2007.07.016
- Woolf, C. J., & Salter, M. W. (2000). Neuronal plasticity: increasing the gain in pain. *Science*, *288*(5472), 1765-1769.
- Xuan, M., Wang, S., Liu, X., He, Y., Li, Y., & Zhang, Y. (2016). Proteins of the corneal stroma: importance in visual function. *Cell Tissue Res*, *364*(1), 9-16. doi:10.1007/s00441-016-2372-3
- Yao, Y., & Mayer, M. L. (2006). Characterization of a soluble ligand binding domain of the NMDA receptor regulatory subunit NR3A. *J Neurosci*, *26*(17), 4559-4566. doi:10.1523/jneurosci.0560-06.2006
- Yerokhin, V. V., Carr, B. K., Sneed, G., & Vassar, M. (2016). Clinical trials registries are underused in the pregnancy and childbirth literature: a systematic review of the top 20 journals. *BMC Res Notes*, *9*(1), 475. doi:10.1186/s13104-016-2280-3
- Yuzaki, M., & Aricescu, A. R. (2017). A GluD Coming-Of-Age Story. *Trends Neurosci*, *40*(3), 138-150. doi:10.1016/j.tins.2016.12.004
- Zakharov, A., Vitale, C., Kilinc, E., Koroleva, K., Fayuk, D., Shelukhina, I., . . . Giniatullin, R. (2015). Hunting for origins of migraine pain: cluster analysis of spontaneous and capsaicin-induced firing in meningeal trigeminal nerve fibers. *Front Cell Neurosci*, *9*, 287. doi:10.3389/fncel.2015.00287
- Zhang, S., Chiang, C. Y., Xie, Y. F., Park, S. J., Lu, Y., Hu, J. W., . . . Sessle, B. J. (2006). Central sensitization in thalamic nociceptive neurons induced by mustard oil application to rat molar tooth pulp. *Neuroscience*, *142*(3), 833-842. doi:10.1016/j.neuroscience.2006.06.063
- Zhou, S., Bonasera, L., & Carlton, S. M. (1996). Peripheral administration of NMDA, AMPA or KA results in pain behaviors in rats. *Neuroreport*, *7*(4), 895-900.
- Zhuo, M. (2017). Ionotropic glutamate receptors contribute to pain transmission and chronic pain. *Neuropharmacology*, *112*(Pt A), 228-234. doi:10.1016/j.neuropharm.2016.08.01

VITA

Branden Kenneth Carr

Candidate for the Degree of

Doctor of Philosophy

Thesis: GLUTAMATE RECEPTOR SUBUNITS IN THE RAT CORNEA

Major Field: Biomedical Sciences

Biographical:

Education: Received bachelor degree of Psychology at the University of Central Oklahoma Edmond, Oklahoma in May 2010. Received bachelor degree of Biology at Oklahoma State University Stillwater, Oklahoma in May 2011. Completed the requirements for the Doctoral of Philosophy degree in Biomedical Sciences at Oklahoma State University Center for Health Sciences, Tulsa, Oklahoma in May 2017.

Experience: Employed as teaching assistant for clinical based histology and neuroanatomy by Oklahoma State University Center for Health Sciences, 2013 – 2014.

Professional Memberships: Society for Neuroscience